Characterisation and Biomedical application of Fabric Sensors

A thesis submitted for fulfilment of the requirements for the degree of Master of Engineering

Michael A Mestrovic
B.Eng. Grad.Dip.

School of Electrical and Computer Engineering
Science, Engineering and Technology Portfolio
RMIT University
June 2007

Declaration

I certify that except where due acknowledged has been made overleaf, the work in this research project is that of the author alone; the work has not been submitted previously, in whole or in part, to qualify for any other academic award; the content of the thesis is the result of research work which has been carried out during the period of candidature.

Michael Mestrovic

30th June 2007

Acknowledgements

Special thanks to CSIRO Textile and Fibre Technology who allowed me to conduct this research as part of the divisions research efforts.

I also wish to especially thank the following people for their valuable contribution to the work presented here:

Associate Professor Dinesh Kumar for his direction, support and guidance. Dr Richard Helmer for his encouragement, support, guidance and help in maintaining focus. Dr Graham Higgerson for coding the ECG analysis algorithm. Mr. Brendan Darcy for his help in building signal conditioning electronics. Dr Bill Humphries for his ongoing support. Mr. Peter Herwig for his patience in preparing the large number of numerous knitted electrodes for testing. Mr Phil Smale for construction and modifications of the pressure test rig.

List of Figures

List of Tables

Abbreviations

AgN	Silver coated nylon
AgCu	Silver coated copper (s) single filament, (m) multifilament
AgCl	Silver chloride
BP	Blood pressure
CLR	Carbon loaded rubber
CV	Coefficient of variation
ECG	Electrocardiogram, electrocardiographic
EDR	Electrodermal response
EEG	Electroencephalogram, electroencephalographic
EU	European Union
FFT	Fast Fourier transform
FR4	Standard grade of fiberglass printed circuit board material
GSR	Galvanic skin response
HR	Heart rate
HRV	Heart rate variability
MMG	Mechanomyogram
MVC	Maximal voluntary contraction
NN	Normal-to-normal heart beat interval
PPY	Polypyrrole
PSD	Power Spectral Density
RMSSD	Root mean square of successive RR interval differences
RR	Heart beat interval, RR interval
SC	Skin conductivity
σ_{NN}	Standard deviation of NN (or RR) intervals
σ_{RR}	Standard deviation of successive RR interval differences
SEMG	Surface electromyography
SENIAM	Surface Electromyography for the Non-Invasive Assessment of Muscles
SPL	Skin potential level
SPR	Skin potential response
SSt	Stainless steel(thick)
TBW	Total body water
TEB	Thoracic electrical bio impedance

Abstract

The sensors commonly used today to measure human physiological parameters are hard and discrete and not suitable for long term monitoring. A wearable garment with integrated fabric sensors incorporated in an unobtrusive way is highly desirable for long term physiological monitoring, particularly in a non-clinical environment.

The aim of this work is to investigate fabric sensors which can be integrated into a garment to allow the unobtrusive monitoring of physiological parameters, primarily for measuring the electrocardiograph (ECG) and respiration.

The work focuses on using only *dry fabric* electrodes where skin preparation and the use of chemical gels or adhesives are not employed. The textile structure used in this study was designed to provide controlled contact pressure, enable construction using common textile processing methods, allow accurate placement of electrodes on the body, allow comfortable fit and be unobtrusive to wear. It was decided to use the knitting method to make bands which incorporated conductive electrodes in order to evaluate different fabric electrodes materials. The detection of respiration using fabric strain sensors did not require electrical contact with the skin.

Preliminary experiments were conducted on a single subject to develop a device and methodology. Galvanic skin response and ECG was initially investigated to determine the effectiveness of electrode materials. ECG was established as a more reliable measure and was subsequently used to evaluate the initial performance of the fabric electrodes, and further refine the test methodology on a single subject. Experiments were then conducted on 10 male volunteer participants of reasonable general health having no known heart conditions, with ages 30-55 and BMI 20-30.

It was found that fabric sensors which were soft, pliable and flexible have advantages in terms of ability to provide better quality ECG signals and a comfortable bio-interface. Variation in the pressure applied to the electrode directly affects the acquired signal level and a pressure of 2.5KPa is preferred. Multifilament conductive yarns are more easily processed into fabric than monofilament yarns and are generally preferred.

Electrodes comprising a conductive polymer treated fabric gave better performance than metal or metal coated yarns.

Fabric strain sensors were tested and used to detect respiration on a single subject. It was found that human respiration can be measured using strain sensors such as those comprised of a conductive polymer treated fabric or a fabric incorporating a rigid conductive monofilament fibre.

Chapter 1

1 Introduction

1.0 Research Questions

The sensors commonly used to measure human physiological parameters such as body core temperature, heart rate, blood pressure, movement or gait, position or respiration are hard and discrete. It is difficult to use these types of sensors in a variety of applications, in particular where continuous monitoring is required during regular physical activity.

Recent commercial solutions lack the look and feel of 'conventional' garments and are costly. The aim of this study is to investigate whether it is possible to integrate sensors into a regular textile garment that can be worn all the time. Textile sensors for monitoring of physiological parameters, primarily electrocardiograph (ECG) and respiration will be investigated.

Hence, the aims of this research are:

(i) to investigate suitable options for non-invasive garment based physiological recording, and,

(ii) to identify the limitations and reliability of the garment based recordings.

This study is directed to investigate whether;

i) incorporation of a conductive yarn into a textile fabric can be used as a biosignal sensor to measure ECG and respiration rate (RR);

ii) Are measures of ECG and RR with these fabric electrodes reproducible.

These practical considerations are important in enabling the application of such a garment based system. Further, determining if the system is suitable for clinical or

non clinical application is also useful. This will allow the physiological monitoring of an individual to be performed in a simple, easy to use and unambiguous manner without the immediate presence of a skilled clinician or the need of a clinical environment.

1.1 Sensing physiological parameters of humans

Clinically, biomedical sensing has been extensively used for the maintenance of human health for a considerable period and is now of increasing importance with the aging of the world's population and the general medical expertise skills shortage.

The focus now is turning to the need for home based monitoring of individuals [1-4]. For practical sensing of the physiological condition of a human being to be successful, it must be unobtrusive (comfortable and invisible) and thereby inherently non invasive. Whilst invasive techniques are used and can play a part in ratifying and confirming the validity and accuracy of non-invasive methods, they in themselves do not provide an acceptable or practical measurement regime for the routine monitoring of an individual's physiological parameters.

It is desirable to have simple wearable systems that can be used for biomedical and health applications [5-7]. Bonato [5], summarises current wearable technologies related to medicine and rehabilitation and specifically recognises the benefits of unobtrusive monitoring in *other than the clinical setting*. Such systems need to be economical, non–obtrusive and reliable. Due to the ubiquitous nature of clothing, integration of a sensing system into a garment has great merit.

The investigations are directed to;

- determine suitable types of yarns or fibre compositions for effective bio-potential detection and
- ascertain whether the outcomes resulting from this research, are able to be applied in the *clinical* or *non-clinical* environments.

Chapter 2

2 Background and Theory

2.0 E-Textiles and Materials

E-Textiles, i.e. electronic textiles, are textiles that contain or carry electronic functionality or components, is a growing area of current research in the advanced materials textiles field and is dependant upon the development of a range of flexible conductive materials. The aim is that the materials used are compatible and meet the requirements of a wearable comfortable garment, are robust and able to withstand harsh physical environments, are biologically compatible and in some cases, enable accurate and precise measurements to be made.

One of the first practical examples and application of the idea of wearable computing was that displayed by Post [8]. Although implemented using mostly discrete electronic components the garment was functional and displayed some basic attributes required of a wearable system. Numerous types of conductive threads are being used in the fabrication of conductive paths, areas and/or layers within such textile structures. The most reported of these being metal coated polymer or hybrid, metal fibres combined with core yarns or threads which have the required level of flexibility necessary for textile processes such as sewing, knitting and weaving[9, 10].

Sewing and embroidering are common methods for creating conductive electrodes areas within a fabric. These methods are less demanding and threads comprised of a nylon core wrapped with three continuous stainless steel fibres have been used successfully in garments [8]. Other composite threads made from short, stainless steel multifilament fibres alone or combined with polyester have been used. The exposure of short fibres extending from the processed thread can present practical problems with electrical shorting with adjacent connections/paths and use may be limited.

Connection of conductive threads is one of the major problems. Metal coated yarns/threads can offer conductivities as good as pure metal ones, whilst also allowing easier connectivity and flexibility. The use of high melting point polymers as the inner

cores on which the metal is deposited allows these to be soldered (Aracon by DuPont). Conductive paths in *S* shapes have been sewn into garments and the self inductance of the wire coil varies with movement of the fabric [11, 12]. Conducting polymer piezo resistive sensors, have been proposed and prototypes demonstrated, but these have been shown to have problems with resistance stability and time response [13]. User interaction is often a requirement of e-textiles and solutions by many researchers have been offered almost all based upon interaction between different layers of a textile. These can be of a direct contact, resistive or capacitive nature. Optical fibres have also been 'integrated' into fabric [14] and used as strain/stress sensors where the mechanical stresses modulate optical signals which can be detected.

Many problems present themselves dependant upon the textile implementation of a wearable garment, but two predominant problems remain; corrosion and connectivity. Even particular grades of stainless steel corrode in the presence of body secretions. If not disposable the garment needs to be laundered, a harsh and demanding environment for any textile.

2.1 Biosignals

'Biosignals' is a term used for signals that can be (continually) monitored and/or measured from biological entities. These may be electrical or mechanical signals (e.g. the mechanomyogram (MMG)), acoustic signals (e.g. phonetic and non-phonetic utterances, breathing) and visual signals (e.g. movements). These signals in many cases are generated by nerve and/or muscle cells, by conscious and unconscious actions within the body. The bioelectric signals often are very low amplitude voltages of the order of a few millivolts or less.

There are a number of bio-electric signals that are routinely measured. The electrodermal response (EDR), the main measure of which is galvanic skin response (GSR), measures changes in skin resistance. Electrical activity of the brain is determined using electroencephalogram (EEG). The variability of the heart beat interval (heart rate variability, HRV) is measured using the electrocardiographic (ECG) recording. Similarly, the variation in physical dimension of the chest and/or abdominal regions causing the lung volume to vary in unison is linked to respiration. Changes in biosignals reflect the changes in the physiological state of an individual.

2.2 The Skin Interface

The skin is the common point of contact between garments and the body and represents a key interface for detecting bio-mechanical and bio-electrical activity. The interactions that take place at the skin-sensor interface are complex and are dependant on the physical and electrical characteristics of both mediums. It is important to understand each, in order to determine the effects of these interactions on the detection of biosignals.

2.2.1 The Human Skin Model

The skin is an essential and complex organ of the human body. A large body of work has been done on the basic physiology of human skin [15-17]. As the skin's electrical properties are of major importance in the detection of physiological signals, it is important to identify the inherent structures that contribute to its conductivity. A diagram showing the ionic pathways through which conduction takes place is shown in Figure 1.

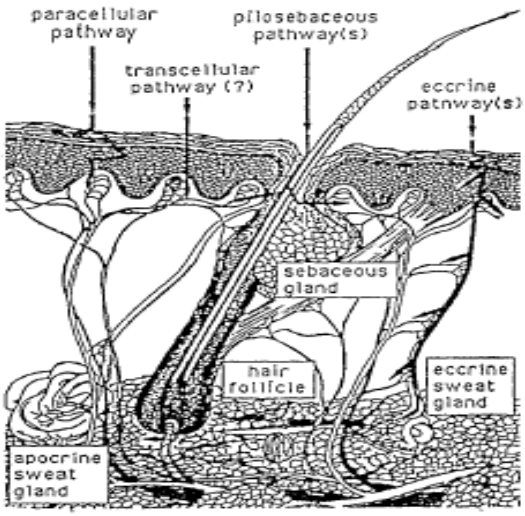

Figure 1. A schematic representation of human skin, showing conduction pathways(redrawn from[15]).

Ions can pass through the stratum corneum via paracellular pathways and through the skin's appendages (hair follicles, sebaceous glands and imperfections in the integrity of the skin) [16, 17]. A large portion of the DC current flows through the skin appendages and this flow can be represented electrically as a large resistance [18].

The structure of the skin and its relationship to blood vessels is shown in Figure 2. Skin reacts to any change in environment such as the contact with a material and this can create an increase in the superficial blood circulation and induce perspiration [19].

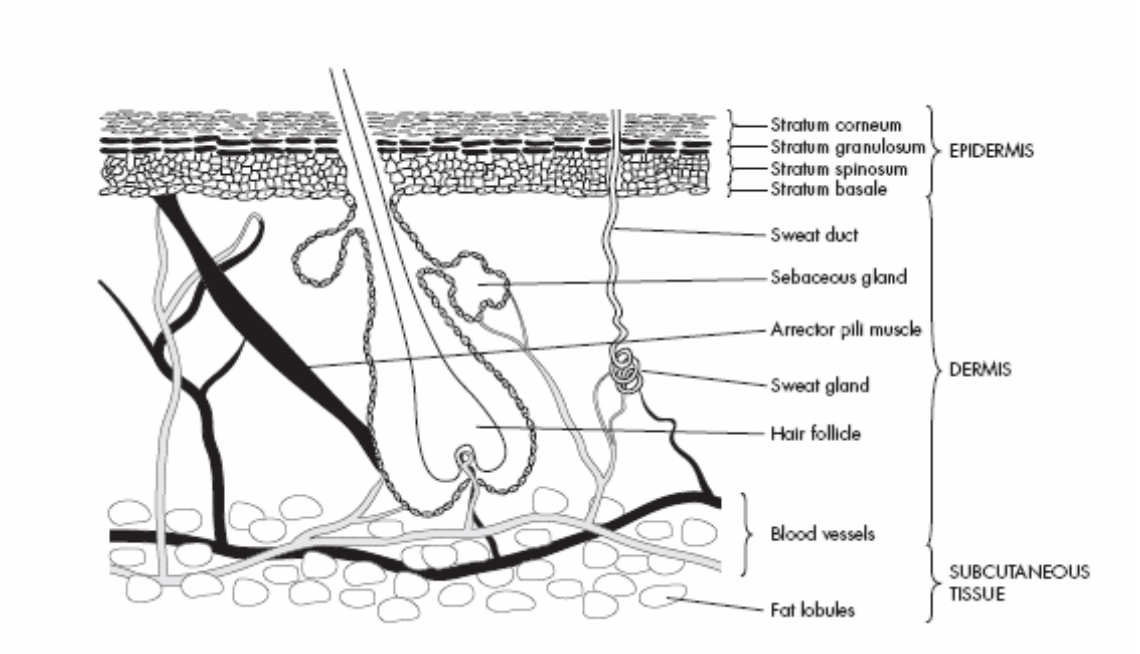

Figure 2. Cross-section through human skin, redrawn from [20].

The sweat ducts have a direct path from the inner layers direct to the normally dry outer layer of the skin, the stratum corneum. This outer layer is relatively thin (of the order of 10-20 microns). The mechanism of surface moistening occurs when the sweat glands secrete fluid which travels to the surface of the skin. The introduction of sweat which comprises a range of salts (e.g. sodium chloride (NaCl)), acts as an effective conductive electrolyte to reduce the resistance of the skin surface. This also causes a lowering of the impedance from the skin surface to the viable tissue below. The production of sweat depends upon a range of physical and physiological parameters and can vary within seconds.

Whilst a large body of work has been reported on the skin, providing an insight into the mechanisms leading to skin resistance, little information is available to accurately characterise skin tissue [21].

The effect of applied voltage across an electrode measuring system has also been shown by many researchers to directly effect the absolute value of skin resistance

measured. Chizmadzhev [15] has reported practical and theoretical models that describe the relationship between voltage and skin resistance. It is shown that for direct current and voltages less than 1 volt minimal, less than 5% reduction in skin resistance is observed. Thus to minimise the effect of voltage a measuring system needs to apply DC voltages of less than 1 volt.

The Cole skin model is considered to be the most useful in describing the impedance of the skin [22], i.e.

$$\mathbf{Z = R_s + j\, X_s} \qquad \textbf{(1)}$$

Where

Z, is the total skin impedance (ohms),

R_s, is the skin resistance (ohms) and

X_s, is the complex skin impedance (ohms, comprising capacitance).

This can be expanded and as derived from Yamamoto [23].

then

$$\mathbf{Z} = \mathbf{Z}_\infty + \frac{R_2}{1 + (j\,\omega\,\tau_m)^\beta} \qquad \textbf{(2)}$$

where $Z_\infty = \lim_{\omega \to \infty} Z$, $Z_0 = \lim_{\omega \to 0} Z$,

and $R_2 = Z_0 - Z_\infty$, is a resistive component(ohms), based on ionic conduction;

τ_m ($f_m = 1/2\pi\,\tau_m$), is the central relaxation time (s);

β (<1), representing the degree of deviation from Debye type ($\beta = 1$);

ω, is angular frequency(2π x frequency in Hz);

Z_∞ is usually taken to represent the deeper skin layers, always less than 1KΩ.

Yamamoto [23] and further studied by Martinsen et al [24], proposed another model based on a parallel resistance, where

$$\mathbf{Z = Z_e \; // \; (Z = R_s + j\, X_s)} \qquad \textbf{(3) from [23]}$$

where Z_e is the resistance of the outer cellular solution

A wide range of both capacitive and resistive values have been reported for these models [21]. Recent reports have suggested other similar models but again there is considerable variation in measured values [22, 25, 26].

2.2.2 Skin surface measurement considerations

International standards have been developed for safe electrical exposure limits for medical measuring equipment [27]. All commercial biomedical equipment needs to adhere to applicable electrical safety and exposure standards.

Direct current measurements such as skin conductivity (SC) or galvanic skin response (GSR), electromyography (EMG) or even electrocardiography (ECG) can cause localised polarisation in the vicinity of the measurement electrodes placed on the surface of the skin [15]. To verify this effect, measurements can be made by reversing the polarity of the measuring potential or current.

Bioimpedance measurements of the human body are performed via the skin surface. As the human body is largely comprised of water and muscle, bioimpedance has resistive and capacitive components. As this bioimpedance is frequency dependant, characterisation is performed using AC signals. Bioimpedance is measured by injecting a known low level AC current (in the 10's -100's of micro amp region) between two outer surface electrodes and measuring with two inner surface electrodes the resulting potential that developed due to this current.

The integrity of the tissue near the electrodes and the electrode area itself will effect the impedance measurement. Skin resistance itself is inversely proportional to contact area between the electrode and the skin [28]. Typically bioimpedance measurements are made at frequencies of 50 KHz to 100 KHz. Bioimpedance is a measure of biological tissue and is dependant upon a range of parameters within and between

individuals. In fact the stratum corneum is the predominant impedance component in impedance measurements up to a few kilohertz and viable skin is significant at higher frequencies [29, 30]. In a study involving SEMG [31], the electrode-skin impedance was measured at low frequencies(1-512 Hz) and found to vary from 2.36KΩ to 135KΩ. Attempts were made to determine if there was any relationship between impedance and the SEMG spectrum but no conclusion was reached because of the large variation between subjects. With this in mind and as the signals of real interest in this research are ECG and respiration, which are very low frequency < 100Hz, bioimpedance was not considered a useful measurement to use. The ECG signal QRS complex has most of it's frequency content within the frequency range of 5 – 30 Hz [32].

Measurements that are considered are EMG, GSR, ECG and respiration.

2.2.3 Skin Conductivity and Galvanic Skin Response

Galvanic skin resistance (GSR) is one of several electrodermal responses that can be measured and is basically the DC resistance measured on the surface of the skin. Skin conductivity as a measure of physiological activity is not new and many studies have been described since 1888 [33].

Skin potential response (SPR) is effectively the measurement made in ECG where voltages at the skin surface are monitored. Skin potential level (SPL) and SPR are affected by lower layers of the skin including the dermal, epidermal layers and sweat pores. Skin resistance is greatest in the stratum corneum, followed by the epidermis and then the dermis. If measurements are made between two electrodes for example, at short distances the resistance is large as the current mainly passes through the stratum corneum but as distance increases, the resistance decreases, since current passes through the dermis and epidermis [34]. Ionic transfer between the outer layer and inner layers of the skin are the primary cause of these sensed voltages [18].

The measurement itself is dependant upon many factors including the physical and emotional state of the subject. This can result in widely varying results as there are

large inter subject variations. There are also large intra-experimental variations for the same individuals. Many researchers in this field have reported this common effect as cited by Aberg [35]. Sweat glands in the outer epidermal skin layer especially during exertion for example, results in the excretion of fluids including salts which increase the conductivity of the skin's surface resulting in a lower GSR.

GSR generally reflects sweat gland activity and changes in the sympathetic nervous system. Measured typically from the palm or fingertips, changes occur in the relative conductance of a small electrical current between the electrodes. The activity of the sweat glands is in response to sympathetic nervous stimulation. Increased sympathetic activation results in an increase in the level of conductance. There is a relationship between sympathetic activity and emotional arousal and investigations are ongoing, in attempts to identify the specific emotion being elicited. Fear, anger, startle response, orienting response and sexual feelings are all among the emotions which may produce similar GSR responses. Singular discrimination and the identification of discrete emotions from GSR measurements have not been reported and are yet to be determined.

Skin conductance can be classified into two types, namely tonic and phasic. Tonic skin conductance is the baseline value of skin conductance in a static environment i.e. one in which there is no singular or discrete environmental event and is generally called Skin Conductance Level (SCL). This SCL as described is different for each person and may typically range from 10-50 μS. Phasic skin conductance is the change in skin conductance when an environmental event takes place, which can be physical or emotion. These time related changes are generally called Skin Conductance Responses (SCRs). The time from an event to a change in SCL i.e. an SCR is called latency. This latency (delay) and the SCR rise time itself, have values in the seconds range. After reaching a peak the GSR value diminishes over a longer time (tens of seconds). In practical measurements, generally a time of a minute should be adequate to acquire a representative SCL for electrode comparison purposes.

Traditionally GSR has been measured on the fingers, hands or feet but it has been reported that the best places for the measurement of GSR is the soles of the feet where the effects of a varying emotional state of a subject is most apparent [36].

However to allow measurements to be made in a simple garment, the aim of this research, consideration was given to implement this in a garment (vest) worn on the torso. Such a garment may allow points of contact to be made in other appropriate places although less ideal, such as the chest and/or abdomen. It was initially thought that electrodes might be better applied to the arm to allow easier and less obtrusive tests on a subject.

2.3 Heart activity and electrocardiography

Current methods for heart activity detection are predominantly based on the detection of electro-physiological conditions using multiple conductive electrodes attached to the skin and a physical hardwired connection to local signal conditioning, filtering, amplifying circuitry and display.

The accepted origination [37] of the ECG waveform components resulting from this detection is shown in Figure 3. The different waveforms for each of the specialized cells found in the heart are shown. The latency shown approximates that normally found in a healthy heart.

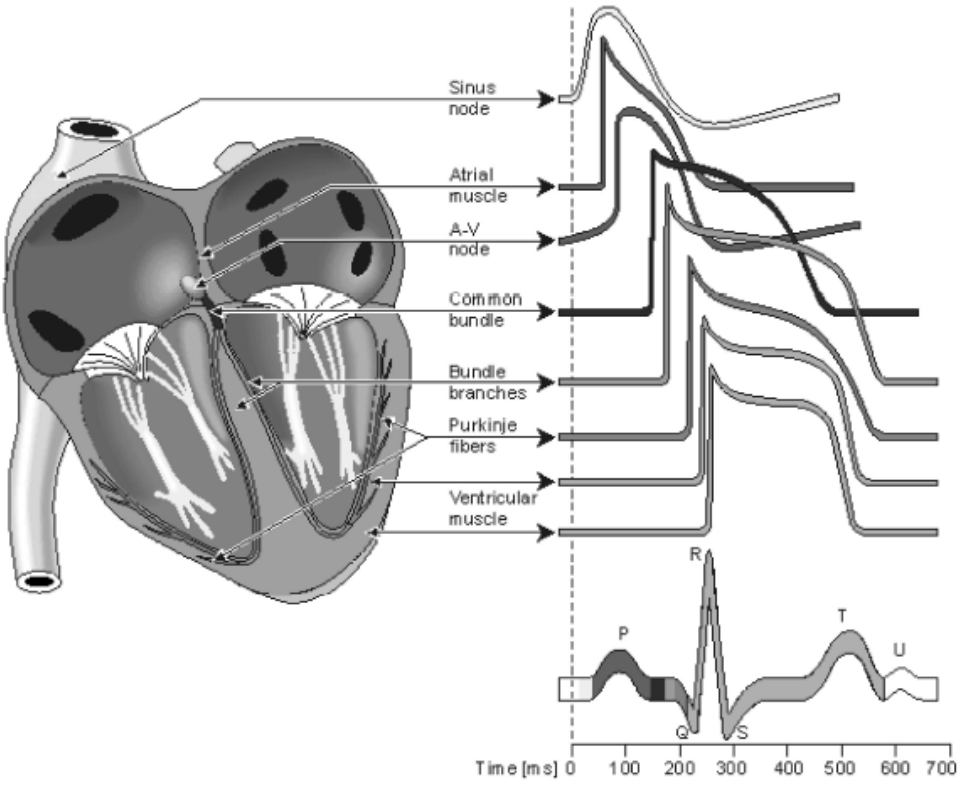

Figure 3. Electrophysiology of the heart, composition of the ECG signal and how signals originate (redrawn from [37]).

Most analysis of electrical signals assumes short term stationarity of the considered signal (the characteristic does not vary with time). If the signal is nonstationary, which is often the case for biosignals, analysis methods must take this into account.

2.3.1 Equipment and Methods of electro-Physiological Monitoring

ECG based monitoring systems use contact electrodes in conductive gels with high levels of chloride ions (namely silver chloride) to ensure generation of half cell potentials. When a conductor is placed in contact with an electrolyte, contact potentials are produced. A layer of ions emitted from the electrolyte collect over the surface of the conductive material, known as Nernst polarisation or 'half cell' effect. If the same two electrodes are used then the potential effect is cancelled.

Clinical heart monitoring and diagnosis are based on the placement of 'standard' electrodes in set positions on the human body. Traditionally up to 12 can be used, but a smaller number of electrodes are more often used. A typical subset of positioning electrodes based on the Einthoven triangle [37] is shown in Figure 4, where three electrodes are used and are denoted as, Lead I, Lead II and Lead III signals.

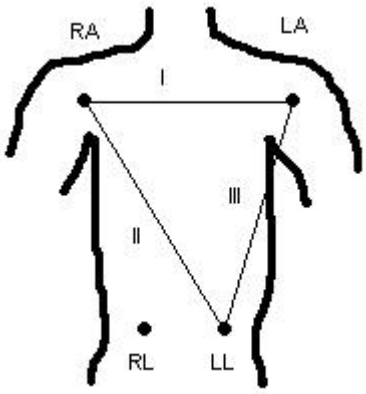

Figure 4. Simplified Einthoven triangle of ECG measurement connections[37].

The biosignals, conditioned with appropriate electronic hardware (see section 3.1.1), are sent to a display device for observation. The right arm (RA) and left arm (LA) are signal inputs and the right leg (RL) or left leg (LL) connection can be used as a reference electrode.

To improve signal integrity in the sensing of ECG biopotentials, commercially available 'active' electrodes are available from BioSemi [38]. Whilst these electrodes can aid in the provision of better signal detection, they not widely used as they are costly and bulky compared to traditional adhesive surface electrodes.

2.3.2 Limitations with Existing ECG Measuring Techniques

In the clinical environment there is a fixed regime that is followed in order to obtain reliable physiological signals, including ECG and EEG[39]. The method draws special attention to the skin/electrode preparation, electrode placement, sensing equipment and instrument operation.

The instruments used to monitor physiological signals are application specific and are designed to meet health and safety regulations [27]. The sensors used to detect the physiological parameter being monitored are also application specific. For example, silver/silver chloride adhesive electrodes are commonly used for ECG. Set procedures need to be followed in the setup and operation of all these instruments to ensure safety and accurate and reliable results.

Commercial electrodes such as those supplied by 3M^{TM}, Kendall, Conmed, HeartTrace and Leadlok are widely used for medical or hospital applications and are generally fabricated using highly conductive materials such as Ag-AgCl. The electrolyte gels have been reported to cause an allergic reaction in some individuals[40-42].

Another shortcoming with the use of gel is that while electrodes with gel may have improved electrical performance in the short term, the gel tends to dry, making the performance subject to time [43-45]. One of the requirements for the development of textile sensors is to remove the need for electrode gels which will allow continuous monitoring using a traditional textile garment.

Work reported in this thesis concentrates on the application of *dry fabric* electrodes where skin preparation and the use of chemical gels or adhesives are not required.

2.4 Methods for ECG Signal Characterisation

The ECG provides a visual insight into the condition and operation of the heart and its function. In order to use ECG as a measure of electrode comparison it is important to understand the ECG waveform and its important parameters. Most clinical information is found in the characteristic wave peaks and time durations (i.e. the amplitudes and intervals). These features and the changes from 'normal' ECG characteristics of a given subject/patient are used by clinicians in the diagnosis of heart related health conditions [39, 46].

Many signal processing techniques are presently used to improve the signal quality such as curve fitting. Chebyshev curves [47] and other polynomial approximations [47, 48] have been used to fit to portions of the raw or mean ECG such as the ST and PR intervals shown in Figure 5. These smooth curve approximations make feature extraction easier.

Another method for signal conditioning of ECG signal that is becoming more popular today, is to use wavelet transforms [49]. A wavelet is a windowed waveform that has similar characteristics to the waveform being studied. It requires the correlation of different 'scaled' versions of the wavelet with the original signal. The purpose is to enhance desired portions of the waveform, particularly the QRS complex and reduce the undesirable effects of either low frequency noise, high frequency noise or both, resulting in a smoother waveform. Considerable research has been reported on the use of wavelets for feature extraction and many different wavelets have been proposed [50, 51]. However, no one single wavelet has been agreed as being the most useful.

A high pass filter is often used (part of the Biopac ECG settings, see Appendix D) to limit the influence on the detected signals from 0 ~ 0.04Hz related to movement, .04~ 0.15Hz called mayer wave and 0.15~ 0.45 Hz, related to respiration. The effect and contributions of the components within these bands, on detected ECG signals for HRV have been studied[52, 53]. A 0.5Hz-35Hz bandpass filter is used to reduce DC artefact and high frequency noise. To discriminate between the signals measured with different electrodes it is necessary to compare the measured waveforms. For this purpose, the

commonly studied features of ECG need to be extracted. The 'typical' ECG signal has common characteristics and can be divided into four main sections.

P wave: depolarisation of atria

QRS complex: depolarisation of ventricles

T wave: ventricle repolarisation

U wave (usually masked by T): atria repolarisation

The heart beat period is defined as the time difference between two successive P waves, but as the signal to noise ratio of the P wave is lower than that of the larger and easily detectable QRS complex, the period of the complex or more generally RR interval is used. A 'normal' ECG waveform [54] with typical values is shown in Figure 5.

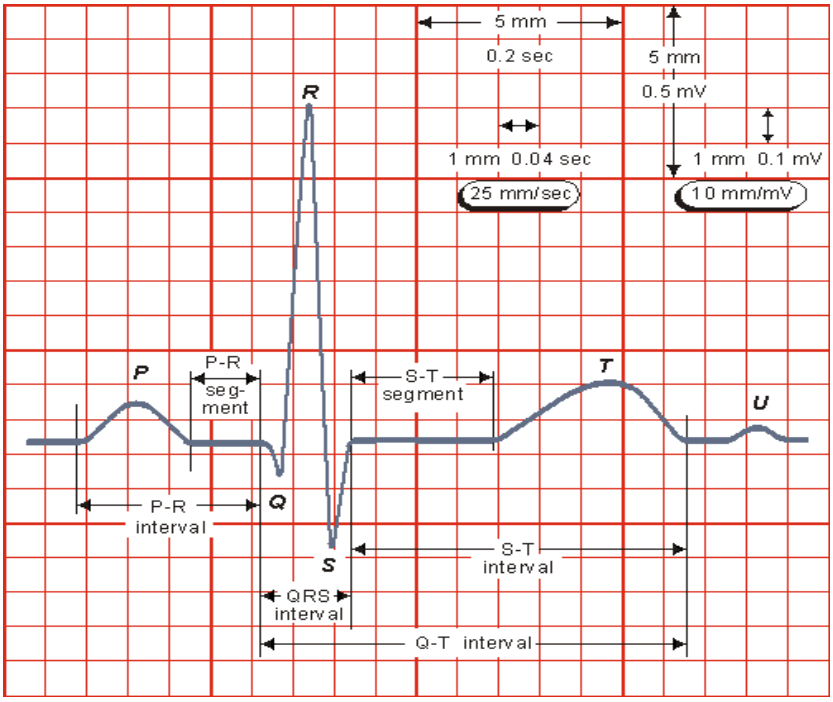

Figure 5. A 'Normal' ECG waveform, redrawn from [54].

2.4.1 Features of the ECG

Characteristics of the ECG waveform have been considered in many ways such as [55] where QRS interval and the R-T interval alone have been chosen for simple identification. A large number of attributes of the ECG waveform have been reported as important for the diagnosis of the condition and state of the heart [46]. No one single

set of attributes and ECG features has been agreed upon by those in the field, that provides a simplified and suitable measure. This is not surprising as ECG diagnosis has grown over a long period of time and is based upon the development of an empirical knowledge of the waveform data base and its interpretation. The state of the art suggests it is necessary to initially resolve and analyse fifteen major parameters of the ECG waveform. These aspects of the waveforms can be calculated and then compared and a reduced set of parameters selected for discussion. These parameters include, the height of the peaks P, Q, R, S and T and the length of intervals QRS, QT, PR, PQ, ST, peak intervals SR, RQ, TR, RP and RR.

An important characteristic of the ECG waveform is the QT interval. This is the time for both depolarisation and repolarisation of the ventricles to occur and is an estimate of the duration of an average ventricular action potential. QT interval varies with heart rate. QT intervals that are abnormally long or short have been shown to be associated with an increased risk of life threatening arrhythmias and sudden cardiac death [56, 57]. Considerable research has been done on attempting to accurately characterise the variation for diagnosis purposes. QT interval changes are normalised with respect to heart rate. The purpose of correction for heart rate is to get a 'standardised' value that would have been measured in the same subject if the heart rate was 60 BPM. There is large inter-subject variation of QT interval but it generally varies in a manner inversely proportional to heart rate [57]. Figure 6, shows typical QT interval variation in healthy adults.

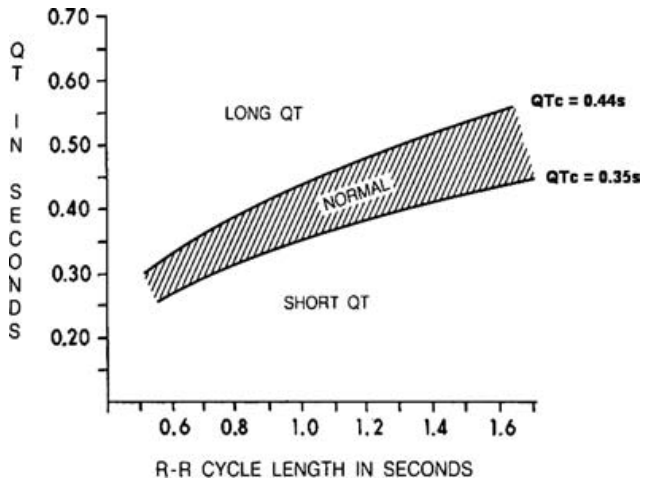

Figure 6. QT interval, upper and lower limits for different RR cycle lengths in healthy subjects (redrawn from [57]).

QT interval has been extensively studied in relation to cardiac diagnosis and the literature abounds with attempts to validate a particular approach in incorporating some method of correction for changes in QT caused by HR. QT hysteresis would need to be considered if dynamic testing was to be performed [58, 59]. This effect results in a time delay of about 2 minutes [60] between a change in RR and the QT interval stabilising at the new RR.

It has been also been reported [61], that the changes in characteristics of a 'normal' electrocardiograph, due to exercise are;

- P wave increases in height
- R wave decreases in height
- QT interval shortens and
- T wave decreases in height

As a result, any comparison of measurements on a single subject, other than at complete rest will result in an erroneous evaluation. To reduce the number of variables, dynamic ambulatory conditions (where the subject is moving), are not desirable during testing. Hence it is important to test subjects in a rest and controlled condition, to minimise rapid changes in RR during individual test sessions.

The use of a singular correction formula for the QT interval to enable accurate diagnosis is not ideal [62-64] because of the variations not only within an individual but between individuals. Many researchers [64, 65] have suggested that the ideal solution to arrive at precise heart corrected QT, is where each individual has a correction derived and optimised from their own ECGs, taken at different heart rates and conditions. Strategies have also been proposed to address this problem [66]. A normal QT correction range is from 0.2 to 0.4 seconds depending upon heart rate. It has been reported that this also varies with posture [67] and variations between male and female subjects have also been reported [68, 69].

Whilst the nominal interval values of the parameters listed above are similar between male and female, considerable variation of the parameters with cardiac cycle time was shown. This variation has been characterised [68] using different measures such as,

fitting each component of the ECG waveform to second order equations in the square root of the cardiac cycle time (T_{R-R}) of the form;

$$\mathbf{T_{(interval\ or\ segment)} = A\ (T_{R-R})^{1/2} + B\ T_{R-R} + C} \qquad \mathbf{(4)}$$

where

$T_{(interval\ or\ segment)}$ is the interval or segment time, (s), and,
A, B, C are constants dependant on the ECG component concerned
(e.g. ST segment, PQ interval) and whether subject is male or female.

The variation of a number of other parameters is also reported by [68]. These are listed below:

- ST segment and QRS duration remain constant with changes in RR.
- QT and PQ interval and T wave duration trend in the same manner with RR.
- P wave duration and PQ segment vary in the same manner with RR.

The trends of the components with RR [68], have not been reported by other researchers in the field and as the study population was small, it was decided not to place reliance on the characterisation.

2.4.2 HR based normalisation of QT segment

The study by Hekkala, showed that HRs of the same subjects at different times are not the same but were expected to be closer(CV 5%) within the same test session compared with separate sessions (CV of 10%) [70]. If same session RR variations are apparent, then in order to allow comparisons to be made between a subject's waveforms, QT values need to be corrected to allow it to be assessed independently of HR. Traditionally Bazett's [71] is the most popular and widely used formula in clinical practice, research and education for the correction of QT. Many other approaches such as Framingham, Hodges have been proposed for QT correction and used clinically [72] but there is no general consensus on the best formula to use for clinical practice [57, 58]. It has been suggested that the heart rate dependence of the QT interval over a wide RR may be best described by an exponential function, but that for the normal HR range

the QT-RR relation is approximately linear [57]. This is also supported by recent research [69], that suggested that the QT_C based on Hodges [73] linear formula see Equation 5, is far less correlated with HR than others studied and is generally more appropriate for broad populations.

$$\mathbf{QT_CH = QT + 105(1/RR-1)\ (Hodges)} \qquad \mathbf{(5)}$$

Hodge's correction has just been used in a coronary risk assessment study using a large population [74]. If heart rates are low, Framingham's may provide a lower correlation [69].

From the above, it is evident that there is no single solution to the correction of QT interval based on HR. It is perhaps best if the HR variation is reduced by the experimental protocol when possible.

2.5 E-Textile Biomedical Sensors

To date most research reported in the literature involves the incorporation of an assortment of sensors into 'garments'[6]. An overview of current developments in biomedical e-textiles is described in [75]. Most of the research is titled 'wearable' but although outcomes are indeed this, solutions are obtrusive. Sensors used range from large and small standard discrete types [76, 77], including discrete conductive elastomers types [78, 79], to carbon or silver loaded silicon rubber which are coated onto textile substrates [80, 81]. DeRossi [9, 10, 82] describes the use of carbon loaded rubber(CLR) and polypyrrole(PPY) coated fabrics to add piezo-resistive properties to garments that are used to monitor respire trace (RT) or movement and conductive fabrics (made from steel threads, acrylic and cotton) used as electrodes to detect ECG. However there are inherent limitations with these sensors eg the CLR sensors have a relatively long response time(seconds) to mechanical stimulus [10], when compared with conventional strain sensors. Repeatability of these sensors is poor and this is undesirable if accurate representation of the physiological signals is to be achieved. To overcome the response/ relaxation time limitations of these sensors, post processing algorithms have been described to derive the causal signal waveform [83].

New methods for the clinical monitoring of physiological parameters have taken the physical form of a shirt(SmartShirt^{TM}) [84]and vest(LifeShirt ^{TM} [11]), or even a loose fitting bodysuit(Hokie) [85]. Many research institutes worldwide are actively involved in the area of garment based health monitoring including: MIT [86], Georgia Tech [87], Philips [88], Infineon Technologies (now InteractiveWear) [89], Fraunhoffer Institute [90], ETH Wearable Computing Laboratory [91], Smart WearLab – Tamper University of Technology, and, MyHeart (WEALTHY) [92]. The emphasis has been placed on replacing the traditional methods of acquiring physiological signals based on direct contact stick on silver/silver chloride electrodes. The aim is to replicate the traditional physiological monitoring techniques with low contact resistance methods. It should be noted however that in all solutions so far reported, Lorigo et al [93], an electrolyte (usually a gel) is applied over the electrode area to enhance the electrode's electrical performance. An example of a fabric electrode with gel by Fraunhofer IZM [94] is shown in Figure 7.

Figure 7. Embroidered circular electrode with solid gel covering for better skin contact (redrawn from [94])

It has been acknowledged that a key challenge is the removal of the membrane which would allow very long term monitoring [95].

2.5.1 The Conductive Yarn Electrode

As the aim of this research is fabric sensors, it is fundamental in a first approach, that yarns that comprise everyday textile apparel be the basic building block of the research. Building on the present methods used to measure ECG, emulation of a simple contact electrode in a fabric form is the first need.

In order to provide the basic requirement of a contact electrode i.e. conductivity, a conductive yarn is required to be used. Conductive yarns have been used commercially for at least two decades in the field of electrostatic or ESD protection in the electronics industry. (The human body can accumulate electrostatic charge amounting to tens of thousands of volts which if discharged into electronics/devices can cause immediate and/or long term damage and performance degradation.) These yarns have been woven into fabrics used to make overclothes e.g. laboratory coats, overalls and the like. These have afforded protection to sensitive electronics by providing a high impedance discharge path for any built up or accumulated electrostatic charge. These yarns have generally been made from low cost carbon based materials, as only relatively high resistances are needed. The conductivity of these yarns is in the order of a thousand ohms/meter and would not be suitable for a low conductivity application such as this. However due to the ever increasing noisy

electrical environment that the world presents there has been the ongoing need for electrical protection in the form of shielding. In this regard, fine conductive fibres initially from stainless steel were developed to allow shield materials such as screens and gaskets to be fabricated to protect sensitive electronics from the effects of electromagnetic emissions. Since then other conductive fibres/yarns have been developed, Bekaert being one of the first commercial manufacturers of different materials [96].

A wide selection of electrically conductive fibres and yarns is now becoming available. To determine suitability for use in an electrode, a detailed analysis of their characteristics is required. These will include conductivity, continuous or multifilament, size of fibres, length of fibres, size of yarn, knittability or weavability, density of needles. Conductivity is important and recent research by Mirtaheri [97] related to the application of biomedical electrodes has shown interesting differences between the most commonly used metals. Mirtaheri shows that the polarisation resistance of all metals reduces with increasing frequency from the DC value and stainless steel has a significantly higher value than other metals at DC. This may result in poorer signal performance for stainless steel when considering the electrode/skin electrical model.

Common conductive yarns commercially available today are made by numerous manufacturers and include;

- Silver coated nylon from Shieldex Trading [98].
- Stainless steel yarn from R Stat [99]
- Silver coated copper from Elektrisola [100]

In order to test the suitability of any of these yarns for the sensing of ECG signals it was proposed to fabricate, in fabric form, a range of electrodes made of these conductive yarns.

The conductive yarns used to date in previous work at the CSIRO Division of Textile and Fibre Technology (CSIRO TFT) which have proven the most successful are silver coated nylon. Two fold yarns (two singles yarns twisted together) made of nylon coated silver have been successfully sewn and knitted into textile materials (at TFT).

Whilst stainless steel has been knitted into fabrics as well, the practical fabrication and knitting of these into a structure has proved more difficult than the silver coated nylon yarn.

Practical implementations of some aspects of the sensor garment may require insulated conductors to prevent inadvertent connections. Insulation of conductors may be provided by the physical separation of conductive yarns via the design and construction of a garment. This may also be able to be achieved by the application (sizing) of a suitable and flexible insulating layer of polymer over the surface of the yarn. Sizing of the yarn is a textile term given to the process of applying a coating to the surface of a fibre or yarn. Polymers could be designed [101] that could readily be removed in a selective manner (screen printing of a form) or dissolving, without damaging the based garment fabric. This would allow electrical connection to be made with the conductive fibre core.

2.5.2 Skin-Fabric Electrode Contact within a Biomedical Sensor Garment

Use of a conductive electrolyte gel to enhance the contact resistance is not desirable. The detection of signals therefore must be done with inherently higher contact impedance.

It has been suggested [38] that contact electrodes without a conducting gel work in either of two modes. That is either capacitive or resistive based on any surface conductive electrolyte, such as natural perspiration. For practical measurements it has been suggested that electrode impedances less than 100kohm are required. For capacitive detection an electrode capacitance of about 100nF is required. In order to maximise the detected signal and minimise the effects of coupled, power line interference (50Hz), a major contributor to overload and measurement errors, dry and insulating electrodes are rarely used without buffering [102]. With simple buffering, that is, using an amplifier of unity gain, the effective electrode impedance present can be reduced, resulting in reduced differential mode interference voltages [43, 103, 104]. If necessary, electrode-skin imbalances can be simply and directly measured [105].

Common mode electrical interference can become differential mode if contact impedances are not low or are unequal or there is an imbalance in amplifier input impedance (very small with current amplifier technology). The common mode voltage detected at + and – electrodes will appear as a differential mode signal if the electrode resistances Rea/Reb and input amplifier resistances Ria/Rib, are not the same for each input. This effect is shown in Figure 8.

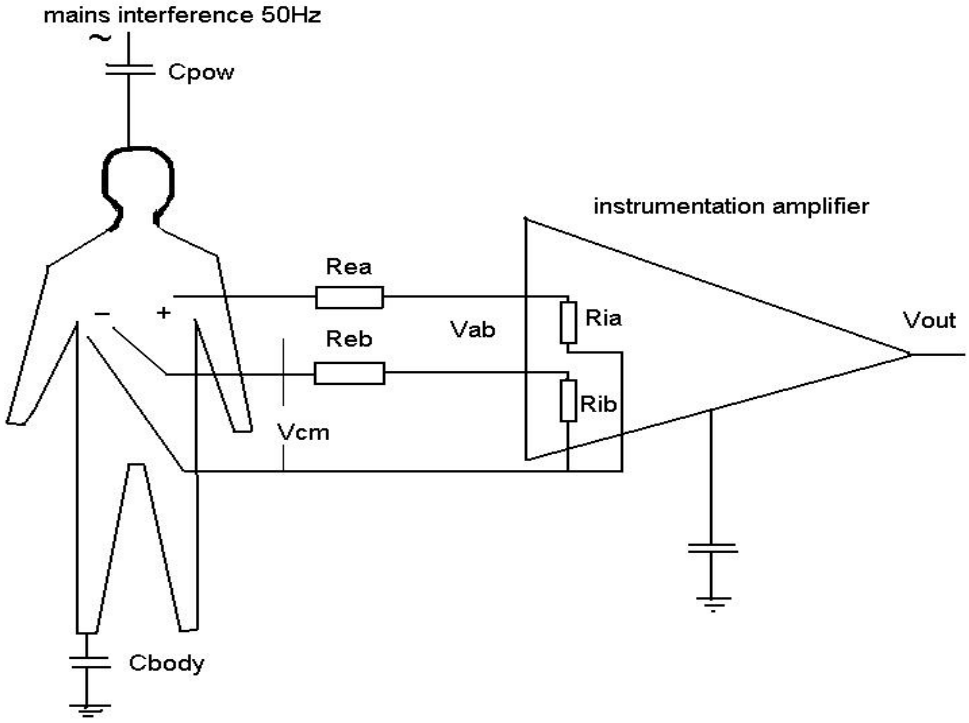

Figure 8. Common mode voltage induction from mains interference and the resulting differential voltage generation from electrode resistance imbalance.

The differential mode interference voltage is given by;

$$\mathbf{Vab = Vcm\ [\ Ria / (Ria + Rea) - Rib / (Rib + Reb)]} \qquad \mathbf{(6)}$$

and $$\mathbf{Vout = Av \times Vab} \qquad \mathbf{(7)}$$

where,

Vout, is the output signal from the amplifier (volts),

Av, is the amplifier voltage gain (a constant),

Vab, is the differential interference voltage (volts),

Vcm, is the common mode voltage (volts),

Ria/Rib, is the input resistance of amplifier input (ohms),

Rea/Reb, is the electrode resistance of each (ohms),

C_{body} , is the human body capacitance to ground (~ 100-300pF[103]),

C_{pow} ,the human body capacitance to ambient mains sources (~ 10-30pF[103]).

In the model above (Figure 8) the resistances may in fact be impedances (i.e. have a frequency dependence) and Z can simply replace R in the formula. If Z is used as the characteristic symbol for electrode impedances and common-mode impedances, then the common mode rejection ratio (CMRR) can be calculated.

The CMRR (e.g. 50Hz signal) is the ratio of the differential signal component to the common mode component causing it. Assuming the common-mode impedance at the amplifier terminals is Z_c +/- Δ_c Z_c and the electrode impedance is Z_e +/- Δ_e Z_e

$$\mathbf{CMRR_{\Delta Z} = 20\log_{10}[Z_c/Z_e]+20\log_{10}[(1-\Delta^2_c)/2(\Delta_c+\Delta_e)} \qquad \mathbf{(8)}$$

Where,

Z_c , is the common mode input impedance of the amplifier,

Z_e , is the electrode impedance,

Δ_c , is the common-mode impedance difference,

Δ_e , is the electrode impedance difference,

$CMRR_{\Delta Z}$, is the common mode rejection ratio due to change in Z.

The CMRR depends not only on the magnitude of Ri in relation to Re, but also the degree of variation in these resistances.
If Z_c = 60 Z_e and the change in Z_e and Z_c are within 10%, then $CMRR_{\Delta Z} \approx$ 44dB, well below that required to suppress common mode interference [106].

The skin-electrode interface itself involves a range of complex physical and chemical interactions and has been widely studied [107-109]. A simplified equivalent electrical model for the skin electrode interface [106] with values is shown in Figure 9.

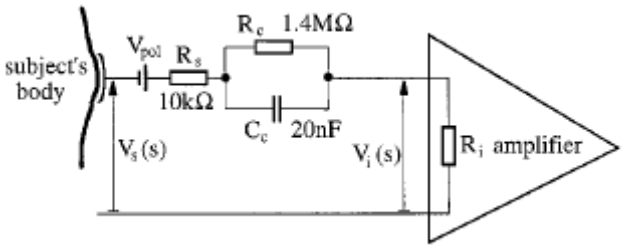

Figure 9. Burke model of the skin electrode interface with typical values(redrawn from [106]).

Where

R_s , is the minimum series contact resistance (ohms),

C_c , is the coupling capacitance (farad),

R_c , is the coupling resistance (ohms),

V_s , is the voltage (volts), detected at the skin and

V_{POL}, is the DC polarisation potential (volts), at the skin electrode interface.

Other researchers in recent times [110] have used the same model and arrived at different values, where R_s = 300Ω, R_c = 450kΩ and C_c = 3nF.

It has been shown that compared with the commonly used Ag/AgCl wet electrodes, a dry stainless electrode has twice an order of magnitude increase in a 50Hz interference signal [43]. A mismatch of electrodes types e.g. the wet and dry resulting in a large contact impedance mismatch, causes a further order of magnitude increase in interference. The work by Searle and Kirkup [43] has shown that the contact impedance (at 50Hz) for a selection of dry conductive electrodes; stainless steel, titanium, aluminium and Red Dot™ 2258, begins in the Meg ohm region and decreases exponentially with time. Clinical electrodes are not re-useable and can cause skin irritation if worn for extended periods (normally much less than 48 hours). Impedance values below 1 MΩ are not reached until a few minutes after application. Values of impedance indicated by 3M for a typical large area (10cm^2) Red Dot repositionable electrode are of the order of 50Kohms. However, it has been observed [111] that through improved electronic conditioning, higher electrode to skin surface resistances can be tolerated facilitating the acquisition of quite acceptable signals.

2.5.3 Skin Microclimate

Humidity within the area of the electrode contact may play a part in both the initial contact resistance and that measured after a period of time. It has been reported [17], that gels placed on the skin can take a considerable time to be fully absorbed into the skin and that this directly effects the resultant conductivity of the skin. Humidity also plays a role as in dry environments the outer layers of the stratum corneum have the lowest water content and hence are not highly conductive. The level of hydration at the skin's surface is normally low to very low. Dry skin is not conductive due to the nonconductive nature and chemical composition of dead skins. However water absorbed into the skin provides the mechanism for ionic conduction. Sweat ducts provide an additional mechanism, as presence of sweat provides an improved conductive medium.

Tagami [112] and later Yamamoto [23] have shown and quantified the effect of hydration and skin admittance. Skin admittance is proportional to the level of inherent hydration and low-frequency susceptance measurements are reported as the correct determinant of skin hydration [113]. Others researchers suggest that a high frequency range is better [114]. It is agreed that characterisation requires multi-frequency analysis but over what range is unclear. The value of skin admittance varies greatly between individuals and even more significant differences have been found between races [79]. It has been described that after initial application of electrodes to the skin's surface, there is a rapid increase in the value of skin admittance. This however has been observed electrodes of a solid metallic nature [43].

2.5.4 Movement, Skin Potentials and Sweat

Other considerations related to contact are the presence of movement artefacts generated by the body and physical movement. This skin fabric/electrode interface is a dynamic environment further complicated by the hyperelastic behaviour of the skin which varies between individuals. Motion artefact is the noise on the ECG or any biosignal. This results from motion of the electrode over the skin's surface, including relative movement between subcutaneous layers and can produce large amplitude changes in any measured biosignals. Traditional electrolyte gels due to their adhesive nature minimise the effect of movement of the electrodes and limit the size of the

resulting signal artefacts. ‘The skin potential artefact (also known as skin-stretch or skin-motion) arises from the change in voltage between the inner and outer layers of the skin under deformation. Skin movement can produce a change in potential at the skin surface of several millivolts [43]. Past research into effects on electrodes by Searle et al [43] and temperature by Cornish et al [115], has shown that reduction in impedance with time is likely the result of perspiration on the skin surface where the electrodes are placed. This also results in a reduction in artefact due to less effective movement between the electrode and the skin surface [116, 117]. This study [117] shows that fabric to skin friction for dry skin increases 50% from 10 to 90% RH and up to 200% when wet. Similarly, another study reveals that, the static friction μ_s , between ‘normal’ skin in vivo and wool is 0.4 and increases by 40% with hydration [118].

This mechanical interaction at the skin-electrode interface is a useful feature that will be considered further with investigations into the design of practical garments. Taking this into account it was decided that any testing needs to consider the effects of time on the measured contact impedance, in that equilibration of value may take some time. Movement may also change electrode pressure which may result in a change in detected signal. Other researchers have mentioned this problem [81] but have not quantified it in any way. Conditioning algorithms may need to take this aspect into account if practical results show this to be true. Buffering of the signal at the sensor electrode may be required in practice as has been indicated in the literature [43] if the sensed signal is unusable for analysis.

The study described in [43] shows a positive effect of sweat but may exaggerate the positive effect of perspiration in a practical situation due to the experimental setup of the electrodes as these were all mounted together on a plastic plate. Total occlusion of the skin with a sealed membrane may induce excessive sweating. The results from this study do show that ‘dry’ electrodes seem to perform comparable to or better than wet electrodes. For long term monitoring this is of particular importance as the wet electrodes performance related to motion artefact degrades over time [43, 45].

A model used in a study that includes the sweat/perspiration element is shown in Figure 10. Electrical equivalent circuit of combined skin-electrode contact is redrawn from [79].

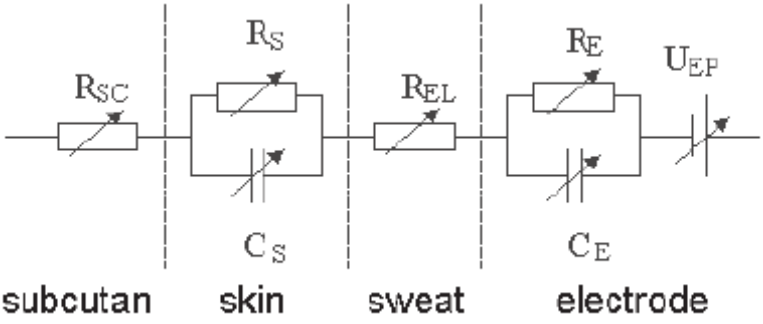

Figure 10. Electrical equivalent circuit of combined skin-electrode contact

The impedance Z of this equivalent circuit is given by:

$$Z = R_{SC} + \frac{R_S}{1 + j\omega R_S C_S} + R_{EL} + \frac{R_E}{1 + j\omega R_E C_E} \qquad \textbf{(9)}$$

where

R_S, is the surface skin resistance (ohms),

R_E, is the electrode resistance (ohms),

R_{EL}, is the resistance of sweat (ohms),

C_S, is the surface skin capacitance (farad),

C_E, is the electrode capacitance (farad).

Here the sweat element is modelled as a pure resistance but no correlation was made between the model and measured results although possible values have been given as $R_{SC} + R_{EL} = 8k\Omega$, $R_S = 140k\Omega$, $C_S = 3uF$, $R_E = 150k\Omega$, $C_E = 180nF$

Results from this study and other studies however highlight the difficulty in quantifying in absolute terms an accurate skin-electrode model.

2.5.5 Conductive Electrode Contact Pressure

It is apparent that the contact resistance between the skin and dry sensor electrode (in the absence of any electrolyte) is a function not only of the nature of the conductive sense area i.e. the conductive medium, but also, of the surface area and applied pressure. The amount of pressure required to achieve an acceptable contact resistance to allow 'useful' signals to be obtained has not been reported and is unknown. Researchers have mentioned greater pressure reduces skin electrode impedance [79, 106, 119] but only one researcher [110] has performed skin electrode tests in which he states that 'firm electrode-skin contact is of primary importance' and actually tests with a single pressure value. It has been shown [120] that clothing pressure is dependant on fabric extensibility stretch level and curvature of the skin surface. Skin comfort perception is related to a range of parameters [121] including clothing pressure so it is desirable to minimise the pressure applied by a garment on the wearer. The perceived pressure is different for different people and may be related to Body Mass Index(BMI) [120, 121].

Miyatsuji [122] reported that high clothing pressure (above 2.5KPa) applied to the human body, adversely affects the physiological homeostatic mechanisms through altering the autonomic nervous system, a co-ordinator of internal environment in the human body. Miyatsuji suggests that clothing pressures of 1.5KPa have less affect and are preferred.

2.5.6 Fabric Electrodes, Physical Compatibility with the Human Body

As described previously any practical fabric electrode must not only allow detection of physiological parameters but be unobtrusive and easy to wear. When worn against the skin surface it has been shown that fibres that protrude out from a fabric surface of diameter larger than about 30 microns will cause unacceptable prickle [123]. Fibres around 20 microns or less in diameter offer good comfort. Hence any multifilament yarn, whether constructed from short or continuos filaments of 'large' diameter (>30 microns), may cause irritation and thus be inappropriate for use against the skin. Yarns constructed from stainless steel yarns may fall into this category. However the silver coated nylon yarns, which comprise smaller continuous fibres, seem to be more

appropriate. Receptors at the skin surface are responsible for the perception of ‘prickle’ but once over stimulated can become ‘immune’ and the prickle effect becomes less apparent. Perhaps this can be exploited in allowing more prickly electrodes that may provide a better contact with the skins surface, but still be acceptable to the user. Yarns made from continuous fibres generally result in less hairy yarn which tend to exhibit less prickle.

The aim of this research is fabric electrodes and the research on prickle [123] based on textile fibres indicates that prickle needs to be considered further in developing electrodes that are not only acceptable, but comfortable for the human user to wear.

2.6 Wearable Technologies - where are they now?

By default most wearable technologies presented in the literature by their very nature are wireless and in all implementations the devices are discrete and generally miniaturised in some form.

The research undertaken at MIT, involves the application of wireless unobtrusive sensors to sense body parameters. A wireless sensor in the shape of a ring has been developed by MIT d'Arbeloff Laboratory for Information Systems and Technology [124, 125] for continuously monitoring a patient's heart rate and oxygen concentration.

Wearable sensor electrodes resembling bandages have been developed by NASA's Jet Propulsion Laboratory, Pasadena, California [126]. These sensors are powered briefly and interrogated by a local hand held transceiver. Similarly miniature sensors less than a cubic millimetre in size are being developed in the SMART DUST project at Berkeley University [127].

A consortium called 'WEALTHY' [82] was established in the European economic union in 2002 to research a wearable health care system. The 'wealthy' system used a fabric vest type garment embedded with biosensors to detect ECG and respiration with knitted conductive electrodes and a strain sensor respectively. It was reported in outcomes of this 'WEALTHY' research in 2005/2006 that the fabric electrodes used, also required the use of a conductive gel or gel layer to reduce the undesirable effects of motion artefact. A recent report in the literature [128], states that 'to improve the electrical signal quality in dynamic conditions the electrodes have been wet'.

Tampere University of Technology's, Institute of Electronics has reported work on smart clothing [129], where a bioimpedance measurement system was used to determine total body water (TBW). This research was aimed at determining whether a bioimpedance measuring system could be integrated into clothing and reliable impedance measurements taken to establish if TBW could be determined. The method of sensing uses conductive fabric electrodes attached to clothing with clip fasteners.

The research methods that were reported were not rigorous and the resulting measurements only indicated a trend of total body water with time.

2.6.1 Commercial Products.

Many commercial products that are in development include:

Smart Shirt [87] by Sensatex Inc [84]. This system is designed as an under shirt embedded with various sensors that records heart rate , body temperature, motion, position and barrier penetration etc. This comprises a complex arrangement of optical fibres and data buses to achieve the desired functionality.

The LifeShirt ^{TM} by Vivometrics [11], which is described as a 'comfortable' garment embedded with a range of sensors to monitor physiological signs of sickness and health.

SenseWear^{TM} Pro Armband [130] by BodyMedia Inc. shaped like a cuff that can be worn on the upper arm and has embedded sensors that allow monitoring of movement, skin temperature, heart rate, heat flow, near body ambient temperature and galvanic skin response to be monitored.

Polar [131] also produce a range of sensing products that rely on the integration of discrete sensors into belts, straps or bra type garments for the monitoring of numerous body parameters. A range is also produced for equines based on the same measurement principles.

The commercial systems generally include a central processing and logging unit to collect the sensor data and a transmitter to send it, usually wirelessly, to a remote device for further action.

The predominant trend in most research reported and commercial products to date has been the incorporation of a range of small discrete sensors or sensing elements within a shirt like garment. However very little has been presented that addresses the specific method of sensing parameters using only fabrics or textiles based integrated sensors.

Chapter 3

3 Preliminary Investigation and Method Development Strategy

The diagram of the relationship between elements within the physical measurement system is shown in Figure 11.

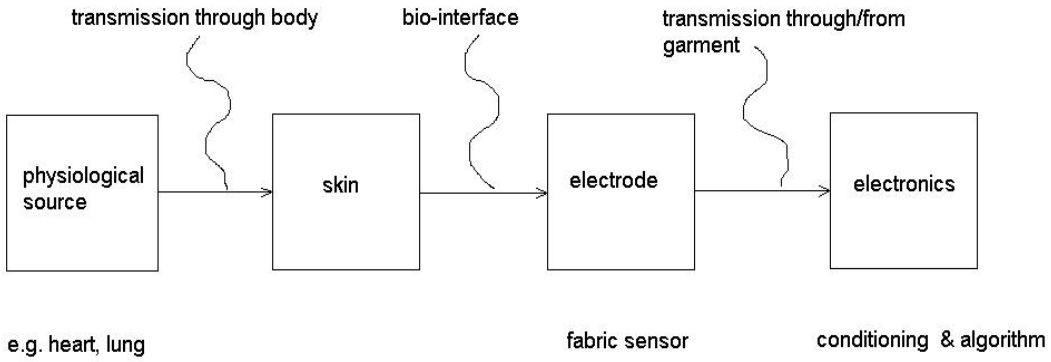

Figure 11. The measurement environment for physiological sensing.

Each aspect of the physiological sensing system is discussed in the following sections. This includes specific requirements of the electronics and instrumentation, fabric electrodes as sensors, measurements on the skin and finally physiological measurements of ECG and respiration.

Ethics approval for the experiments was obtained from the RMIT University Human Ethics Committee.

Participants were made aware of the nature and details of the experiments and were informed that they could stop the experiments at any time. Each participant completed the approved consent forms before the experiments began.

Experiments were conducted on male participants assumed to be of reasonable general health having no specific known heart conditions. Preliminary experiments were conducted on a single volunteer subject to develop test procedures and validate measurement setups. Indicative preliminary measurements helped to highlight limitations and the effectiveness of test strategies.

After the test methodology had been confirmed the experiments were conducted on 10 male volunteer participants.

3.1 Electronic Acquisition Tools and Measurements

3.1.1 Electrode Electronic Conditioning

Signals such as ECG are conditioned, via high input impedance circuits (10M-100Mohm) which need high common mode rejection at low frequencies due to the pickup by the body of 50 Hz signals (inherent in the environment). These signals can be of the order of 10VRMS, due to the human body's inherent capacitance to ground and the 50Hz source of 10pF-100pF (see Figure 8). Filtering of this 50Hz signal with a notch filter is generally also required as this may also appear as a differential mode signal. A bandpass filter is also generally required from 0.1Hz -50Hz, to allow the complete heart signal to be amplified. The AC coupling also eliminates the resistive component of motion artefact.

Commercial biomedical instrumentation that meet specified safety requirements are used in this research for all measurements on the body. Specifications for the instruments used are shown in Appendix D.

3.1.2 Instrumentation

To help determine the initial feasibility of detecting the ECG signal, a short series of initial tests were performed. These were conducted using a portable commercially available Electrocardiograph (ECG) acquisition system called 'QRS Card' from Pulse Biomedical Inc (Figure 12). A description and specification for this instrument are detailed in the Appendix D. The QRS Card hardware was configured and controlled via the laptop running the QRS Card software and was used to monitor, display and save the heart signal waveforms. The laptop was running on its internal battery so that measurements were electrically isolated from the mains voltage.

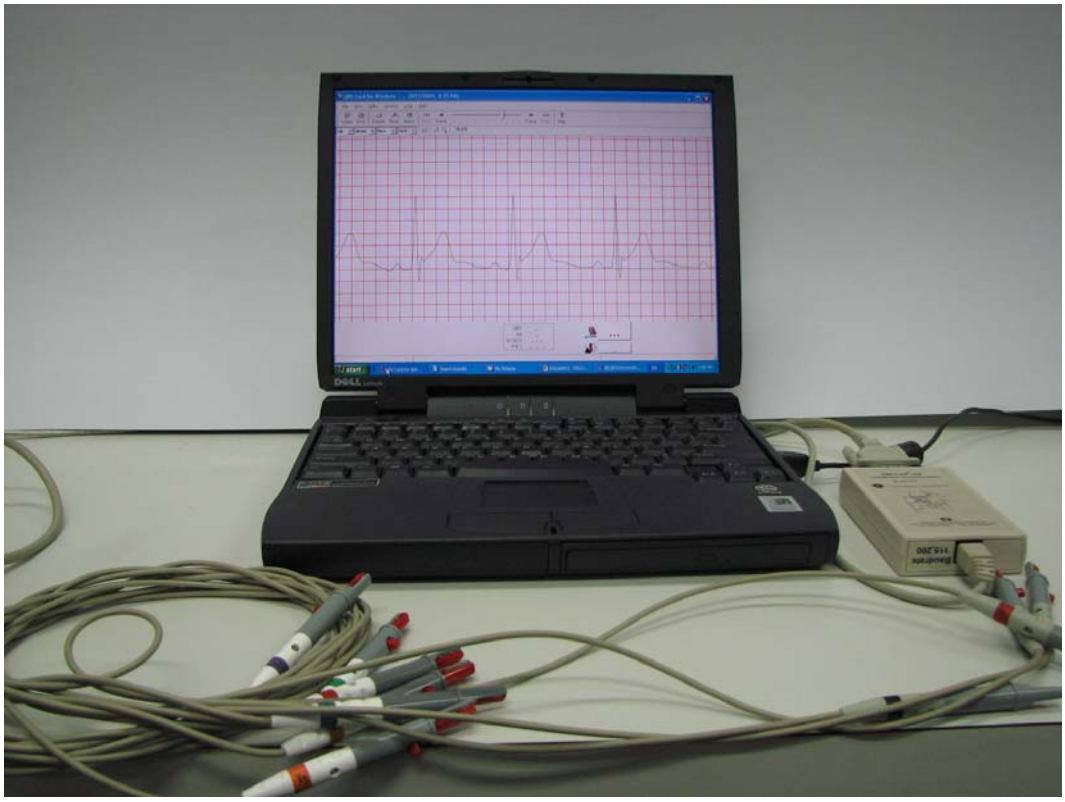

Figure 12. QRS Acquisition system, laptop and RS232 acquisition pod.

To measure GSR a commercial instrument from Autogenic Systems AT64 SCR meter was used initially (Figure 13). Although this displayed values of SCL and/or SCR it did not permit direct logging of the measurement (e.g. by a laptop computer). The pressure meter used initially to display force values from the sensors is also shown in Figure 13.

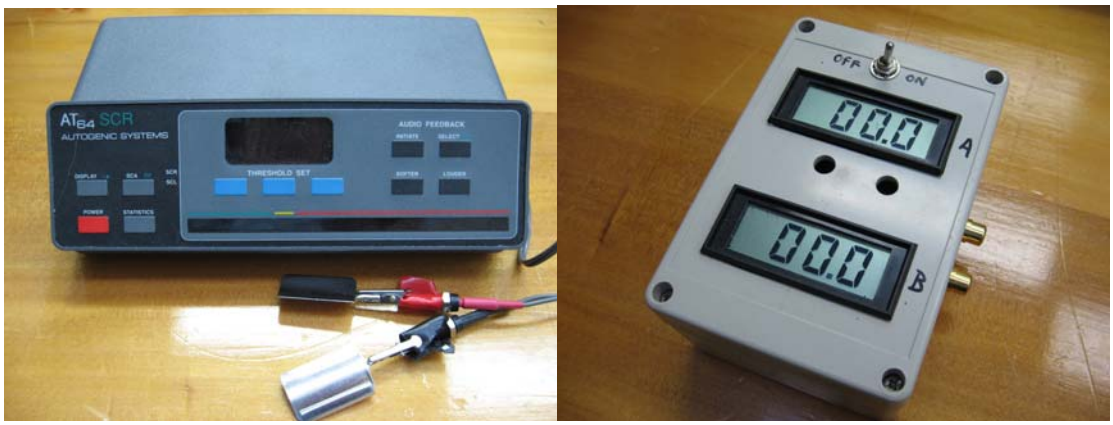

Figure 13 SCL/SCR meter used initially for GSR tests (left) and Pressure meter (right).

This equipment though good as stand alone instruments for ECG and GSR measurements, did not allow the easy automation or acquisition of other externally derived biosignals. Signals from other specially built sensors, such as strain and pressure sensors also needed to be measured. To allow simultaneous acquisition of a range of signals, including analog ones (e.g. from respiration sensors), a Bipoac system was obtained (Figure 14). This was connected by a universal serial bus cable to a laptop computer that controls and receives acquisition data from the Biopac interface. Biopac system software called AcqKnowledge version 3.8.2 was used for measurements.

Figure 14 Bipoac system hardware used for GSR and ECG tests.

The Biopac system can be configured (dependant on the modules chosen) to measure every conceivable biosignal, including analog voltages. It provides simultaneous acquisition of all these signals and allows the measured biosignals to be synchronised in time. The specification for the Biopac system used is given in Appendix D. All electronic conditioning circuits were powered from the Biopac +/- 12V, 5V outputs to ensure galvanic isolation from the mains voltage.

3.2 Garment Design Concepts

The textile structure used in this study needs to possess a number of specific attributes to enable it to meet performance and practical needs and ideally would:

- enable one size fits all, i.e. be adjustable over a reasonable size range
- have the ability to provide controlled contact pressure
- enable construction using common textile processing methods
- allow accurate placement of electrodes on the body
- allow comfortable fit and be unobtrusive to wear

These attributes depend not only on characteristics of the materials used but on how these can be incorporated seamlessly into a functional garment. To fulfil these requirements within a single garment is a challenging problem.

3.2.1 Garment Construction

Textile garments can be fabricated using woven, non-woven or knitting technology.

Weaving uses a continuous fibre or yarn to produce a continuous planar textile structure. The fabrication of a garment from a woven fabric is achieved by the traditional cut and sew method. To add conductive areas, pieces of conductive material would need to be sewn into or onto the base fabric. Mechanical stability is based on the regular interweaving of yarns in the two directions (warp and weft) of the fabric. These fabrics generally, do not allow garments to be produced which are as flexible or as form fitting as knitted garments [132].

Non woven textiles are formed by an arrangement of short length fibres and have a matted structure. Mechanical stability within the fabric is afforded due to the entangled nature of the construction. These textiles are stiffer and less conformable than woven

textiles and not widely used in apparel, hence were not considered for this application [132].

Knitting is used to construct textile garments (apparel) because it provides solutions which are mechanically flexible and may be loose fitting or conformable. They can be made from a large variety of natural or man made yarns or fibres. Knitting technology is comprehensively described by Spencer [133].

Knitting, a well established and widely used technique was used to fabricate the first trial, tube like vests at the Commonwealth Scientific Industrial Research Organisation's Division of Textile & Fibre Technology (CSIRO TFT). The first prototypes using knitting technology incorporating specific areas with conductive electrodes is shown in Figure 15.

Although not a practical garment as it was not form fitting which would provide pressure on the electrode area and electrode placement was arbitrary, it did demonstrate that typical conductive yarns can be knitted into complex structures. Electrodes can be placed within most areas of such a garment but connection of these electrodes to a common site (for connection to conditioning electronics) within the garment is difficult.

Figure 15 First knitted vests with conductive electrodes for ECG measurements (inside view).

The foundation yarn used was wool/lycra to provide some elasticity. (Lycra, a DuPont product, is an elastomeric fibre with stretch and recovery abilities and is commonly used to add stretch and comfort to clothing.) However the garment was found to be inadequate as it could not provide a consistent pressure between subjects.

Conductive fabric electrodes can be fabricated using the methods described above, but for purposes of detailed study, it is not yet feasible to test a range of different types of electrodes in a full garment form. Conductive electrodes can be added to a garment by the cut-n-sew method in which an electrode is cut from a piece of conductive fabric and sewn onto a foundation garment, e.g. a Tshirt. Two problems with this method were apparent. However it is difficult to make electrical connection to the electrodes and the pressure applied was uncontrollable.

It was decided to use the knitting method to make bands which incorporated conductive electrodes. These fabricated circular bands when applied around the torso could be easily removed and repositioned to allow different configurations.

To enable these electrodes to be tested, a section of each band including the electrode was cut out and sewn into an elastic/Velcro band to allow fitment on any size subject. The elasticity also allowed pressure to be adjusted. In the knitting process, tails of conductive yarn were left which extended from the conductive electrode area. This allowed easy connection of the electrode to a snap fastener which could then be connected to the measuring instruments.

3.3 'Real' Conductive Fabric Electrodes

A number of preliminary test electrodes were constructed from a range of different conductive yarns so as to test the initial viability of sensing heart function with fabric electrodes formed from conductive yarns in a knit structure. Silver coated nylon, stainless steel and silver coated copper yarns were first tested. All yarns were knitted as patches on a Shima Seiki SES-SWG 3D knitting machine into conductive electrodes within a textile fabric at CSIRO TFT. The silver coated copper (monofilament) yarn did have practical problems due to it's reduced mechanical flexibility and brittleness when compared with silver coated nylon (AgN) and stainless steel and although difficult to knit was considered adequate for further test use. The stainless, a multifilament yarn, did however present more problems than did the silver.

Samples of silver and stainless conductive electrodes were initially tested for conductivity on the skin with a multimeter (measuring ohms). Both provided similar values in the 1- 10-20 Megohm region. The readings obtained varied considerably with time and with the amount of contact pressure applied to the electrode area. These results indicated, as described earlier, that a certain amount of controlled pressure over the contact area of the electrodes would be necessary to help reduce the contact resistance and aid in detection of stable signals. In the case of fabric electrodes, applying pressure to the contact area also results in an increase in the actual conductive contact area between the skin and electrode as the loops of conductive yarn flatten. Fabric electrodes have a non uniform surface and have fibres protruding from the surface. A diagram displaying these features is shown in Figure 16. Dependant on electrode fabrication, they may be bulky and hairy or relatively smooth with small protruding fibres. Bulky electrodes or ones constructed with a coarse knit are generally more compressible and will have a more pronounced variation of skin-electrode impedance with pressure when compared to smooth and densely knitted ones which have a low level of compressibility.

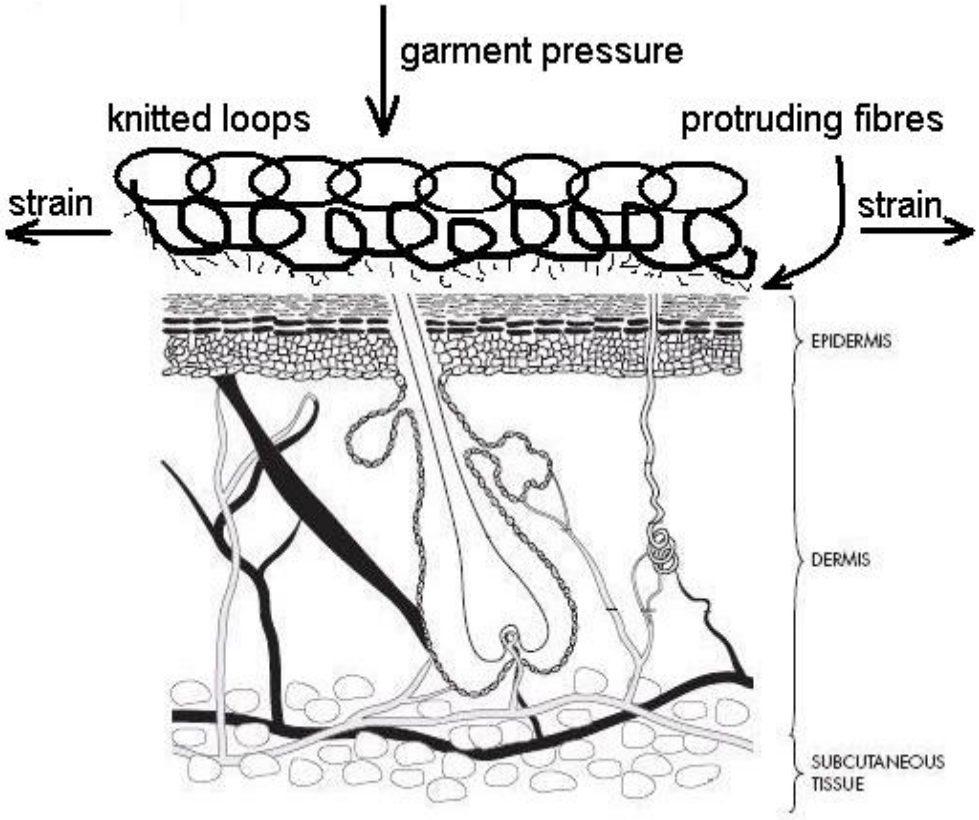

Figure 16. Mechanical interaction of a fabric electrode with the skin.

The observed decrease in resistance value with increased pressure involved a number of variables. The electrode to skin surface contact resistance is reduced, the skin layers immediately under the contact area are also compressed and perhaps there is a better contact (conduction path) from the skin's surface through the stratum corneum /epidermis and dermis layers, along these layers parallel to the surface and then back through the dermis/epidermis/stratum corneum layers to the other electrode. An appropriate model to describe this effect needs to be developed but is beyond the scope of this research.

In its simplest form, the skin/electrode contact model can be reduced to one of a complex impedance, comprising a resistor and capacitor in parallel. Other models also without the effects of pressure have been described in the literature and most are similar to that of Cole [134]. Detection of any signals (the heart can generate voltages in the order of 1-5mV on the skin surface under ideal conditions) under these circumstances, relies upon the sensing of a very low current through the SC. The heart

signal source appears like a current source, i.e. a voltage source connected via a high impedance. Detection of this low level current is easily done with current amplifiers generally configured as instrumentation amplifiers in order to amplify the differential signal. Even though these may have input impedances in the order of 100Mohm, considerable reduction in signal sensitivity can be expected if the contact impedance is less than an order of magnitude below this, i.e. if it is greater than 10Mohm. As a result, testing was conducted with the silver and stainless electrodes to determine their effectiveness to detect heart beat.

3.3.1 Conductive Electrode Materials for ECG

Ag/N and stainless steel yarns both have advantages and disadvantages as conductive electrodes. Stainless steel yarns are comprised of many strands of fine stainless steel filament spun together. Monofilament stainless fibres in themselves generally cannot be practically fabricated into an electrode due to the stiffness and brittleness of the single filament. AgN or other conductive multifilament yarns being inherently more flexible were used. A silver coated copper yarn was also included for testing.

The materials mentioned above were knitted into electrode form (in knitted bands). These are shown in Figure 17 and Figure 18.

Figure 17. Knitted electrodes on loose knitted band (used for first single trials), left to right; Silver Copper, Stainless steel and Silver Nylon.

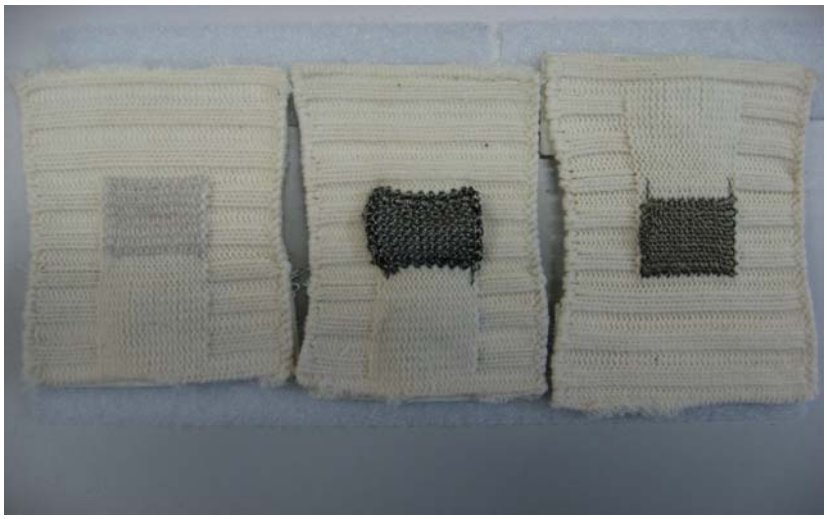

Figure 18. Actual knitted removable electrode assemblies, used for multiple trials, left to right; Silver copper, Stainless steel and Silver Nylon.

The electrodes in Figure 18 were made so that they could be easily interchanged within a supporting structure.

3.3.1.1 Fabric Electrode Characteristics

The object of this study is to develop totally *dry* electrodes. The primary aim of the electrode is that it has a low contact impedance. The fabric's method of construction will have an effect on the surface roughness and hairiness of a conductive electrode and this may affect the effective resistance between the electrode and the skin's surface. The stainless electrodes for example, used for testing on multiple subjects, were knitted with SSt yarns that were 'coarse', compared to the other yarns. This resulted in the electrode area being relatively rigid when compared with the other electrodes and also less compressible and conformable. It was thought "the more fabric like the electrode the better it contacts with the skin's surface" so as to provide an improved contact area. An electrode size of 20mm x 20 mm was chosen giving consideration to motion artefact, signal level and noise [19].

Characteristics of the yarns used for the electrode construction are provided in Appendix G (where supplied by manufacturer) and summarised in Table 1. AgN is a multifilament two fold yarn where each fibre (34 in total) is comprised of a central nylon 66 monofilament core coated with silver. The stainless is a multifilament two fold yarn in which the fibres (550 in total) are composed of 68% iron, 18% chromium,

12% nickel and 2% molybdenum. The stainless is a larger diameter yarn and was the only available for testing at the time. Two different types of the AgCu were tested, a continuous single filament and a multifilament. The AgCu single filament (AgCu(s) was used for multiple subject tests. Although these fibres had a reasonable tensile strength, malleability was low and during initial knitting trials these would not knit without breaking. Both of these were then knitted with another non conductive yarn (wool) to allow them to be knitted. The continuous monofilament silver coated copper core fibre (1x 0.08mm) was twisted with a wool yarn and the other, the continuous multifilament(20 x 0.04mm) silver coated, copper core fibre which was knitted in parallel with a polyester yarn. The final AgCu test electrodes are shown in Figure 19 and for AgN and SSt in Figure 20. It can be seen that the effective surface contact area for the single composite yarn, AgCu(s), is greatly different to that of the multifilament yarn, AgCu(m).

Table 1.

Characteristics of the conductive yarns used to knit electrodes.

Material	Manufacturer	Tex	Dia (M)	Construction	Resistance (ohms/cm)
Ag N	Statex	NA	170u	117 tex x 2	40 -60
Stainless	R Stat	9D	NA	12u 275 filament x 2	60 - 80
Ag Cu(s)	Electrisola	NA	NA	1 x .08 single	0.06
Ag Cu(m)	Electrisola	NA	NA	20 x 0.04	0.02

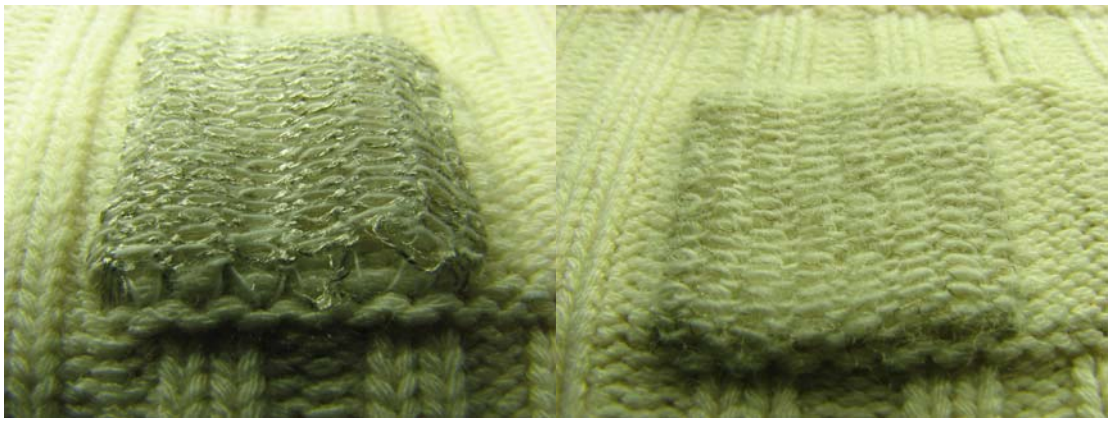

Figure 19. Knitted fabric electrodes, AgCu(m) (left), AgCu(s) (right).

The fabric electrodes were knitted using a Shima Seiki SES-SWG knitting machine with needle density of 14gauge (14 needles per inch). The square electrode area was knitted in such a way that it is joined at each end to a wool lycra band. The lycra is included to provide a stretch component within the band (to aid in placement directly on the torso if required, but this was not done). This allowed an area of electrode totally comprising the selected conductive yarn to be knitted.

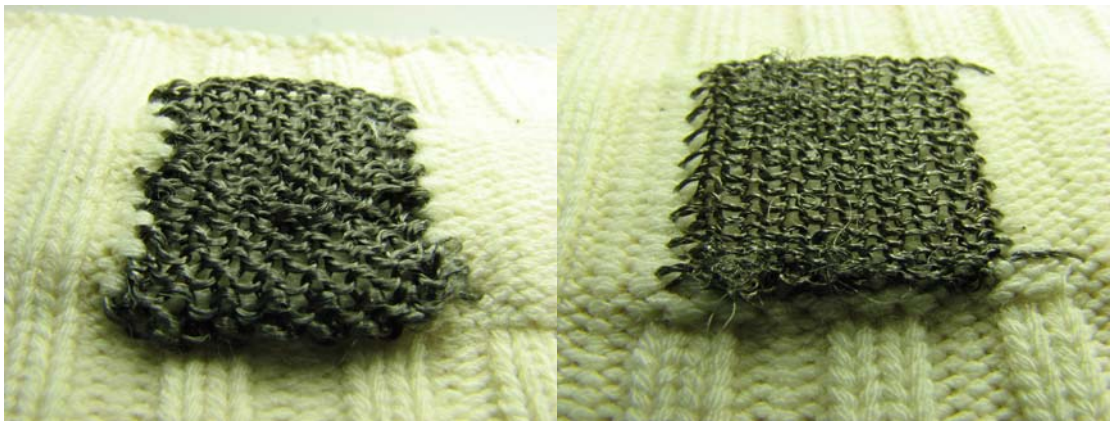

Figure 20. Knitted fabric electrodes, SSt (left), AgN (right)

3.3.1.2 Electrical Characteristics of Sample Fabric Electrodes

The knitted electrodes were cut from the knitted bands. The tails of the conductive yarn from the electrode were wrapped around fingers of the top of the ring of a metal snap fastener and this was pressed onto Velcro (hook) which contained a backing adhesive. This was then stuck onto one end of the base wool fabric of the band. Another piece of Velcro (hook) was stuck to the other end. The Velcro hook present at

each end of the assembly allowed it to be easily attached to the test band. An example of the AgCu(s) electrode is shown in Figure 21. Notice on the back side of the electrode an effective recess is available for placement of the discrete pressure sensor assembly without upsetting the top surface profile.

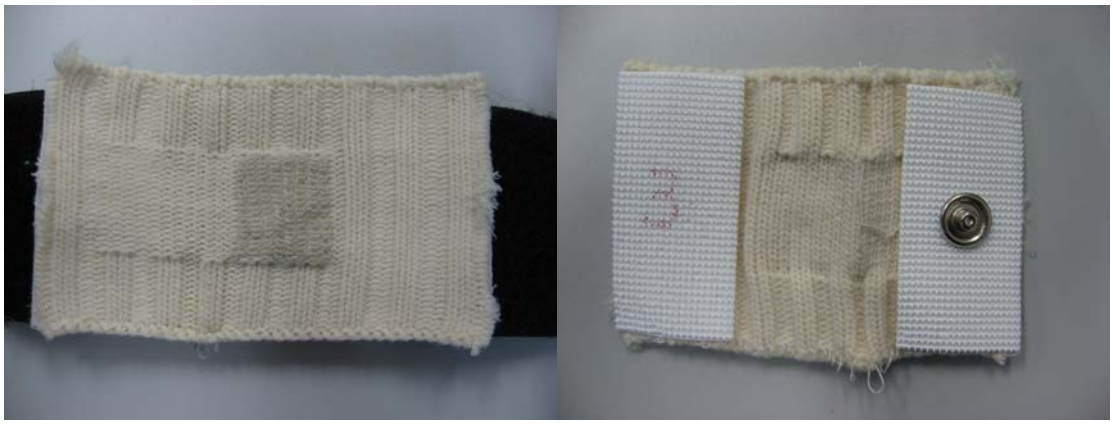

Figure 21. Detachable fabric electrodes (AgCu(s) example), front and rear views

The electrodes themselves were knitted as similarly as possible, but due to the differences in the conductive yarns' physical characteristics, some variations were necessary. Details of the physical construction and resistance of each electrode are shown in Table 2.

Table 2.

Knitted electrode characteristics

Electrode Material	Electrode ~Area	Lycra loop length	Conductive yarn loop length	Resistance (across electrode) Ω
AgN	20 x 20	9.5 mm	6 mm	0.6
Stainless steel	20 x 20	9.5 mm	8 mm	0.2
Ag Cu(s)	20 x 20	9.5 mm	7.5 mm	0.2
Ag Cu (m)	20 x 20	9.5 mm	7.5 mm	0.1
LV9315PPY	20 x 20	NA	NA	~300
WoolPPY	20 x 20	NA	NA	~160

The electrical conductivity of the yarn provides the basis upon which the contact resistance of the electrode is obtained. It has been reported that the difference between the resistance of a homogenous conductive fabric sheet can be four orders of magnitude lower than that of the yarn that it was fabricated from [135] as seen in Table 1 and Table 2.

The fabricated electrodes were tested for overall resistance by placing each sample in a test jig. The samples tested were the 20mm x 20mm electrodes. In this way any differences between electrodes from different yarn types and construction methods can be determined. The results indicate that the fabric electrodes with the lowest surface resistance were the SS and the AgCu fabric. Even so, the other fabric electrodes have are very similar and low values of resistance, except LV9315PPY and WoolPPY. Due to the relatively higher surface resistance of the outer layer of the skin, the stratum corneum, this may not present any problem. It has been shown [15], that at low electric field levels, i.e. low voltage conditions, that the lower layers of the skin namely the dermal and epidermal layers are not involved in conductance between surface electrodes in close proximity. The conductivity of these lower layers is considerably higher than that at the surface and is the prime contributor at higher sense voltages.

3.4 Development of Skin Contact Pressure Tests

3.4.1 Physical measurement considerations

To maximise the signal to noise ratio of the measured signal it is desirable not only to have a minimum contact resistance but also for maximum common mode rejection the impedances need to be the same, any inequality, will result in unequal common mode signals being present at the input to the input amplifier. Unequal pressures on test contacts may subsequently result in a reduction in signal to noise ratio and hence degraded performance and poor discrimination of the desired signal. Variations of these resistances with time may also contribute to variations in acquired signals.

EMG a commonly measured biosignal, may vary in amplitude from the μV to low mV range [136] and depends on many factors unique to the individual. Amplitude, time and frequency domain properties are dependent on factors such as [137]:

- the timing and intensity of muscle contraction,
- the distance of the electrode from the active muscle area,
- the properties of the overlying tissue
- the electrode and amplifier properties and
- the quality of contact between the electrode and the skin (from Bortec)

These factors are common to measurements made on the skin's surface and have an effect on all biosignals.

Studies by numerous researchers [138, 139] show that maximum voluntary contraction (MVC) repeatability, within and between individuals, is affected by experimental noise e.g. due to random factors such as mood, motivation, psychological and physical conditions. Rainoldi [138] has shown that maximal voluntary contraction of 50% can provide the highest EMG signal repeatability. If electrodes remain in place reproducible surface EMG is possible [139].

In developing the test protocol, consideration was given to this and to the European Union(EU) project; Surface Electromyography for the Non-Invasive Assessment of Muscles (SENIAM), recommendations for Bipolar sEMG Electrodes [140]. Tests pads were made 10mm x 10mm and the distance between centres was 20mm. Initial practical measurements on two subjects indicated, at least in the case of the biceps and forearm that repeatable values could not be obtained using one single set of electrodes. This result is supported by others [31, 79] who identify that the primary cause of differences in impedance, is the different properties of the skin between individuals. To limit the effect of physical conditions, a measurement method is needed which is independent of the physical state and position of the subject.

3.4.2 GSR Pressure Testing

As GSR relies on DC contact characteristics of the electrode connection to the skin's surface, it was decided to investigate the effect of electrode contact pressure on GSR. Initially a quick trial was performed on a single subject. The schematic of the testing arrangement is shown in Figure 22. Electrodes were mounted onto the one piece of plastic (not shown) with a gauge length of 10mm between the electrode edges. Pressure was applied by an elastic band 50mm wide placed around the forearm.

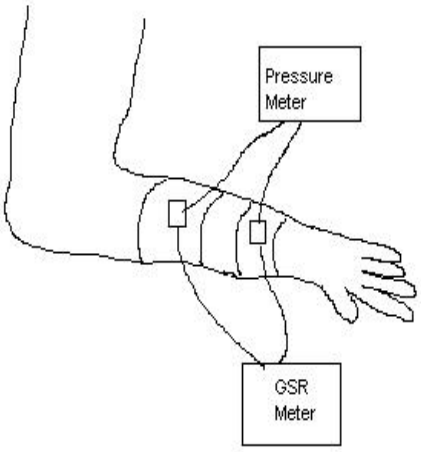

Figure 22. Setup for initial GSR pressure measurement.

Foil Force foil based sensors were used as the sensing elements and with appropriate electronic conditioning and calibration. The electrodes were connected to a commercial GSR meter; Autogenic Systems AT64 SCR, that could measure SCL and SCR.

GSR results were erroneous and it was extremely difficult to apply a constant test pressure in this setup. EMG was also measured with the subject holding a mass in their hand as a load but with similar results. Further tests with this setup were discontinued.

In an effort to obtain a level of consistency in measurements, a mechanical support to cradle the arm was designed to aid electrode placement, permit pressure to be adjusted and maintained and allow electrodes to be changed with minimal effort. This was fixed on a stand which could be positioned next to the arm of an office chair. The bicep was chosen as a suitable site for measurement as it was thought more stable readings would be achieved. The elbow and rear of the upper arm were supported and adjustments were provided in three degrees of freedom to enable correct alignment of the electrode pair on the bottom part of the bicep.

The schematics of the mechanical design of the adapter heads used to house the pressure sensors and support the test electrodes, is shown in Figure 23.

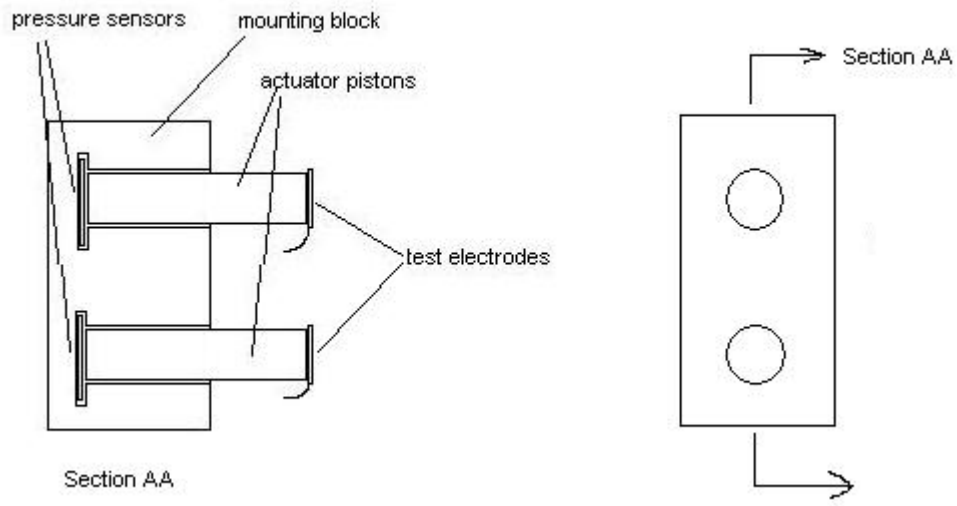

Figure 23. Simplified diagram of mechanical adapter for GSR/EMG pressure measurements.

The circuit schematic for the pressure sensing conditioning is shown in Appendix E. The sensors were calibrated with a range of weights over the range of 50gram to 650gram (~5 KPa to 62 KPa).

The foil sensors were placed between a solid base and a moveable, 10mm diameter piston, upon which the conductive test electrodes were placed. The design of the electrode tips designed is shown in Figure 24. The snap male fastener clips into the top of the mounting piston as shown above.

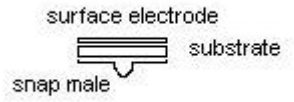

Figure 24. Electrode tip assembly for testing of conductive fabric electrodes.

Initially electrodes of 10mm square were used but later changed to 10mm diameter. The electrodes were placed in the middle of the biceps as shown in Figure 25. The skin was not prepared in any way for these tests.

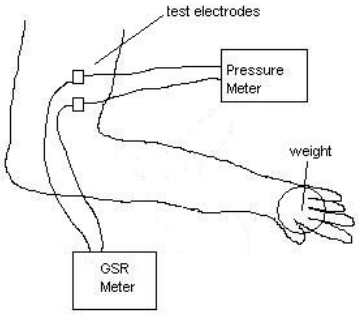

Figure 25. Setup for second GSR/Pressure measurements on bicep.

To help maintain the arm in a controlled state GSR was measured with 50% MVC (weight in hand). Due to application of electrodes (AgN in this case) to the surface of the biceps it was difficult to test a subject whilst maintaining a fixed contact pressure because of absolute position of the muscle and the fixed physical nature of the pressure rig. Any relative movement between the two translated itself into a modulation of the applied pressure and hence measuring electrode signals with a constant pressure was not possible. This problem was compounded due to the type of sensor chosen to measure the pressure.

Two problems with this type of sensor became apparent, namely repeatability at light loads and settling time. It was observed that it could take tens of minutes for the measured force value to asymptote and settle to within 5% of a final value. The repeatability of the sensed value at small applied forces was also poor with a variation of up to 20%. To overcome this problem the foil sensors were replaced with a pair of button force sensors obtained from Sensor Developments Inc. (see Appendix C). These are housed in metal in the shape of a button and were shown to exhibit good repeatability and settling time over the whole force range used.

Tests were repeated but measurement of GSR with the test rig on the biceps was still found to be unsuitable. The measuring site of the forearm was reconsidered. The pressure rig was modified to allow testing on the inner forearm (Figure 26). This was hoped to help to reduce the effect of variation in the applied pressure and also to accommodate the new sensor.

Figure 26. Final pressure electrode test rig used for GSR tests on subject forearm.

Better results were then obtained in that a pressure could be adjusted and maintained more easily and GSR values could be measured.

3.4.3 Experimental Test Protocol for Singular Fabric Electrodes

To improve the measurement system for GSR, Biopac with a single GSR input amplifier was used. Specifications are shown in the Appendix D. One important operating characteristic of the GSR amplifier is that the test voltage applied across the electrode terminals is 0.5V. From the earlier discussion on the human skin model it is obvious that this voltage is well suited for testing without having undue voltage effects on the measured skin resistances.

3.4.3.1 Experimental Plan for skin-electrode pressure & conductivity measurement

The following method was used to initially characterise contact materials.
The pressure sensors are calibrated (see Appendix C), for 0 to 4V for loads of 0 to 1000gm. Biopac was used to measure GSR of the subject.

1. Measure pressure/GSR response with a range of test electrode materials.
    a. Brass alloy disc of 10mm diameter
    b. Ag plated contact disc 8mm diameter, derived from the centre of Red Dot 5650 electrodes.
    c. Silver coated nylon yarn 20gg knitted fabric electrode nominally 11mm diameter.
    d. Stainless Steel multifilament metallic yarn 20gg knitted fabric electrode nominally 11mm diameter.

Conduct tests on a single subject initially to determine validity of test setup.

2. From initial results, select the most suitable electrode materials to test on multiple subjects.

Selected electrode materials include

    a. AgNylon knitted fabric
    b. Stainless steel knitted fabric
    c. Aluminium foil
    d. Polypyrrole conductive polymer fabric.

Aluminium was considered for use as an electrode material, but as the chemical response of aluminium oxides to human perspiration has been shown to have problems [141] it was not included.

A series of ECG tests will be conducted on 10 subjects with 3 of these materials. An ECG analysis program will be used to quantitatively discriminate between electrodes.

Initial single subject Test Procedure
The subject was placed in a seated position in a conditioned environment (25 degrees centigrade and 60% relative humidity)
The right arm of the subject was placed in and supported by the test rig which was positioned next to the subject's chair.
The test rig was connected via two shielded cables and connectors to the GSR input amplifier of the BIOPAC measuring system and two shielded wires from the pressure sensors to the pressure display unit.
Test electrodes were carefully placed onto the electrode support posts.
The test electrode assembly was carefully adjusted to make initial light contact with the forearm of the subject.
The pressure knob was adjusted until the required pressure reading was obtained.
The GSR and Pressure values were recorded for a number of minutes.

Due to the difficulty in obtaining constant pressure readings, a limited number of pressure steps were used. To test if there was any polarisation effect a single measurement was made and then alternating the input amplifier connections and measuring again. No effective change was apparent and values remained within a 5% range.

Testing was then performed on a single subject. The first of these tests revealed a change in the GSR even though the initial pressure setting was not adjusted, (see Figure 27). The pressure was set to minimum, to provide contact, but changed during the test time due to unsolicited physical movement of the subjects arm.

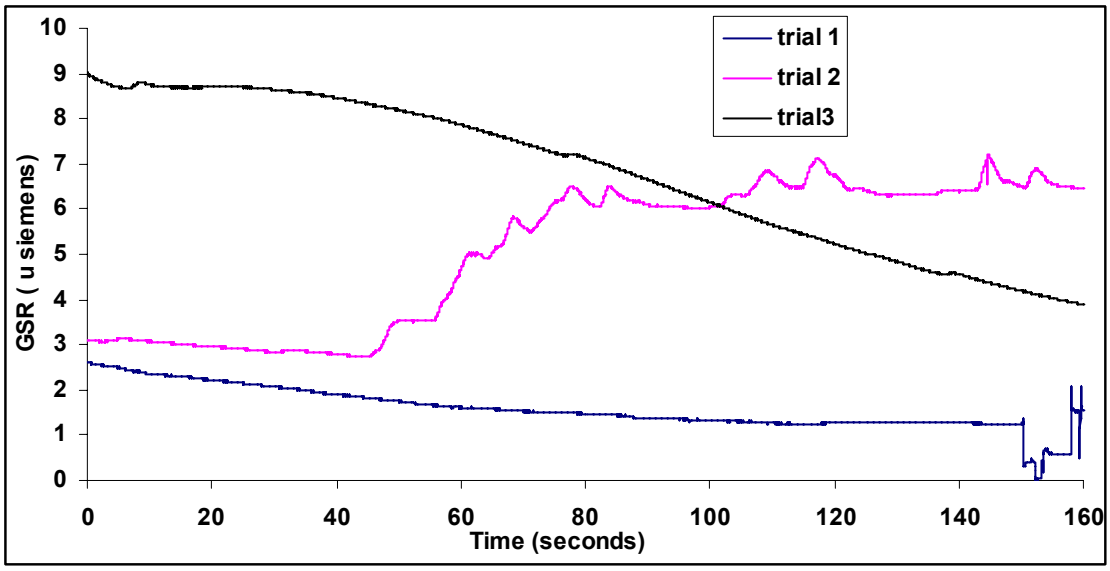

Figure 27. GSR Subject 1: minimal (10 gms load) 3 trials, conducted 5 minutes apart.

GSR varied throughout the conduct of three trials. Further trials were conducted and the results are shown in Figure 28 and Figure 29 for nominally 250 grams and 20gms applied force respectively. Subject 2 provided more stable results than did subject 1. The effect on GSR to a step change in applied load is shown in Figure 30 for brass/alloy tips and Figure 31 for bare fastener tips (no electrode surface).

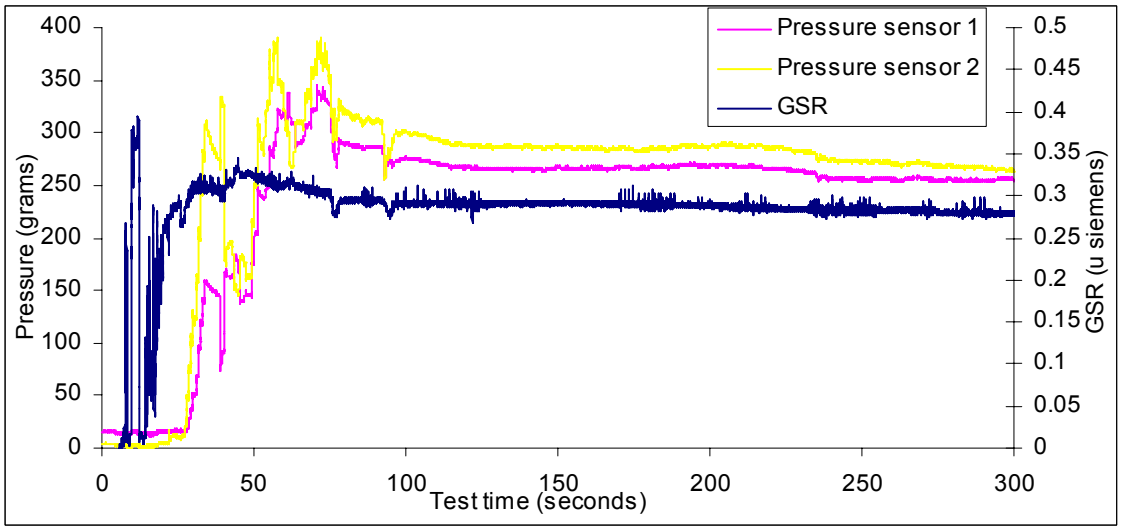

Figure 28. GSR/load (nominal 250gm): Subject 2, Red Dot centre metal electrode.

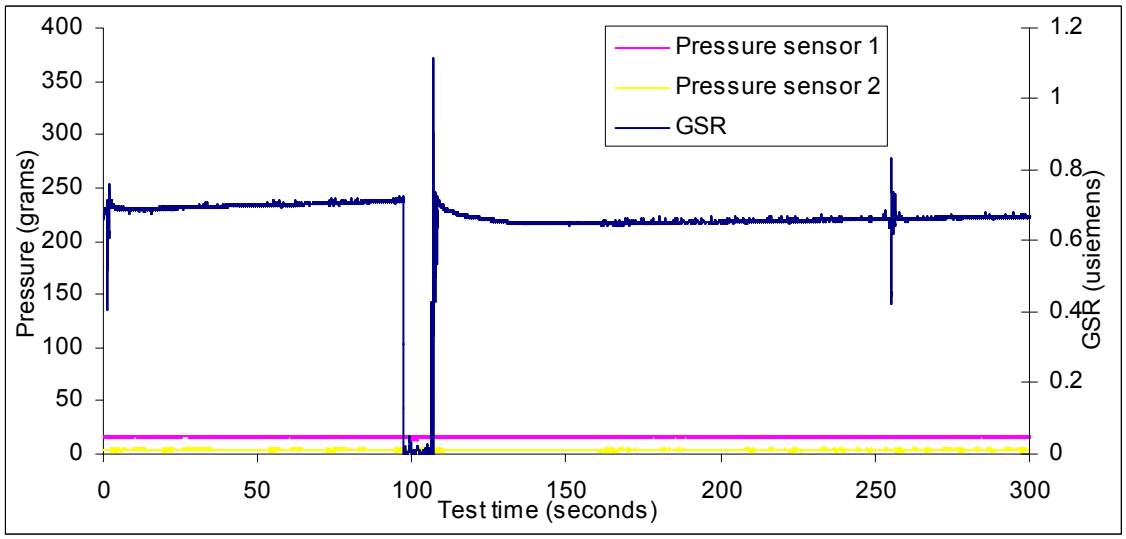

Figure 29. GSR minimal load (20grams), contact only, Subject 2, Red Dot centre metal electrode.

At small pressures GSR varies to a large degree because the effective contact resistance between the electrode and the skin is higher and any small movements of the forearm (small pressure changes) will directly affect the resistance. Note that upon application the GSR begins generally lower and increases with time, i.e. the resistance goes down in value.

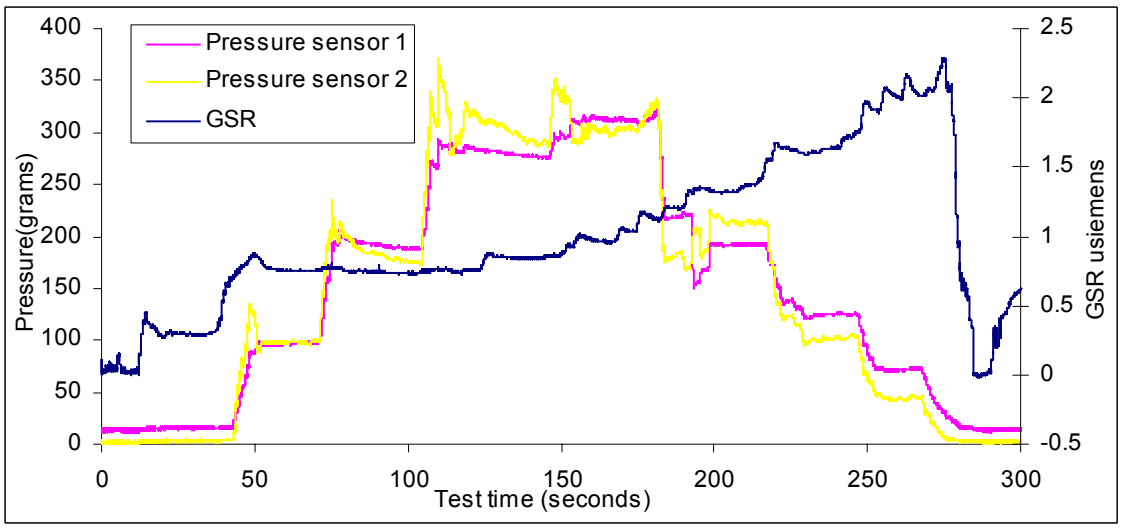

Figure 30. GSR/load step response, Subject 1: over 300 seconds (brass/alloy).

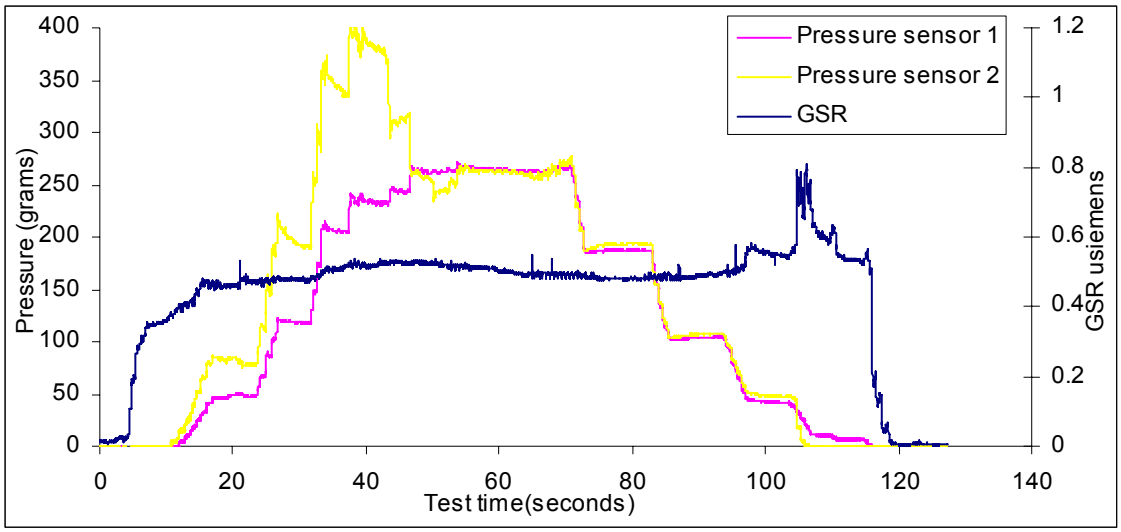

Figure 31. GSR/load step response, Subject 1, bare fastener tips no electrode.

The effects of step changes in load in Figure 30 and Figure 31 show that the GSR response is unpredictable. Initially at light loads a step change in GSR is observed but this diminishes above ~ 50-100gm. It seems that once a good connection is made to the skin any change in pressure is not reflected in a change in GSR. With reduction of pressure, GSR increases, which is opposite of what is expected (increase of GSR is a reduction in ohmic resistance). This may be due to conductance through the lower viable skin layers which have lower resistance.

3.4.4 Experimental Results from initial Pressure/GSR Measurements

Preliminary static testing and calibration of the pressure sensors used in the pressure/GSR test system revealed that the results were within +/-5%.

From the previous description and discussion on GSR measurements, it was experimentally confirmed that the use of GSR to help determine the effectiveness of an electrode material was fundamentally flawed due to the variable nature of the skins surface conductivity. The inherent resistance of the electrode materials chosen for experimentation are in themselves low with the aim of producing an effective contact resistance when placed on the skin's surface. A setup is required that will permit any differences in contact resistance to be quantified. Because the actual measurement of GSR is in itself not repeatable with temporal variability of the skin's conductance being predominant and the absolute values of GSR not of the same order of magnitude

as that expected for the electrode materials used, the ability to measure any electrical differences between electrode materials was not possible. In order to limit the number of experimental variables a 'skin' which has more repeatable characteristics with an inherently lower resistance is required.

3.4.4.1 Artificial Skin

Having used conductive materials as part of other research work it was decided to try a conductive rubber sheet as a 'skin'. The conductivity of the sheet is approximately 50 ohms/square and although significantly lower than that of natural skin which is many hundreds of kilo ohms or higher, it should allow a level of discrimination between electrode materials to be determined. Like skin, it too has a temporal effect relating to the measured resistance across the sense electrodes. In order to reduce the variability within a measurement series, at each change in load, the associated resistance value was taken after a 1 minute. Three conductive electrodes were chosen for comparison, a brass alloy, Red Dot (Ag centre portion) and AgN.

Experiments were conducted by increasing the load from zero. The results for brass/alloy tips, including loading and unloading (hysteresis) are shown in Figure 32. The 'skin' was moved slightly between the two tests which would account for the slight difference in initial value. Red Dot and AgN tips are shown in Figure 33. Differences are also due to the temporal dependence of the 'skin's recovery from deformation caused by the application of pressure.

Results show that a measurable difference can be seen as the pressure on the electrode is increased up to a value of about 300gram/cm^2. In most if not all cases, values asymptote to within 5-10% of the final low resistance value when a 200gm load is applied. This suggests that forces up to this order of magnitude are a good first estimate of a suitable test force to apply when testing electrodes.

The figures show that for the Ag (Red Dot) electrode the 'skin'-electrode resistance is 107 ohm and for brass alloy electrodes 122 ohm. The AgN electrodes have a value of 75ohm. This can be attributed to the fact that this electrode provides a total coverage of the contact area ~ +10% due to some hairy peripheral fibres providing a contact as well. Figure 34 shows the lower load range (below 50g) for the AgN electrode.

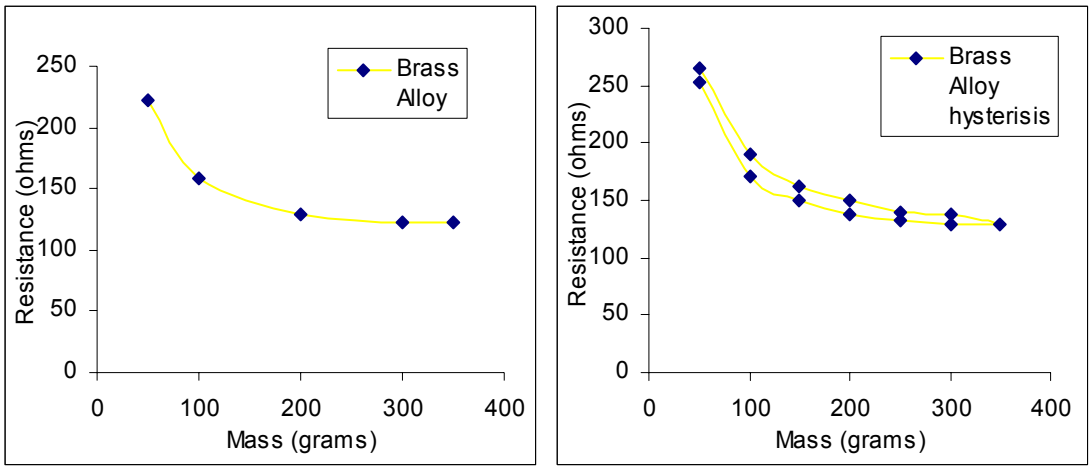

Figure 32. Pressure/Resistance for brass alloy tips, trial1 (left) and trial2 with hysteresis (right).

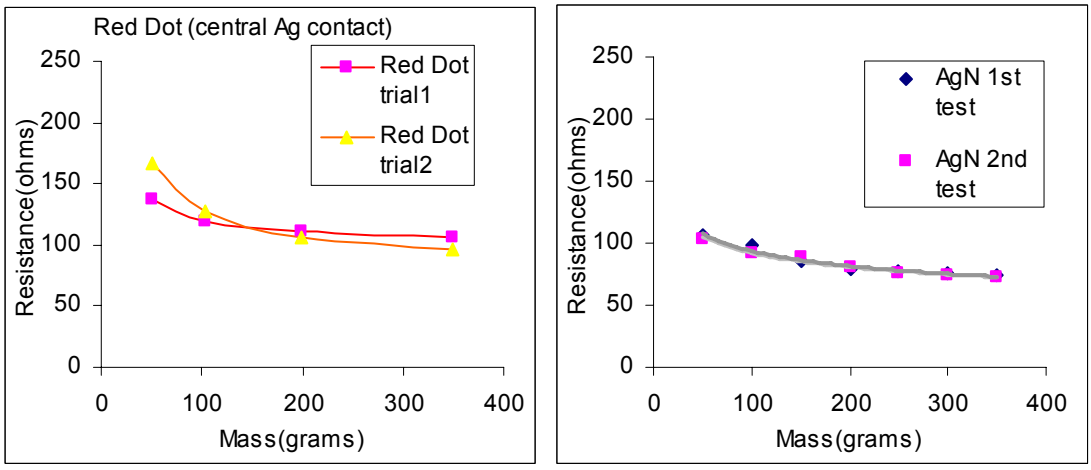

Figure 33. Pressure/Resistance for Red Dot and AgN for two trials.

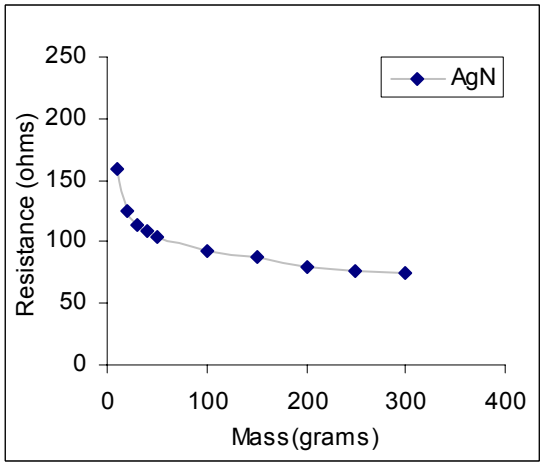

Figure 34. Pressure/resistance low load range for AgN.

The repeatability of the results shown for Red Dot and AgN in Figure 33, is reasonable given the elastic nature of the 'skin' and considering that electrodes were removed from

the surface between tests. AgN measured consistently lower in resistance than did the Ag electrodes. The discernable differences in resistance between materials, helps to confirm the validity of the pressure measurement approach. These experiments verified that repeatable results could be achieved using the new pressure sensor and that a stable pressure around 100g may be suitable within a test garment.

The artificial skin, whilst useful to observe differences in electrodes does not replicate the physical or electrical properties of human skin. This pressure level may not be appropriate for torso measurements on human subjects. It was noted during previous GSR testing that at a pressure level even of 100gm, large indentations of the subject's forearm skin was observed. Lower levels may be preferable.

3.4.5 Pressure Sensor assemblies for use in test bands

The sensors (Sensor Developments Inc) with a diameter of 10mm were glued and mounted onto a square 20 x 20 mm, 1.5mm thick plastic substrate. A small ring of sponge rubber was positioned around the sensor to act as a separator and a 20 x 20 mm, 1.6mm thick piece of PCB circuit board FR4 material was glued to the spacer. The spacer was dimensioned so that only a minimal force was applied to maintain the upper plate in position. One of the two pressure sensor assemblies is shown in Figure 35.

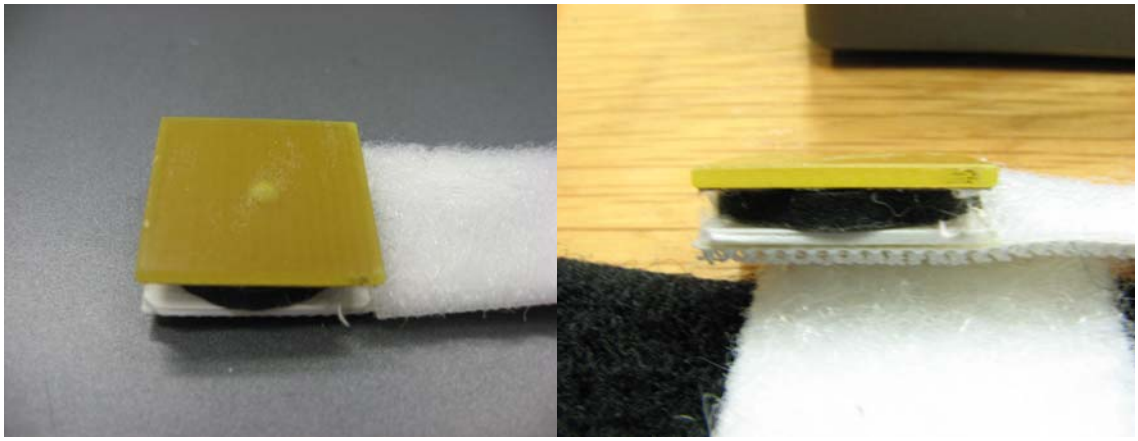

Figure 35. Pressure sensor assembly sandwich for measuring load on the fabric electrode.

Velcro was placed onto the back of the assembly to allow it to be positioned on the stretch test band immediately underneath the electrode. The pressure sensor assemblies were calibrated on a Hounsfield H5000M Tensile Tester TFT 1479 (see Appendix C).

3.5 ECG Measurements

ECG is easy to measure compared to EMG or GSR as it is of relatively large amplitude, relatively consistent and has a high temporal correlation within an individual. The heart muscle generates a reliable signal which can be readily detected over most of the human body. An individual's heart rate (HR) depends on their physical and emotional state [142] and is no measure of differences between electrodes. The ECG signal though, has a range of other characteristic features (described in section 2.4) which can be extracted and used for electrode comparison purposes. The decision was made to conduct further testing based upon ECG measurements.

3.5.1 Initial ECG Tests

Clinical ECG measurements often involve a 12 lead electrode configuration. To validate the measurement set- up, a twelve lead measurement was performed on a single subject. The arrangement of the 3M 2560 electrodes used is shown in Figure 36.

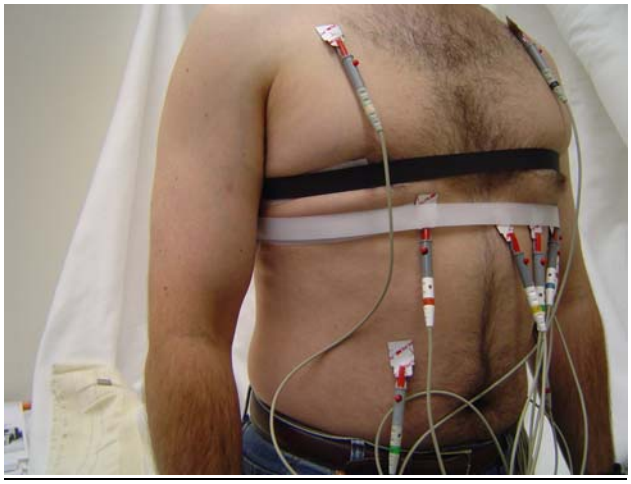

Figure 36. Initial ECG testing with 12 lead Red Dot electrodes.

The waveform obtained from this measurement compared well visually, with that expected from the literature as in Figure 5 and demonstrated that the system was appropriate for preliminary testing. It was decided that a reduced set of electrodes was more suitable, which reduced the complexity of measurement and simplified the

analysis. The initial approach concentrated on a simple system that comprised up to four electrodes.

A similar arrangement to the Einthoven triangle using the right arm (RA), left arm (LA), right leg (RL) and left leg (LL) electrode setup was used. As a reference, initial measurements were conducted on a subject using Red Dot electrodes (3M commercial Ag/AgCl adhesive electrode used for clinical ECG measurements). Measurements were conducted at 22 degrees centigrade and 60% relative humidity, with the subject at rest seated on a stool. The positioning of electrodes used for the reference measurements is shown in Figure 37. Typical signals obtained are shown in Figure 38. These were measured with no skin surface preparation but good quality signals were obtained when compared with those described in published ECG data [46].

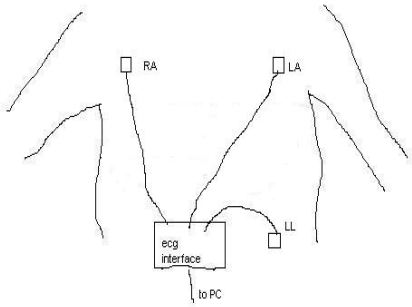

Figure 37. Front view, electrode placement for simplified 3 sensor (2 + reference) measurements.

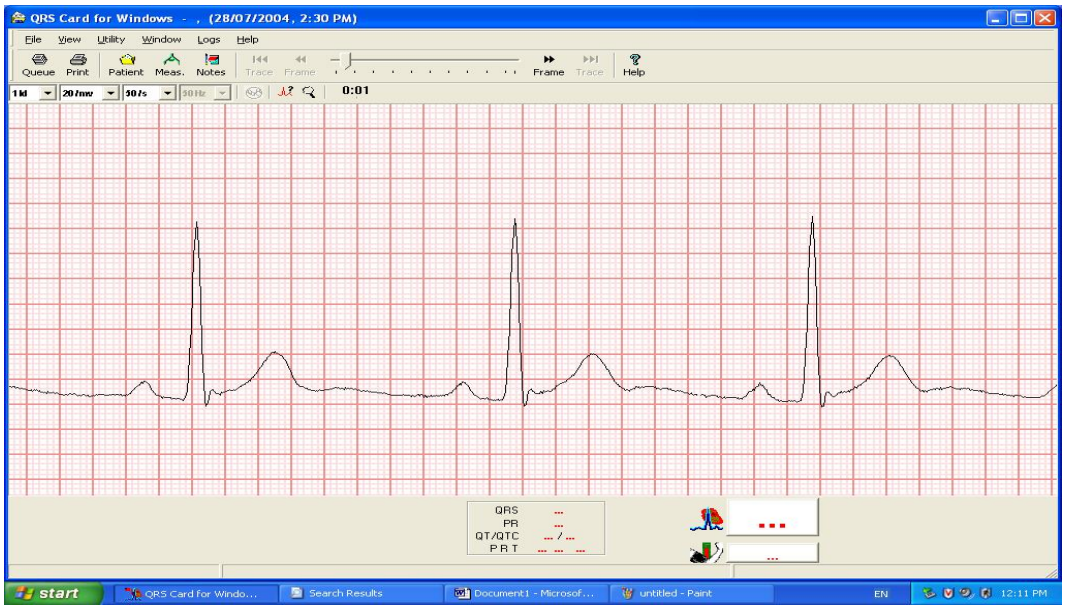

Figure 38. ECG signal as displayed on QRSCard, RA,LA,RL,LL all 3M Red Dot.

The above ECG waveform Figure 38 is visually similar to the 'normal' ECG shown earlier in Figure 5, although in this case no skin preparation was done prior to application of the electrodes. This demonstrated that useful ECG signals may be detectable with a suitable fabric electrode constructed using materials and facilities at CSIRO TFT.

3.5.2 Preliminary Tests with bands

In order for these measurements to be conducted and sensitivity optimised, the electrodes needed to be placed on and maintain some contact pressure with the skin. Fabric electrodes, each of 20mm by 20mm, were knitted into band loops about 50mm wide. The electrodes were then cut from the knitted bands and sewn onto 50mm wide elastic. On the ends of the elastic Velcro^{TM} hook and loop were sewn to alternate ends of the elastic (Figure 39). Two bands were used one for each test electrode and were joined together. This allowed the sensors to be individually placed in position on the body location first marked with a pen dots and permitted adequate pressure to be provided over the electrode contact areas.

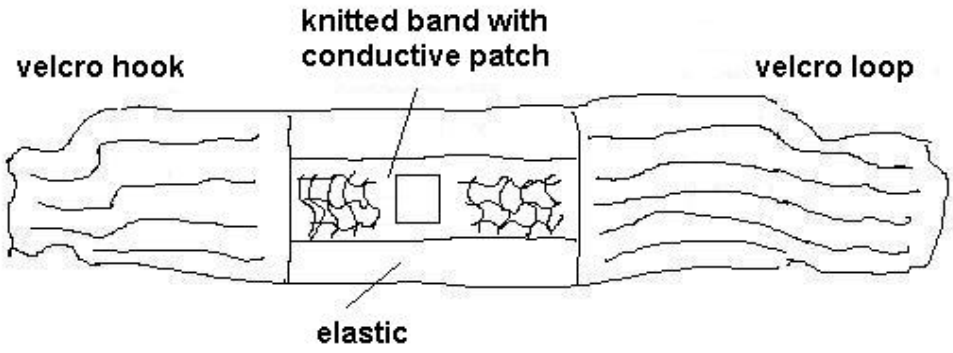

Figure 39. Single conductive sensor electrode band.

The bands containing the conductive electrodes, allow the two upper sensors to be placed on either side of the subject's torso just below the armpit and the lower ones placed 50mm below and in front, as shown in Figure 40. Measurements were made within 2 minutes of application. The subject was at rest seated on a stool for these tests. Tests were done using silver nylon and stainless steel electrodes. Two silver

nylon electrodes were placed in the upper position with the stainless steel below and the positions were then exchanged. The waveforms for stainless steel are shown in Figure 41. The response of AgN was visually the same. The waveform above is reasonable in quality, although lower in amplitude than the reference Red Dot baseline signals has basic attributes of the 'normal' ECG as shown in Figure 5.

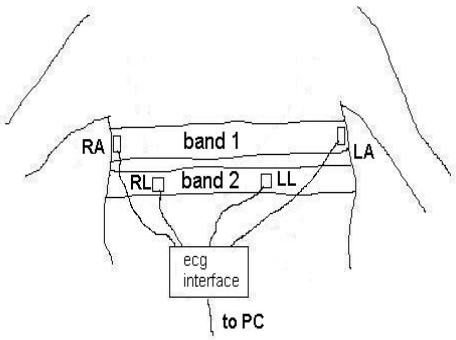

Figure 40. Conductive AgN/Stainless steel electrode placement.

Figure 41. ECG signal as displayed on QRSCard, RA, LA AgNylon, RL, LL Stainless steel.

A reasonable position for the sensors that results in usable signal waveforms is under the armpits and over the heart. This is not necessarily the optimum placement for the

detection of the heart beat signal but it would allow signals to be sensed from a typical sample group of either male or female test subjects more easily.
Further tests were conducted using sensors placed in these positions.

3.5.3 ECG test band with knitted test electrodes

The testing of the different fabric electrodes was performed with three of the same type of sensor attached to the elastic/Velcro bands. One band held the left side electrode and the other band held the right side and reference electrodes, which were placed adjacent to each other. The test electrodes were placed in position on the bands over the pressure sensor assembly described earlier. A photo of the pressure sensor assembly and the elastic/Velcro band is shown in Figure 42. The bands were constructed with the elastic and Velcro sections to not only cope with the varied size of subjects' chests but also to enable pressure to be adjusted. This allowed the simultaneous measurement of pressure applied to the electrode and the detected ECG signal.

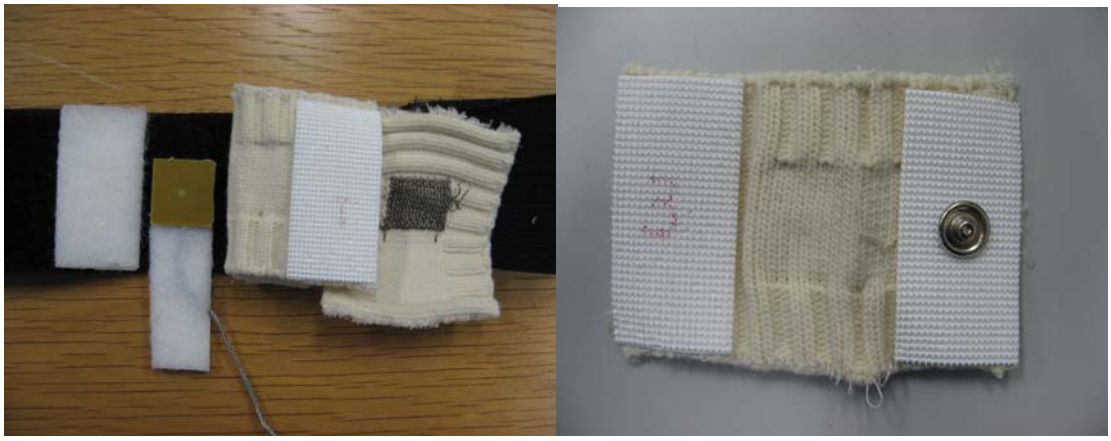

Figure 42. Pressure sensor mounted on test band, under test electrode (left) and rear of fabric test electrode (right).

The ECG electrodes were connected to the Biopac ECG amplifier module and the pressure signals were conditioned (amplified and scaled) and connected to the Biopac analog input module. The setup, shown in Figure 43, also shows the laptop which was used to show a series of videos to subjects during testing. Subjects were seated on the right and faced the screen.

Figure 43. Basic setup including test band for multi subject testing.

3.6 Fabric Sensors for physiological monitoring

The basic characteristics and use of fabric based strain sensors for the detection of respiration is described.

3.6.1 Strain Sensors and Respiration

Respiration, the rate of breathing, can be detected by measuring the movement of the upper torso and/or the abdomen. Breathing causes expansion and contraction of either the chest and/or abdomen which expands or contracts the lungs. The depth of respiration depends on the oxygen demands of the body, because of exertion and stress and can also depend on the physical position whether standing or seated. By applying strain sensors around the chest and/or abdomen, respiration can be detected. Respiration will cause an increase and decrease in circumference of the chest and/or abdomen which would result in a variation of strain and also a measurable change in the pressure (detected with the electrode contact pressure sensor).

Two different types of sensor that measure movement have been investigated. One, comprising application of a conductive polymer fabric sensor used in collaborative research work between CSIRO TFT and University of Wollongong(UOW) in NSW, the subject of UOW Patent WO 03/014684, 'Feedback Device having Electrically Conducting Fabric'. The other movement sensor, based on a stiff conductive monofilament fibre is the subject of Patent PCT/AU2006/001521 [143]. This had already been practically applied in sensing arm movements as the interface in an 'air guitar'.

The use of a polypyrrole treated fabric for use as a movement sensor has been investigated as part of research conducted on an Intelligent Knee Sleeve [144]. This research used a polypyrrole treated fabric as a strain sensor. This was used to monitor the movement of the human knee and indicate when a certain angle of bending had been reached. The sensor's resistance changes with changes in strain. The resistance is due to the fabric's surface coating of conductive polymer. The multitude of individual adjacent yarn/fibres within the fabric, mechanically interact and touch each other creating a conductive path through the fabric. In an unstrained fabric these interactions are based

on the inherent connectivity between yarns. When strained, more yarns are forced together that increases the overall interconnections across the fabric, thus reducing the resistance. Absolute values of base resistance can be tailored in manufacture and are dependant upon the type and amount of conductive polymer dopent used. This same sensor should be able to also monitor any movement on the surface of the body. The use of 'piezo' strain sensors (carbon loaded polymers) has been reported for use in this application [95], but these have the inherent disadvantage of relatively slow response and settling times. They are useable to monitor respiration rate but are unsuitable to characterise respiration. The mechanical characteristics of the base fabric, determines the dynamic electrical response of the sensor to changes of strain.

A sample of polypyrrole treated fabric from Marktek (Eeonyx Corporation) was procured and was used to make the sensor. This fabric was a double knit lycra and it had no specific design requirements and stretch resilience was poor. This had a resistance when manufactured of nominally 10KΩ per square. A sensor was made by cutting a strip of the fabric 150mm long and 20mm wide. Due to the fabric's construction, a strip cut on the wales direction (down the knit) had a rest resistance of 400KΩ and in the courses direction (across the knit) had a resistance of 150KΩ.

A trial was conducted on a single subject to determine the feasibility of using this sensor to monitor respiration. This was mounted in line and over an elastic portion of the test band and held in place with Velcro at each end. Two male press studs were also attached (facing outwards) to each end of the sensor to allow electrical connection to the BioPac leads. This allowed the sensor to be mechanically held in place on the outside of the band and also permitted electrical connection. The gauge factor is a measure of a strain sensors sensitivity and is defined as

$$\mathbf{K\ (gauge\ factor) = \ (\Delta R/R_0)\ /\ \varepsilon} \qquad \mathbf{(10)}$$

where,

ΔR is the change in resistance in ohms,

R_0 is the initial resistance in ohms and

ε is the applied strain.

Another sensor, a conductive filament strain sensor developed at CSIRO TFT is described in Patent PCT/AU2006/001521 [143]. This sensor has the advantage that the resistance change due to strain involves only two electrical points of connection, (whereas conductive polymer sensors rely on a large number of interconnections within the sensor). As the reliability of any electrical system is inversely proportional to the number of connections, a generally poorer performance of polymer sensors can be expected.

Use was made of an existing monofilament sensor assembly. The assembly was attached to an elastic portion of the electrode test band using Velcro so that during respiration, expansion or contraction of the band the strain sensor would monitor strain. The two sensors (Figure 44) are attached with Velcro to the front left and right sections of the test band.

Figure 44. Strain sensors, CSIRO monofilament (left), PPY (right).

This sensor's resistance is inversely proportional to strain. Nominal gauge length (between pinch points) for zero strain is 160mm. The characteristics for both sensors are shown in Figure 45. These measurements were made after the test cycle and the base resistance of the PPY sensor has changed from ~ 400 KΩ to ~ 1000KΩ due to mechanical fatigue and breakdown of the fabric structure.

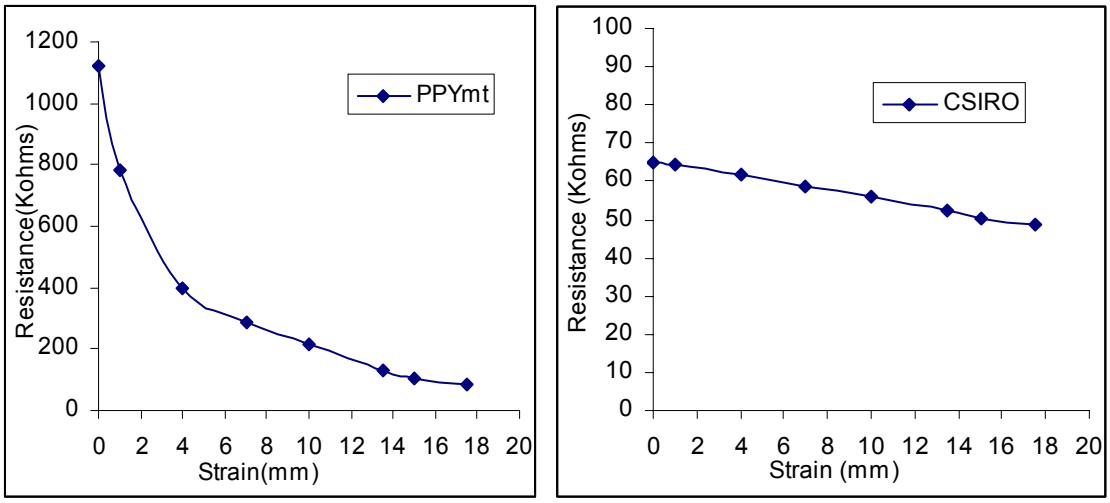

Figure 45. Strain resistance characteristics for PPY and CSIRO strain sensors.

The figure shows that the PPY sensor has a logarithmic response which needs to be linearised, whereas a more desirable linear characteristic is displayed by the CSIRO sensor. For electrical testing, the CSIRO sensor was connected to a constant current conditioning circuit that provided a voltage output proportional to strain, which was connected to an analog input of Biopac. The PPY sensor was connected directly to the GSR input module of Biopac which was scaled and displayed units of μsiemen (conductance, the inverse of resistance).

Cycle tests were performed on the two different strain sensors to get an indication of the strain performance and repeatability. The sensors were placed in a test rig built at CSIRO TFT (Figure 46) for the cyclic testing of this type of sensor. The test specimen is extended in a longitudinal manner with extensions up to 50% possible. The cyclic rate can be varied over a range of 0.5 to 5 cycles per second and tests were done at 1Hz, with a fully relaxed (sagged) position present in the cycle.

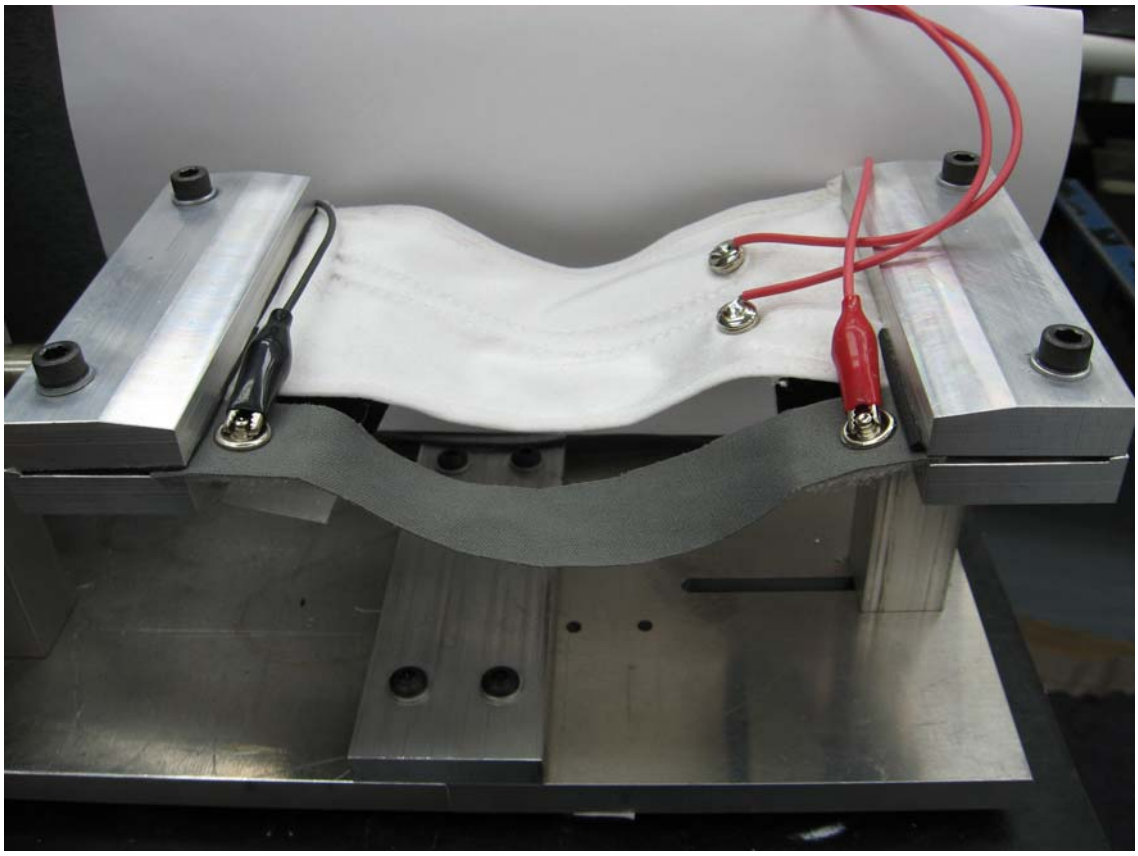

Figure 46. Cyclic tester for strain sensors, CSIRO and PPY (sag in cycle).

The sample strain sensors were mounted in the test jaws. As the sensors were not exactly the same length the strain to each was not applied at exactly the same time and there is a small time difference in the response. The measured waveforms are not related or scaled in any way other than to show the responses. A plot of the response of the two different sensors with strain is shown in Figure 47. Both sensors show very similar responses although it was observed that the PPY sensor's resistance changed over the length of the test cycle. The base rest resistance fell from 570KΩ to 470KΩ ~ 20% reduction and the maximum extension value dropped from 76KΩ to 65KΩ. This is due to the mechanical fatigue and abrasion within the fabric structure in which the yarns make more intimate contact with each other thereby reducing the resistance. The fabric used was not optimised in any way, but it demonstrates the capability of this type of sensor. The CSIRO monofilament showed no signs of resistance change and long term tests have shown it to be robust and stable.

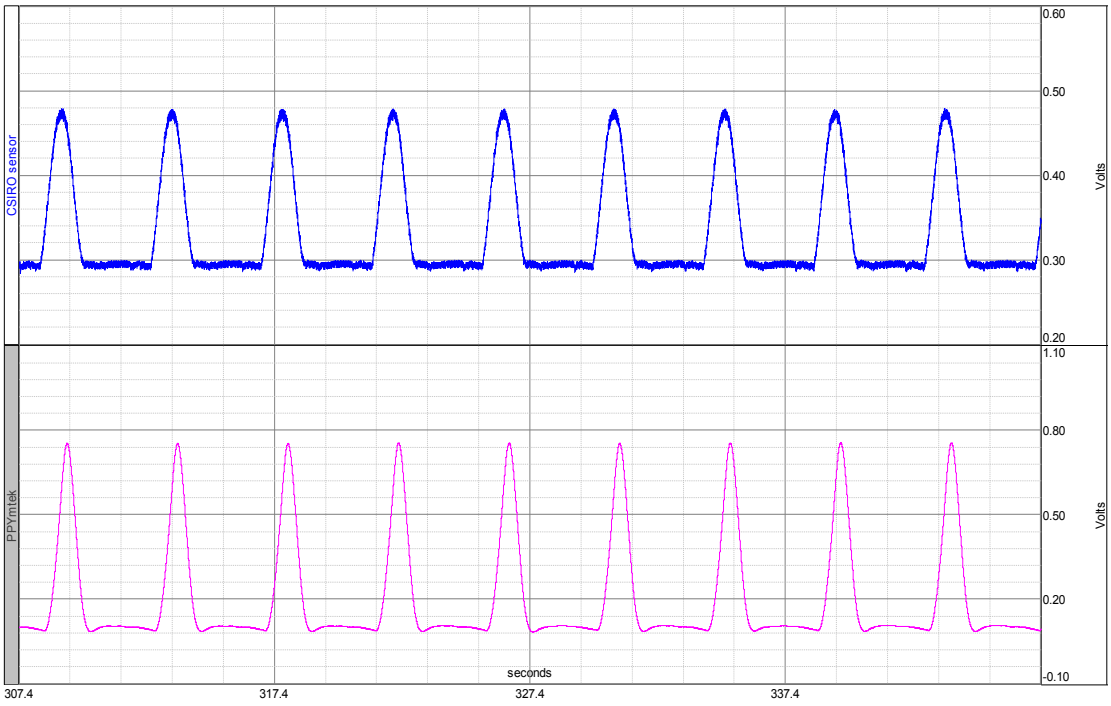

Figure 47. Plot of the cyclic response (as displayed on Biopac software), for CSIRO monofilament (top) and PPY (bottom), horizontal time(s), vertical (volts).

The CSIRO monofilament sensor has been trialled for washability and has been found to give repeatable results over five 5A wash cycles (effectively means fully washable) and more than 100,000 mechanical cycles.

Testing of respiration detection was performed in the same way as for ECG, with subject seated and calm (again watching a video). Test bands with the attached CSIRO and PPY strain sensors were placed around the subject and pressure adjusted to 100g. This test began with some initial torso movement and deep breathing to settle the sensors. This lasted about a minute and provided data at higher pressures. Respiration settled to a shallow level, inherent for this subject, which accounted for low signals.

The results of these tests indicate the possible use of both types of sensor for the detection of respiration and/or movement of the human body. Although the polypyrrole sensor tested did not have ideal characteristics with low K and only limited repeatability, respiration was readily detected. These results repeat the early research at CSIRO TFT and other reported research [45, 145-147], using polypyrrole coated fabric or carbon loaded rubber as sensors, which also highlighted stability problems. These

were due to oxidation of the surface, mechanical fatigue of the base fabric and yarn interactions, but further recent work by others has improved this lack of performance. Methods have been proposed, reported in current research that allow PPY coated fabric strain sensors to be fabricated that possess high strain sensitivity and better short term stability [148]. Implementation of these research outcomes could result in a repeatable and stable respiration sensor, if stimulus response times and longer term stability are further improved. Integration of such a sensor into a garment will need special attention, such as how to selective apply a PPY coating to a specific area.

The CSIRO TFT monofilament sensor however has an inherently better repeatability and stability than the PPY and with advances in design could be integrated more easily into a practical garment.

3.7 Specific Test Procedures

As a result of the previous investigations into ECG, respiration and pressure, a method for measurement was developed and is described in this section.

3.7.1 Verifying the method of electrode discrimination using ECG

Preliminary tests were performed on a single subject to verify the test method. The signals obtained using the Red Dot electrodes were used as the prime reference for comparison.

Red Dot electrodes were placed on the subject in selected areas as previously described, namely one under each arm pit, positive lead connected to LA and negative lead connected to RA. A test was done to determine the most appropriate position for the reference electrode. Two positions were tried, one at the waist on the left hand side of the torso and the other mid chest where the surface is relatively flat. The raw waveforms as acquired from Biopac are shown in Figure 48, indicating that the signal quality from either reference positions is almost identical. There is a small increase in 50 Hz noise present in the mid chest reference waveform, but this is of little consequence and has no effect on the displayed ECG, PQRST waveshape.

Positioning of the reference electrode in the mid chest region in this instance produced a slightly noisier signal primarily due to the less than ideal contact resistance which is increased due to the presence of surface hair.

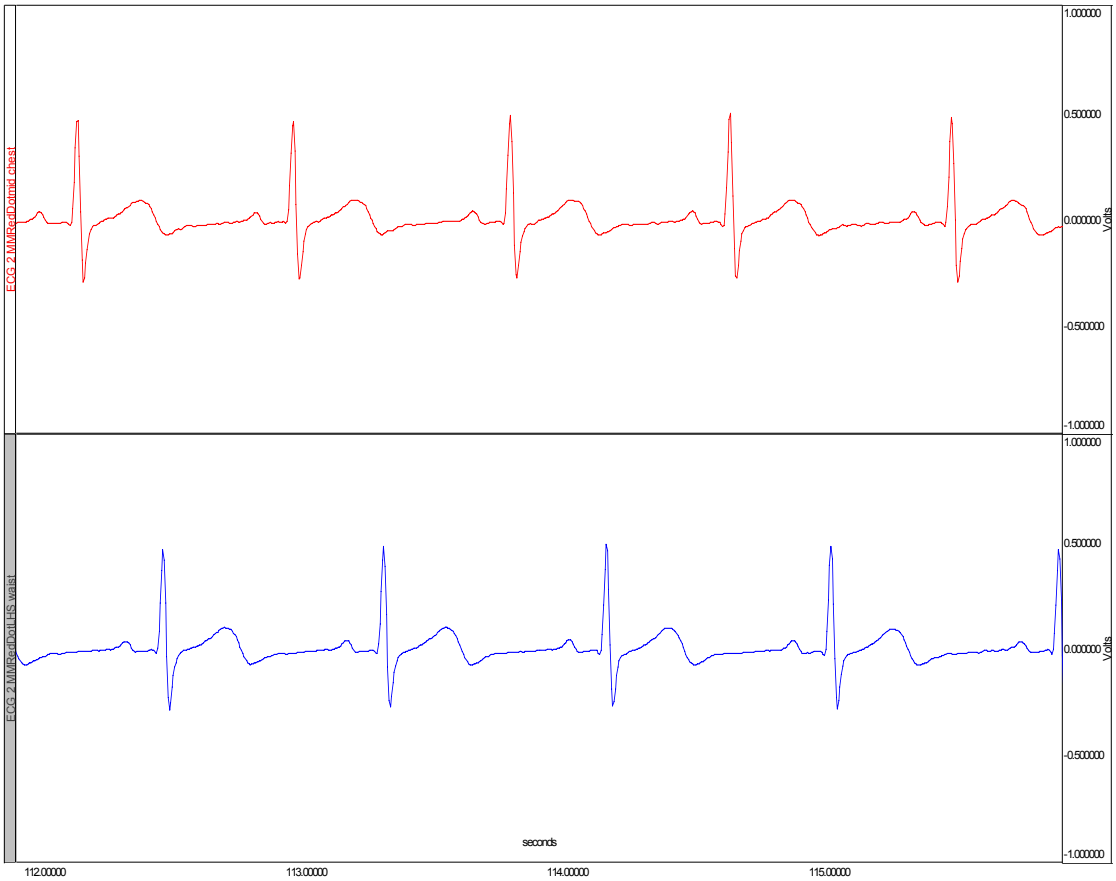

Figure 48. Raw ECG with Red Dot electrodes, (as displayed on Biopac AcqKnowledge software); reference positions, top plot mid chest, bottom plot left side waist.

These results demonstrated that suitable waveforms were able to be detected and tests on a single subject were then conducted using the Red Dot and four different conductive fabric electrodes. The reference electrodes used upon which the relative performance of these test electrodes is compared was initially the 3M Red Dot 2560, used for results in Figure 48. These have a silver plated contact area of ~10 mm diameter and are surrounded by a conductive AgCl gel adhesive. This affords a highly effective low resistance skin electrode contact. It should be remembered that there is no preparation of the skin.

The duration of time that an electrode remains in contact with the skin also affects its performance. Temporal changes in the electrode impedances of 'typical electrodes' have been reported by Kirkup [43] who has shown that impedance values have equilibrated to within a few percent of their final value within 120 seconds of the application of the electrode to the skins surface. This work used both stainless steel

and pre-gelled Ag/AgCl electrodes. It was therefore decided that all measurements will be taken over a four minute period which would include the initial temporal effect (over 120 seconds) and also provide stable data for comparison and analysis of the acquired waveforms. The actual bands and fabric electrodes used for these tests are shown in Figure 49. Preliminary tests on the single subject are shown in Figure 50.

Figure 49. Pairs of fabric test electrodes sewn onto bands for initial single subject tests, top AgCu, mid SS, bottom AgN.

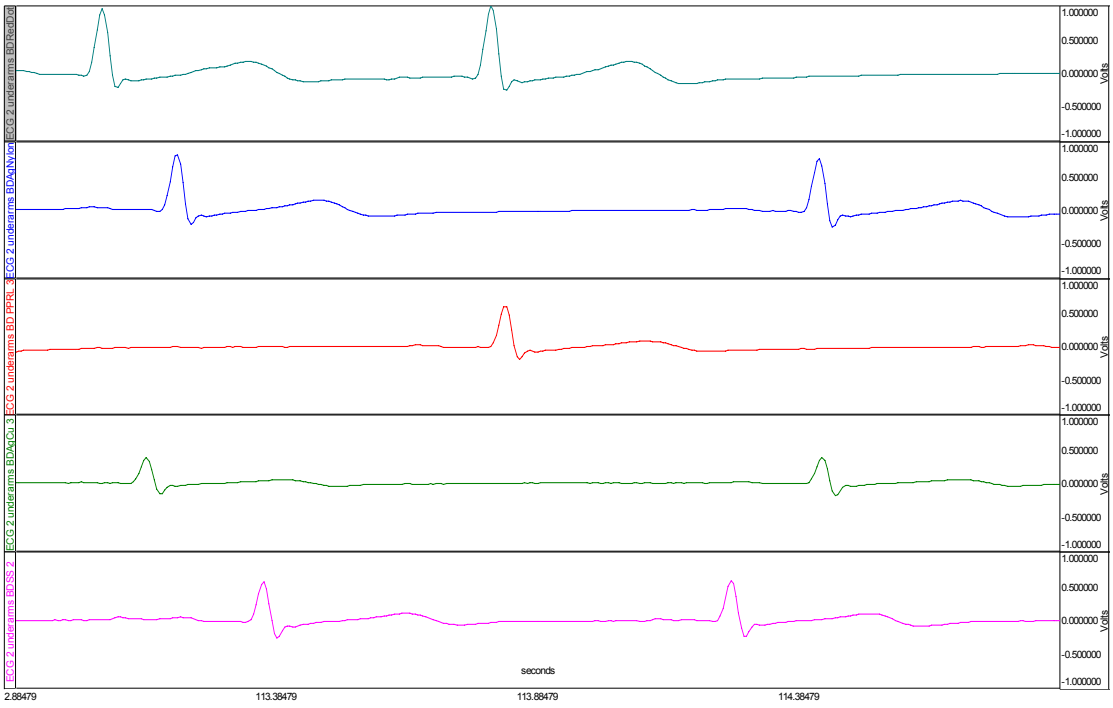

Figure 50. Initial tests on single subject (as displayed on Biopac AcqKnowledge software), multiple electrodes (mid chest reference). Top to bottom, Red Dot, AgN, PPY, AgCu, SS.

Detailed waveforms and tabulated results are described in section 4.1. From visual inspection it is evident that the detected ECG signal is different for different electrodes. This is most likely due to the differing electrode skin surface resistance (impedance). The normal or typical skin model described earlier in Chapter 2.6.3, Figure 10, incorporates a resistive component together with a shunt capacitive component. In the case of Red Dot which exhibits a low resistance value for the skin contact and hence the shunt capacitive component is bypassed by this and has a minimal effect on the acquired signal. The surface electrode capacitance for the Red Dot or any electrode is directly proportional to the separation between the effective conductive layers of the skin and the surface of the electrode.

$$\mathbf{C = \varepsilon A/d = \varepsilon_0 \varepsilon_r A / d} \qquad \textbf{farads} \qquad \textbf{(11)}$$

where,

C is the capacitance in Farad

A is the electrode surface area in square meters,

d is effective the spacing between the skin and electrode in meters,

ε is the permittivity,

ε_0 is the dielectric constant for a vacuum = 8.854pF/m and

ε_r is the relative dielectric constant for the medium in the skin-electrode space.

The values of parameters for fabric electrodes with uneven irregular surfaces have not been reported and any capacitance values quoted have only been empirically deduced. Practical fabrication of the electrodes in the knitting process allowed a conductive area to be constructed, but the conductive surface contact area of the fabric is by observation not a continuous or contiguous coverage over the electrode area. The cover factor varies dependant on a number of factors including yarn tex, number of knitting needles used and the density. If placed under tension which is the case in tests or indeed in fact in a practical garment or vest the cover factor will change. In general, is has been observed in the test electrodes that the cover factor may change from 80% to 60%.

Due to the nature and availability of the conductive yarns used to fabricate the different electrodes it was not possible to construct the electrodes so that they had

precisely the same physical characteristics other than the same overall conductive area. To better compare the effects of only a change in the conductive base yarn e.g. AgN, AgCu, SS or Polypyrrole (PPY), it is desirable that the physical characteristics of the yarn were the same but this was not possible. Hence fabric electrodes were constructed from available materials with generally similar characteristics as detailed in section 3.3. The actual electrode area was designed to be 20 x 20 mm but in practice electrodes were within +/-20% of this value.

All tests on multiple subjects were conducted using the same reference electrode as the test electrode (not Red Dot as used for single subject). To permit more reliable skin contact for the reference electrode than offered by mid chest position a measurement was done with the reference electrode next to the RA electrode (under arm). This provided good signals and this position was used in multiple subject tests.

During initial testing on subjects it was observed that when pressure sensors were placed in the electrode test band the pressure values were not constant. Investigation showed that this was partly due to movement of the subject but the variation was cyclic in nature and found to be due to the effect of respiration. Adjusting of the band for desirable pressure was therefore based on an average value.

3.7.2 ECG Feature Extraction Algorithm

In order to permit comparison of electrodes, features of the ECG waveform as described in section 2.4 need to be determined. An algorithm was developed in Matlab script to extract the following features from ECG waveforms as shown in Figure 5.

- Peak Amplitudes: Pmax, Qmax, Rmax, Smax, Tmax
- Intervals: QRS, QT, PR, PQ, ST and
- Peak Intervals: SRpi, RQpi, TRpi, RPpi and RRpi

The raw waveforms acquired from the Biopac system are saved in Matlab format allowing direct input to the algorithm. No additional filtering or manipulation of the data was performed before analysis.

The R peak is used as the reference point for extraction of all features. The R peak is not always the dominant peak but it is the sharpest and the derivative of the spectrum will highlight this point. The start of the waveform data set is aligned to be between R peaks and a search is started looking for the maximum derivative within the search window, which identifies where R peak lies. Rmax is then found as the maximum value of the data around this point. With the position and value of Rmax found the extraction of features is found by finding the positions and values of the other waveform peaks;

Searching forward from R peak to find the next minimum, S peak
Searching backward from Rpeak to find the next minimum, Qpeak
Searching forward from Speak to find the next maximum, Tpeak
Searching backward from Qpeak to find the next maximum, Ppeak

The positions of derivative minimums of the ECG waveform around these points, is used to identify the start and ends of the intervals QRS, QT, PR, PQ and ST. The intervals between peaks are calculated from the positions of the peaks previously found. This sequence is repeated for each period of the ECG waveform. On reaching the end of the waveform data set, the mean and standard deviation for each feature is calculated from each individual period. A detailed description of the feature extraction algorithm Matlab script is in Appendix H. As mentioned earlier, the signals analysed by the algorithm are raw and any embedded noise or arrhythmia directly affects the standard deviation. This is apparent in some of the results tabulated in the Appendix.

3.7.3 ECG electrode performance tests - multiple subjects

To determine whether the results and differences observed on a single subject were repeatable, further test were performed on a larger number of subjects.

Subjects were recruited from within CSIRO TFT. Male subjects were selected for testing to limit variability and remove the need for extra supervision for female subjects. Ten subjects were selected at random and their physical characteristics such as age, height, weight and build, varied, see Appendix F, Table F. The single subject used initially for the first trials is also retested as part of this group and is subject 9.

Tests were performed in a Lead 1 configuration, i.e. right under arm, left under arm with right under arm as reference ground potential.

Each subject was tested with four types of electrode, including the reference Red Dot electrode. Heart rate (HR), (listed as RRpi in the tables) is no measure of differences between electrodes as it has been shown that there is a close correlation between HR and emotions [142].

To reduce heart rate variability during testing sessions it was decided that subjects would be seated and to avoid being distracted were asked to watch a different video for each test. This not only helped to minimise variations in heart rate (and maintain emotional state), but also helped to reduce movement or motion artefact which is a common cause of signal degradation.

The first four subjects were tested first with Red Dot, then AgN, followed by stainless steel and then AgCu(s). The remaining 6 subjects were tested with the electrodes in a random order, but with Red Dot tested last. Time between testing of each electrode within a session was 5 minutes.

When testing a single subject and measuring the electrode pressure it was found that to obtain a pressure of 200 g/cm^2 the elastic /Velcro bands needed to be tightened to an unacceptable level. The maximum pressure that was perceived to be acceptable was less than 50 g/cm^2. Based on this, it was decided to adjust the band tension so that the force applied across the electrode was nominally, 100g (25g/cm^2) ~2.5KPa. This pressure is lower (1/4) than that suggested by GSR measurements, but is compensated by the increased contact area (x4).

It is interesting to note that the earlier tests on the single subject which used a common signal Red Dot electrode were of better quality(generally better S/N) than that obtained in the later multi-subject tests. This suggests that the reference electrode connectivity is very important to signal quality.

3.7.4 Repeatability on a single subject

In order to evaluate the repeatability of measurements, further tests were performed as follows.

1. Testing the same subject with 3 different pressures, low, medium and high. (3 electrodes)
2. Testing the same subject, with the same electrode/band on and off 3 times *
3. Testing the same subject, with all electrode types including improved electrodes

Electrodes tested were AgN; AgCu (s); AgCu(m); SS; WoolPPY; LV9315PPY. Results of this test are presented in section 5.4.

*A test for the temporal performance of a typical fabric electrode was included. This test was incorporated in the refit trial in which the same AgN electrodes were fitted (or refitted) then measured three times. Each trial was for 10 minutes. The band was then left and measured during the next two, 10 minute periods. The overall test time for this trial was 50 minutes.

The metals Ag, Cu, or SS have been applied to human skin for various purposes for a considerable time and are not considered toxic when placed on the skin. Conductive polymers are a relatively new field of research and as yet little has been reported as to the toxicology of these materials. A literature search on the toxicology of polypyrrole (used to prepare some of the test samples) was done but resulted in no suitable information. It was decided that it would be unwise to use these for long term testing on a human subjects until safety aspects are better understood. Testing according to a toxicology standard such as Oko-Tex Standard 100 [149, 150] is required. Therefore testing with polymer coated fabric electrodes although desirable, did not proceed on multiple subjects.

Chapter 4

4 Results and Discussion

The ECG signal formed the basis for the comparison of fabric electrodes. The feature extraction algorithm described in section 3.7.2 is used to extract the key characteristics of the ECG waveform (as described in section 2.4). This will enable determination of how accurately fabric electrodes can detect a signal consistent with that of conventional electrodes.

Motion artefacts were considered and only sections of waveforms without large signal artefacts were selected for analysis. In general there was little motion artefact.

4.1 ECG Performance of prototype Fabric Electrodes – Single subject results

These initial tests were performed on a single subject to test the first versions of the knitted fabric electrodes sewn into the first prototype bands (section 3.7.1 Figure 49). The PPY/AgN fabric electrode used in this test was a knitted AgN fabric patch polyester backed and coated with conductive polymer which is different to the LV9315PPY and WoolPPY tested in section 4.4. The AgCu used here was a multifilament yarn. The time domain response of the five electrodes, Red Dot, AgN, PPY/AgN, SS and AgCu from tests on a single subject are shown in Figure 51, Figure 52 and Figure 53.

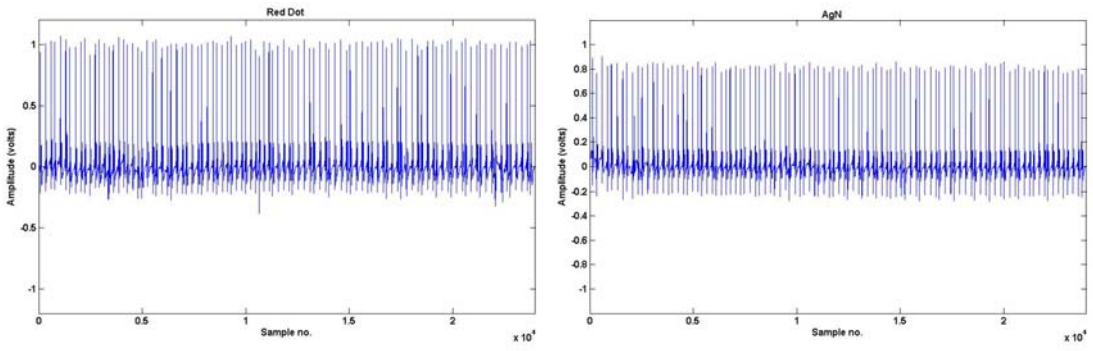

Figure 51. Time domain response (sampled every 5msec) of Red Dot, left and fabric AgN electrode, right.

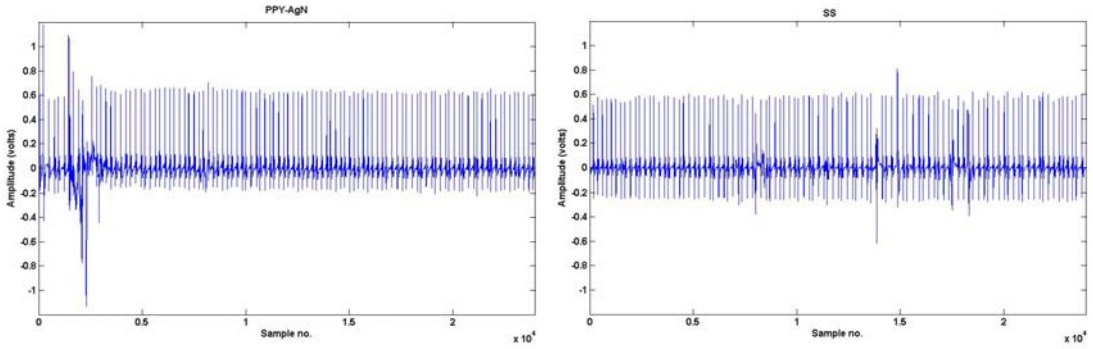

Figure 52. Time domain response (sampled every 5msec) of fabric PPY/AgN electrode, left and SS, right.

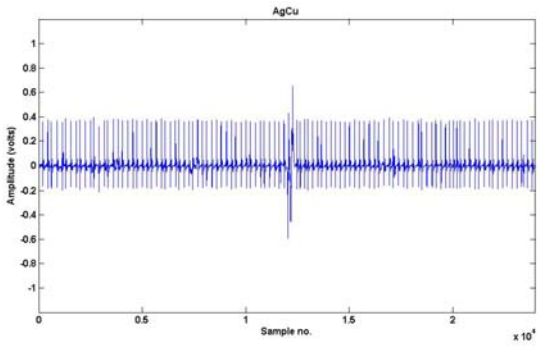

Figure 53. Time domain response (sampled every 5msec) of fabric AgCu electrode.

It can be seen that the amount of artefact present on the signals (seen as transient disturbances in the waveform) is low. The level of the signal envelope is the highest for Red Dot and reduces for the other electrodes. A comparison of typical electrode waveforms is shown in Figure 54 for a single heart beat.

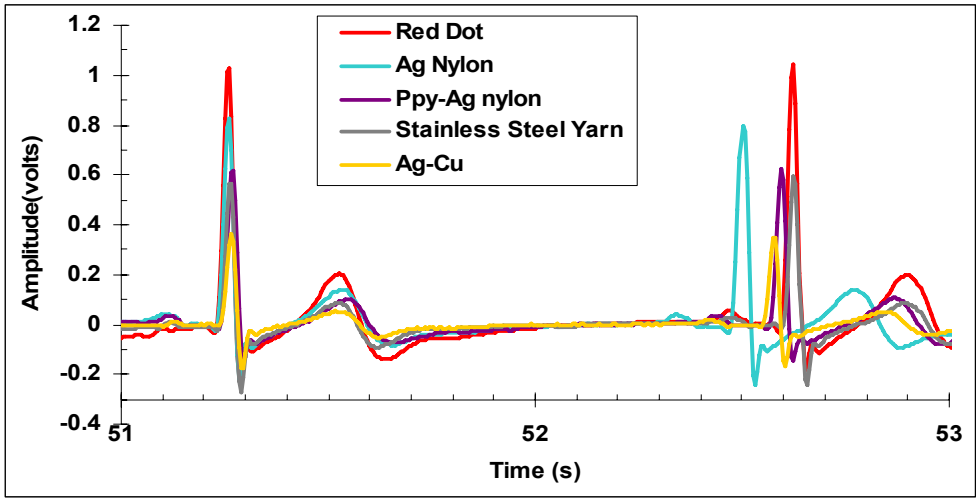

Figure 54. Comparison of a typical ECG waveform of 1 heart beat, during 2 minute test period showing ECG Signal of Red Dot and four fabric electrodes tested on the same subject.

Figure 54 shows that the waveforms are not periodic; this is described as arrhythmia (irregular heart beats). This made feature extraction algorithm analysis sometimes difficult and accounted for the apparent large standard deviation in RR for some subjects, including subject 9 (see Appendix F). The visual morphology of the signal is not changed in the detected waveforms, with only amplitude differences apparent. The signals are also devoid of noise, likely due to the use of Red Dot reference electrode. As mentioned, a Red Dot reference electrode is not used for the fabric electrode tests on multiple subjects.

The results obtained from the feature extraction algorithm for these waveforms are shown in Table 3. The subject used was the same subject identified as subject 9 in the multiple subject tests.

Table 3.

Results from feature extraction algorithm for subject waveforms in Figure 54.

SUBJECT 1	ELECTRODE TYPES mn = mean value, sd =standard deviation									
Peak	RD mn	RD sd	SS mn	SS sd	AgN mn	AgN sd	AgCu mn	AgCu sd	PPYmn	PPYsd
Pmax(volts)	0.03	0.04	0.02	0.01	0.02	0.03	0.01	0.01	0.02	0.02
Qmax(volts)	-0.05	0.02	-0.02	0.02	-0.03	0.02	-0.01	0.01	-0.02	0.01
Rmax(volts)	1.00	0.03	0.57	0.02	0.81	0.03	0.37	0.01	0.63	0.02
Smax(volts)	-0.21	0.03	-0.25	0.02	-0.23	0.02	-0.18	0.01	-0.17	0.02
Tmax(volts)	0.19	0.02	0.08	0.01	0.14	0.02	0.05	0.01	0.09	0.01
Intervals	Interval times are the number of samples, each sample is 5msecs.									
QRS	22.30	1.90	22.55	4.95	22.20	2.37	23.12	5.15	21.63	2.64
QT	85.03	2.73	79.16	6.47	83.33	3.08	75.46	10.23	81.91	5.87
PR	26.86	8.29	25.80	3.00	28.33	4.06	23.30	6.18	25.82	4.61
PQ	8.78	4.09	11.84	4.96	11.05	5.31	8.13	5.45	8.20	5.45
ST	11.22	4.60	5.81	5.40	7.54	1.01	5.38	1.43	7.88	2.03
SR pi	5.62	0.49	5.47	0.51	5.48	0.50	5.40	0.50	5.54	0.50
RQ pi	7.11	1.23	7.22	3.12	7.11	1.30	8.60	4.28	7.75	2.77
TR pi	54.57	2.01	52.16	2.33	53.56	1.02	51.75	1.80	53.60	1.53
RP pi	26.30	7.92	31.44	3.85	30.85	3.89	29.73	3.61	30.09	2.65
RR pi	239.35	52.40	231.23	42.35	236.37	47.64	228.84	39.85	229.08	39.68
Intervals	in msecs									
QRS	111	9	113	25	111	12	116	26	108	13
QT	425	14	396	32	417	15	377	51	410	29
PR	134	41	129	15	142	20	117	31	129	23
PQ	44	20	59	25	55	27	41	27	41	27
ST	56	23	29	27	38	5	27	7	39	10
SR pi	28	2	27	3	27	3	27	2	28	3
RQ pi	36	6	36	16	36	7	43	21	39	14
TR pi	273	10	261	12	268	5	259	9	268	8
RP pi	132	40	157	19	154	19	149	18	150	13
RR pi	1197	262	1156	212	1182	238	1144	199	1145	198

The waveforms for all electrodes on this subject displayed a large amount of arrhythmia which was not catered for in the algorithm and standard deviations for some measurements are large. For example, RR peak interval (RR pi). Slight adjustment of search windows in the feature extraction algorithm improved performance of extraction for later tests (for subject waveforms with arrhythmia).

With some people, P and Q waves are very low in amplitude, similar to noise level (30mV) and information related to these is unreliable. A low or non existent P or Q wave is apparent in some healthy people and those with cardiac problems [46]. If the P or Q wave is of low level, the accuracy in determining its amplitude, peak position and onset is reduced. For interval measurements related to these waves particularly, PR, PQ, RPpi and RQpi results have a large standard deviation.

The key features of ECG signal derived from the feature extraction algorithm analysis; peak intensity, peak-peak intervals, and feature interval, for a wide variety of electrodes tested with this subject is shown in Figure 55. These results have not been corrected for time interval variations due to any changes in RR (e.g. QTc), as the RR variation over the four tests within the single session was 6% and 9% for the last test (PPY) a separate session.

It can be seen from Figure 55a that the overall peak amplitudes have been preserved best with the AgN and PPY/AgN fabric electrodes. The peak to peak intervals in Figure 55b, show that again these are best preserved with the AgN and PPY/AgN electrodes. Similarly Figure 55c shows the same trend with AgN and PPY/AgN electrodes being the best in maintaining interval widths. Overall SS performed worst than these electrodes based on the extracted features and AgCu was worst of all.

For main ECG interval features excluding those related to P and Q waves, the values are within 10% of Red Dot. From these results, based on the comparison of extracted features of the ECG, it can be seen that both AgN and PPY/AgN fabric electrodes can reproduce ECG waveforms without loss of feature information.

a).

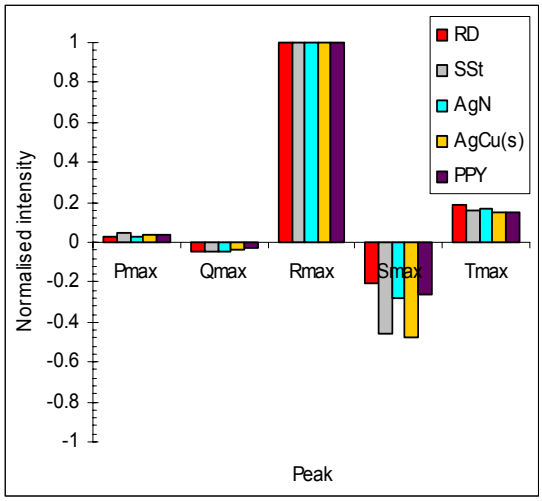

b).

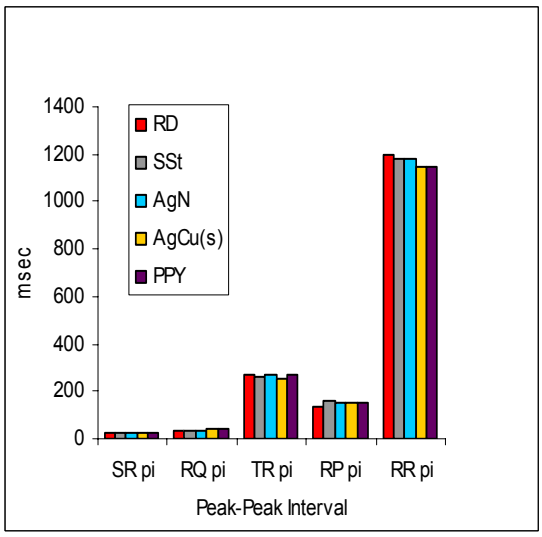

c).

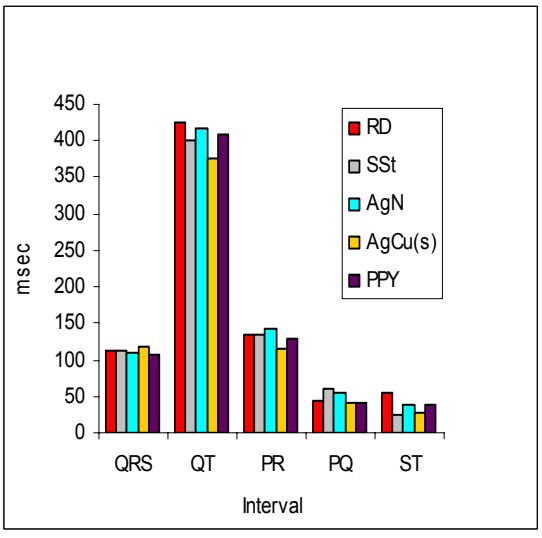

Figure 55. First trials, algorithm analysis of 4 minute test waveform of Red Dot and four electrodes (Red Dot chest reference) on single subject, a). peak intensity, b). peak-peak intervals, and c). feature interval.

The observed difference in the transient response of electrodes when compared with the Red Dot response can be accounted for due to the differences between electrodes contact coupling resistance and coupling capacitance as described earlier in section 2.5.2.

Of particular interest is the response of the stainless steel electrodes. This result is supported by recent research [97], where studies with typical metals used as biomedical recording electrodes in weak aqueous NaCl solutions were discussed. This is relevant as the skin electrode interface will include a sweat component which is of similar composition. It was shown that all metals studied, including Ag and stainless steel, display a decrease in serial resistance R_p and capacitance C_p as frequency increases. Electrode polarisation impedance is also inversely proportional to electrode area [28, 97], so a large area will provide lower impedance. The construction of the electrodes that were tested was such that as the SSt yarns were 'coarse' the electrode area was relatively rigid when compared with the other electrodes and also less compressible and conformable. The more fabric like the electrode the better it contacts with the skin's surface and helps to provide an improved contact area. With the stainless steel electrode according to [97] it had the largest serial resistance at 0.01Hz (essentially DC) ten times that of other metals and a serial capacitance an order of magnitude lower. These signals are of low frequency and this is where the capacitance is lower and the resistance for stainless steel is highest. As a result the capacitive impedance is even higher at low frequencies. This could account for the observed poorer performance during experiments and noise of the stainless electrodes particularly with movement.

The average waveform for each electrode is shown in Figure 56.

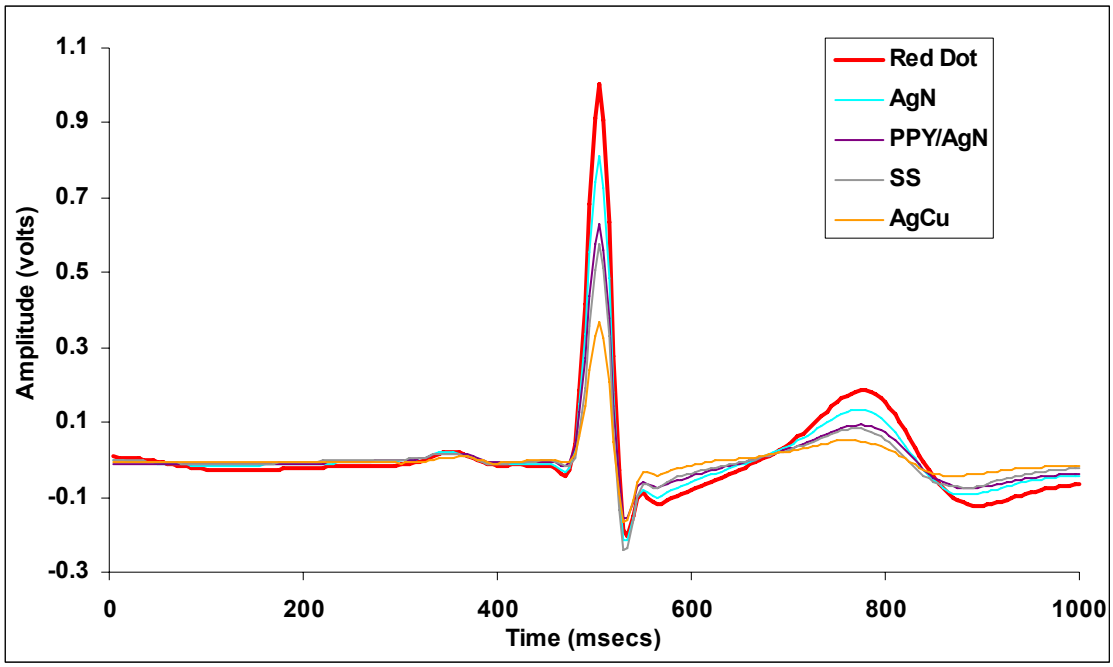

Figure 56. First trials on single subject, average ECG waveforms for Red Dot and four fabric electrodes.

From Figure 56 average ECG results, compared with Red Dot(1V), AgN (0.8V) has the largest amplitude, followed by the PPY/AgN(0.63V) and SS(0.58V) electrodes. AgCu (0.37V) has the lowest. All except the AgCu (monofilament) electrode show promise as the basis for use as practical electrodes.

4.1.1 ECG detection using fabric electrodes - multiple subjects

These tests were performed using the new knitted detachable electrode assemblies (described earlier in section 3.3.1.1), together with the associated band. The electrodes tested were Red Dot, SSt, AgN, Ag Cu(s) as shown earlier in section 3.3.1 Figure 17 and Figure 18 .

Test results for each subject's feature extraction algorithm analysis and composite plot of each electrodes average waveform are shown in the Appendix F. As subjects were seated during test periods motion artefact was minimised.

It was observed in subjects with higher levels of body fat that the detected ECG signals were generally of lower absolute amplitude. In subjects with medium build and lower

levels of body fat, better signals were detected. Motion artefact is also more apparent in subjects with higher levels of body fat. Body Mass Index (BMI) is defined as the ratio of weight/height^2 and is a measure which can indicate the amount of body tissue. Subjects in this study had a BMI that varied from a minimum of 20.4 to a maximum of 30. The amplitudes from subjects near these two extremes are shown in Figure 57.

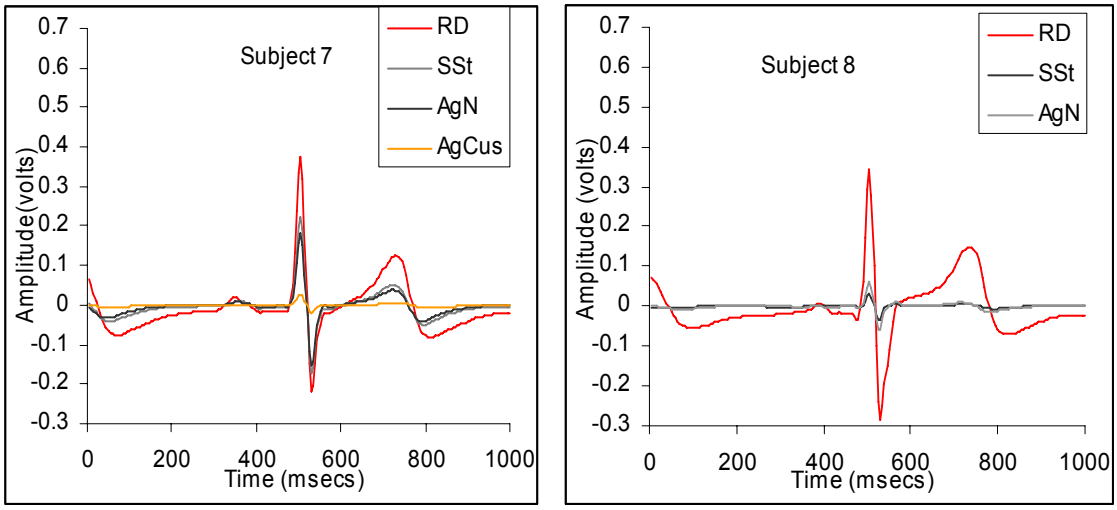

Figure 57. Average ECG electrode waveforms for two subjects with different BMI. Subject 7, BMI 29, Subject 8, BMI 21.

The subject with low BMI produced low signal levels from the fabric electrodes, 1/5 of the value of the Red Dot, which could not be analysed using the feature extraction algorithm. The high BMI subject produced similar Red Dot values but the fabric electrode levels were much higher (2/3 of Red Dot). A study conducted by Shen et al [151], has suggested that there is a relationship between BMI and some aspects of the ECG signal. It is also suggested that BMI may be an indicator of abdominal volume.

4.1.2 Waveform Analysis and Comparison Multiple subjects

The full results from the feature extraction algorithm analysis across the sample population are tabulated in Appendix F, which show the mean and standard deviation for each feature of the ECG waveforms for each electrode.

4.1.2.1 Body Mass Index, electrode pressure and ECG amplitude

To determine if there was any relationship between the physical characteristics of the subjects (Appendix F, Table F1), electrode pressure and ECG signal level, the BMI was determined for all subjects. A plot of BMI vs. the electrode signal amplitude is shown in Figure 58.

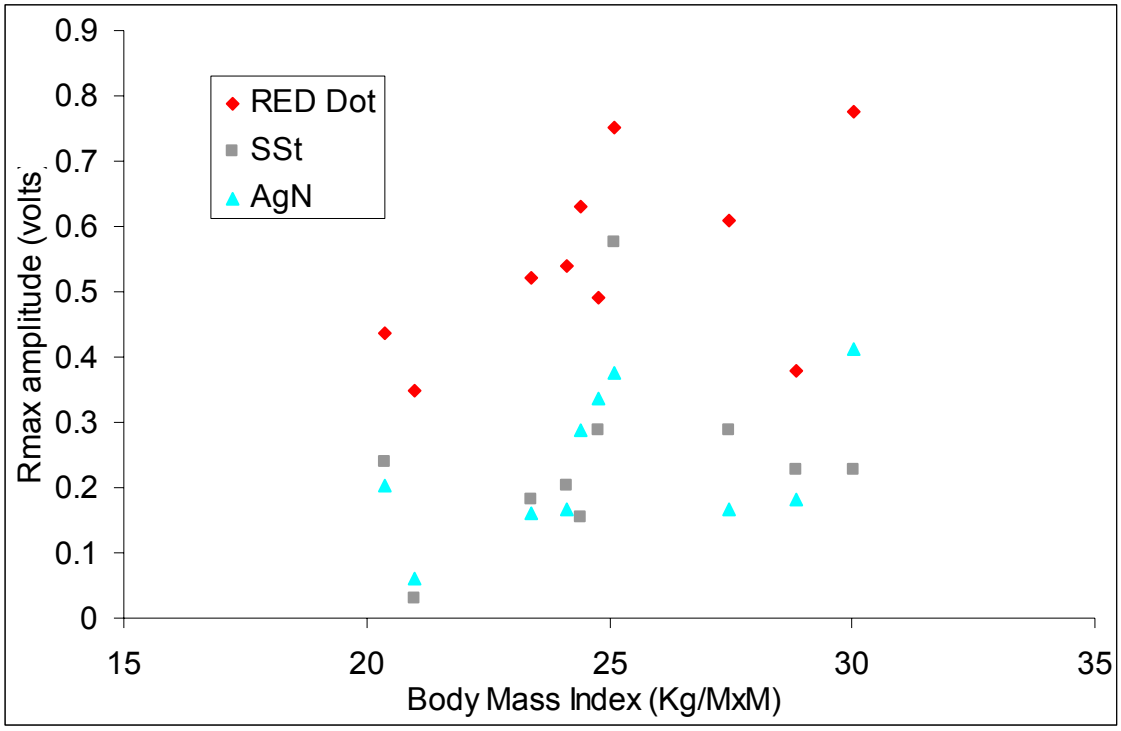

Figure 58. BMI versus Rmax amplitude across the sample population.

Due to the scattering of data an overall trend cannot be determined but Figure 58 indicates that signal levels from subjects increase with increase in BMI value. It is important to note that the trend measured with Red Dot electrodes is also apparent with the fabric electrodes. Attempts have been made to determine the effect of torso impedance on epicardial and body surface potentials by modelling [152]. The modelling of the electrical pathways from the cardiac source to the body surface includes skeletal muscle, subcutaneous fat layers and the epicardial and lung surfaces. This work shows that surface potentials are affected by changing torso loads. The largest change of potentials was seen with highly anisotropic (which displays directional properties) skeletal muscle layers which greatly effects current flows within the torso. Isotropic (homogenous) layers showed the smallest effect, which implies that, the fat to muscle ratio effects ECG surface potentials levels. Interestingly subjects 7 (BMI 28.8) and 10

(BMI 30) had almost the same BMI but subject 7 had a visually higher level of fat tissue (less muscle) and a lower signal level.

As clothing pressure is dependant on fabric extensibility, stretch level and curvature of the skin surface [120] it can directly affect electrode pressure. The average pressure during testing (for both sensors) on each fabric electrode across the sample population is shown in Figure 59.

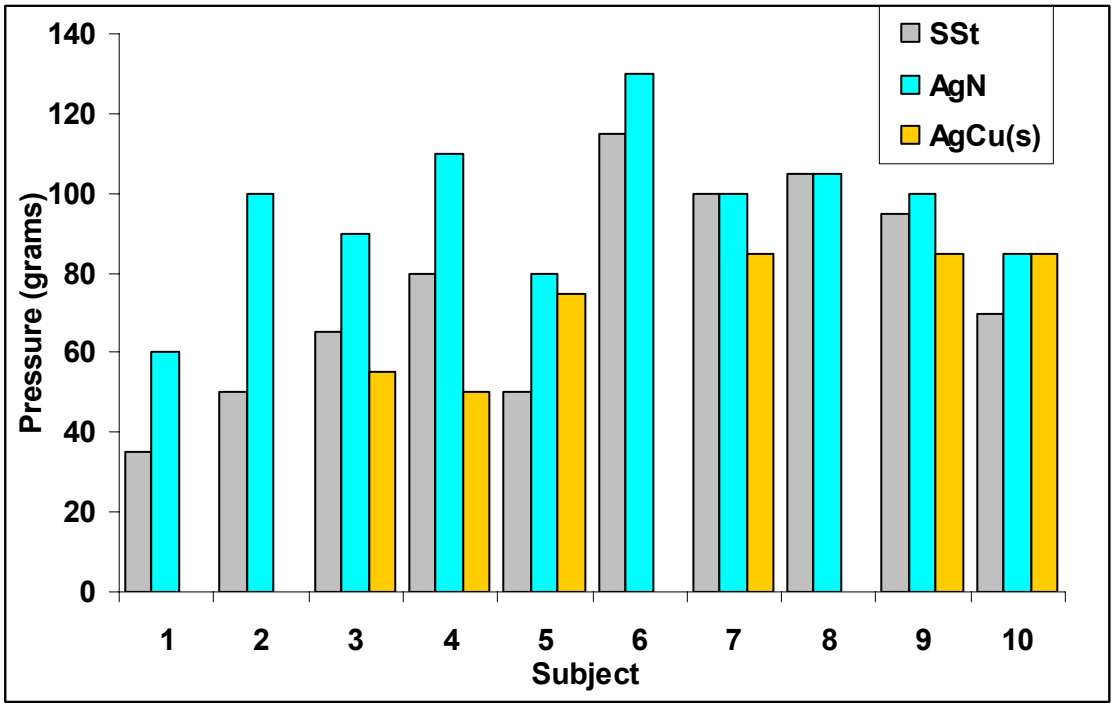

Figure 59. Average electrode pressure achieved for each fabric electrode, across the sample population.

The maximum electrode pressures achievable for each subject depended on what was considered acceptable by each subject. In general, the chest band pressure achieved was consistent with comfortable garment chest pressures reported in other studies [122]. With some subjects it was difficult to set the target pressure of 100 grams load (derived from section 3.7.3 earlier and subject comments on comfort). It can be seen from Figure 59 that AgN settings are higher than SSt. It was generally more difficult to achieve high pressures with SSt than the other electrodes, perhaps due to the bulky and less conformable structure of this electrode. As pressure directly affects surface friction and the level of artefact due to motion, performance of the SSt electrode may have been affected.

In general it was found difficult to set consistent pressures for the different electrodes on individual subjects and across the population. The ability to apply consistent pressure depends not only on BMI but the muscle/fat structure of the subject. To highlight this, the average and standard deviation electrode pressure for each subject's set of electrodes is shown in Figure 60.

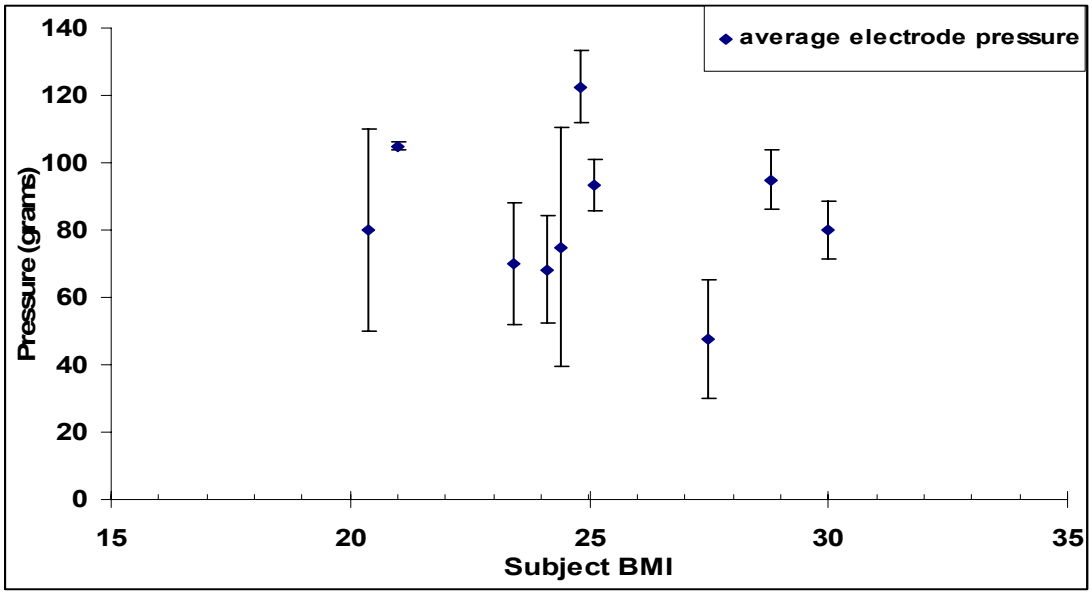

Figure 60. Average electrode pressure with standard deviation and BMI across the sample population.

Across the sample population the average pressure values vary over a wide range from 45 grams to 120 grams. Pressure effects contact resistance as described in section 2.5.5 and can affect detected biosignals. This will contribute to ECG signal amplitude variation between subjects.

During overall testing and adjustment of the test bands including feedback from all subjects, it was concluded that a pressure of 2.5 KPa (100gram force) for each electrode was deemed an acceptable (maximum), comfortable level.

4.1.2.2 ECG results

With the need to make useful comparisons between the electrodes, it was decided as discussed in section 2.4, that the features of the ECG, amplitudes of peaks and time intervals of the acquired waveforms would be used. The analysis results (Appendix F) allows direct comparison of these features and are used to derive the following charts.

As QT interval is an important measurement this could be corrected according to the formula of Hodges [73] and Framingham [153] (see section 2.4.2). As the variation of RR during test sessions was low (<5% except for subject 7), QT correction did not need to be applied to the results. The variation of RR interval for the sample population is shown in Figure 61. Manual calculations are included from the raw SSt waveforms for subject 1, 6 and 8, as these could not be analysed by the algorithm.

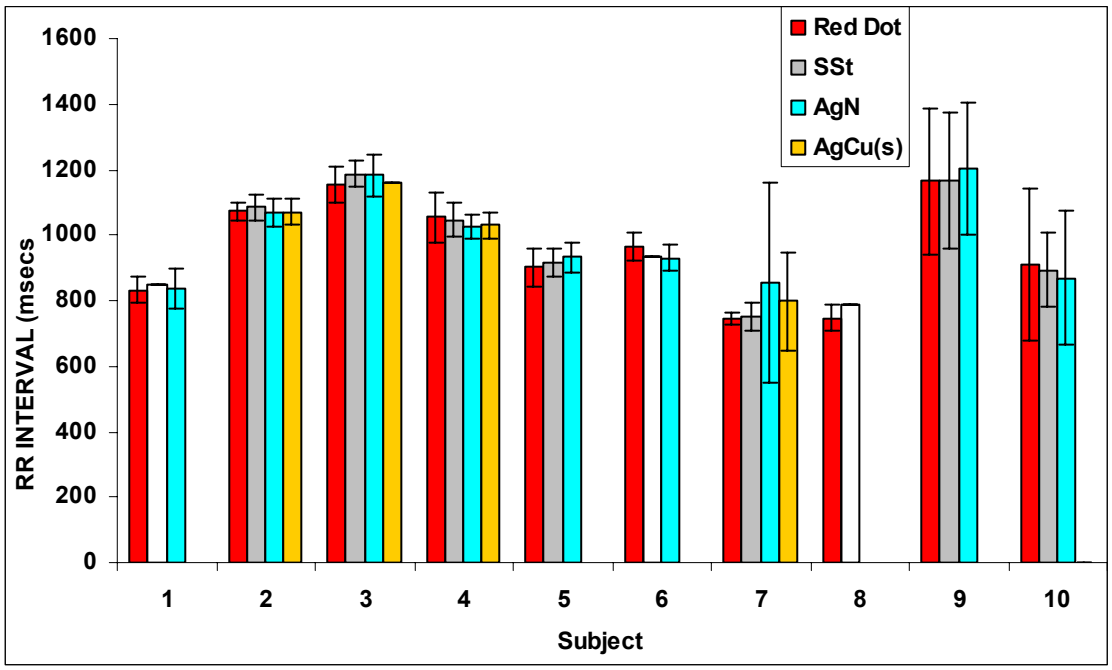

Figure 61. RR interval variation for Red Dot, SSt, AgN and Ag(s) electrodes across the sample population.

Though the RR of the subject population was consistent for individual subjects, significant variation of the detected ECG signal amplitudes was observed. The absolute Rmax values acquired across the sample population are shown in Figure 62.

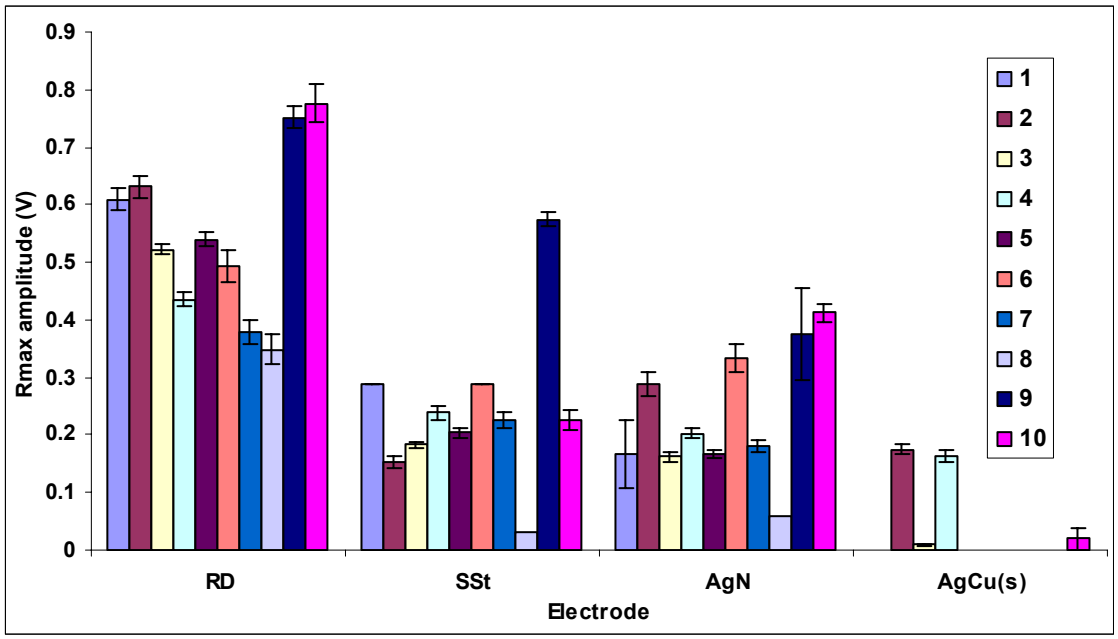

Figure 62. Rmax of ECG signal relative peak amplitudes for all electrodes across the sample population.

The difference in signal amplitude between subjects varies from an average of 0.55V for Red Dot to 0.24V for SSt and 0.235V for AgN. Subject electrode waveforms, generally with amplitudes lower than 0.1V with a high noise component and those with a high level of signal artefact, could not be analysed. Other than poor signal amplitude, arrhythmia or excessive departure of the waveform from that expected of the typical ECG were difficult to analyse. This was particularly apparent with the AgCu(s) electrodes. The raw signals acquired from Biopac were analysed with the feature extraction algorithm and no processing was performed on the data sets. The raw data includes not only artefact, but embedded noise which has an effect on the standard deviation (σ). As described earlier, the algorithm measures the features of each individual cycle ECG cycle. Any noise on the signal directly affects the σ values of the data set. Two features of the ECG waveforms are shown for the sample population. Values of QT interval and the coefficient of variation (CV) are shown in Figure 63 and values of QRS interval and the CV of QRS interval are shown in Figure 64.

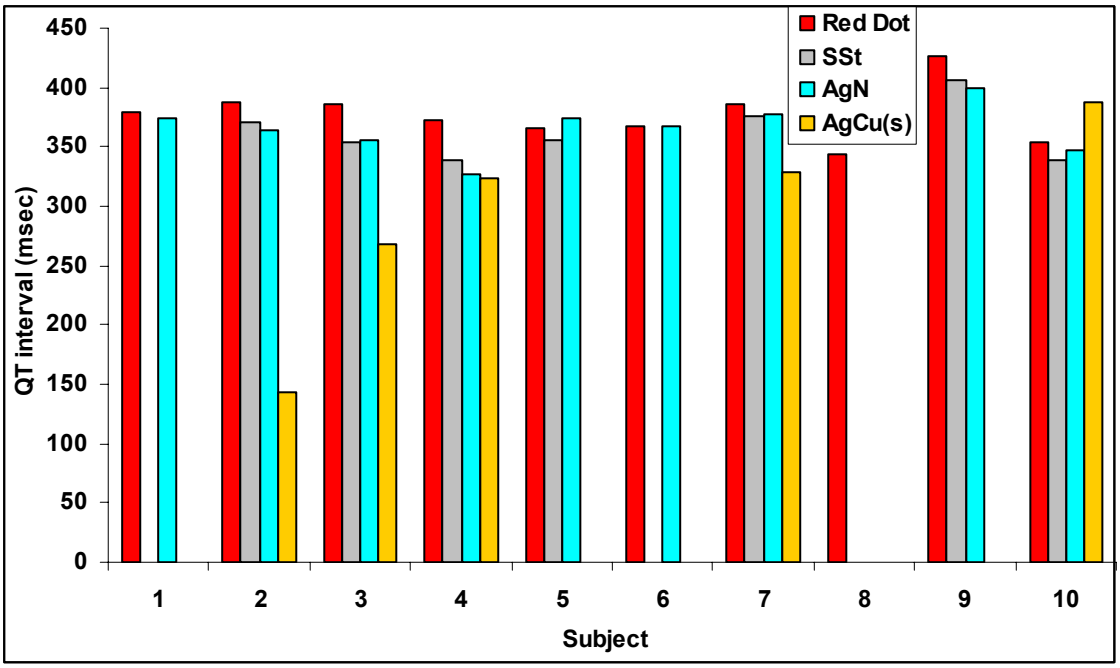

a).

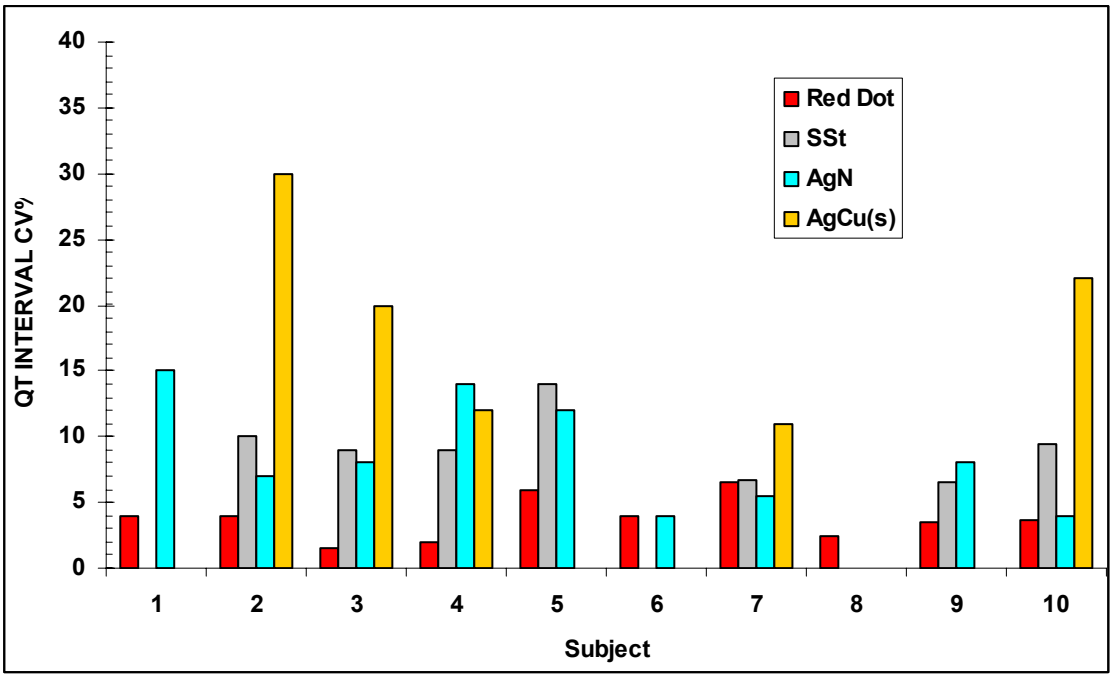

b).

Figure 63. QT interval variation, a). QT interval value for all electrodes across the sample population, b). QT interval CV% for all electrodes across the sample population.

For Red Dot (the reference), the CV of QT interval is less than 6%. Generally AgN has a better CV than other electrodes.

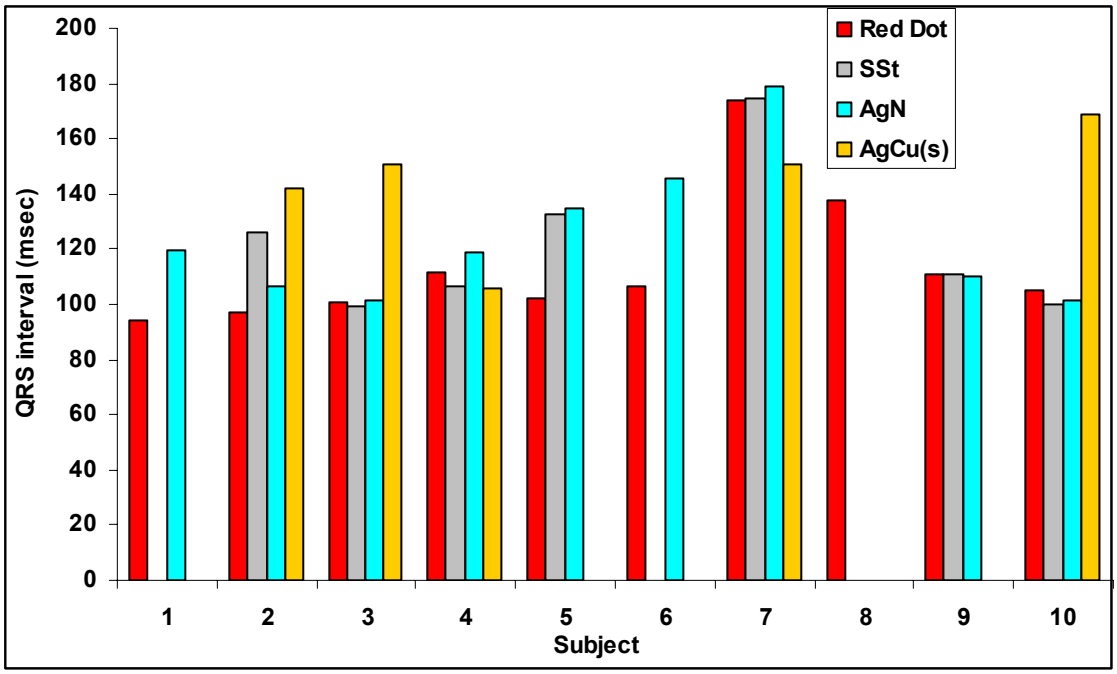

a).

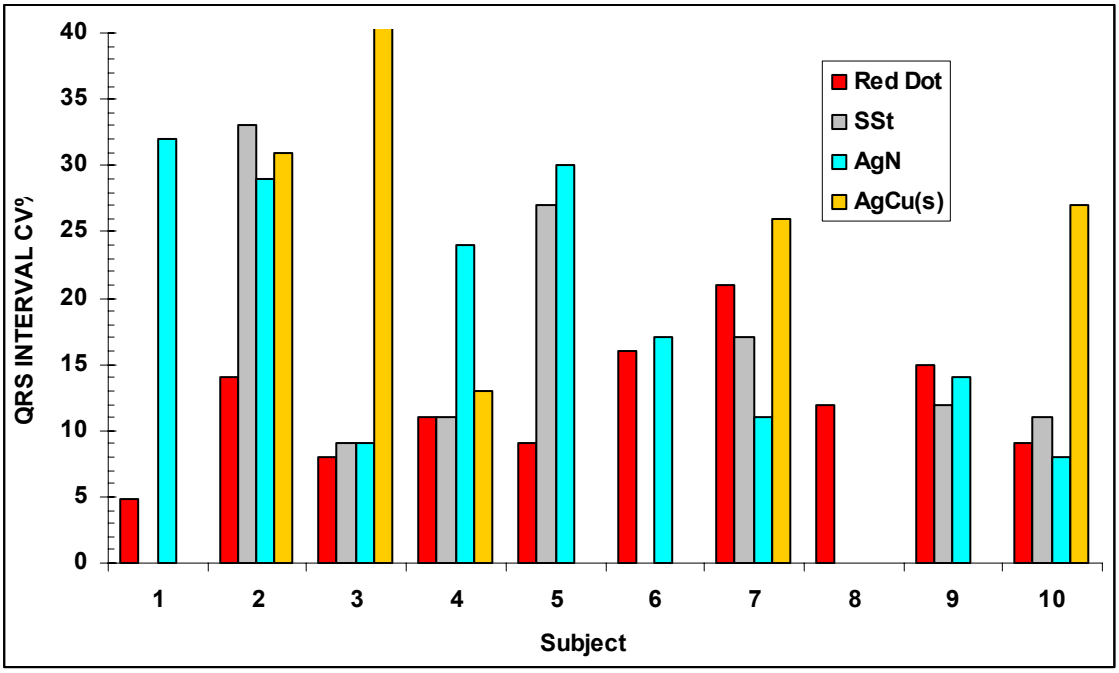

b).

Figure 64. QRS interval, a). QRS interval value for all electrodes across the sample population, b). QRS interval CV% for all electrodes across the sample population.

For Red Dot the CV of the QRS interval is large with a mean of 10%. SSt and AgN gave similar results, with AgCu(s) showing the largest variation. This may be due to the presence of low levels of P and Q waves in the waveforms of many subjects (as described earlier in section 4.1).

A comparison of features of the electrode waveforms for one subject, derived by the feature extraction algorithm are shown in Figure 65.

a).

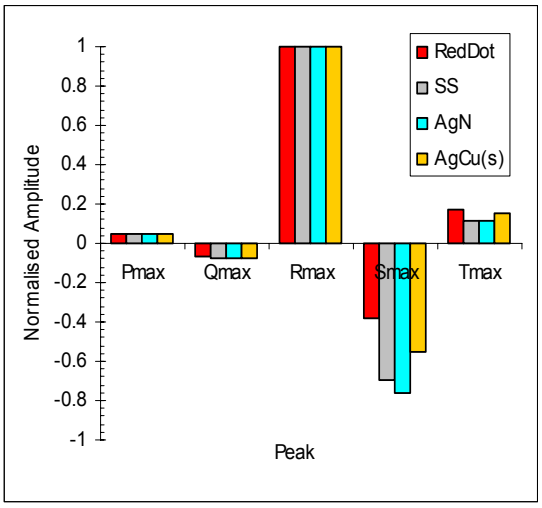

b).

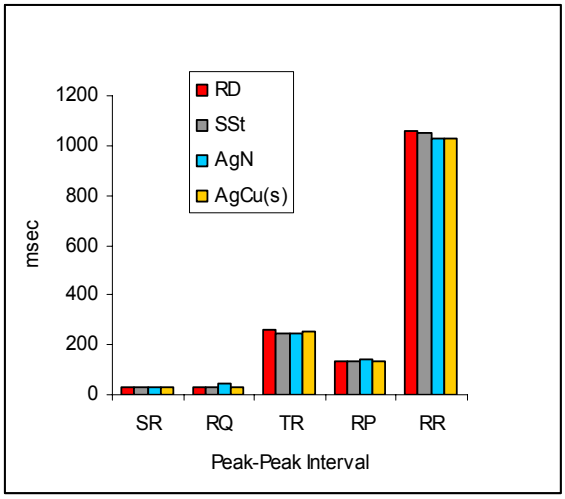

c).

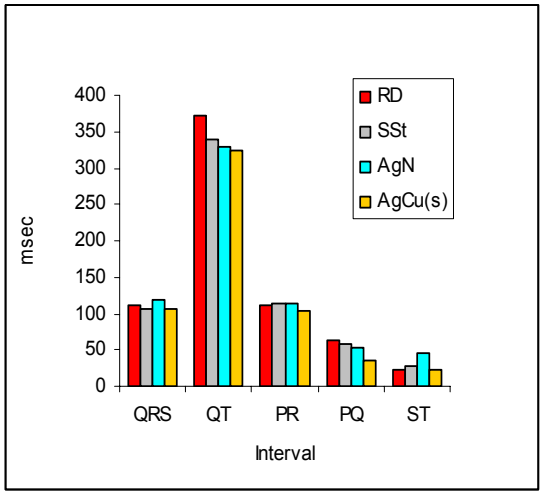

Figure 65. Characteristics of the ECG waveform for a single subject [subject 4 BMI 20.3] for all electrodes, a). Rmax normalised Mean Peaks, b). mean peak to peak intervals, and c). feature mean interval times.

Figure 65 shows that intervals and relative peak amplitudes have been largely preserved across all electrodes, even though the amplitudes were lower in all electrodes compared with Red Dot. For this subject, peak amplitudes were best represented by the AgCu(s) electrode, whereas for peak to peak intervals SSt and AgCu(s) performed better. For intervals SSt was best. The AgCu(s) result was not supported by the sample population as only one other subject provided waveforms that could be analysed. The AgCu(s) electrode waveforms of other subjects were too low in amplitude. The observable difference in S_{peak} amplitude is discussed later in section 4.3.

4.1.2.3 Temporal changes of ECG amplitude

Visual analysis of the results from the 4 minute tests are also interesting. In all subjects there was a change in signal amplitudes with positive and negative peaks being affected equally. Generally the amplitudes for the AgN and the SS electrodes increased from the start of the test to the end by 10-20%. This would be due to the wetting effect of sweat over the electrode contact area which reduces the electrode-skin impedance and reduces the skin resistance due to conductance through the appendages. These electrodes are comprised entirely of the conductive yarns used for each. For the AgCu(s) electrodes where signals were measurable, a reduction of up to 50% in amplitude with time was evident, totally opposite to that of the other electrodes. In all subjects, the amplitudes of the signals from the AgCu(s) electrodes are also lower than all other electrodes, (possibly due to the much lower density of conductive to non conductive area of this particular electrode).

The temporal effect over a 4 minute test session for AgN and AgCu(s) electrodes is shown in Figure 66.

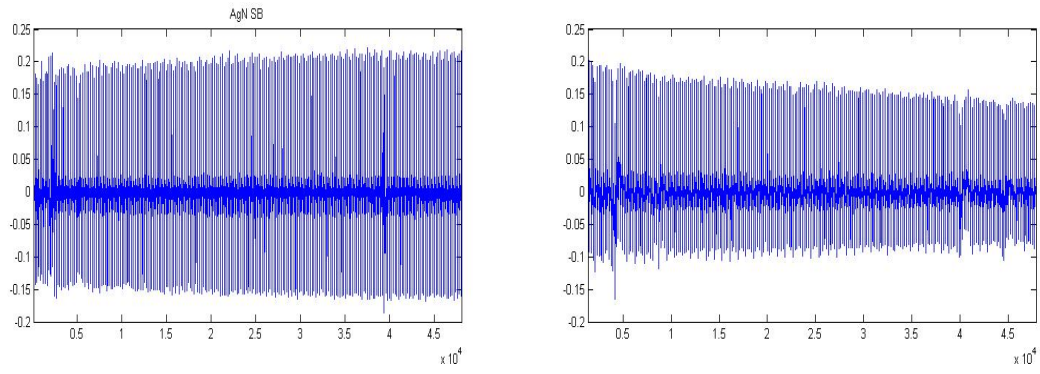

Figure 66. Typical amplitude temporal response(sampled at 5msec), AgN electrode left, AgCu(s) electrode right.

The reduction of signal level with time for AgCu(s) may be attributed to absorption and wicking of sweat away from the surface of the skin and away from the small individual contact area that each conductive fibre provides. The density of the conductive fibres is low in this electrode (compared to other electrodes) due to it's method of fabrication. Longer term tests using this electrode need to be conducted to determine if the signal recovers. Results suggest that electrodes with a higher density of conductive surface as is the case with AgN or SSt can provide larger amplitude signals. A higher density AgCu(m) electrode comprising a multifilament yarn can offer better performance.

4.1.2.4 Electrode signal quality

A simple measure of performance of the electrodes is whether the acquired signals can be analysed using an algorithm. The features extraction algorithm as described earlier is based on the typical ECG waveform. The algorithm used is not optimal or robust for use with any waveform and its ability to cope with abnormal ECG waveforms is limited. The tabulated subject results (Appendix F) are indicative of an electrodes similarity with Red Dot. The Red Dot waveforms for each subject did not present problems in analysis. A partial measure of the signal quality from fabric electrodes is whether features of the waveform can be extracted. Figure 67 shows a plot of the number of subject waveforms that could be successfully analysed with the algorithm, against the type of electrode. Success is based on the algorithm being able to derive all ECG parameter values.

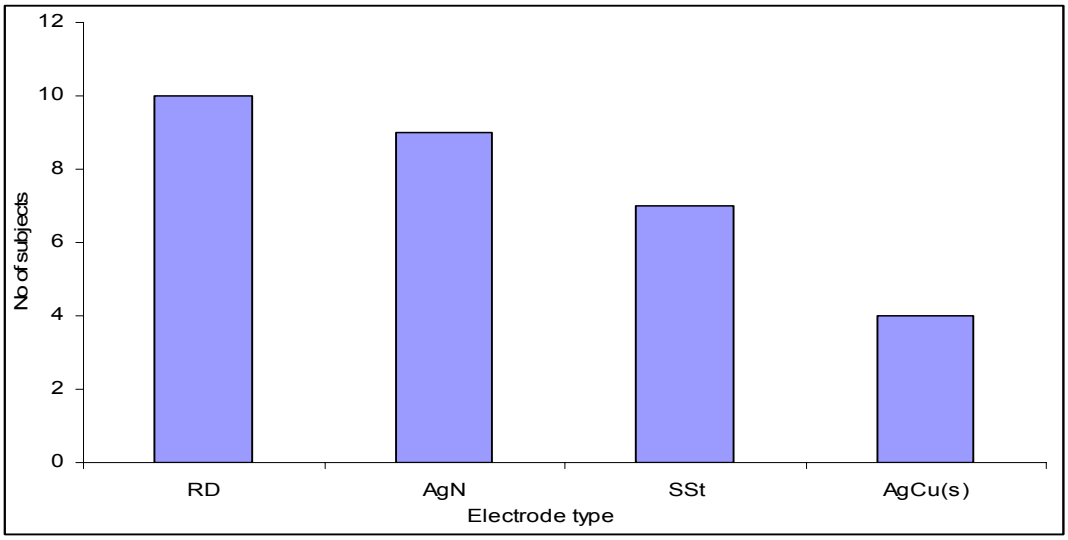

Figure 67. Analysis success for different electrodes across the sample population.

For low level signals or those with significant noise, all ECG parameters can not be determined. The trend of the ability to analyse subject waveforms, shown in Figure 67 shows that for the electrodes tested, the more fabric like the electrode, the better the detected signal. AgN is the most fabric like of these electrodes and these ECG waveforms had lower noise and artefact between QRS intervals. SSt has higher inherent levels of artefact present in ECG waveforms than other electrodes (e.g. see example Figure F1 in Appendix F). These signal artefacts corrupt the underlying subject ECG wave and characteristics cannot be derived using the feature extraction algorithm. Although the signal amplitude of the SSt is similar to AgN the level of artefact is higher which resulted in lower success. The AgCu(s) electrodes have generally low amplitude signals (more noise) across all subjects and feature extraction is less reliable. As a result these electrodes had the lowest level of success.
In some subjects, Rwave was not observed in AgCu(s) electrode waveforms and these were not saved.

4.2 Spectral characterisation of Electrode Measurements

During measurements it was observed that subjects which appeared to have dry skin did not produce good signals, whilst those with moist skin did. This is in contrast to higher levels of surface moisture which results in lower contact impedance and improved signals. As described earlier, the introduction of an electrolyte of any form is beneficial and essential in reducing skin electrode impedance.

Electrolyte in the form of sweat begins to form at the skin-electrode interface soon after application of the test electrode. The signals were not manipulated to optimise the waveforms so that the low frequency performance of electrodes could be highlighted. A plot of typical FFT spectral response from Red Dot and SSt electrodes is shown (from Matlab) in Figure 68. A reduction of spectral components below 5Hz can be seen, due to the Biopac high pass filter whose 3 db point is set at 0.5Hz. For Red Dot the spectral lines can be seen for the major ECG waveform components. This is not the case with the SSt electrodes (potential response and artefact) which generally have a large increase in spectrum below 5 Hz. AgN shows a lower level of low frequency components than SSt but still higher than Red Dot. The in band signal for both SSt and

AgN has more in band noise component and also lower in amplitude compared with Red Dot as seen in the time domain response (Figure 69 and Figure 70).

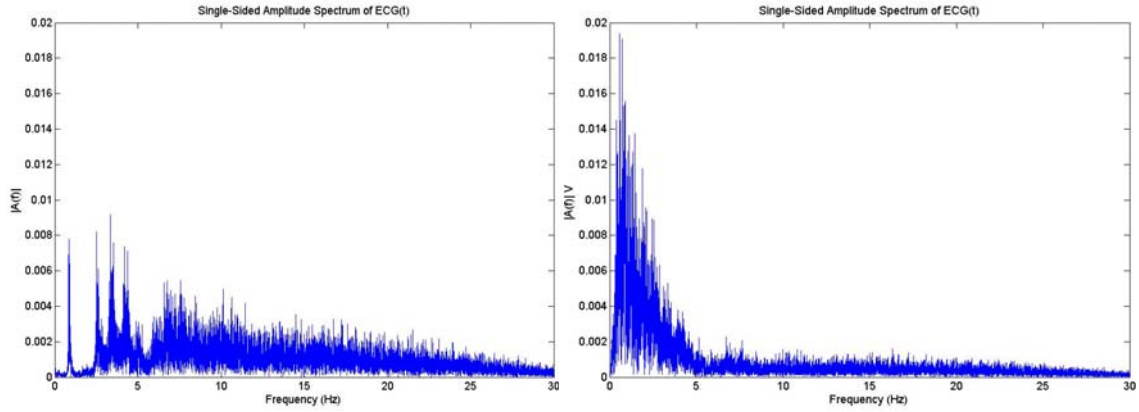

Figure 68. Typical spectral response, linear amplitude scale, Red Dot (left), SSt fabric electrode (right).

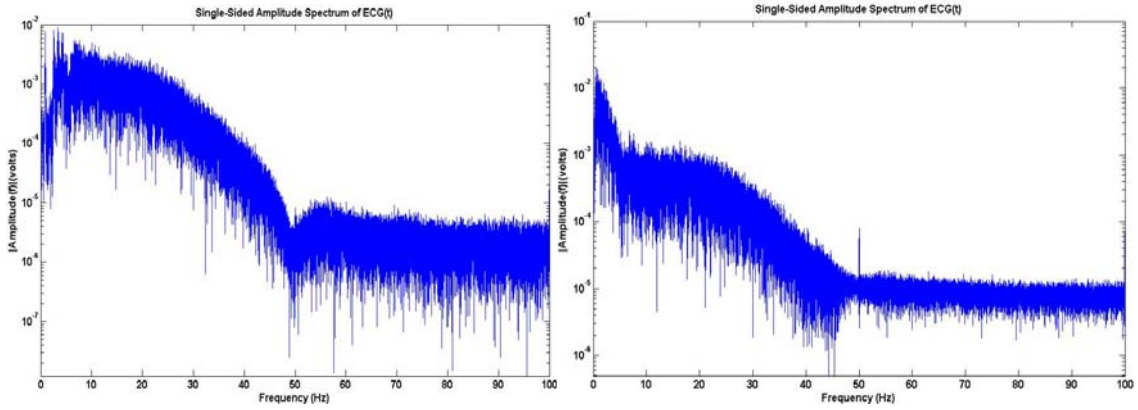

Figure 69. Typical spectral response, log amplitude scale for Red Dot (left), SSt fabric electrode (right).

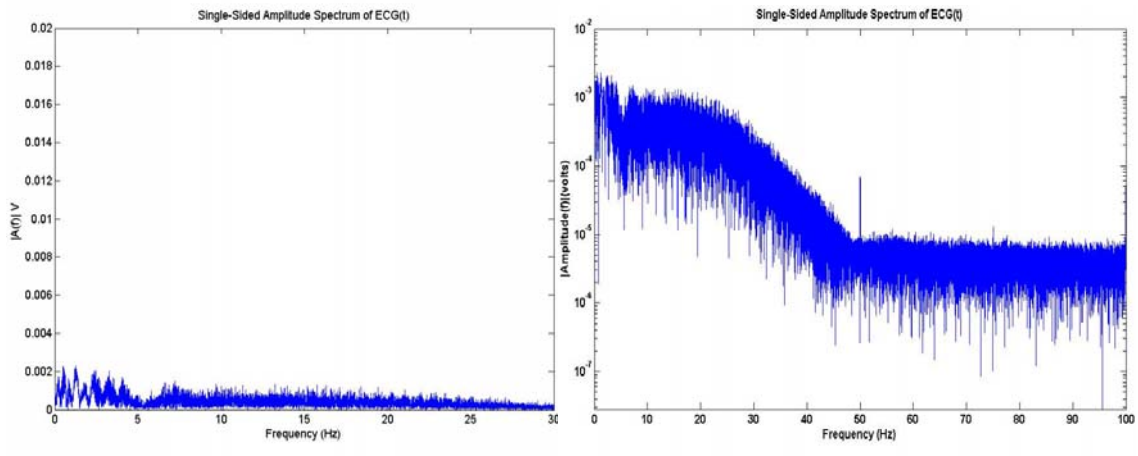

Figure 70. Typical spectral response for AgN fabric electrode, linear amplitude scale (left), log amplitude scale (right).

From Figure 68 it ca be seen that the stainless has poorer low frequency performance

than the reference Red Dot and AgN. (Note: A special component at 50Hz is noticeable for both the SSt and AgN electrodes)

4.2.1 Power Spectral Density (PSD) analysis

Another method of analysis, being used for HRV is the power spectral density (PSD). This is basically FFT^2 and is a measure of the where the power (or energy at various frequencies) within a waveform resides. PSDs were performed using Matlab (Welch's) on a sample of 'good' and 'poor' signals in order to help quantify the visually observed differences in the raw waveforms. These waveforms included any artefact that was detected during the measurement session. Examples are shown in Figure 71 and Figure 72 that highlight the result of poor connectivity. Similar responses (-45dB in-band levels) are obtained for both the AgN and SSt electrodes but the AgCu(s) shows a marked increase in low frequency component power at the expense of the desired ECG components.

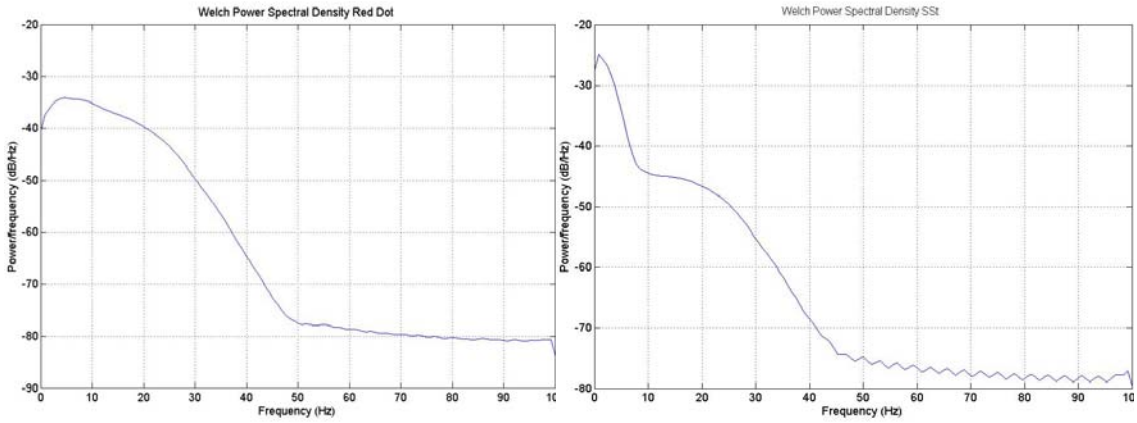

Figure 71. Typical PSD response for Red Dot (left), SSt fabric electrode (right).

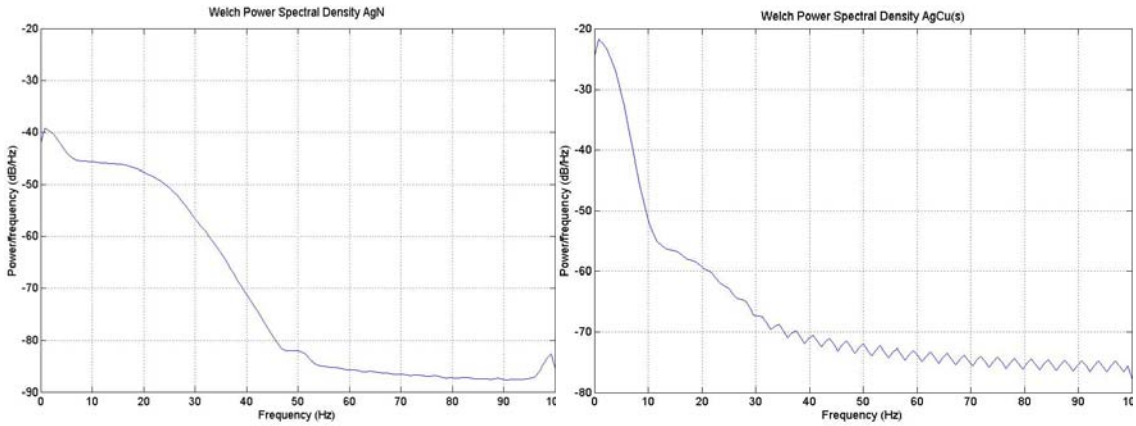

Figure 72. Typical PSD response for AgN fabric electrode (left), AgCu(s) fabric electrode (right).

The full effects of motion artefact can be seen in Figure 73 and Figure 74 for a set of SSt and AgN electrodes during a full measurement session, which shows both the time and PSD responses. These results are from the same subject and have very similar in-band ECG amplitudes. Note the high level of low frequency power component of the artefact evident for the SSt electrode. The higher degree of artefact for SSt was found to be the case across all subjects.

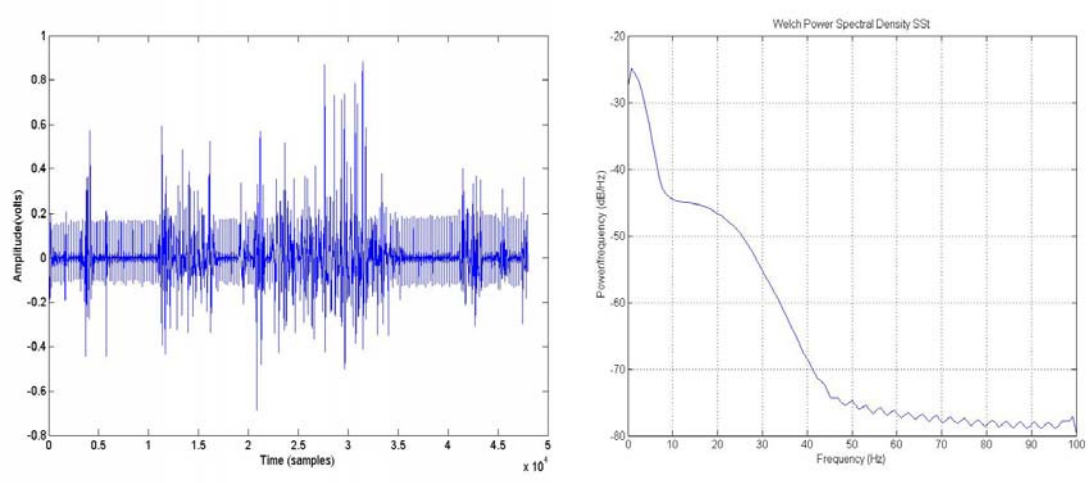

Figure 73. SSt fabric electrode motion artefact in time(left) and PSD(right) domains.

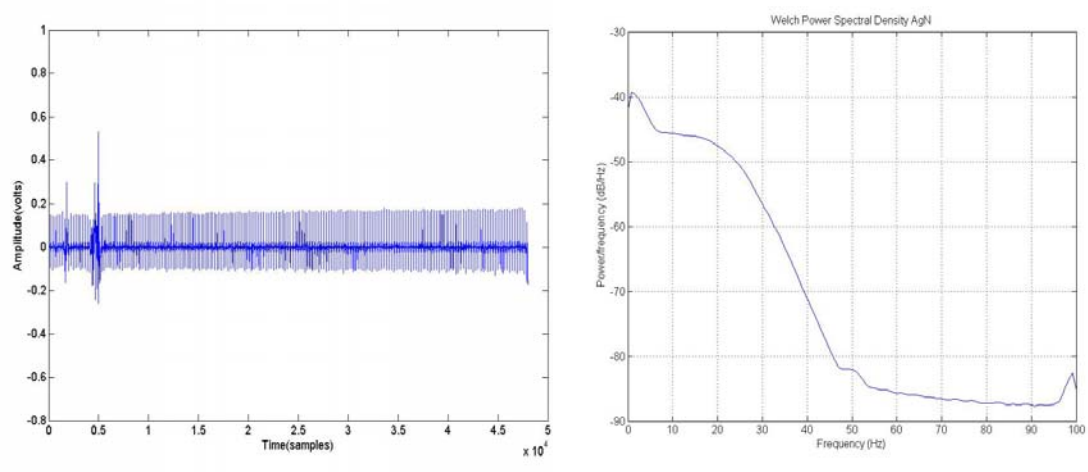

Figure 74. AgN fabric electrode motion artefact in time(left) and PSD(right) domains.

The signal waveforms amplitudes for some subjects were found to be inadequate to allow useful analysis and comparisons to be made. This was found generally with the AgCu(s) electrodes. This was partly due to the performance and repositioning of the reference electrode from the earlier single subject tests (ref mid chest with Red Dot), but

more importantly, to the poor performance of the AgCu(s) electrode itself which had reliability problems with continuity of connection across the surface of the electrode.

4.3 ECG Signal Variation

The ECG signal sensed by fabric electrodes is subject to change, due to variations in contact pressure, described in section 2.5.5 and time, referenced in section 3.7.1 and observed in earlier results in section 4.1.2.1. The ECG signal detected with the fabric electrodes tested has been observed to increase with increases in pressure and time. Experiments were conducted to measure the effects that contact pressure and time have on the acquired signals.

4.3.1 Effect of pressure on ECG signal

The tests on multiple subjects were performed at a nominal electrode pressure of 100gm. A test was done on a single subject to determine the magnitude of this effect. A test band was used with AgN electrodes and a series of tests were performed at three different electrode pressures, chosen arbitrarily at an average of 65gm (low), 75gm (med) and 120gm (high). The graph in Figure 75 shows that the amplitude of the detected ECG signal is proportional to electrode pressure. The highest amplitude, 0.6V is at the highest pressure and the amplitude falls with reduction in pressure to 0.4V. Figure 76 shows the amplitudes normalised to the highest pressure to ease visual comparison of the waveform shapes.

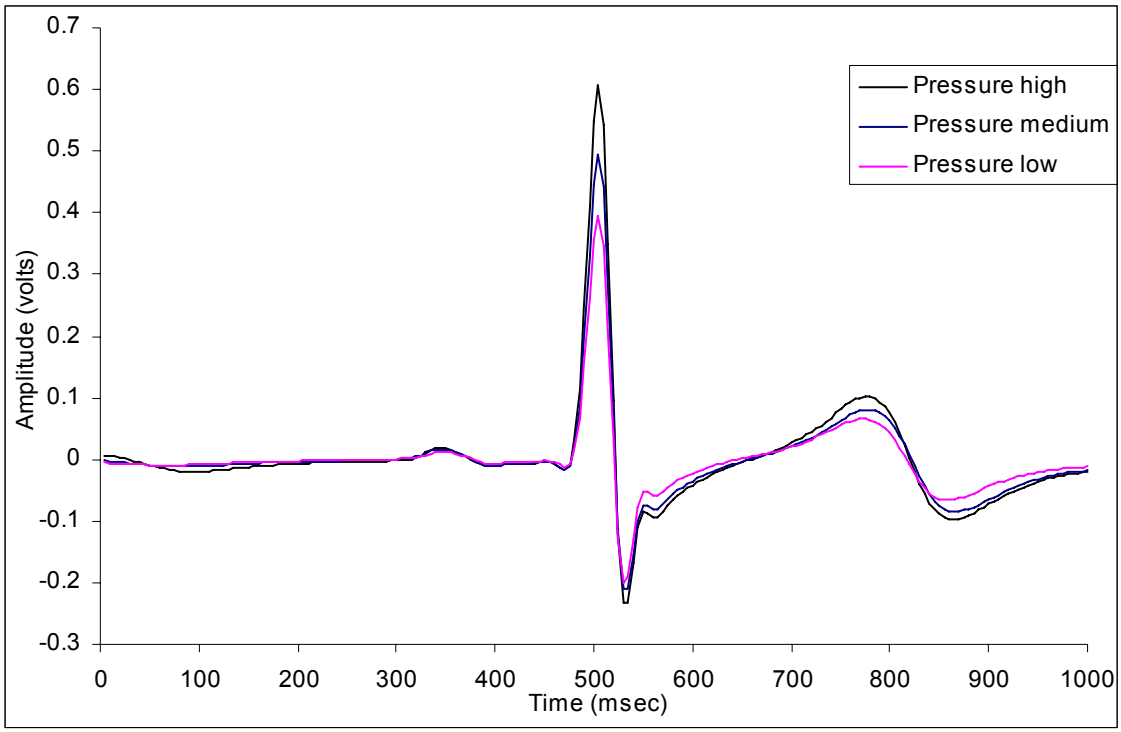

Figure 75. Effect of Pressure on detected ECG for AgN fabric electrodes.

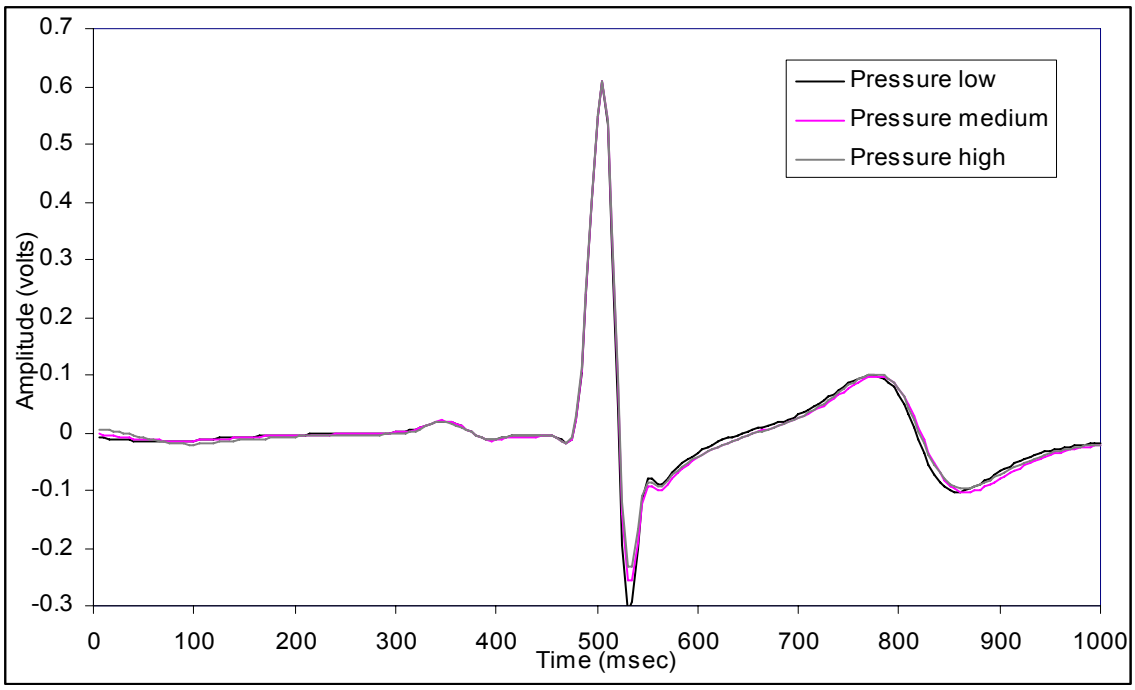

Figure 76. ECG waveforms normalised to highest pressure for AgN fabric electrodes.

The resulting curves in Figure 76, show that the waveshapes for the three pressures tested are almost visually identical. The effect of increase in pressure does not affect the detected signal in any way other than to provide an increase in amplitude and the visual

morphology of the signal remains the same. The absolute difference in amplitude of the signals (of the major peaks) with the change in pressure is shown in Figure 77.

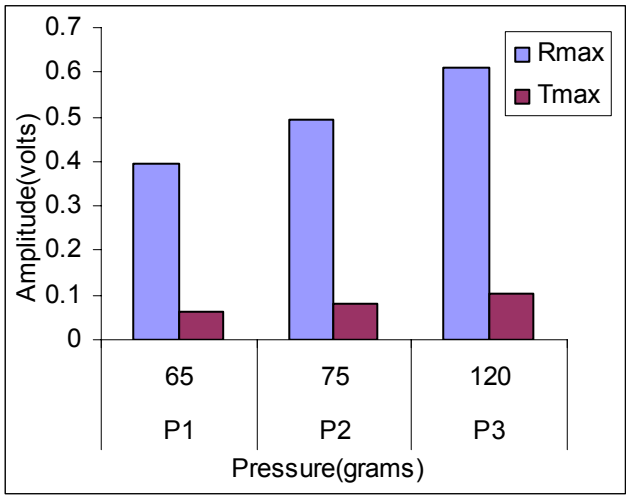

Figure 77. ECG amplitudes of Rmax and Tmax with pressure for AgN electrodes.

Although not thought clinically significant, an interesting difference between the waveforms is the variation of the S_{peak} amplitude. There is a noticeable increase in amplitude of the S_{peak} as the pressure is reduced. This presence in waveforms has been noted by other researchers as well, but no reason has been offered to explain it [154]. This may be due to the change in skin-electrode impedance i.e. the capacitance/resistance ratio and/or the imbalance or change in electrode impedance. As the pressure increases, the skin-electrode capacitance (as described in section 2.5.4) increases, but the contact resistance reduces. The basic input equivalent circuit of the skin-electrode interface is a differentiator circuit whose output is affected by ratio of impedance between the two shunt components C_E and R_E. The morphology of the QRS waveform is such that the gradient of the leading flank, QR, is lower that that of the trailing flank, RS, which falls more rapidly. Any differentiator action (due to capacitance) applied to the detected signal will be more apparent on this RS portion of the QRS interval. At lower pressure where the effective contact resistance is higher the capacitive path is predominant and this causes an increase in level of this derivative component. At the higher pressure the effect of the derivative component is diminished as it is shunted by the lowered value of contact resistance. It is proposed that the negative peak is affected by the relationship between the resistance and capacitance at the skin-electrode interface. The position of the reference electrode in relation to the sense electrodes may also contribute to signal imbalance and the S_{peak} value.

4.3.2 Temporal Variation of ECG

A longer term test was performed on a single subject to determine any effect on the detected ECG signal with time. The average ECG waveforms at the start and at the end of each time segment are shown for comparison in Figure 78. The waveform amplitude increased from the beginning to the end of the test by 35%, but the wave structure was otherwise unchanged. There was no apparent degradation or change in waveshape observed due to refitting of the band during this experiment.

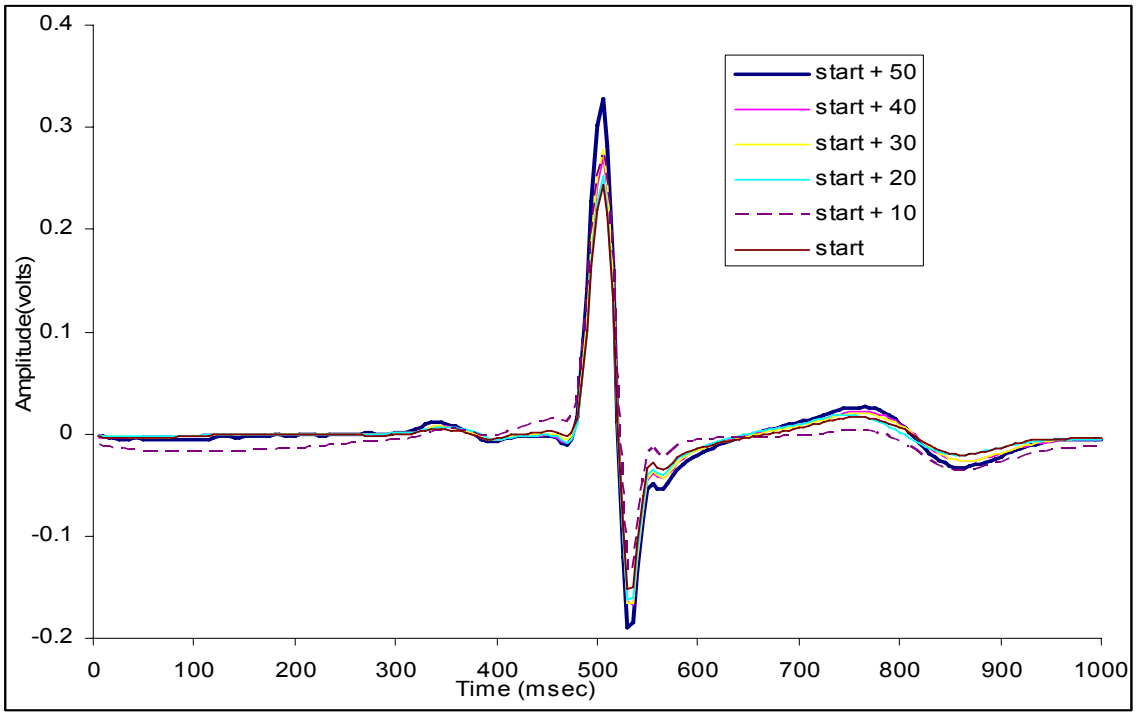

Figure 78. Temporal variation of AgN fabric electrode over 50 minutes at low pressure setting.

4.4 Improved electrode design - single subject test

It was observed that the overall performance of the AgCu(s) fabric electrodes is poor. Some measurements did indicate that the AgCu(s) electrode made from a single monofilament fibre, did not adequately test the suitability of AgCu as an electrode material. To fully test AgCu suitability a multifilament AgCu yarn was sourced and a few electrodes were knitted from this yarn. This electrode AgCu(m), along with SSt, AgN and two new conductive polymer based electrodes were tested on a single subject. The conductive polymer electrodes are designated LV9315PPY, a PPY coated fabric and a WoolPPY, a PPY coated wool fabric. The waveforms acquired are shown in Figure 80. These tests were conducted using three test electrodes of the same type. The AgCu(m) and the AgN electrodes gave almost identical performance. The SSt electrodes in this test gave the lowest signal levels.

For comparison, the spectral response of polypyrrole electrodes is shown in Figure 79. It can be seen here that the LV9315PPY has a similar response to that of Red Dot (see Figure 73 earlier) with only a small increase in artefact noise below 5Hz. The LV9315PPY and WoolPPY electrodes performed the best of the fabric electrodes in this respect.

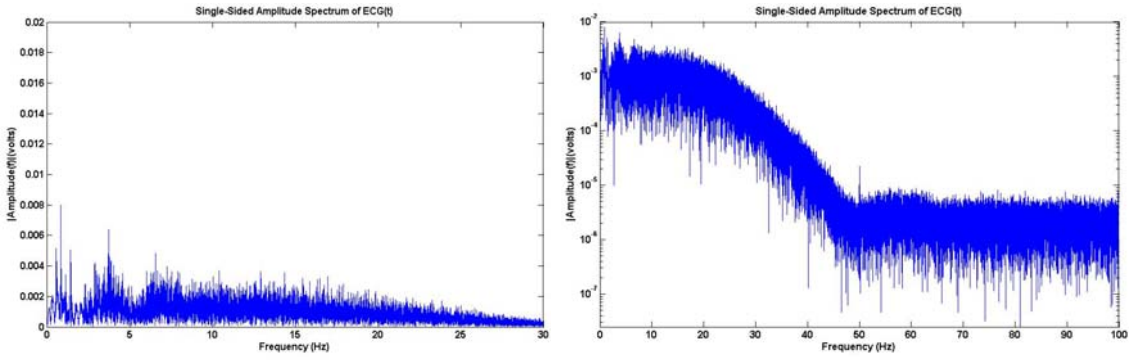

Figure 79. Spectral response for LV9315PPY fabric electrode, linear amplitude scale(left), log amplitude scale (right).

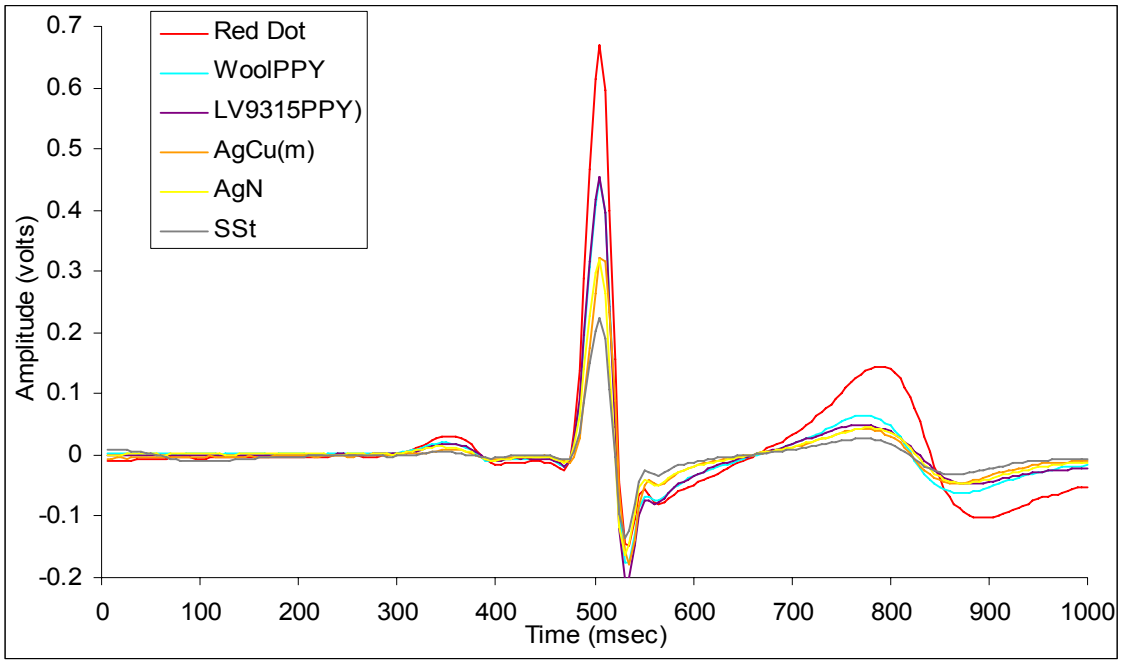

Figure 80. Comparison of Red Dot, 3 metals and two totally fabric PPY electrodes

It can be observed from Figure 80 that the amplitude of both PPY fabric electrodes is higher than the metal or metal coated electrodes. Figure 80 also indicates that WoolPPY and LV9315PPY are visually very similar (WoolPPY showing marginally better Twave amplitude). The improved amplitude from PPY fabric electrodes may be due to the redox potential difference between the polypyrrole and the metals.

4.5 Fabric Based Respiration Sensing

The subject tested was seated as in other tests. It should be noted that the depth of respiration (expansion and contraction of the thoracic area) of this subject was low and recorded signals were of low amplitude. It was noted that the particular subject did have shallow breathing. Deeper breathing results in larger amplitudes. Respiration rate can be derived from the waveforms with simple low pass filtering and thresholding. Step changes in level were due to large breaths being taken. The signal from the PPY strain sensor and the pressure sensor are shown in Figure 81. It can be seen that the signal from the strain sensor is essentially the 'same' as that from the pressure sensor. The signal from the conductive polymer sensor is reasonable but does show a limited response and is in agreement with others researchers, whether polypyrrole or conductive elastomer [128]. The CSIRO strain sensor shows a similar relationship with the pressure sensor positioned adjacent to it and its response is shown in Figure 82.

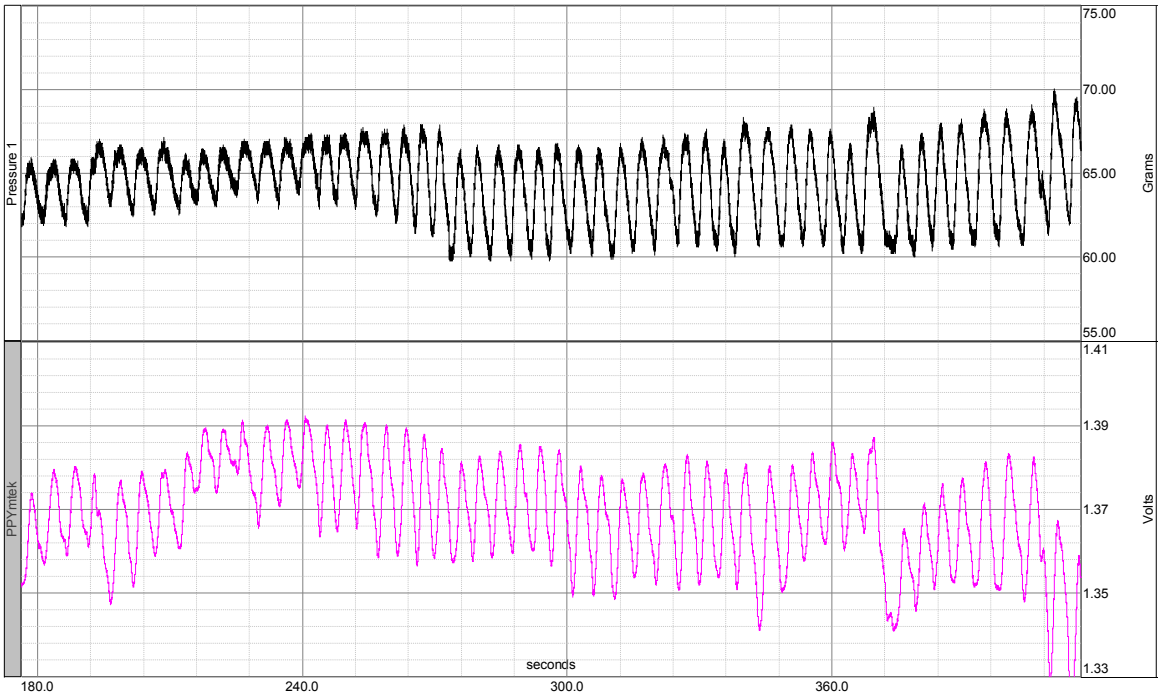

Figure 81. Thoracic respiration (as displayed on Biopac AcqKnowledge software), correlation between Pressure sensor 1 and PPY sensor, horizontal time(s), vertical(volts).

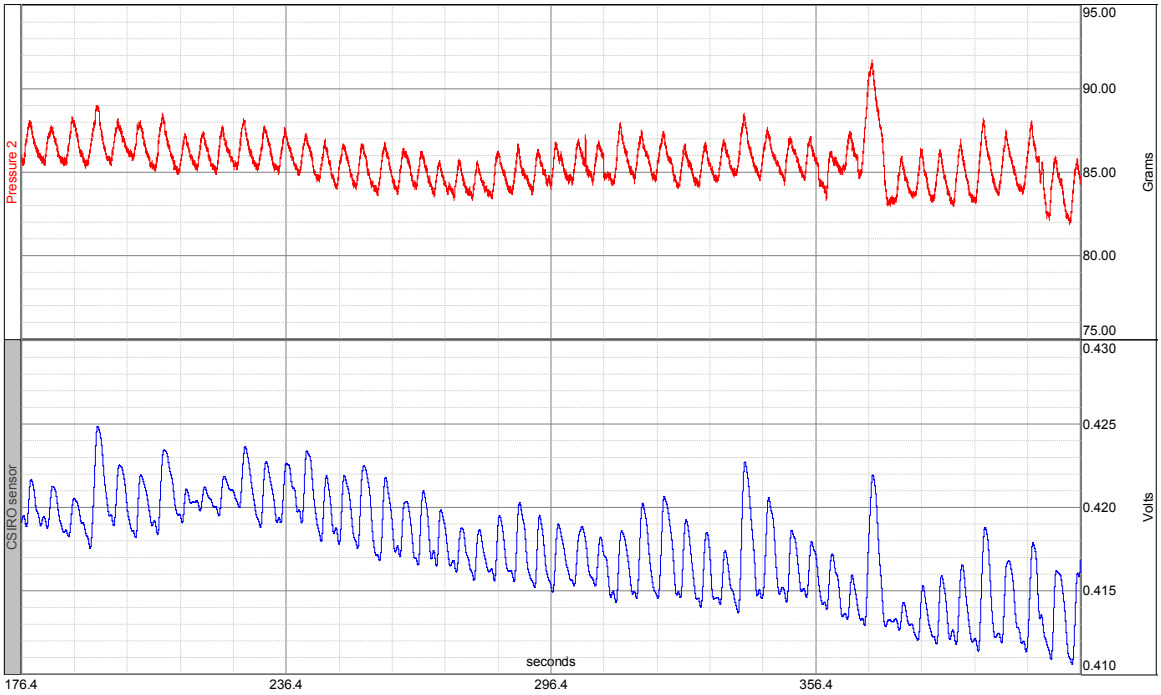

Figure 82. Thoracic respiration, (as displayed on Biopac AcqKnowledge software), correlation between Pressure sensor 2 and CSIRO sensor, horizontal time(s), vertical (volts).

The observation that the measured electrode pressure varied with respiration is of significance. The variation in pressure can be monitored and this signal is directly related to, and is a measure of the respiration of the subject. This pressure sensor can be used to correlate the signals derived from the fabric sensors.

Plots of the relationship between pressure sensor 1 and pressure sensor 2 are shown in Figure 83. Even though the two pressure sensors are under each armpit and the absolute pressures are not the same, there is a very good linear relationship between the measured pressures. Plots of the correlation between pressure sensor 2 and the CSIRO sensor and between pressure sensor 1 and the PPY sensor are shown in Figure 84.

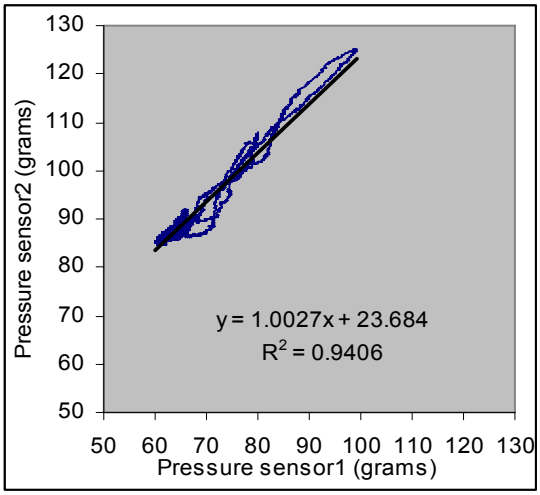

Figure 83. Relationship between values measured by Pressure 1 and Pressure 2 sensors.

a).

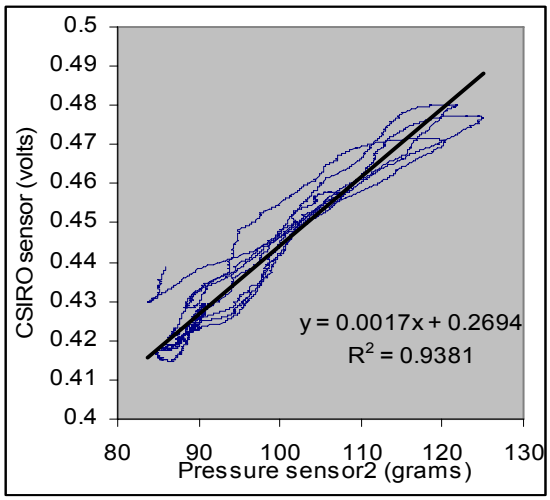

b).

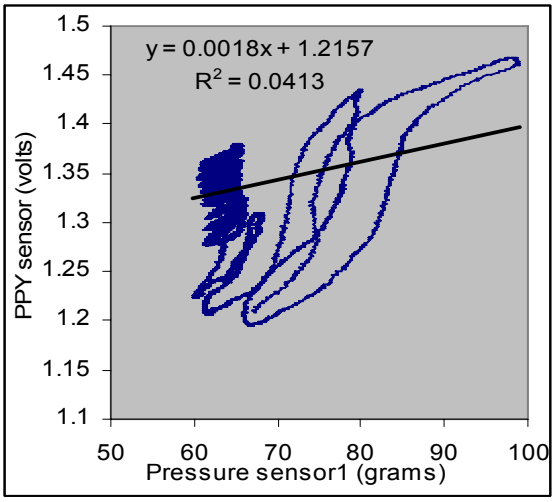

Figure 84. Relationship between values measured by a). Pressure sensor 2 and CSIRO sensor and b). Pressure sensor 1 and PPY sensor.

The two strain sensors, although adjacent to the pressure sensors, are over the chest area and not subject to the same mechanical conditions. Even so the relationship between pressure sensor 2 and the CSIRO strain sensor (Figure 84) is linear. The pressure sensor 1 versus PPY sensor result (included for information, as it could not be repeated), shows a shift in value during the test due to small movement of the band and a change in the sensor's resistance due to its continual mechanical fatigue. As testing progressed the PPY strain sensor's resistance changed due to the mechanical breakdown of the fabric structure. The sensor was physically longer in its relaxed state after the test. However the PPY sensor does exhibit a linear relationship with pressure1 sensor when at the higher strain end of its stretch range when positioned on the subject (see section 3.6.1, Figure 45).

As described earlier, the strain sensors used, monitor the expansion and contraction of the thoracic (or abdominal) area of the torso. Measurement of the change in linear dimension of these areas is a measure of and can be directly related to the volume of air inhaled or exhaled. From the characteristics of the respiration waveform such as the rising and falling gradients, the proportional rates and volumes/unit time can also be derived. To measure this, both thoracic and abdominal areas need to be monitored simultaneously and correlated with the rates and volumes of inspired and expired air. As there is reasonable correlation between the strain sensors' responses and that of the pressure sensors, this suggests that pressure sensors may be used instead to derive the same information. This may result in a more effective, useful and less obtrusive sensor solution.

Chapter 5

5 Discussion of contributions to state of the art

5.1 Comparison of fabric vs standard electrodes

The results using fabric electrodes demonstrate that many biosignal measurements can be made and ECG can be readily obtained. The quality of the ECG signals detected using the 'best' fabric electrode, approximates that of the standard Red Dot electrodes routinely used in clinical environments. Importantly, the main ECG characteristics of interval durations and peak amplitudes is maintained and suggests clinical use can be considered. Long term monitoring is feasible with fabric electrodes but is not with traditional electrodes, as these dry out and become noisy after a short time.

Respiration rate may also be deduced from the fabric ECG waveform because heart rate decreases with expiration of air and increases with inspiration of air. This heart rate variation, the RR interval, may be as much as 20% which is a useful change and may permit a reasonable level of discrimination. Respiration can cause a change in electrode pressure which may also increase the level of signal artefacts.

Although the electrode area used in the studies (see section 4) provided good results, this may not be optimum. Building on the results of this study the best dimensions and configuration of the electrodes needs to be investigated further. An oblong electrode may offer improved performance when considering the effects of motion artefact.

During testing and adjustment of the test bands and feedback from all subjects it was concluded that a pressure of 2.5 KPa (100gram force) for each electrode was deemed an acceptable, comfortable level. In any practical comfortable garment this would suggest a level similar to 2.5KPa is a desirable garment pressure in the sensor region. Pressures higher than this, although better for signal amplitudes are not comfortable. Lower levels of 1.5KPa may be preferred to minimise physiological effects (see section 2.5.5) on the wearer. When testing subjects with visually larger amounts of body fat, it was generally more difficult to set this value of electrode pressure when compared with slimmer subjects. It was also noted that the absolute amplitude of the ECG signal varied between

subjects. This is due to physiological factors such as the orientation and size of heart muscle and the amount and composition of the surrounding body tissue as described earlier.

The detrimental affect of artefact is another very important aspect of physiological measurements and is especially important when considering ECG. Of the electrode materials tested, stainless steel was the worst in relation to observed level of signal artefacts created by motion. The stainless electrodes tested are relatively rigid when compared to the other more fabric like electrodes and rather than move with skin would tend to move over the skin. The more fabric like electrodes, the more they conformed to the skin surface and it is proposed that this, together with applied pressure causes the shear friction to be greater which reduced skin-electrode movement. It has been found that for polymeric materials that have both plastic and elastic deformation in the contact zone that the frictional force can be represented by $F = \mu N^n$, where n is the power law exponent and has values between 2/3 and 1 and N is the load normal to the surface [155]. Provided that there is adequate compression of the under lying skin layers, signal artefact due to sub layer movement is less than that due to movement of the electrode over the surface of the skin. The AgN electrode looks and feels like a normal fabric, whereas the SSt was bulky and coarser.

Artefact was consistently observed during tests and presented significant problems with some subjects but detailed investigation was not undertaken. In this respect, positioning of the electrodes under the arms as used in this research may not be optimum, as electrodes in this position are also subject to respiration artefact.

5.2 A comparison of materials used to form fabric electrodes

Analysis of the results from Mirtaheri's research [97] has shown that the polarisation resistance of all metals reduces with increase in frequency from DC (0.01Hz) to 100KHz. So an electrode's effective resistance will reduce as frequency increases from DC and therefore its performance as an electrode increases with frequency. As ECG signals include components close to DC (~0.5Hz), the characteristics of the electrode at

these low frequencies is important. The values of polarisation resistance at DC (0.01Hz) for typical metals which may be used as electrodes are shown in Figure 85.

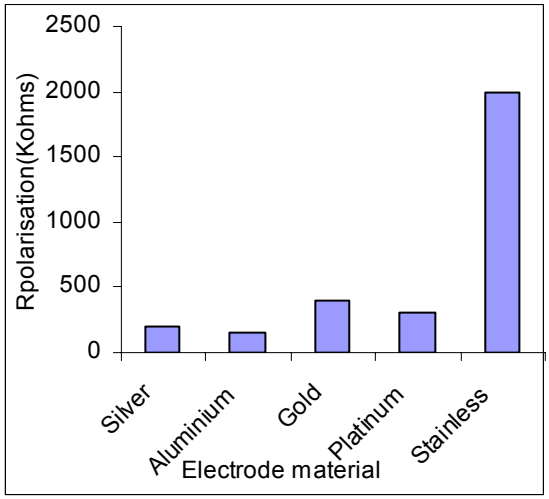

Figure 85. Polarisation resistance of metal electrodes at DC.

Stainless steel exhibits a very high resistance at low frequencies that is markedly different from other metals; at DC it is an order of magnitude higher than that of other metals. Therefore, the combined skin electrode impedance of the SSt electrode at low frequencies (<20Hz) will be higher than that of the electrodes comprised of silver. This is highly significant. As the frequency range of the acquired ECG signals for the subjects is below 100Hz, the values for 50Hz have also been extracted from Mertaheri's results and are also shown in Figure 86.

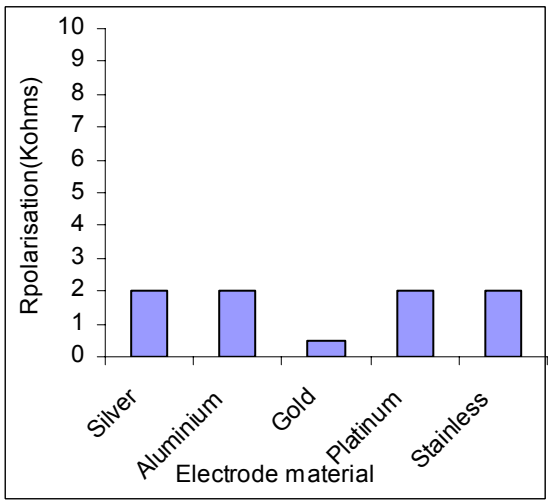

Figure 86. Polarisation resistance of metal electrodes at 50Hz.

The values for all metals are very low ≤ 2KΩ and are almost the same for all metals at ≥ 50Hz. Therefore at low frequencies the impedances of both SSt electrodes (plus the SSt reference electrode) are higher and any impedance differences are amplified by the measuring circuit and variations will appear as undesirable disturbance signals. Any differences between the sense electrodes themselves, is also exaggerated and the effect is more apparent. This would help to account for the observed increase in low frequency signal noise and the increase in disturbance signal due to movement for stainless electrodes (SSt).

5.3 Designing and Applying Fabric Electrodes in garments

The design of fabric electrodes for integration into a physiological monitoring garment requires consideration of a number of aspects, including location, size/shape, pressure, micro climate, conductive contact area, material stiffness and processability and most importantly comfort.

The ability of an electrode to provide a high level signal is important. Even the use of commercial electrodes as in this study, for the detection of ECG, has shown a variation of 2:1 in detected signal amplitudes over the range of subjects. The lower the absolute signal level, the higher the signal to noise ratio, which results in poorer quality waveforms. Population studies need to be conducted and results analysed to determine the best position, although additional redundant selectable electrodes may be of advantage.

The electrodes used in this work are 20mm x 20 mm and the results show that good quality signals can be obtained. This is consistent with a study into electrode noise which showed that noise level is inversely proportional to electrode size and that sizes below 20mm result in unacceptable levels of noise[19]. An electrode of larger size may be better but this has not been investigated.

Electrode shape, an area of research that has been neglected, may provide additional benefits related to positioning and signal detection if investigated. It is proposed that to maximize signal detection and minimise electrode movement thus minimising artefact,

an electrode shape, other than square or rectangular, such as triangular, may be better. A means of maintaining the electrode in a fixed position may be that the area immediately surrounding the electrode is comprised of a material e.g. silicone or other tacky material to increase the surface friction. This is yet to be evaluated.

The textile garment itself needs to be constructed with elastic and/or strain sections similar to the functionality of the test bands. The sense electrode and the area immediately surrounding it must be able to conform to the body's surface with a minimal amount of strain. A small amount of strain is required because for example during movement, exertion or even respiration the volume and physical dimensions of the body change. If the sense electrode does not move in proportion with this change then there will be relative movement between the skin and the electrode resulting in undesirable artefact. This is particularly important where a fabric strain sensor is used to detect respiration. Strain a result of respiration is detected by the longitudinal variation of the sensor. To achieve this each end of the sensor must move in unison with the expansion and contraction of the chest (or abdomen). This may be achieved by attaching each end of the sensor an elastic portion of garment. The strain sensor may also have tacky ends (Figure 87) which allows the sensor to adhere to and move with the skin during respiration.

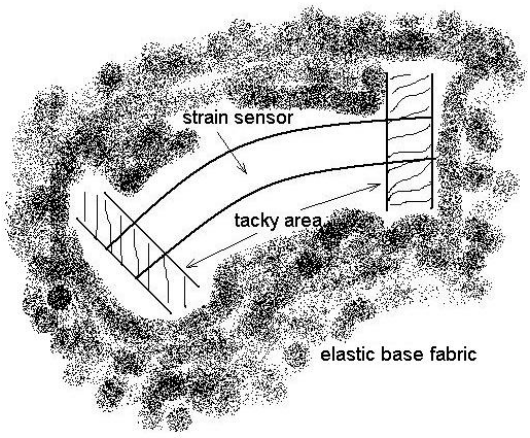

Figure 87. Strain sensor with tacky ends.

The garment also needs to apply a constant pressure over the electrode area of 2.5 KPa to provide adequate signal quality. As comfort for the user is a prime consideration, the electrode itself must contain exposed or protruding fibres with diameter ideally less than 25um to be acceptable to the user for long term use, consistent with existing garment

comfort knowledge [123]. The foundation garment must also meet this criteria. Protruding fibres, whether conductive or not may be beneficial to enhance the conduction path or help in the transfer of sweat to the electrode proper, if of 20 to 25um diameter. These fibres are generally stiffer and will burrow into the SC. Yarns made from continuous fibres generally result in less hairy yarn, i.e. have a low level of protruding fibres.

The microclimate within the electrode region is extremely important to the proper functioning of the electrical signal detection at the skin-electrode interface. For a dry fabric electrode, the development and maintenance of sweat as the conductive electrolyte in this region is essential in ensuring a low impedance contact from the electrode surface through the outer SC. This also helps increase the surface friction which together with an applied pressure, further improves electrode stability. The means described earlier to help maintain electrode position, may also provide a useful mechanism to aid in the creation of a suitable microclimate for the electrode. A suitable microclimate may be achieved through suitable selection of the electrode materials, their structure and the surrounding fabric. The findings of area, pressure and sweat although not quantified, are supported in a report on metallic electrodes by Besio [119].

The electrode must be highly conductive and less than 10Ω (if the surface is metallic) and have a cover factor for the conductive element of the electrode of at least 50%, the higher the better. PPY treated fabrics with a higher resistance of 100 to 300Ω perform just as well or better. A hairy fabric electrode, with protruding fibres may provide a better contact to the skin, but these must be tightly bonded within the foundation yarn to reduce linting and loss of fibres. Of the electrode construction materials tested to date, AgN or conductive polymer have been shown to be of most promise. The electrical stability of the electrode materials and the textile structure needs to be investigated. In general, conductive fabrics based on metal/metal coated yarns have advantages in maintaining their conductive characteristics over time, when compared with conductive polymers. Conductive polymer treated textiles or yarns can be susceptible to dopent loss and oxidation, which results in lower conductivity [156].

In practical application, as the garment is in intimate contact with the skin’s surface, the possibilities of contamination and cross infection of ailments and disease between

subjects is possible. In this context it is thought unwise to use a single garment across multiple subjects but rather the garment should be single use or single user use only.

The monitoring of respiration (whether thoracic or abdominal) has the same physical requirements as sense electrodes, in that the maintenance of sensor position is critical if repeatable signals are to be achieved. In the case of strain sensors which are oblong, each end must be fixed in relation to the skin's surface so that the expansion and contraction of the skin due to respiration is reflected in the sympathetic mechanical response of the sensor. Each end of the sensor would be of a tacky nature e.g. silicone to provide a level of adherence to the skin's surface preventing slippage of each end relative to the skin. The foundation garment must be of an elastic nature to ensure that the ends of the sensor/s do not shift during respiration or activity.

Comfort, an important aspect of traditional garment design, is the prime consideration for the development of intimate physiological monitoring textile garment. To be successful, such a garment must consider, at least, all the aspects described above and any solutions offered must not compromise user comfort.

5.4 Towards Clinical use of fabric electrodes

The preliminary results using an assortment of fabric electrodes, combined with a single Red Dot reference electrode for detection of ECG (see section 4.1), demonstrated that good quality signals can be acquired. The waveform feature extraction analysis algorithm analysis shows that by using a good reference electrode which provides a low skin-electrode impedance, clinical quality ECG signals can be obtained (see Figure 55). Although this is not the ideal solution with all electrodes being of a fabric nature it does allow an ECG to be measured with the minimal intrusion by the use of a single Red Dot electrode. Long term monitoring is possible with two fabric electrodes and a reference Red Dot that can be replaced. A plot of the PPY coated AgN electrode normalised to Red Dot (using a Red Dot reference electrode), extracted from section 4.1 results is shown in Figure 88.

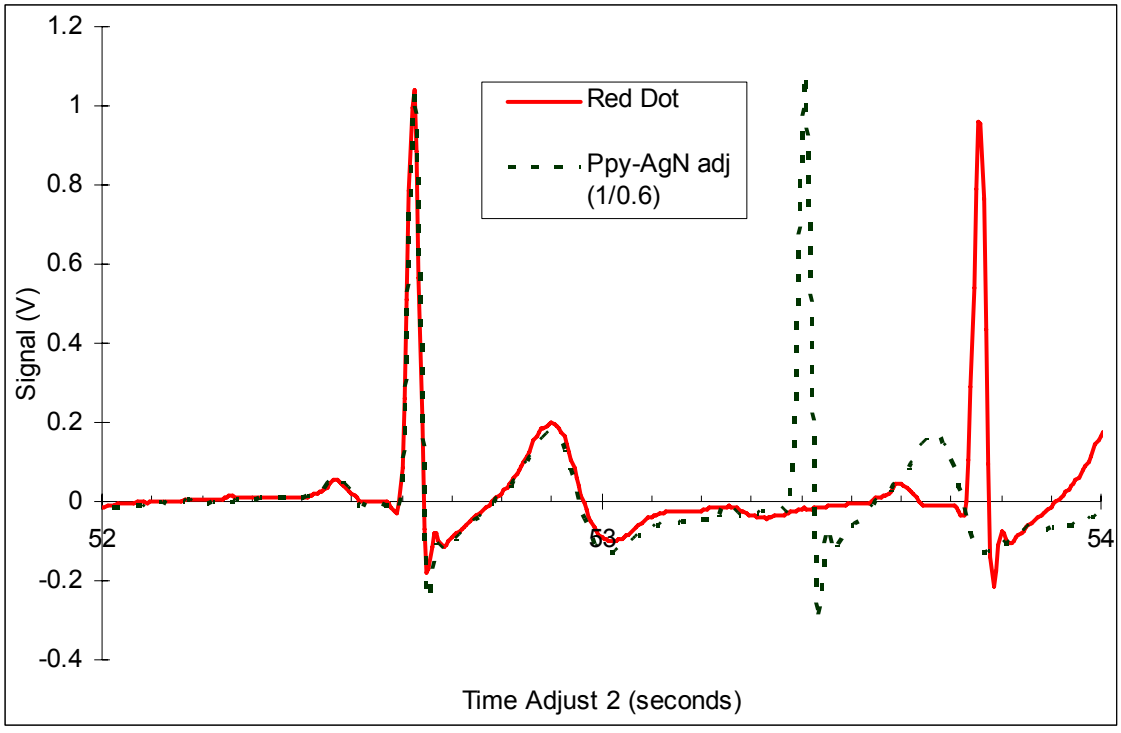

Figure 88. PPY/AgN fabric electrode response normalised to Red Dot

The test results in section 4.4 and above, show that fabric electrodes alone, can be used to detect ECG signals and that the signal quality is approaching that of Red Dot electrodes.

It is acknowledged that movement artefact is a considerable problem and the sensing with fabric electrodes needs to be optimised and conditioning (hardware and software) of the acquired signals will need to be performed to provide clinical quality signals.

This research has shown that sensing physiological parameters such as ECG with dry fabric electrodes is possible in static situations. Ambulatory detection though, requires that special attention be paid to address the underlying causes of signal artefact. With enhancement of the electrodes and garment, together with an optimised measurement system, the signal quality may be improved to the level demanded by clinicians. This is particularly important in diverse, dynamic situations and environments.

It was planned to present a series of acquired waveforms to clinicians for assessment but this was not undertaken.

5.5 Summary of Contribution

Comparison of the fabric electrodes tested indicates that, provided a nominal electrode DC conductivity of < 10Ω is achieved, the closer the electrodes mechanical properties approach that of conventional fabrics, the better is the electrical performance. Electrodes fabricated from AgN, conductive polymer(or conductive materials with similar properties) when optimised through further research for yarn properties, size, shape and knit or weave structure should be capable of providing performance approaching that of Red Dot electrodes. With careful consideration of the conflicting design requirements, garments may be constructed with integral sense electrodes and structures to allow the monitoring of ECG and respiration.

PPY based electrodes have been shown to perform as well as AgN and offer the added benefit of being a 'conventional' fabric and having similar comfort attributes. AgN may be more favourable to use as sense electrodes for physiological monitoring subject to toxicity issues.

For practical ambulatory monitoring situations where clinical performance is not necessary, a less than ideal dry electrode can be used to provide HR, HRV and limited ECG information with the application of appropriate algorithms.

The application of dry fabric electrodes in the clinical environment, where high signal integrity is essential, requires special attention to be paid to the attributes of the reference electrode as well as robust signal processing algorithms to cope with artefact.

Respiration can be measured successfully with fabric based strain sensors or pressure sensors, placed in a band or garment.

Chapter 6

6 Conclusion

The results of experiments show that conductive yarns fabricated into sensors can be used to measure ECG and respiration. The results were obtained with *dry* electrodes.

It was shown that reproducible measures for ECG were possible over multiple subjects. The most suitable material investigated for these fabric electrodes is silver coated nylon yarn which performed better than stainless steel or the silver coated copper yarns. Electrodes comprised of conductive polymer coated silver nylon or conductive polymer treated wool fabric gave even better results. Results have shown that electrode contact pressure is highly important and a pressure of 2.5KPa provides a good compromise between signal quality and subject comfort.

The sensing of respiration using fabric based sensors was shown to be successful, particularly with a conductive monofilament sensor whose response was linear with strain.

6.1 Review

When using *dry* fabric electrodes to measure ECG, the need for a low resistance contact between sensing electrodes and the skin is essential to maximise signal quality and reliability. If monitoring only HR or determining heart rate variability (HRV) derived from ECG signals, contact resistance is less important. With the application of appropriate signal analysis algorithms, any of the electrodes investigated in this work can fulfil this reduced function. Results from the study indicate that;

- Electrodes comprised of 100% stainless steel exaggerate the effect of motion artefact and are not preferred. Other metallic or metal coated yarns are more suitable for use in the fabrication of fabric electrodes.
- Multifilament yarns are more easily fabricated into fabric than monofilament yarns and are preferred.

- Electrodes comprised of a conductive polymer coated silver nylon or conductive polymer treated fabric have better performance than metal or metal coated yarns.
- Metal or metal coated yarns, combined with a textile yarn such as cotton or wool may offer benefits in improving the performance of a sensor in a practical garment. In this case surface coverage of the conductive area within the electrode needs to be greater than 50% to enable useful signals to be obtained.
- Electrodes of 20mm x 20mm can provide good ECG signals.
- The practical use of any *dry* electrodes in the detection of physiological parameters is dependant on the inclusion of sweat at the electrode-skin interface.
- The detection of human respiration can be achieved readily using strain sensors such as those comprised of a conductive polymer strain fabric or a strain fabric incorporating a rigid conductive monofilament. In a practical monitoring garment, it is proposed that respiration would be better sensed with a fabric pressure sensor.

6.2 Considerations/Recommendations for future work

Further research is required to investigate the optimum material, size, shape and positioning of electrodes with the aim of optimising the signal quality to a level clinically acceptable for use in ECG diagnosis, within a conventional host garment.

The effect of movement artefact (not addressed in this study) presents a real problem particularly in ambulatory measurements. For reliable long term ECG monitoring to be achieved, special consideration needs to be given to electrode/garment design and complementary signal processing algorithms.

The incorporation of sensors into a practical garment must ensure that a consistent electrode skin/contact pressure can be maintained. This is especially important for use across a physically diverse population.

Further research is required to determine the best materials to use for fabric electrodes, particularly the use of conductive polymers (once the human toxicity effects of conductive polymers have been determined).

Dependant upon length of use, the long term effects of sweat on the corrosion and conductivity of metallic electrodes may need investigation.

Special consideration needs to be given to the how the interconnection between fabric electrodes and conditioning electronics can be best achieved in a garment.

If a garment is required to be used a number of times the effect of laundering on performance will need to be considered.

To determine the suitability of any fabric electrodes for clinical use, a series of clinician assessments needs to be conducted on a range of acquired waveforms.

APPENDIX

APPENDIX A CSIRO TFT sensor conditioning circuit

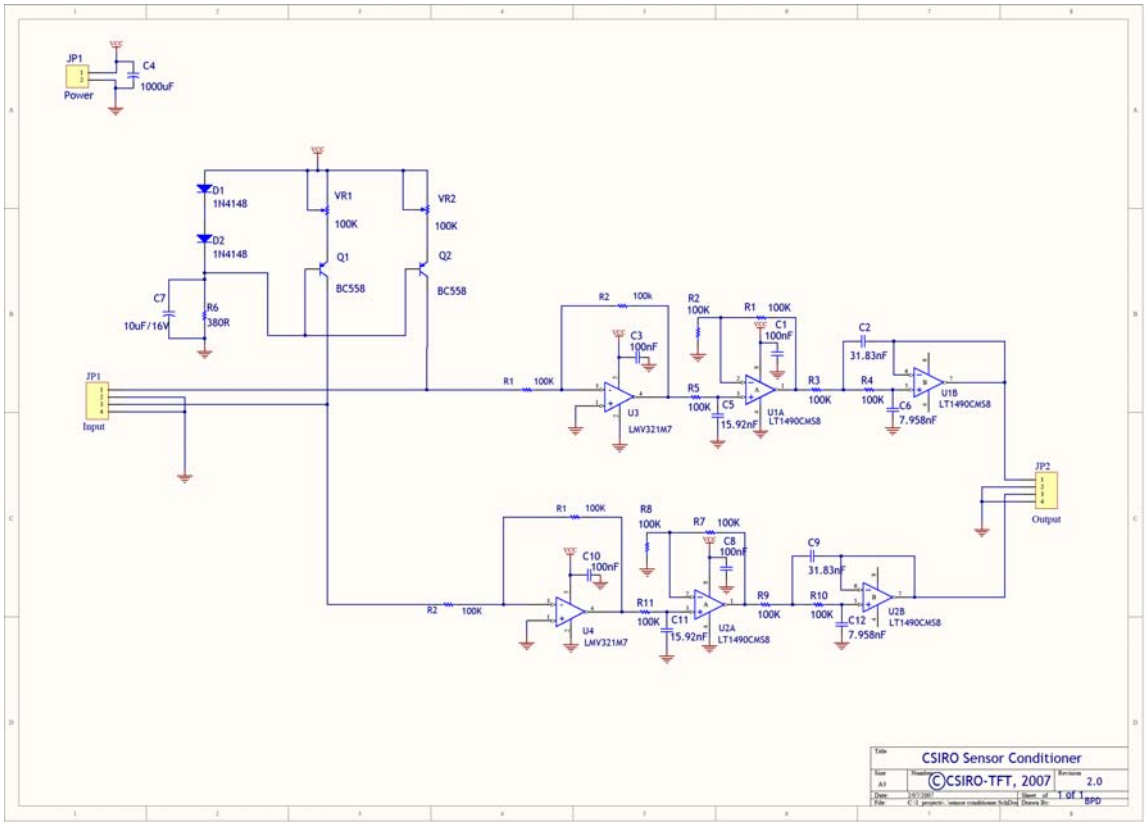

APPENDIX B Pressure sensor conditioning circuit

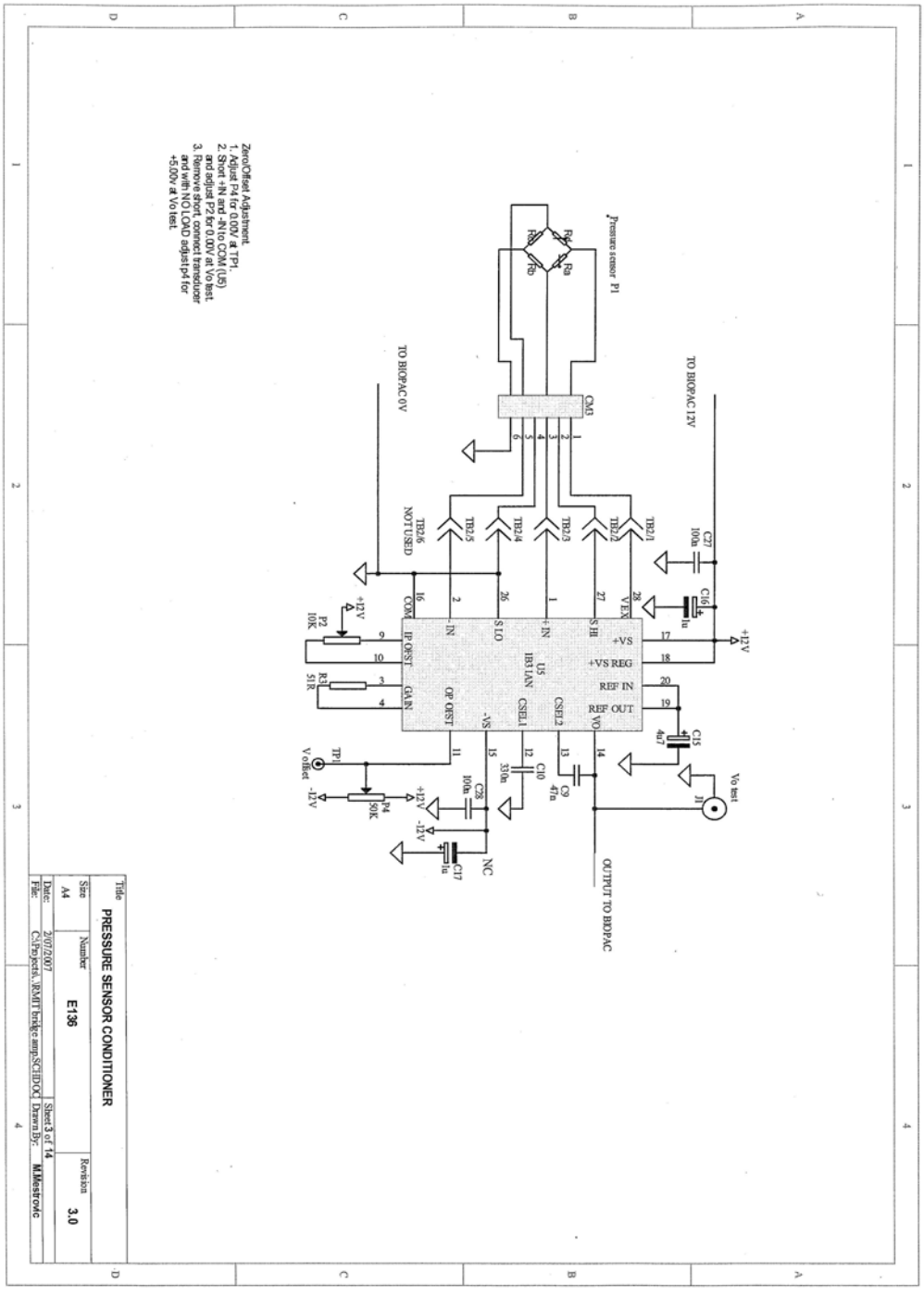

APPENDIX C Pressure Sensor Calibration

The sensors used in the experiments to determine the effects of electrode pressure on the signal integrity of acquired physiological signals were sourced from Sensor Developments Incorporated, type 10244-020. The sensors were connected to a bridge amplifier which was driven from 5V and gain and offset voltage adjusted for 0V at 0 gram load and 4V at 1000gram load. The circuit schematic for the sensor conditioning is shown in the appendix. The output of the bridge conditioning circuit was connected to the Biopac Instrument along with the GSR signals derived from the surface electrode electrodes.

These were calibrated using a Hounsfield H5000M Tensile Tester TFT 1479, by progressively loading the sensors from 50grams to 1000grams and recording the results. The sensors were then unloaded and the results recorded. At each load the average output voltage was recorded and the plotted results are shown in Figure 89. Both sensors were calibrated in the same way and gave the same results within 1%. Hysteresis observed with loading and unloading was less than 2% and is considered acceptable given the experimental error and repeatability of the physiological measurements. The response is linear.

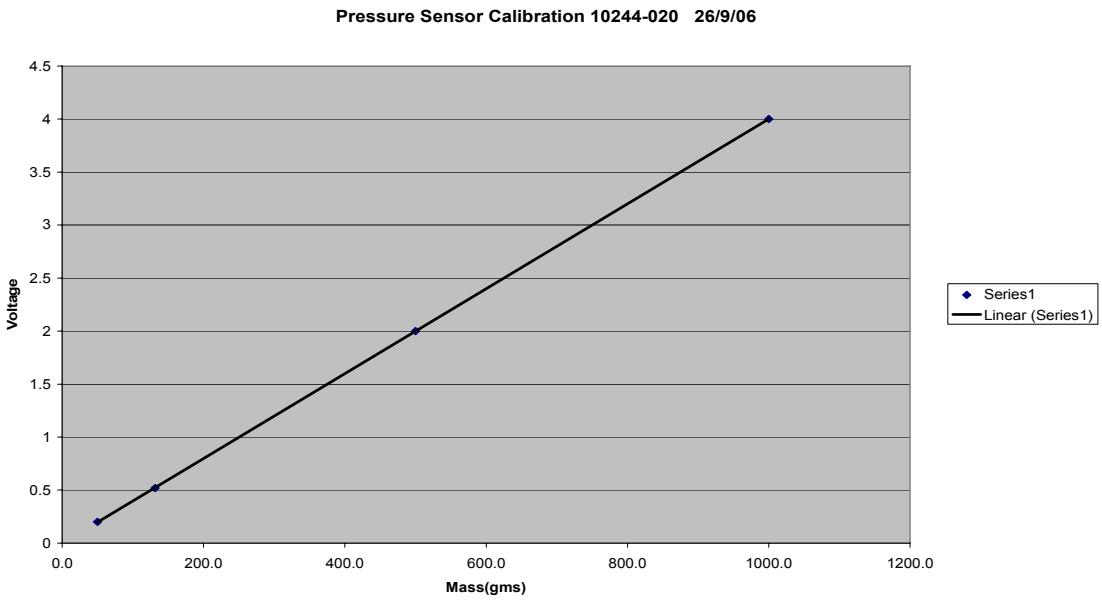

Figure 89. Pressure sensor calibration curve, sensor type 10244-020.

APPENDIX D Hardware

Biopac ECG100C Electrical Specifications

Gain:	500*,1000,2000,5000	
Output Selection:	Normal*, R-wave indicator	
Output Range:	+/- 10V(analog)	
Frequency Response:	Low Pass Filter:	35Hz*, 150Hz
	High Pass Filter:	0.05Hz, 1.0Hz
Notch Filter:	50dB rejection @ 50*/60Hz	
Noise Voltage:	0.1uVrms –(0.05-35Hz)	
Signal Source:	Electrodes(three electrode leads required)	
Z(input)	Differential:	2Mohm
	Common mode:	1000Mohm
CMRR:	110dB(50/60Hz)	
CMIV-referenced to	Amplifier ground:	+/- 10V
	Mains ground:	+/- 1500VDC

Input Voltage Range:	Gain	Vin (mV)
	500	+/- 20 *
	1000	+/- 10
	2000	+/- 5
	5000	+/- 2

Sampling Rate 200Hz*

Modes selected displayed with *

QRS Card Specifications

Frequency response	.05 – 100Hz
Lead leakage	< 10 uA
Input Impedance	> 100M ohm
Gain sensitivity	5,10 and 20 mm/mV
CMRR	> 120dB
Sampling rate	240 Hz or 500Hz
A/D resolution	12 bits
Time base	25 and 50 mm/sec
Electrical isolation	
Patient isolation	Optical
Power isolation	4 kV
Isolated leakage current	< 10uA
Defibrillator protection	360 joules

APPENDIX E Strain sensor cyclic tester

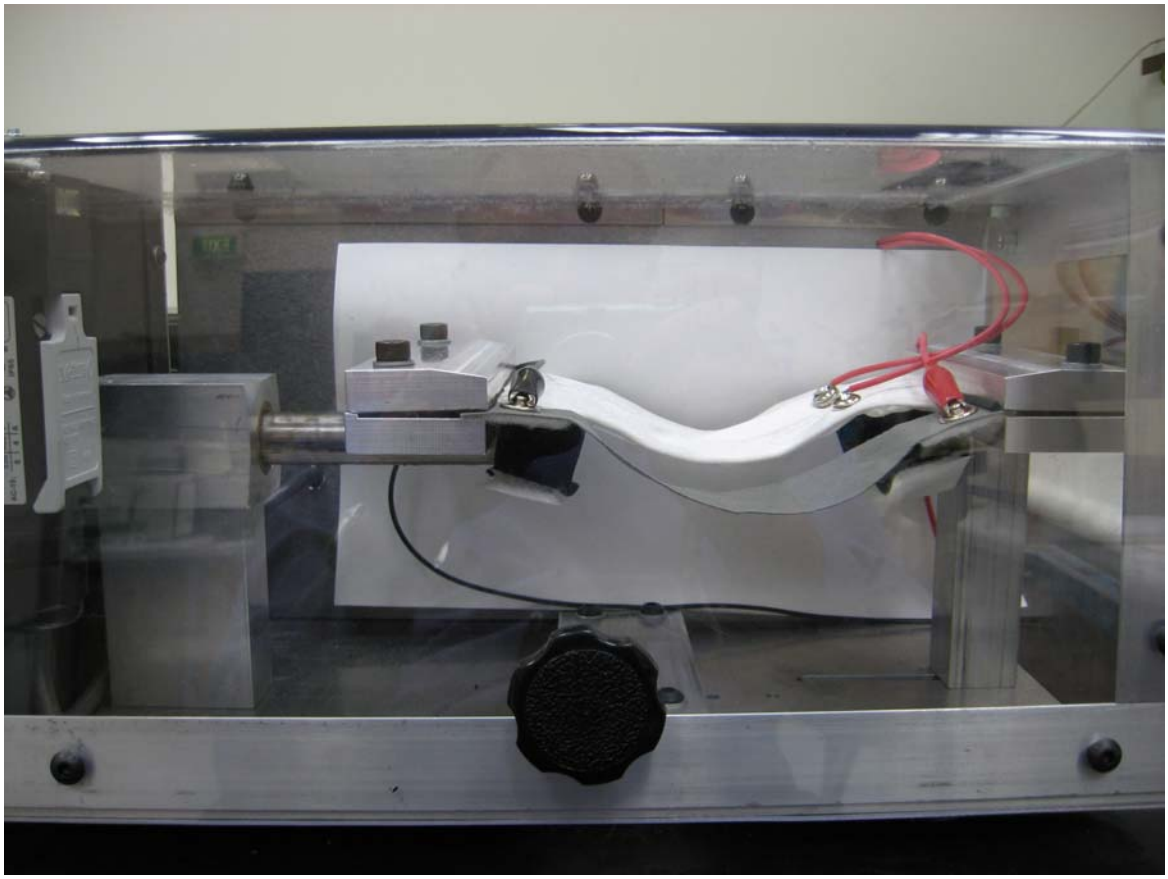

Figure 90. Cyclic test rig used for testing strain sensors.

APPENDIX F Subject data

Table F1 Body Mass Index of Sample Population

Subject	Height(m)	Weight(Kg)	BMI	Age
1	1.8	89	27.46914	56
2	1.73	73	24.39106	53
3	1.79	75	23.40751	45
4	1.73	61	20.38157	43
5	1.74	73	24.11151	39
6	1.74	75	24.7721	44
7	1.89	103	28.83458	44
8	1.8	68	20.98765	35
9	1.74	76	25.10239	34
10	1.75	92	30.04082	40

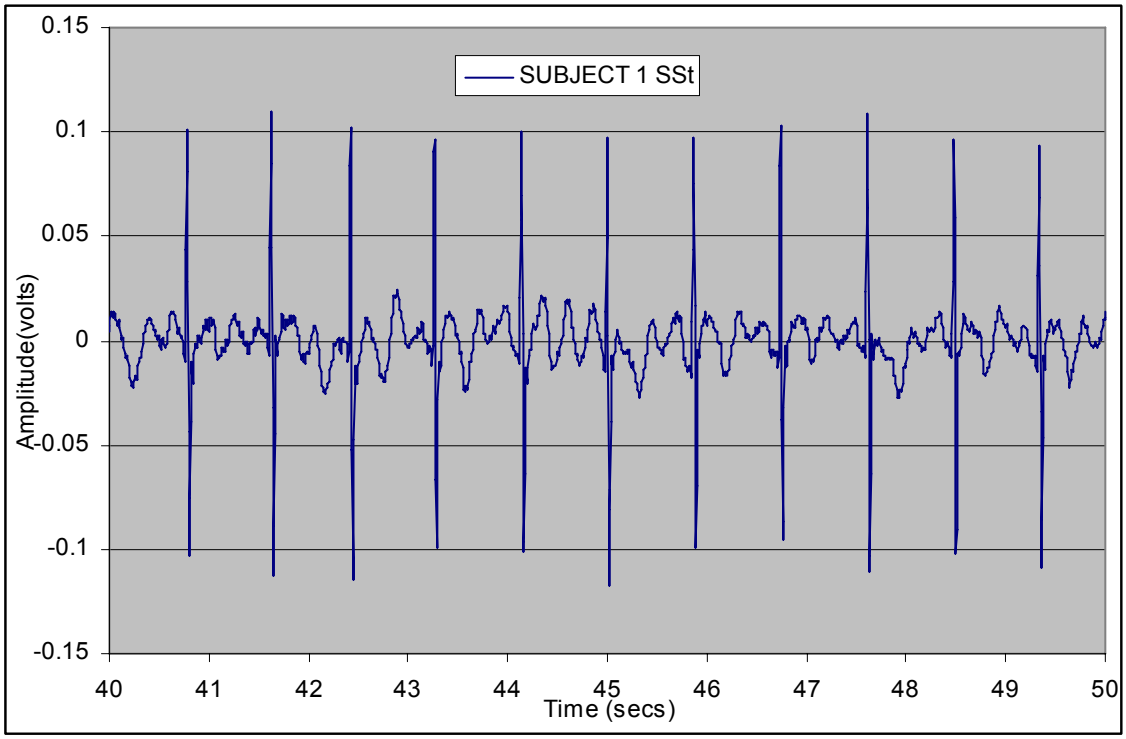

Figure F1. Subject 1, ECG waveform snapshot of SSt electrode.

An example of a poor signal which was unable to be analysed by algorithm.

The raw ECG waveforms and characteristics from the feature extraction algorithm for all subjects are shown below.

Where column data is missing from a table, analysis was not possible.

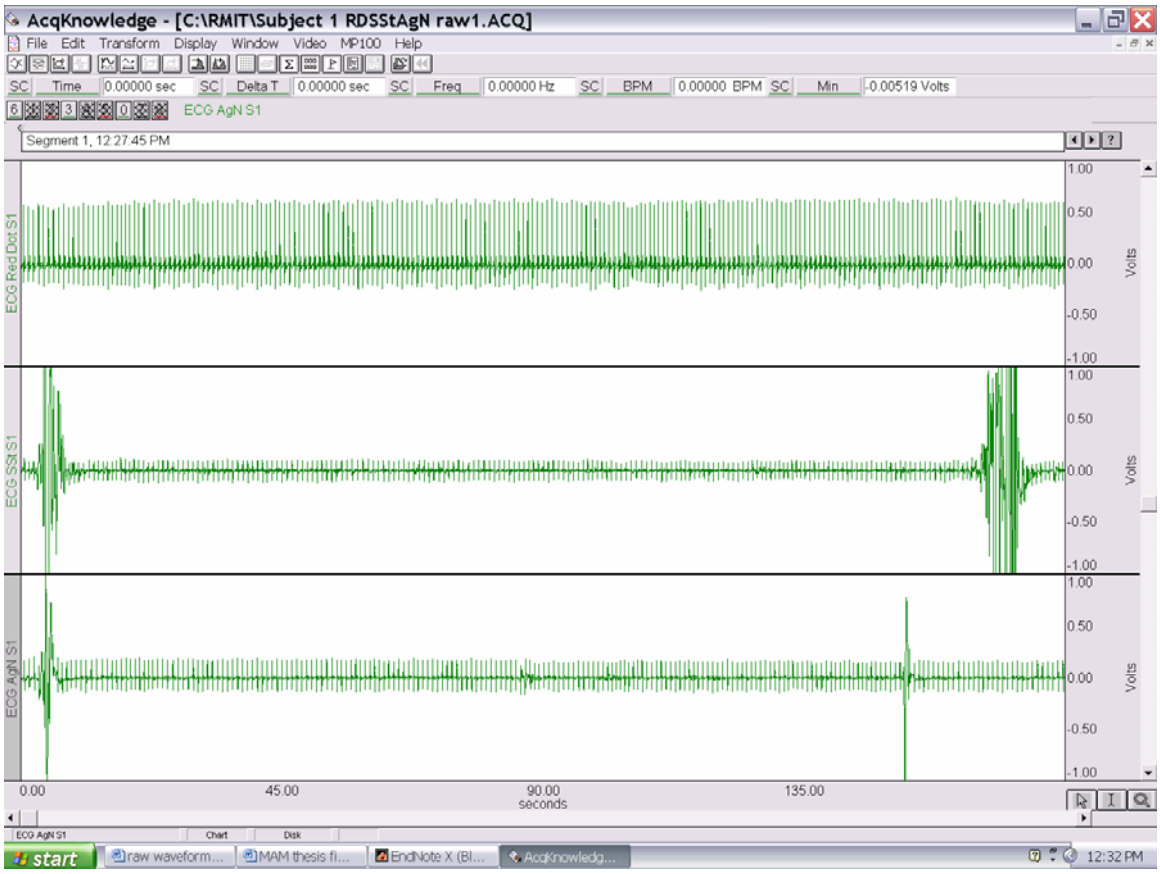

Figure F2. Subject 1, Acquired ECG waveform signals (as displayed on Biopac AcqKnowledge software), (3 mins), top to bottom, Red Dot, SSt, AgN, AgCu(s).

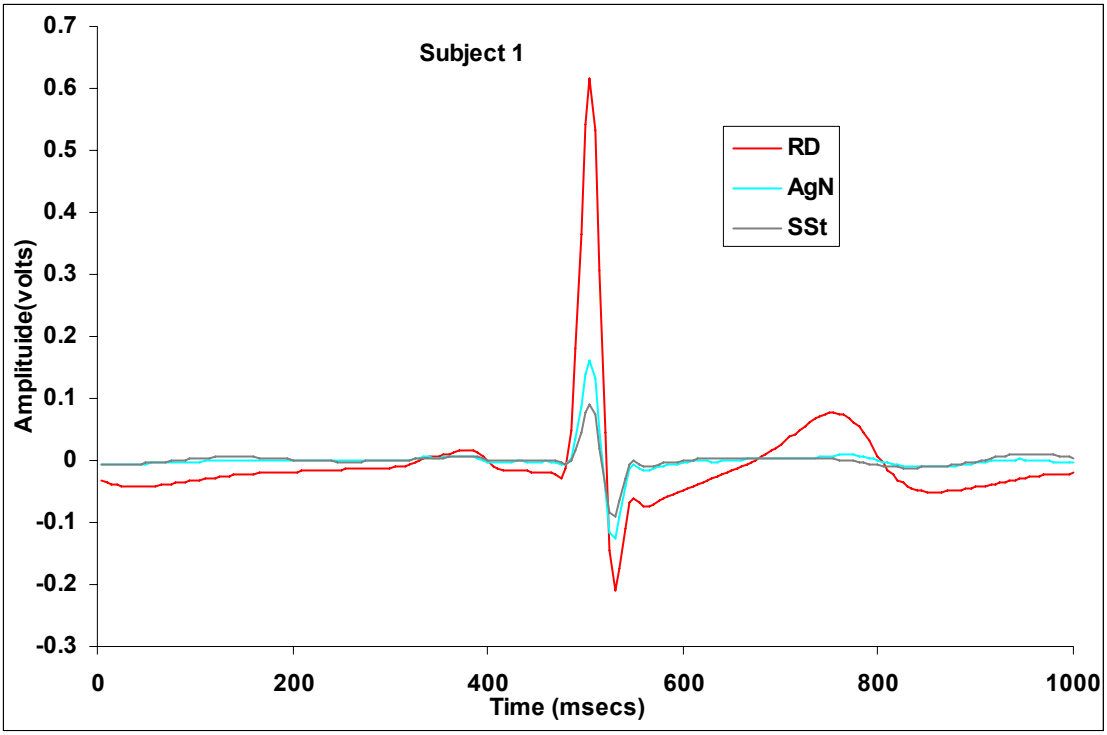

Figure F2a. Subject 1 average ECG waveforms for Red Dot, SSt, AgN, electrodes.

Table F2. Subject 1, Features extracted from ECG waveforms.

SUBJECT 1	ELECTRODE TYPES mn = mean value, sd =standard deviation					
Parameter	RD mn	RD sd	SS mn	SS sd	AgN mn	AgN sd
Pmax(volts)	0.02	0.00			0.01	0.01
Qmax(volts)	-0.03	0.00			-0.01	0.07
Rmax(volts)	0.61	0.02			0.17	0.06
Smax(volts)	-0.21	0.02			-0.13	0.06
Tmax(volts)	0.08	0.01			0.02	0.05
Intervals	Interval times are the number of samples, sample is 5 msec					
QRS	19.2718	0.9513			23.8992	7.6428
QT	75.82	2.85			72.85	11.10
PR	22.35	2.31			22.08	9.03
PQ	7.24	2.98			6.26	4.87
ST	7.93	1.48			9.71	8.65
SR pi	5.03	0.18			4.73	0.45
RQ pi	6.14	0.76			10.27	6.48
TR pi	49.30	0.88			49.87	7.03
RP pi	25.14	1.44			29.44	7.09
RR pi	166.63	7.74			167.04	12.44
Intervals in msecs						
QRS	96	5	0	0	119	38
QT	379	14	0	0	364	56
PR	112	12	0	0	110	45
PQ	36	15	0	0	31	24
ST	40	7	0	0	49	43
SR pi	25	1	0	0	24	2
RQ pi	31	4	0	0	51	32
TR pi	247	4	0	0	249	35
RP pi	126	7	0	0	147	35
RR pi	833	39	850	0	835	62

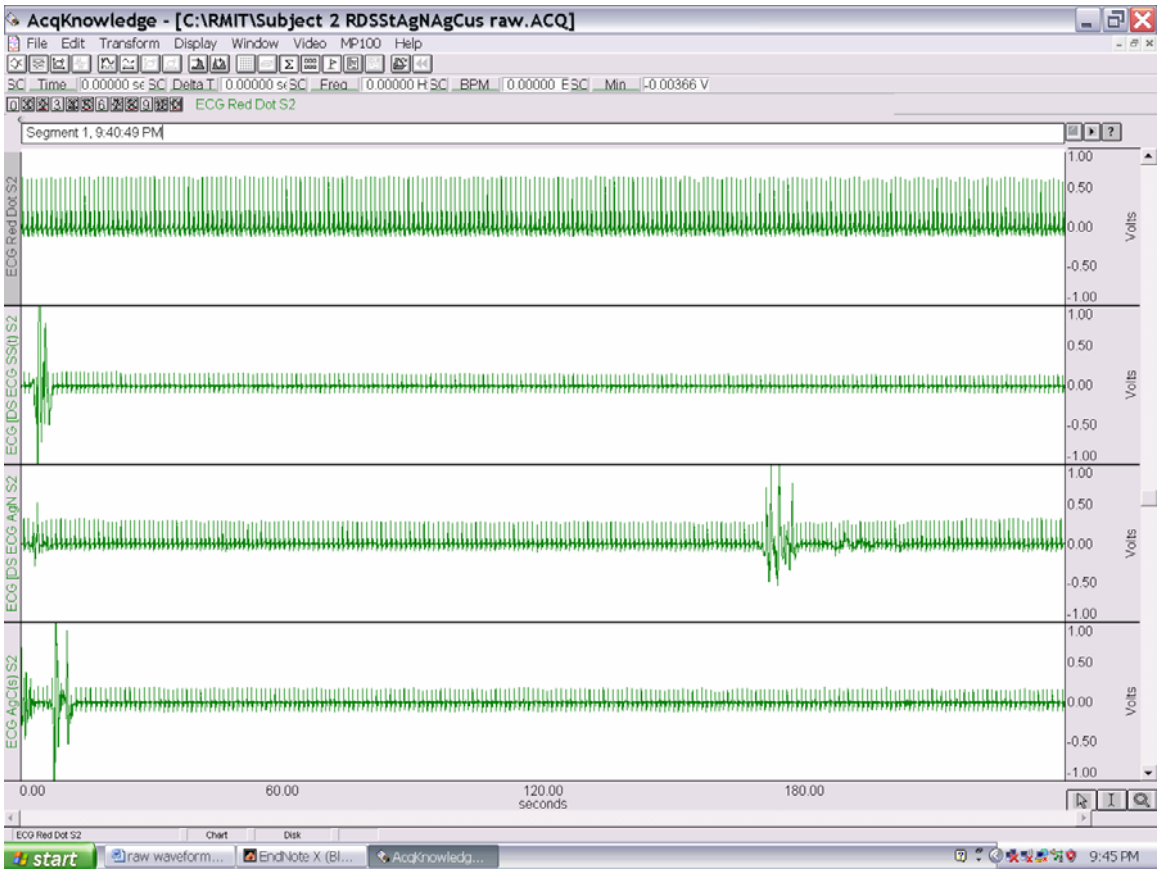

Figure F3. Subject 2, Acquired ECG waveform signals (as displayed on Biopac AcqKnowledge software), (4 mins), top to bottom, Red Dot, SSt, AgN, AgCu(s).

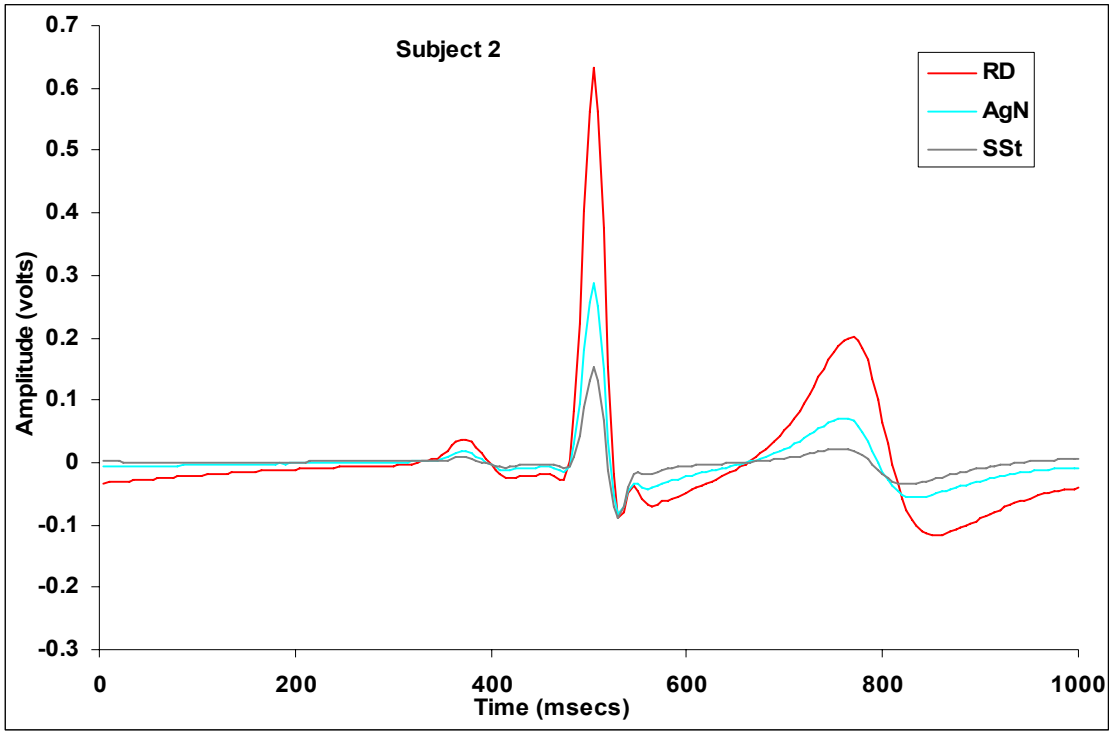

Figure F3a. Subject 2 average ECG waveforms for Red Dot, SSt, AgN, electrodes.

Table F3. Subject 2, Features extracted from ECG waveforms.

SUBJECT 2	ELECTRODE TYPES mn = mean value, sd =standard deviation							
Parameter	RD mn	RD sd	SS mn	SS sd	AgN mn	AgN sd	AgC mn	AgC sd
Pmax(volts)	0.04	0.00	0.01	0.00	0.02	0.00	0.01	0.00
Qmax(volts)	-0.03	0.00	-0.01	0.00	-0.02	0.00	-0.01	0.00
Rmax(volts)	0.63	0.02	0.15	0.01	0.29	0.02	0.18	0.01
Smax(volts)	-0.09	0.01	-0.09	0.00	-0.08	0.01	-0.11	0.01
Tmax(volts)	0.20	0.01	0.02	0.00	0.07	0.01	0.02	0.01
Intervals Interval times are in number of sample, sample is 5msec								
QRS	19.36	2.80	25.35	8.44	21.35	6.33	28.56	8.99
QT	77.41	3.29	74.21	7.22	74.88	5.16	75.80	7.34
PR	26.45	3.73	18.05	8.48	21.83	6.21	20.04	9.92
PQ	10.60	1.42	9.22	5.71	10.64	3.28	8.98	5.46
ST	16.57	2.51	4.69	2.97	7.71	2.22	2.86	3.31
SR pi	5.46	1.07	4.90	0.30	5.10	0.33	4.98	0.25
RQ pi	7.53	3.26	11.38	6.27	9.00	5.10	13.22	6.18
TR pi	52.72	0.48	49.68	1.45	51.09	0.62	48.35	2.68
RP pi	26.60	0.53	27.47	3.69	26.82	0.61	30.15	7.43
RR pi	214.66	5.59	217.19	7.93	213.72	8.65	214.10	8.01
Intervals in msecs								
QRS	97	14	127	42	107	32	143	45
QT	387	16	371	36	374	26	379	37
PR	132	19	90	42	109	31	100	50
PQ	53	7	46	29	53	16	45	27
ST	83	13	23	15	39	11	14	17
SR pi	27	5	24	2	26	2	25	1
RQ pi	38	16	57	31	45	26	66	31
TR pi	264	2	248	7	255	3	242	13
RP pi	133	3	137	18	134	3	151	37
RR pi	1073	28	1086	40	1069	43	1071	40

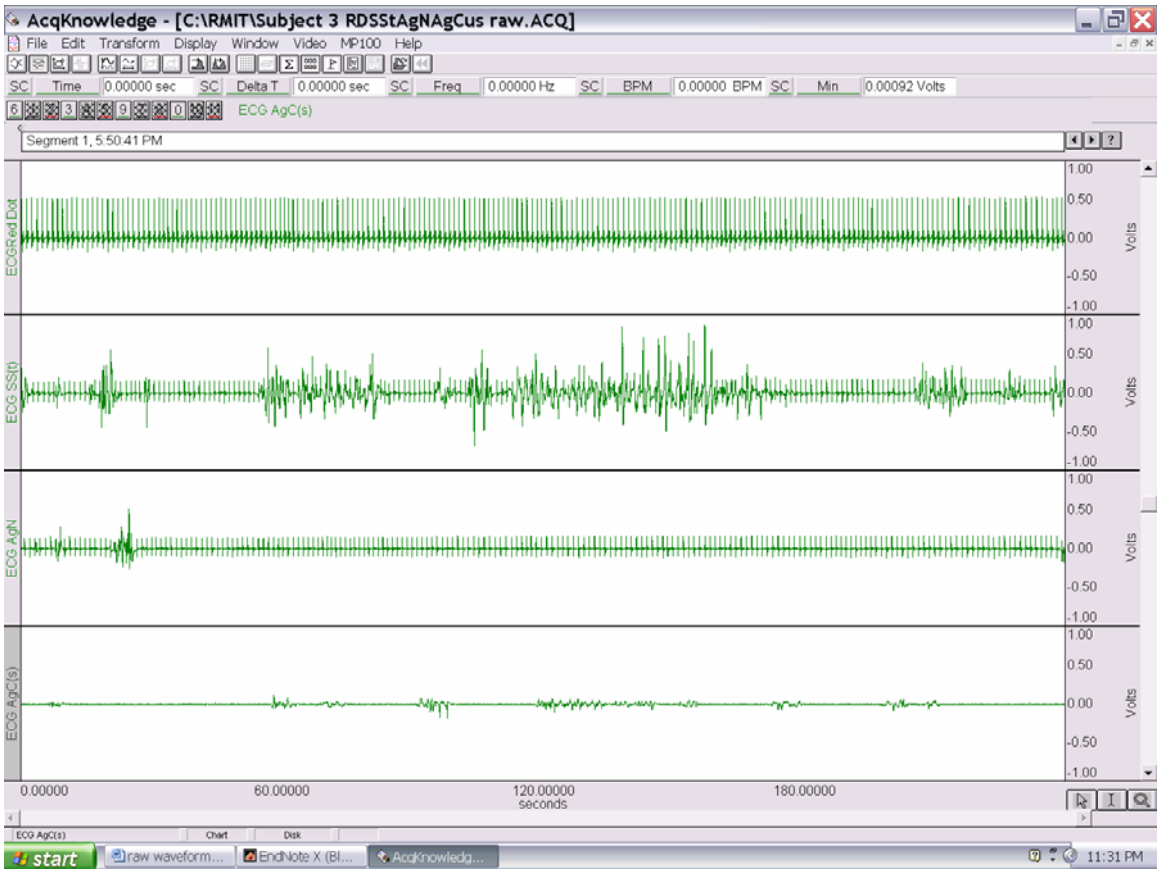

Figure F4. Subject 3, Acquired ECG waveform signals (as displayed on Biopac AcqKnowledge software), (4 mins), top to bottom, Red Dot, SSt, AgN, AgCu(s).

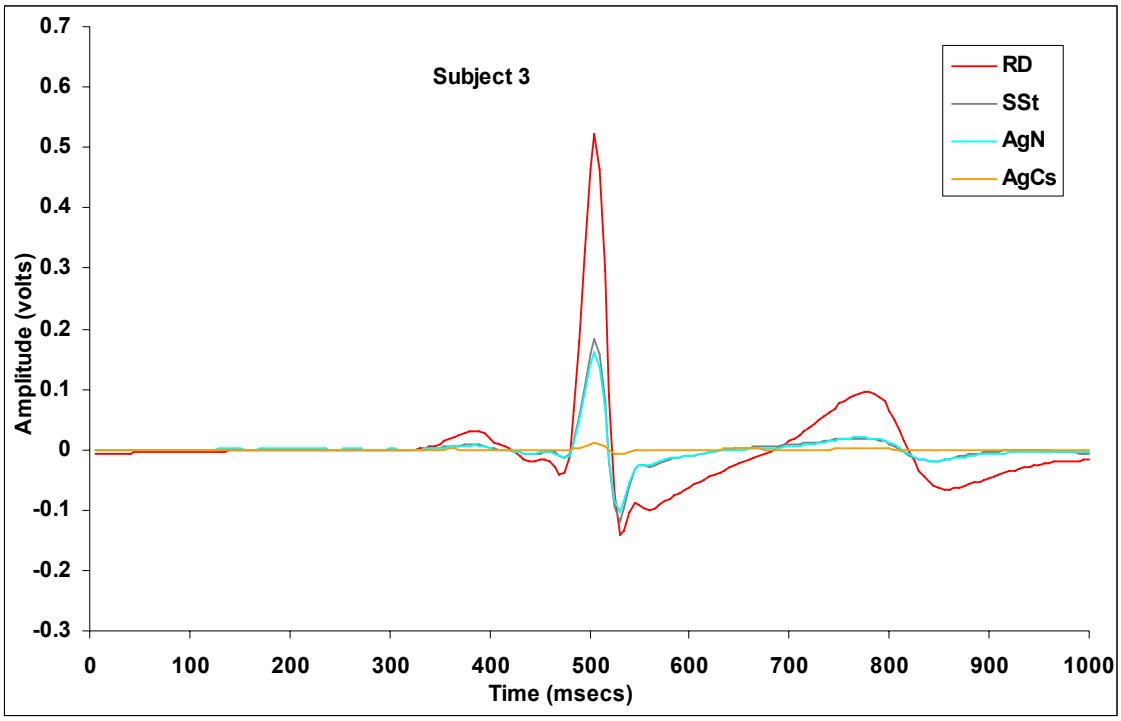

Figure F4a. Subject 3 average ECG waveforms for Red Dot, SSt, AgN, AgCu(s). electrodes.

Table F4. Subject 3, Features extracted from ECG waveforms.

SUBJECT 3	ELECTRODE TYPES mn = mean value, sd =standard deviation							
Parameter	RD1 mn	RD1 sd	SSt mn	SSt sd	AgN mn	AgN sd	AgCsmn	AgCs sd
Pmax(volts)	0.032	0.003	0.009	0.005	0.007	0.003	0.002	0.001
Qmax(volts)	-0.043	0.003	-0.013	0.003	-0.015	0.005	-0.002	0.001
Rmax(volts)	0.522	0.008	0.183	0.005	0.162	0.009	0.010	0.001
Smax(volts)	-0.144	0.021	-0.120	0.008	-0.105	0.008	-0.007	0.001
Tmax(volts)	0.096	0.007	0.021	0.004	0.020	0.004	0.003	0.001
Intervals interval times in number of samples, sample is 5msec								
QRS	20.126	1.617	19.913	1.730	20.318	1.831	30.389	12.912
QT	77.309	1.075	70.870	6.864	71.201	6.022	53.778	11.128
PR	24.174	2.992	21.261	7.368	21.112	3.972	21.611	11.025
PQ	5.185	0.795	7.591	2.039	8.202	1.993	5.923	5.780
ST	6.913	1.345	3.696	2.225	2.793	1.184	16.357	12.201
SR pi	5.362	0.482	4.913	0.288	4.955	0.207	5.000	0.343
RQ pi	6.483	0.501	6.304	1.521	6.056	0.747	11.167	5.597
TR pi	54.372	0.814	51.087	4.926	52.603	2.693	36.389	10.885
RP pi	24.092	0.810	25.043	5.304	25.056	2.398	33.167	8.522
RR pi	231.233	11.076	237.500	8.193	236.562	12.757	306.353	136.412
Intervals in msecs								
QRS	101	8	100	9	102	9	152	65
QT	387	5	354	34	356	30	269	56
PR	121	15	106	37	106	20	108	55
PQ	26	4	38	10	41	10	30	29
ST	35	7	18	11	14	6	82	61
SR pi	27	2	25	1	25	1	25	2
RQ pi	32	3	32	8	30	4	56	28
TR pi	272	4	255	25	263	13	182	54
RP pi	120	4	125	27	125	12	166	43
RR pi	1156	55	1188	41	1183	64	1161	682

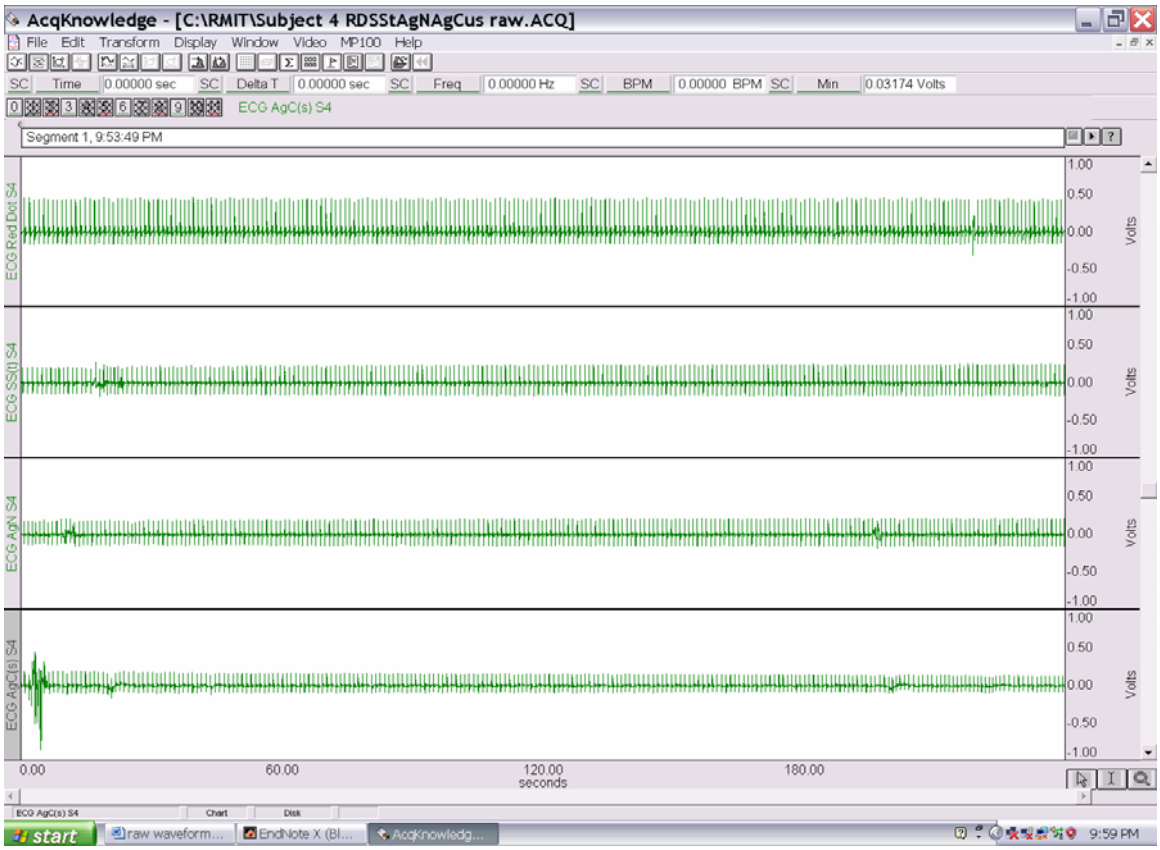

Figure F5. Subject 4, Acquired ECG waveform signals (as displayed on Biopac AcqKnowledge software), (4 mins), top to bottom, Red Dot, SSt, AgN, AgCu(s).

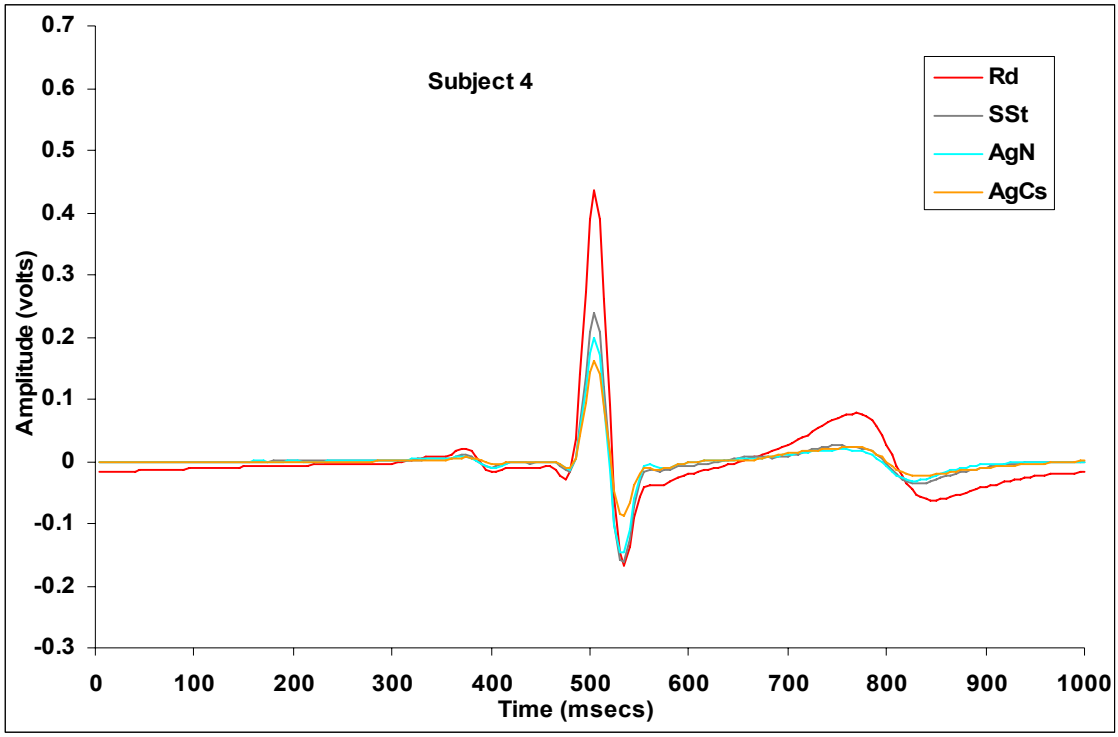

Figure F5a. Subject 4 average ECG waveforms for Red Dot, SSt, AgN, AgCu(s). electrodes.

Table F5. Subject 4, Features extracted from ECG waveforms.

SUBJECT 4		ELECTRODE TYPES mn = mean value, sd =standard deviation						
Parameter	RD1 mn	RD1 sd	SS mn	SS sd	AgN mn	AgN sd	AgCs mn	AgCs sd
Pmax(volts)	0.021	0.003	0.011	0.004	0.010	0.004	0.007	0.006
Qmax(volts)	-0.030	0.003	-0.017	0.003	-0.015	0.004	-0.012	0.006
Rmax(volts)	0.436	0.013	0.238	0.011	0.203	0.009	0.164	0.010
Smax(volts)	-0.168	0.004	-0.166	0.006	-0.155	0.007	-0.091	0.008
Tmax(volts)	0.077	0.007	0.026	0.003	0.023	0.010	0.024	0.006
Intervals intervals in number of samples, sample is 5 msec								
QRS	22.382	2.578	21.243	2.379	23.720	5.897	21.171	2.846
QT	74.436	1.347	67.619	6.241	65.583	9.330	64.636	7.842
PR	22.511	1.284	22.679	2.596	22.640	6.100	20.643	3.868
PQ	12.621	3.260	11.689	5.174	10.420	5.696	7.312	5.822
ST	4.364	1.251	5.390	2.603	9.010	5.469	4.529	1.793
SR pi	5.811	0.393	5.548	0.499	5.446	0.498	5.643	0.481
RQ pi	5.938	0.241	5.533	1.458	8.377	5.728	5.850	2.402
TR pi	52.665	1.014	48.905	2.513	48.843	2.638	50.950	2.912
RP pi	26.286	0.491	26.771	1.738	28.779	4.309	26.143	3.667
RR pi	210.969	14.998	209.589	10.209	205.448	6.903	206.101	7.688
Intervals in msecs								
QRS	112	13	106	12	119	29	106	14
QT	372	7	338	31	328	47	323	39
PR	113	6	113	13	113	30	103	19
PQ	63	16	58	26	52	28	37	29
ST	22	6	27	13	45	27	23	9
SR	29	2	28	2	27	2	28	2
RQ	30	1	28	7	42	29	29	12
TR	263	5	245	13	244	13	255	15
RP	131	2	134	9	144	22	131	18
RR	1055	75	1048	51	1027	35	1031	38

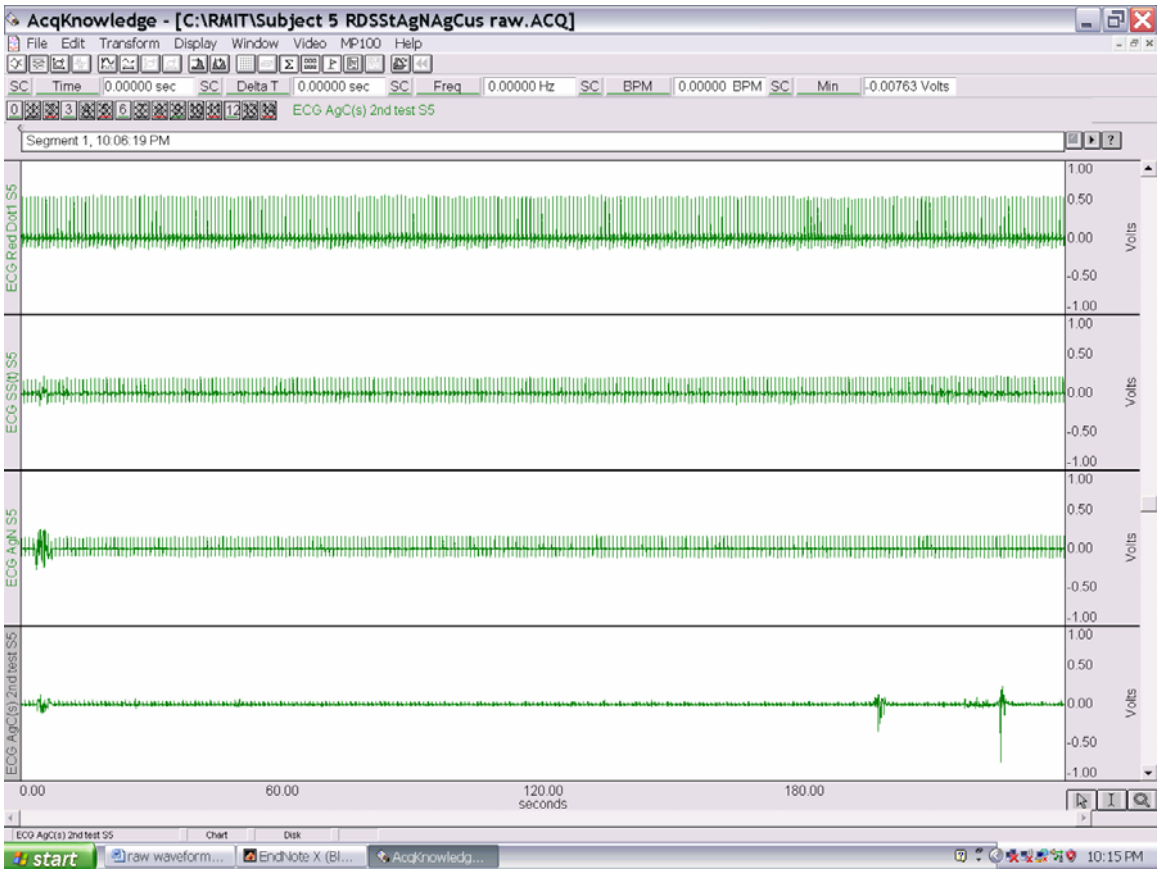

Figure F6. Subject 5, Acquired ECG waveform signals (as displayed on Biopac AcqKnowledge software), (4 mins), top to bottom, Red Dot, SSt, AgN, AgCu(s).

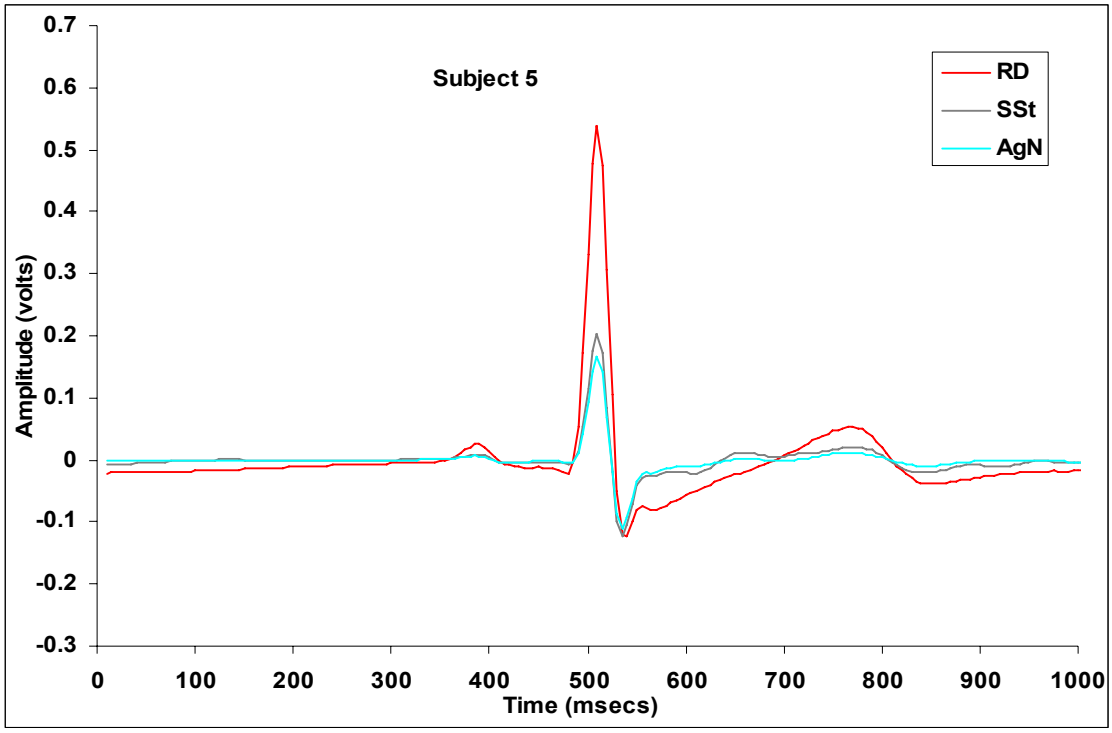

Figure F6a. Subject 5 average ECG waveforms for Red Dot, SSt, AgN, electrodes.

Table F6. Subject 5, Features extracted from ECG waveforms.

SUBJECT5	ELECTRODE TYPES mn = mean value, sd =standard deviation							
Parameters	RD1 mn	RD1 sd	SSt mn	SSt sd	AgN mn	AgN sd	AgCs mn	AgCs sd
Pmax(volts)	0.026	0.003	0.010	0.009	0.007	0.002		
Qmax(volts)	-0.022	0.004	-0.009	0.007	-0.006	0.001		
Rmax(volts)	0.540	0.013	0.204	0.010	0.167	0.008		
Smax(volts)	-0.129	0.013	-0.124	0.009	-0.110	0.007		
Tmax(volts)	0.054	0.006	0.025	0.008	0.012	0.002		
Intervals intervals in number of samples, samples in 5 msec								
QRS	20.502	1.795	26.488	7.352	26.920	8.204		
QT	73.068	4.505	71.211	10.204	74.809	9.147		
PR	23.274	2.422	18.698	8.385	15.596	7.972		
PQ	7.218	2.447	7.296	4.877	8.783	5.506		
ST	6.166	1.450	7.471	5.900	2.630	2.114		
SR pi	5.577	0.495	5.023	0.231	4.996	0.247		
RQ pi	6.536	1.131	10.950	5.604	11.341	6.089		
TR pi	51.653	1.314	47.617	6.813	50.715	2.866		
RP pi	24.494	0.634	26.506	5.049	25.020	1.922		
RR pi	180.727	11.579	183.208	8.908	186.457	8.896		
Intervals in msecs								
QRS	103	9	132	37	135	41		
QT	365	23	356	51	374	46		
PR	116	12	93	42	78	40		
PQ	36	12	36	24	44	28		
ST	31	7	37	29	13	11		
SR pi	28	2	25	1	25	1		
RQ pi	33	6	55	28	57	30		
TR pi	258	7	238	34	254	14		
RP pi	122	3	133	25	125	10		
RR pi	904	58	916	45	932	44		

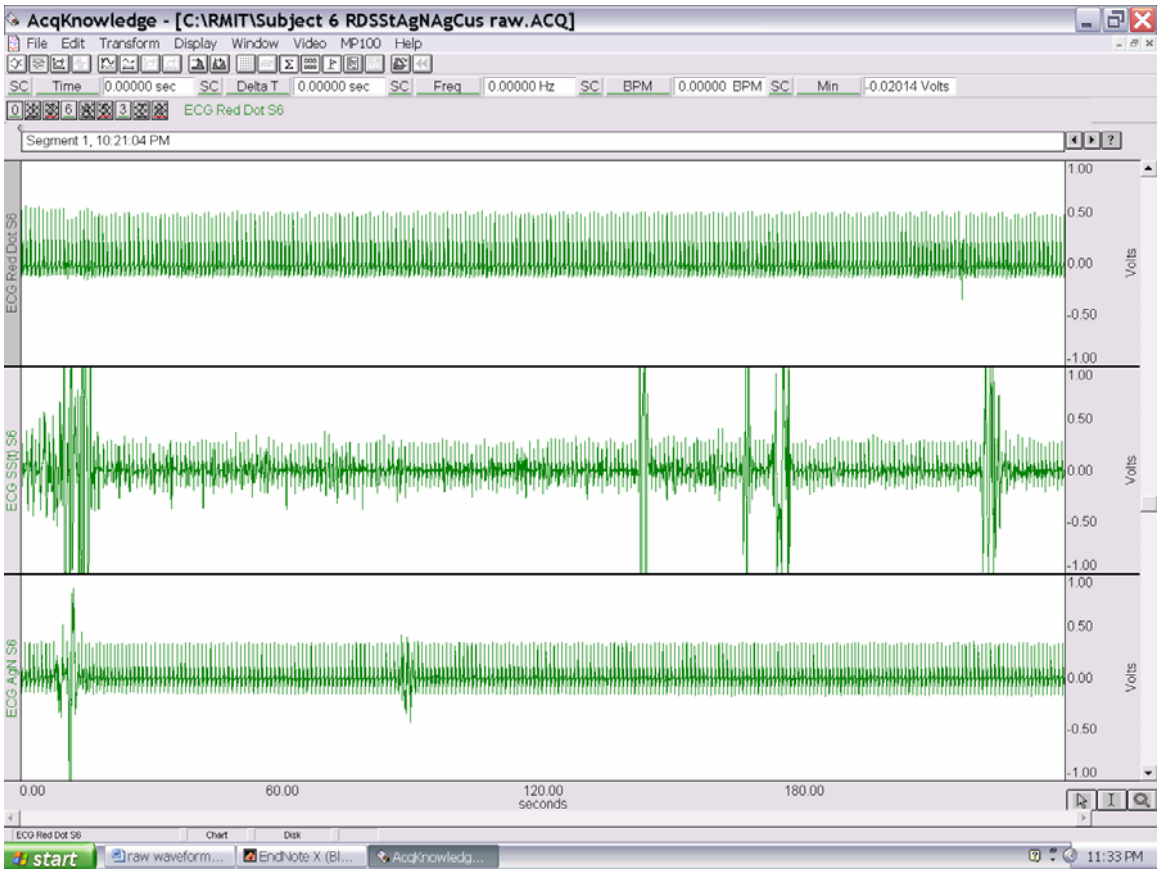

Figure F7. Subject 6, Acquired ECG waveform signals (as displayed on Biopac AcqKnowledge software), (4 mins), top to bottom, Red Dot, SSt, AgN.

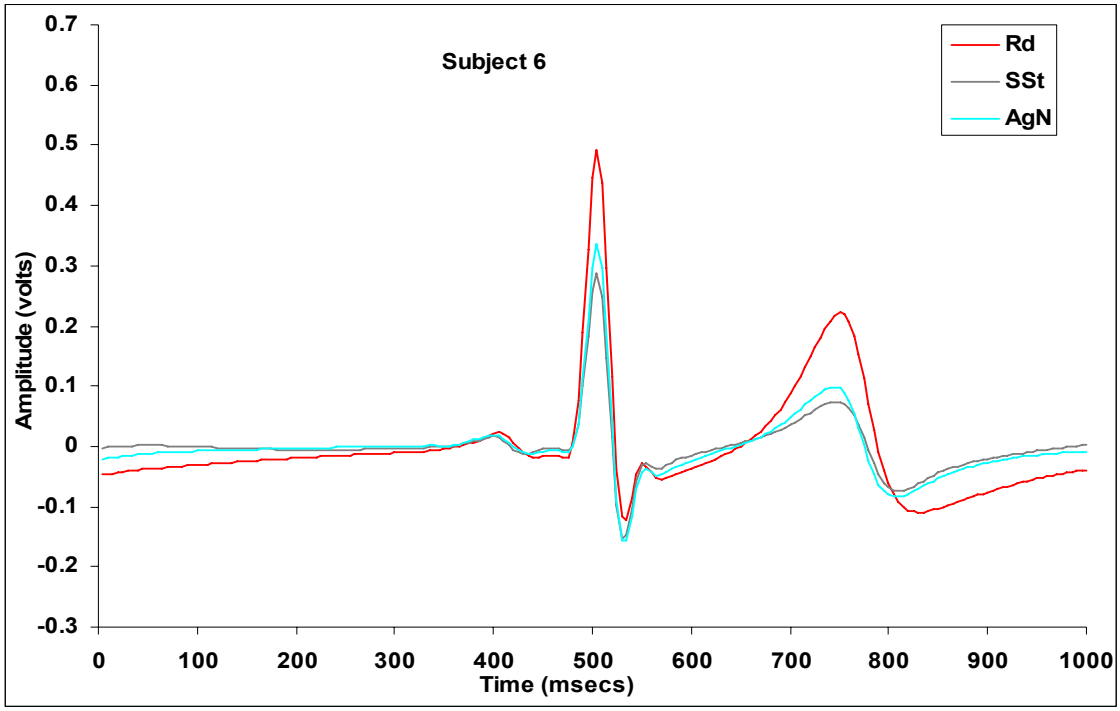

Figure F7a. Subject 6 average ECG waveforms for Red Dot, SSt, AgN, electrodes.

Table F7. Subject 6, Features extracted from ECG waveforms.

SUBJECT6	ELECTRODE TYPES mn = mean value, sd =standard deviation							
Parameters	RD1 mn	RD1 sd	SS mn	SS sd	AgN mn	AgN sd	AgCs mn	AgCs sd
Pmax(volts)	0.024	0.010			0.020	0.028		
Qmax(volts)	-0.021	0.008			-0.015	0.028		
Rmax(volts)	0.492	0.028			0.335	0.024	not	useable
Smax(volts)	-0.130	0.016			-0.161	0.022		
Tmax(volts)	0.222	0.007			0.102	0.027		
Intervals intervals in number of samples, sample is 5 msec								
QRS	21.299	3.435			29.140	5.174		
QT	73.522	2.899			73.665	2.757		
PR	18.469	4.541			10.669	7.793		
PQ	6.213	1.078			9.091	3.225		
ST	15.549	1.670			6.923	2.005		
SR pi	5.502	0.501			5.487	0.501		
RQ pi	8.336	2.745			12.962	2.768		
TR pi	49.138	0.499			47.958	1.395		
RP pi	20.360	1.622			21.555	4.448		
RR pi	193.333	8.238			186.285	7.583		
Intervals in msecs								
QRS	106	17	0	0	146	26		
QT	368	14	0	0	368	14		
PR	92	23	0	0	53	39		
PQ	31	5	0	0	45	16		
ST	78	8	0	0	35	10		
SR pi	28	3	0	0	27	3		
RQ pi	42	14	0	0	65	14		
TR pi	246	2	0	0	240	7		
RP pi	102	8	0	0	108	22		
RR pi	967	41	0	0	931	38		

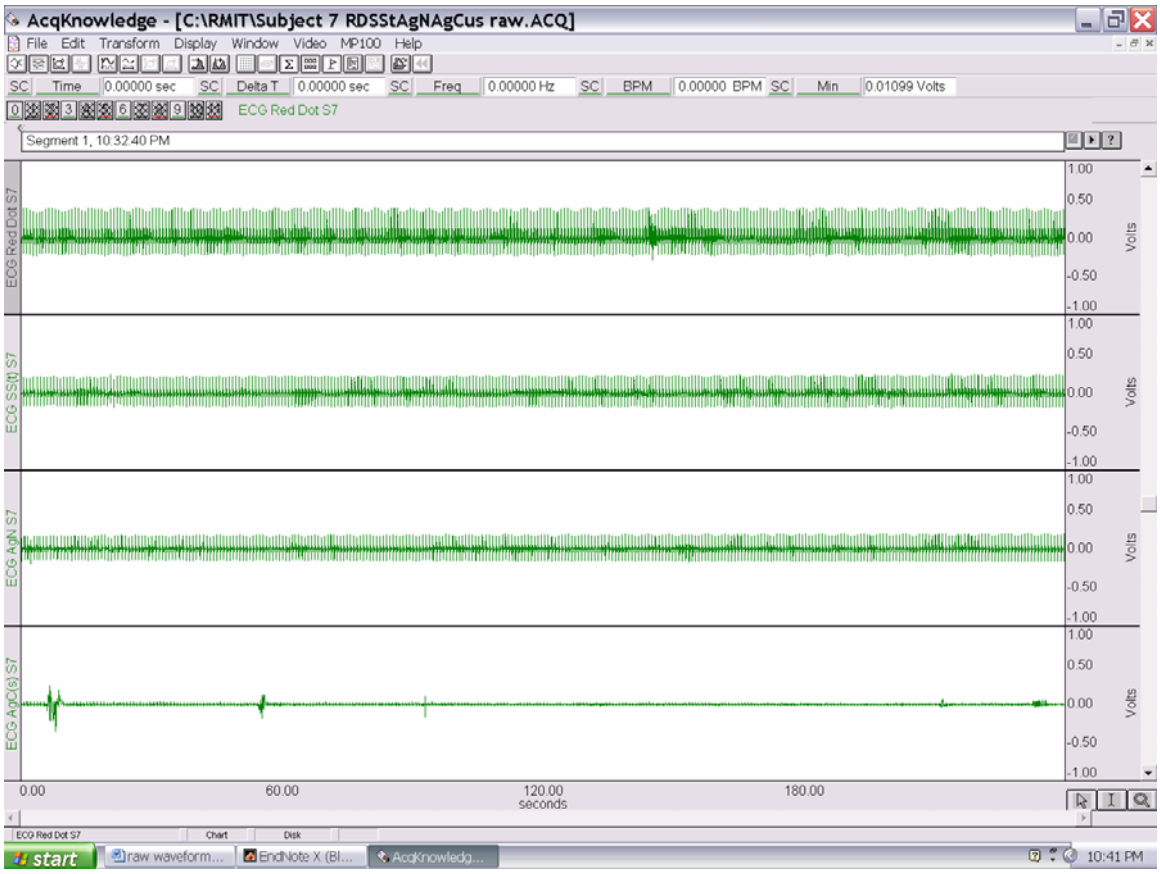

Figure F8. Subject 7, Acquired ECG waveform signals (as displayed on Biopac AcqKnowledge software), (4 mins), top to bottom, Red Dot, SSt, AgN, AgCu(s).

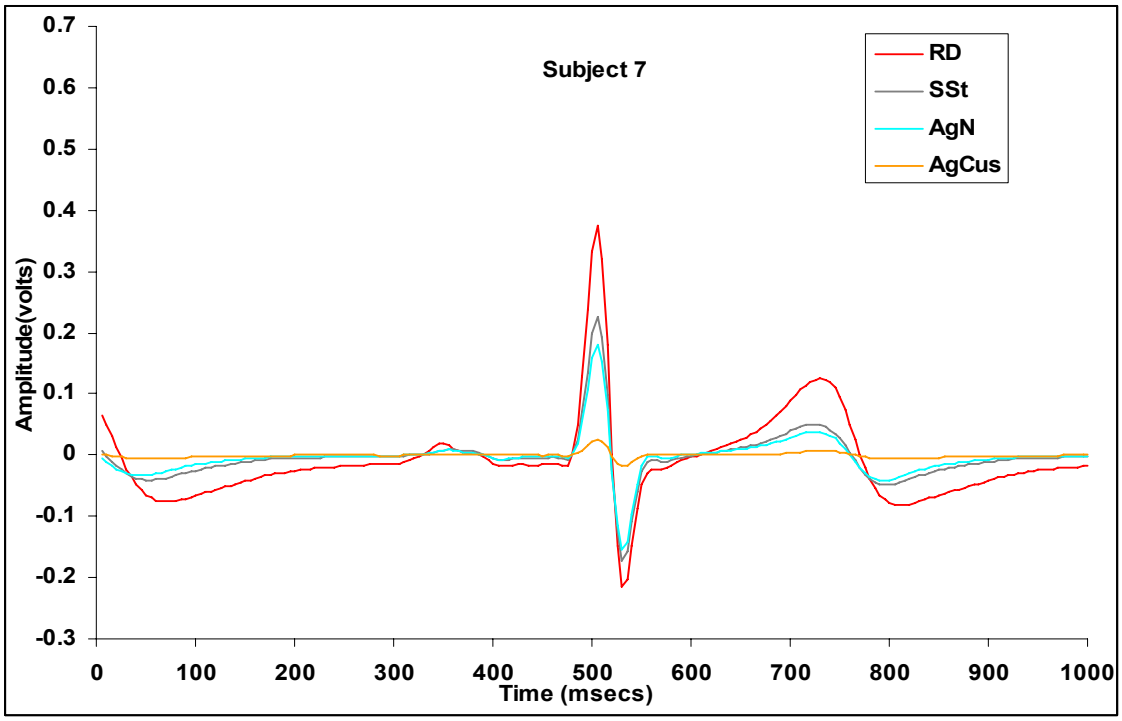

Figure F8a. Subject 7 average ECG waveforms for Red Dot, SSt, AgN, AgCu(s). electrodes.

Table F8. Subject 7, Features extracted from ECG waveforms.

SUBJECT7	ELECTRODE TYPES mn = mean value, sd =standard deviation							
Parameters	RD1 mn	RD1 sd	SSt mn	SSt sd	AgN mn	Agn sd	AgCs mn	AgCs sd
Pmax(volts)	0.020	0.008	0.012	0.004	0.011	0.004	0.003	0.001
Qmax(volts)	-0.019	0.003	-0.010	0.002	-0.008	0.003	-0.003	0.001
Rmax(volts)	0.373	0.021	0.226	0.013	0.181	0.011	0.031	0.003
Smax(volts)	-0.219	0.011	-0.174	0.006	-0.155	0.007	-0.023	0.002
Tmax(volts)	0.122	0.005	0.051	0.004	0.038	0.003	0.008	0.003
Intervals intervals in number of samples, sample is 5 msec								
QRS	34.780	7.583	35.090	6.213	35.784	4.039	30.292	8.050
QT	77.273	5.052	75.296	5.080	75.702	4.045	65.740	7.886
PR	17.703	7.735	12.824	6.450	11.804	4.583	18.745	11.236
PQ	5.937	4.094	4.696	3.921	3.862	2.691	3.243	2.957
ST	3.944	0.950	5.408	2.309	9.344	4.675	13.170	9.361
SR pi	5.299	0.459	5.185	0.389	5.214	0.411	5.140	0.351
RQ pi	16.299	4.913	17.118	4.548	18.340	3.054	11.340	4.529
TR pi	44.824	0.592	43.467	0.930	43.313	1.125	44.180	2.862
RP pi	29.583	2.250	29.185	2.186	29.485	1.685	30.860	7.245
RR pi	149.054	3.730	150.441	8.394	171.199	61.041	159.571	29.670
Intervals in msec								
QRS	174	38	175	31	179	20	151	40
QT	386	25	376	25	379	20	329	39
PR	89	39	64	32	59	23	94	56
PQ	30	20	23	20	19	13	16	15
ST	20	5	27	12	47	23	66	47
SR pi	26	2	26	2	26	2	26	2
RQ pi	81	25	86	23	92	15	57	23
TR pi	224	3	217	5	217	6	221	14
RP pi	148	11	146	11	147	8	154	36
RR pi	745	19	752	42	856	305	798	148

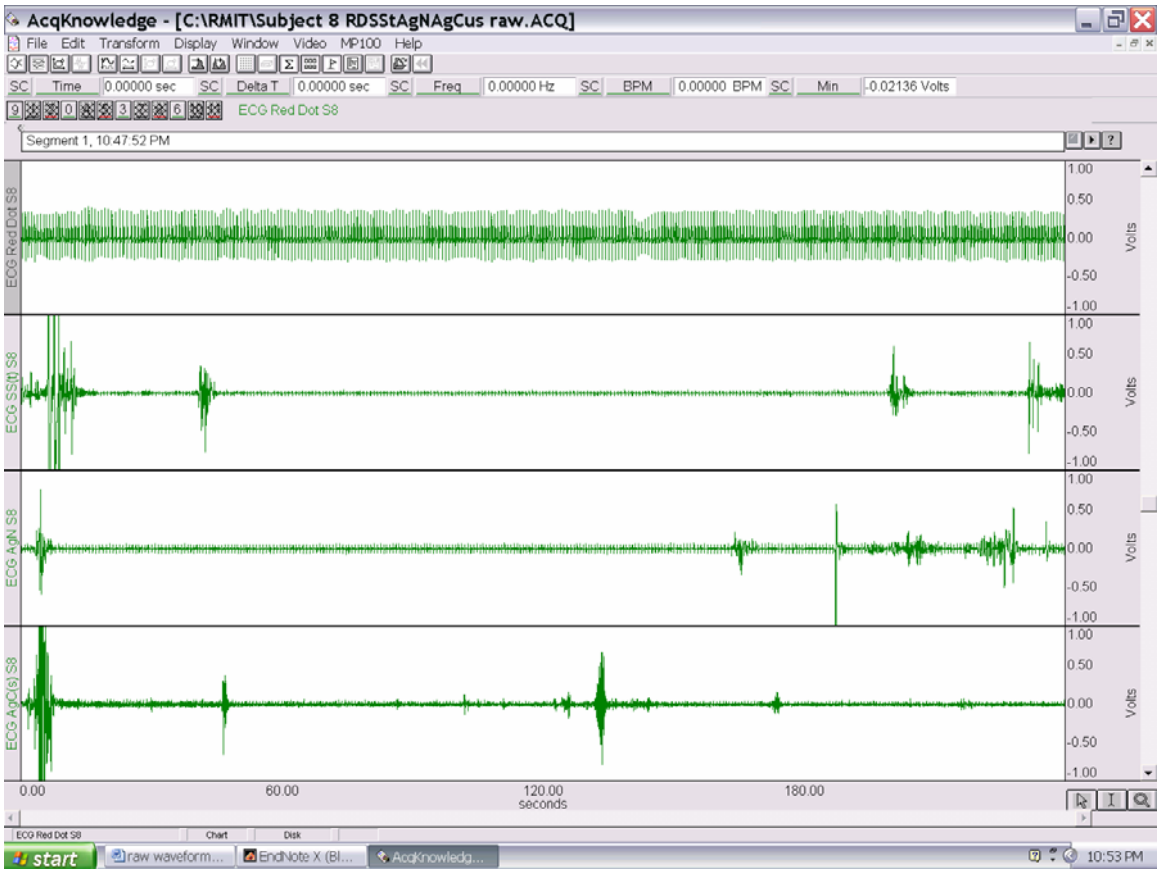

Figure F9. Subject 8, Acquired ECG waveform signals (as displayed on Biopac AcqKnowledge software), (4 mins), top to bottom, Red Dot, SSt, AgN, AgCu(s).

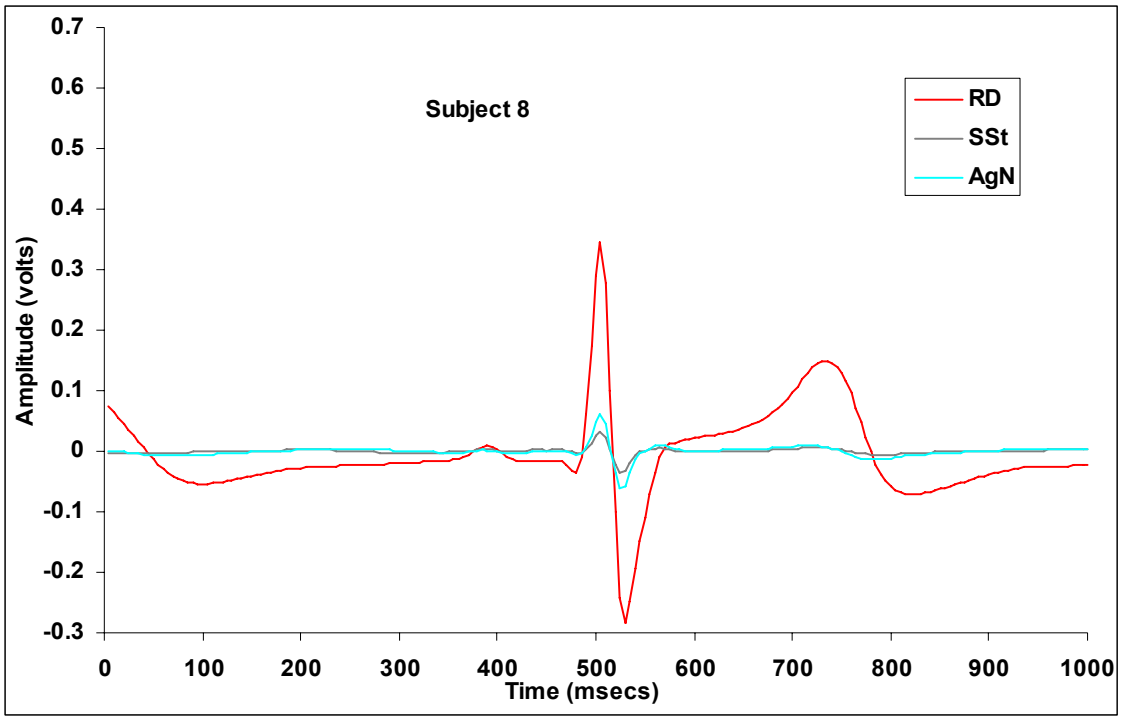

Figure F9a. Subject 8 average ECG waveforms for Red Dot, SSt, AgN, AgCu(s). electrodes.

Table F9. Subject 8, Features extracted from ECG waveforms.

SUBJECT 8	ELECTRODE TYPES mn = mean value, sd =standard deviation							
Parameters	RD1 mn	RD1 sd	SSt mn	SSt sd	AgN mn	AgN sd	AgCs mn	AgCs sd
Pmax(volts)	0.009	0.006						
Qmax(volts)	-0.036	0.007					not	useable
Rmax(volts)	0.344	0.027						
Smax(volts)	-0.283	0.017						
Tmax(volts)	0.148	0.012						
Intervals intervals in number of samples, sample is 5 msec								
QRS	27.665	3.512						
QT	68.750	1.747						
PR	22.073	1.943						
PQ	7.149	2.910						
ST	5.142	2.007						
SR pi	4.941	0.274						
RQ pi	5.472	1.396						
TR pi	45.594	0.697						
RP pi	23.238	0.662						
RR pi	149.674	8.206						
Intervals in msec								
QRS	138	18						
QT	344	9						
PR	110	10						
PQ	36	15						
ST	26	10						
SR pi	25	1						
RQ pi	27	7						
TR pi	228	3						
RP pi	116	3						
RR pi	748	41						

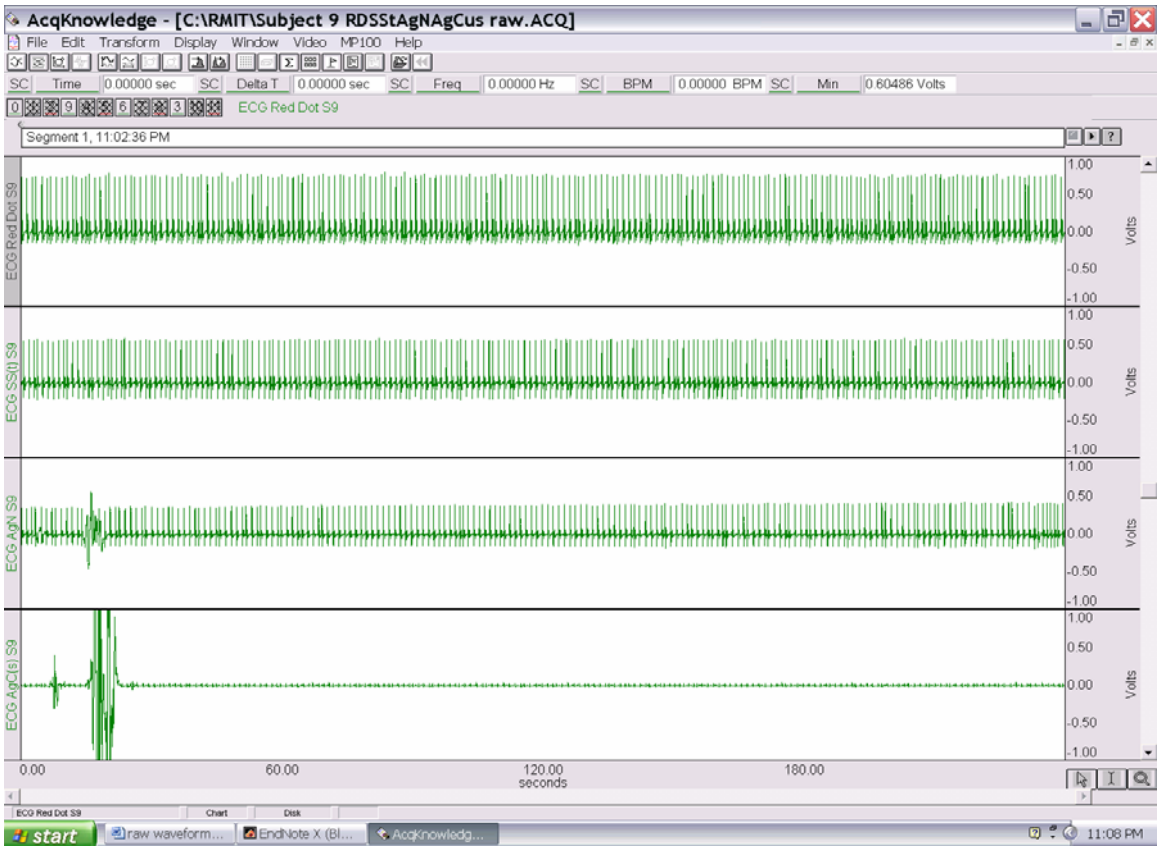

Figure F10. Subject 9, Acquired ECG waveform signals (as displayed on Biopac AcqKnowledge software), (4 mins), top to bottom, Red Dot, SSt, AgN, AgCu(s).

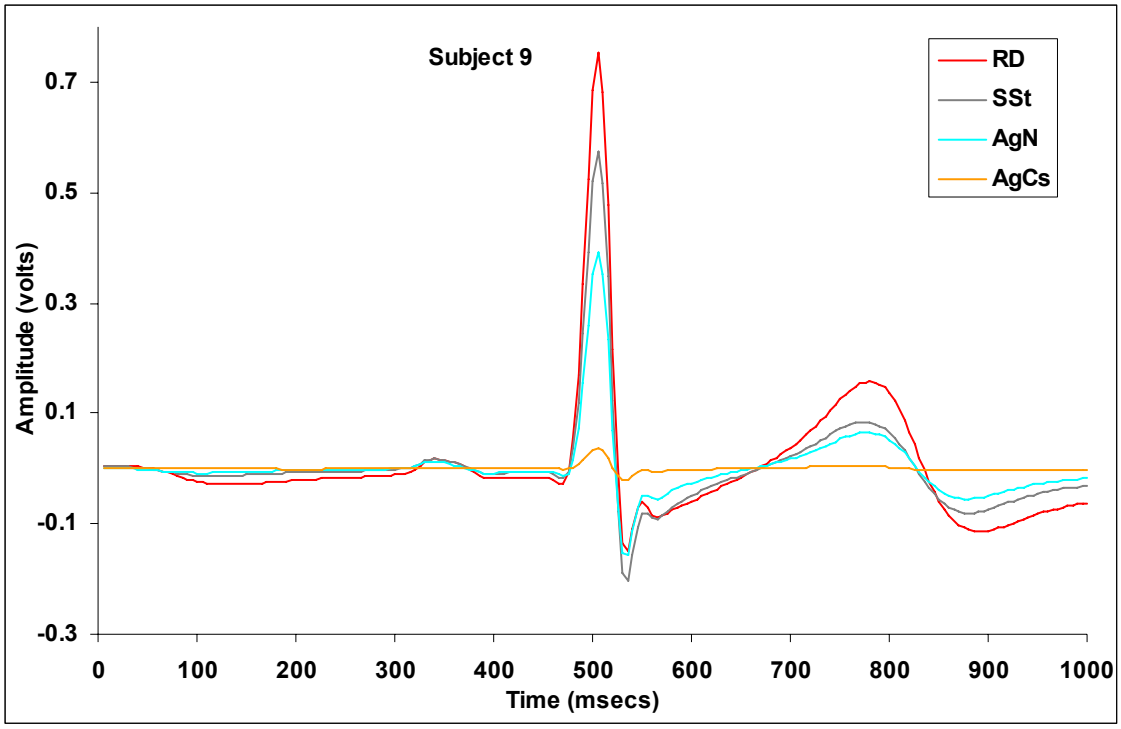

Figure F10a. Subject 9 average ECG waveforms for Red Dot, SSt, AgN, AgCu(s). electrodes .

Table F10. Subject 9, Features extracted from ECG waveforms.

SUBJECT 9	ELECTRODE TYPES mn = mean value, sd =standard deviation							
Parameters	RD3 mn	RD3 sd	SSt3 mn	SSt3 sd	AgN3 mn	AgN3 sd	AgCus mn	AgCus sd
Pmax(volts)	0.021	0.025	0.020	0.013	0.014	0.008		
Qmax(volts)	-0.028	0.007	-0.018	0.003	-0.014	0.006		
Rmax(volts)	0.752	0.018	0.575	0.011	0.376	0.079		
Smax(volts)	-0.156	0.012	-0.208	0.009	-0.157	0.033		
Tmax(volts)	0.159	0.008	0.086	0.004	0.080	0.068		
Intervals intervals in number of samples, sample is 5 msec								
QRS	22.126	3.348	22.149	2.687	21.983	3.140		
QT	85.307	3.032	81.343	5.376	80.016	6.467		
PR	28.637	6.243	27.975	5.852	28.746	3.989		
PQ	9.901	4.494	11.475	5.578	11.788	5.594		
ST	11.595	1.577	4.765	0.802	5.235	2.435		
SR pi	5.649	0.479	5.642	0.481	5.770	1.259		
RQ pi	8.341	3.134	7.662	2.250	7.415	1.956		
TR pi	55.078	1.319	53.397	1.470	53.120	4.466		
RP pi	30.561	5.859	31.441	4.796	32.721	3.736		
RR pi	233.172	44.588	233.291	41.735	240.819	39.940		
Intervals in msecs								
QRS	111	17	111	13	110	16		
QT	427	15	407	27	400	32		
PR	143	31	140	29	144	20		
PQ	50	22	57	28	59	28		
ST	58	8	24	4	26	12		
SR pi	28	2	28	2	29	6		
RQ pi	42	16	38	11	37	10		
TR pi	275	7	267	7	266	22		
RP pi	153	29	157	24	164	19		
RR pi	1166	223	1166	209	1204	200		

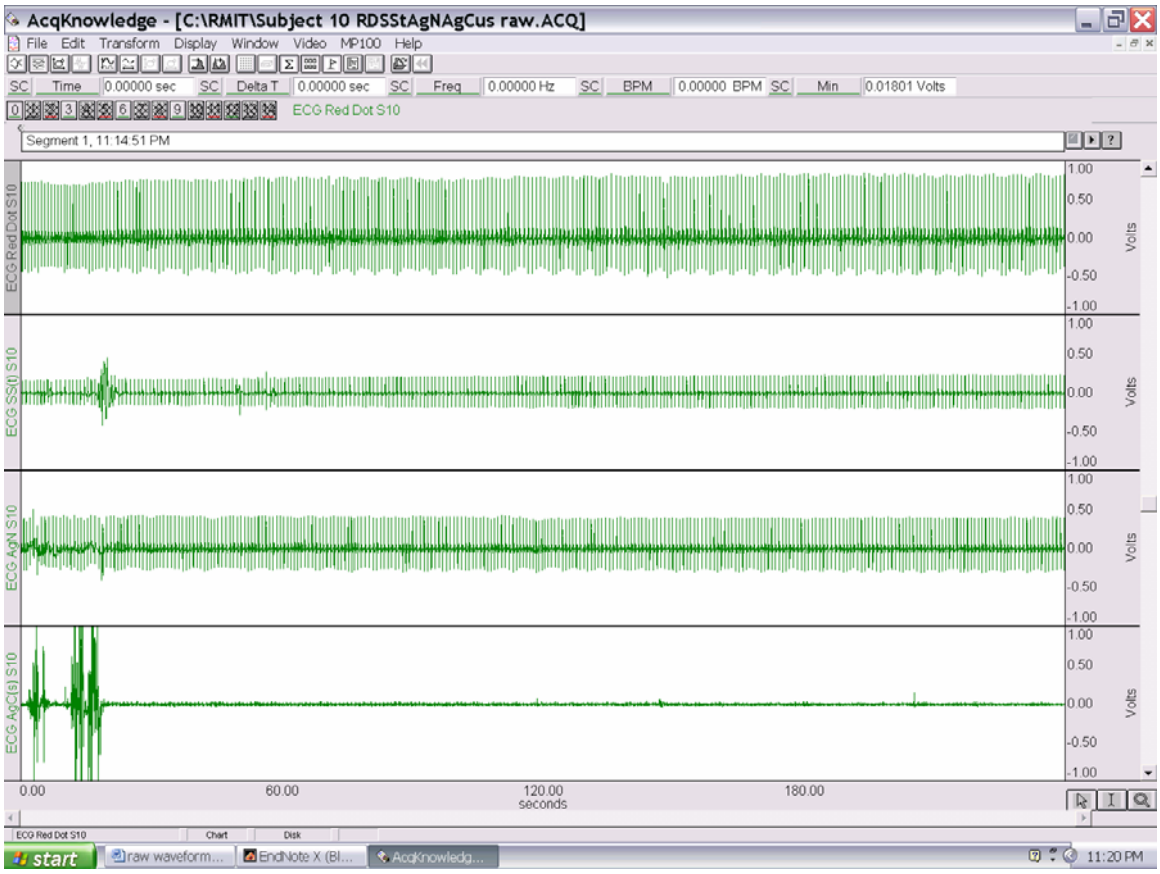

Figure F11. Subject 10, Acquired ECG waveform signals (as displayed on Biopac AcqKnowledge software), (4 mins), top to bottom, Red Dot, SSt, AgN, AgCu(s).

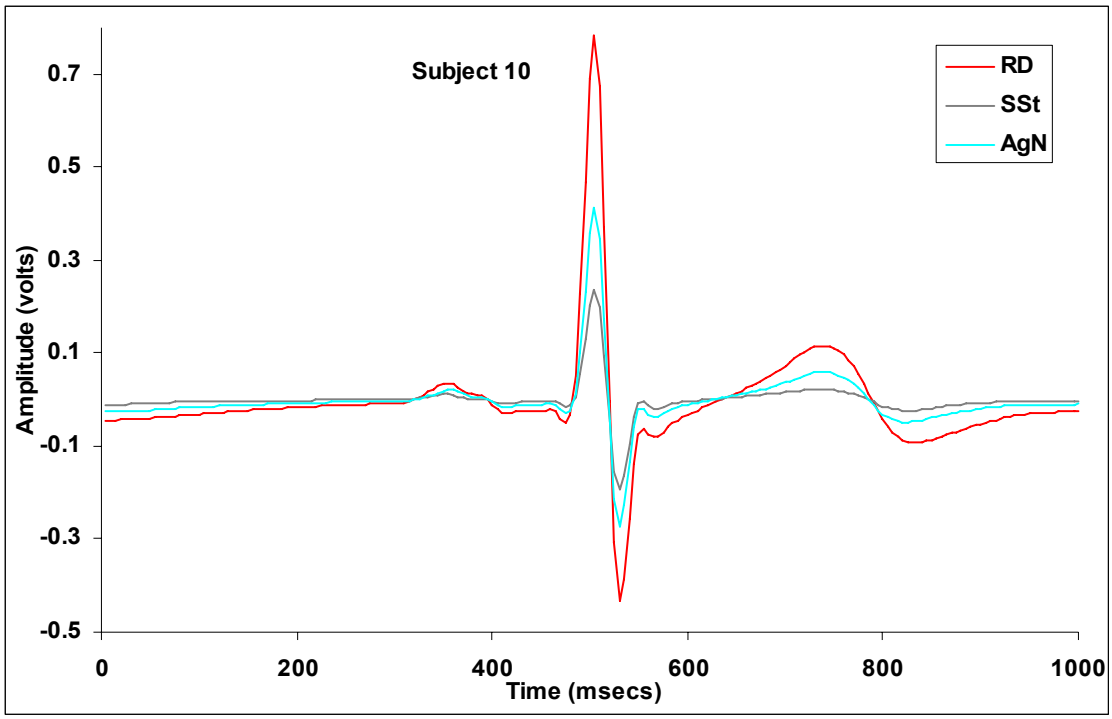

Figure F11. Subject 10 average ECG waveforms for Red Dot, SSt, AgN, electrodes.

Table F11. Subject 10, Features extracted from ECG waveforms.

SUBJECT 10	ELECTRODE TYPES mn = mean value, sd =standard deviation							
Parameters	RD mn	RD sd	SS mn	SS sd	AgN mn	AgN sd	AgC mn	AgC sd
Pmax(volts)	0.038	0.008	0.012	0.005	0.023	0.020	0.009	0.006
Qmax(volts)	-0.052	0.012	-0.016	0.006	-0.032	0.017	-0.008	0.006
Rmax(volts)	0.775	0.033	0.227	0.017	0.412	0.017	0.020	0.019
Smax(volts)	-0.433	0.035	-0.187	0.015	-0.271	0.023	-0.011	0.006
Tmax(volts)	0.115	0.013	0.023	0.004	0.061	0.011	0.020	0.009
Intervals intervals in number of samples, sample is 5 msec								
QRS	21.026	1.901	20.005	2.203	20.319	1.637	33.931	9.464
QT	70.908	2.562	67.740	6.791	69.662	2.740	77.587	17.585
PR	31.451	2.180	27.724	2.722	28.874	2.871	22.097	7.820
PQ	11.410	1.670	12.195	3.566	10.725	3.118	7.403	4.884
ST	5.429	1.439	12.874	5.780	7.880	2.301	21.760	18.652
SR pi	5.173	0.380	4.986	0.152	5.018	0.134	14.707	5.995
RQ pi	5.980	0.917	5.781	1.858	5.865	1.745	11.533	5.522
TR pi	46.204	1.301	45.609	3.377	46.433	1.093	58.600	17.703
RP pi	30.301	1.541	30.609	1.536	29.331	1.586	32.027	8.223
RR pi	182.097	46.513	178.687	22.844	174.069	41.040	559.743	610.709
Intervals in msecs								
QRS	105	10	100	11	102	8	170	47
QT	355	13	339	34	348	14	388	88
PR	157	11	139	14	144	14	110	39
PQ	57	8	61	18	54	16	37	24
ST	27	7	64	29	39	12	109	93
SR pi	26	2	25	1	25	1	74	30
RQ pi	30	5	29	9	29	9	58	28
TR pi	231	7	228	17	232	5	293	89
RP pi	152	8	153	8	147	8	160	41
RR pi	910	233	893	114	870	205	2799	3054

APPENDIX G Yarn data
SILVER NYLON AgN

SHIELDEX Technical Data Sheet PN# PY16125x2

Conductive Yarn

Conductive Yarn — Silver Plated Nylon Yarn 117/17 x 2-ply

PURPOSE:	Conductive thread for ESD, medical and EMI knitted gasket applications
Description:	Silver plated nylon 66 yarn
Material Resistance:	100-150Ω/inch
Material Resistivity:	< 0.025 Ω/sq. cm

General Properties

Nominal Denier:	125/17 x 2 ply
Nominal Diameter:	170 microns
Number of Filaments:	34 nominal
Twist:	16 TPI nominal
Twist Direction:	S
Ply-Twist:	12 TPI Nominal
Ply-Twist Direction:	Z
End Joinings:	air splice only
Splice Frequency:	4 Max/Package
Transfer Tail:	None
Yield	19,800 yards/lb.

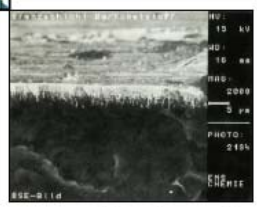

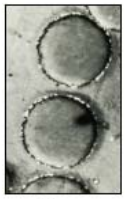

Cross section views of nylon fiber showing silver deposits

Physical Properties

Denier At 11% MR:	Min=200 / Max=260
Breaking Strength (g.)*:	Min=675 / Max=725
Elongation At Break (%):	Min=15.8 / Max=21.4
Shrinkage (%) **:	Min=5 / Max=20
Tenacity (g/den)	5.0

Packaging

Single Case:	21 Packages
Nominal Case Weight:	23 lb.
Standard Pallet:	16 Cases
Nominal Pallet Weight:	468 lb.

Package Properties

Core Type:	3 Deg-30 Min Cone 9"
Core Material:	Pressed Paper or plastic
Product ID Color:	Gray
Package Weight:	0.1 LB Nominal
Package Weight Control:	+/- .1 lb. within single case

SHIELDEX produced by Statex

Shieldex Trading (US)
4502 Route 31 Palmyra NY 14522 USA
Tel: +1 315-597-1678 Fax: +1 315-597-6687
shieldex2@rochester.rr.com www.shieldextrading.net

Statex Productions & Vertriebs GmbH
Kleiner Ort 11, 28257 Bremen Germany
Tel: (+49)421-275047/8 Fax: (+49)421-273643
erichsen@statex.de www.statex.de

APPENDIX G2 Stainless Steel

SSt

High-conductive fibres and yarns with high thermal resistance

R.STAT/S (stainless steel)

	Dtex	Electrical restivity (Ω/cm)	Tensile strength (cN)	Elongation
R.STAT/S 8µ	4	150 - 170	7,5 +/- 10%	1%
R.STAT/S 12µ	9	60 - 80	18 +/- 10%	1%
R.STAT/S 22µ	30	10 - 30	55 +/- 10%	1%

R.STAT/S fibres combine :

Characteristics	Presentation
Cracked fibres Standard cut-length 50-60 mm Other cut-lengths on request	• Pure staple 12/100 (100 % stainless steel 12µ) • Staple blend 12/50 (50 % stainless steel 12µ + 50 % PES) • Staple blend 82/18 (82 % wool + 18 % stainless steel 12µ)
Cracked slivers	• 100 % stainless steel 8µ 2g, 3g, 4g, 5g and 6g / meter standard cut-length 50-60 mm • Staple 12µ in blend with nylon, wool, polyester 0.6 g to 20 g / metre • Special cut-length on request
Spun yarns	• 100 % stainless steel Standard : Nm 11/2 100 % stainless steel 12µ ***Other counts on request*** • In blend (PES, nylon, aramids...) Standard : Nm 50/1 80 % PES – 20 % stainless steel 8µ ***Other counts and blends on request***
Continuous yarns	• Stranded yarn 100 % stainless steel 12µ 275 filaments x 2, 200 tpm

APPENDIX G3

Elektrisola

AgCu(s), AgCu(m)

Typical mechanical values of the metals			
Metal	Density [kg/dm^3]	Breaking strength approx. [N/mm^2] from to	Elongation approx. [%] from to
Copper (Cu) and silver-plated copper (Cu/Ag)	8,9	260 320	10 35
Brass (Ms) and silver-plated brass (Ms/Ag)	8,5	410 590	10 30
Aluminium (Al)	2,7	120 180	5 25
Copper-clad aluminium (CCA)	3,3	180 220	5 15

Supply spools

Spool type	d1	d4 [mm]	l1	Approx. nom. filling weight [kg]	Wire diameter range
79/45	80	16	100	0,7	0,020-0,030
124/45R	125	16	125	2,5	0,025-0,063
159/45R	160	22	160	6,0	0,040-0,080
199/45R	200	22	200	11,0	0,050-0,080

Fineness / Diameter

Nominal diameter of the metal [mm]	Outside diameter approx.	dtex [g/10'000 m]
0,020	0,024	30
0,025	0,030	49
0,027	0,032	56
0,032	0,036	76

0,038	0,043	110
0,040	0,048	123
0,050	0,059	192
0,063	0,075	303
0,071	0,083	385
0,080	0,093	476

Wire types

TW-0 Bare wire without protective coating, silver-coloured, for conductive fabrics, ESD applications

TW-C Wire for fashion with a wide range of colour variations

TW-D Wire with high mechanical and chemical resistance

TW-F Wire with very high mechanical and chemical resistance

Processing

Our metal monofilaments can be used with all types of fibre.

It is important in the twisting-, weaving-, embroidering- and finishing process that neither the silver layer nor the enamel layer on the wire becomes damaged. Therefore the product should be checked after each working process.

Finishing

All piece goods with a metal part have to be finished with care (see also point processing).

Washing

Washing at 40°C with overdrive (ISO 6330, procedure 7A) is possible, if the construction of the piece goods takes into consideration the properties of metal yarns and the metal monofilaments did not become damaged. Therefore the qualities should be tested and repeated periodically by the manufacturer with washing tests.

Guarantee

Elektrisola Feindraht AG guarantees the sample-conforming supply of the metal monofilaments. We have no influence on the properties of the final products.

APPENDIX H ECG Algorithm

```
%% Analyse an ECG data stream to extract to extract the standard
%% descriptors P, Q, R, S, T, PR segment, ST segment, PR interval, QRS
%% duration, QT interval and RR
function ECGparams = AnalyseECG(ECG)
% The RS peak is not always the dominant peak in aberrant ecgs but is
% always the sharpest, so to make sure we select this peak we take the
% derivative of the spectrum and look for the maximum with a
corresponding
% minimum within 15 data points
start = 1;
ECGparams = [];
ECGd = diff(ECG);
ECGlen = length(ECG);
while start < length(ECG) - 155
    % Look for the maximum within the first 150 points
    range = start:(start+160);
    [maxv maxp] = max(ECGd(range));
    [minv minp] = min(ECGd(range));
    if (minp > maxp) && (minp - maxp < 15)
      % we have found the right peak
        % Correct the position for the start of the range
        maxp = maxp + start - 1;
        minp = minp + start - 1;
        [R Rp] = max(ECG(maxp:minp));
        Rp = Rp + maxp - 1;
        % Make sure that we are not too close to the end
        if (Rp + 75) > ECGlen
            Start = ECGlen + 1;
      % Set the start value > length so that the loop will exit
            break
        end
      % Now find S (the minimum value within 20 units of R
        [S Sp] = min(ECG(Rp:(Rp+20)));
      % Correct for the offset
        Sp = Sp + Rp - 1;
     % Now find Q (the minimum value within 20 points to the left of R
        [Q Qp] = min(ECG((Rp-20):Rp));
        Qp = Qp + Rp - 21;

        Qp
        % Next find T within 60 points of S
        [T Tp] = max(ECG(Sp:(Sp+60)));
        Tp = Tp + Sp - 1;
      % The next point we want to find is J - the beginning of the ST
      % segment. To do this we find the first occurrence after S where
      % the derivative rises above -0.001.
        J = find(ECGd(Sp:(Sp+20)) < 0.001,1,'first');
        if isempty(J)
            J=0;
            ST=0;
            QRS = 0;
            QT  = 0;
        else
            J = J + Sp - 1;
        % Get the value at J tp help find the beginning of the T peak
            Jval = ECG(J);
```

```
% The end of the ST segment is the last point in the interval
% ST where the value is less than 5% of the vaule at T
    val = (T - Jval)/20 + Jval;
    ST = find(ECG(J:Tp)<val,1,'last') - 1;
% ST is the offset from J
end
% We now need to find the end of the T peak.
% The first method requires we find a valley floor within 55
% points of the T peak
for i = Tp:(Tp+55)
    if ECG(i+1) > ECG(i)
        break
    end
end
if i < Tp+55
    Tend = i;
else
% Couldn't find a valley so the next method is to find the
% position of the first point in the derivative to fall below
    % 0.001
    Tend = find(ECGd(Tp:(Tp+55))<0.001,1,'first');
    if isempty(Tend)
        Tend=0;
    else
        Tend = Tend + Tp - 1;
    end
end
if Tend > 0
    QT = Tend - Qp;
else
    QT = 0;
end
% Now to find P (within 30 units of Q)
[P Pp] = max(ECG((Qp-30):Qp));
Pp = Pp + Qp - 31;
% Find the end of the PR Interva/Segment. Track the derivative
% back from Q until the value falls below -0.001. This ensures
% we are on the descent to Q and so the end of the PR segment
%is the last point starting from P with derivative above-0.001
% changed from 30 to 40 MAM
for i = Qp:-1:Pp
    if ECGd(i)<-0.001
        break
    end
end
PRend = find(ECGd(Pp:i) > -0.001,1,'last');
if isempty(PRend)
    PRseg = 0;
    PRint = 0;
    QRS = 0;
else
    PRend = PRend + Pp - 1;
% Since we have found an end to both the segment and the
% interval, we cal look for a start.
%The start of the PR segment is the first point in the P-PRend
%interval where the value is less than 5% of P.
    val = (P - ECG(PRend))/20 + ECG(PRend);
    Pend = find(ECG(Pp:PRend)> val,1,'last') + Pp - 1;
    if isempty(Pend)
        PRseg = 0;
    else
        PRseg = PRend - Pend + 1;
```

```
            end
        % Since, like the T peak, the start and end of the P peak can
        % be at different heights the only available technique is to
        % find the first point travelling back from the rising edge of
        % P where the derivative falls below 0.001
            for i = Pp:-1:(Pp-15)
                if ECGd(i) > 0.001
                    break
                end
            end
            Pstart = find(ECGd((Pp-15):i)< 0.001,1,'last') + Pp - 16;
            if isempty(Pstart)
                PRint = 0;
            else
                PRint = PRend - Pstart + 1;
            end
            if J > 0
                QRS = J - PRend + 1;
            end
        end
        % For debugging purposes to find the place where it falls over
         Rp
        ECGparams = [ECGparams; [P Q R S T QRS QT PRint PRseg ST (Sp -
Rp) ...
            (Rp - Qp) (Tp - Rp) (Rp - Pp) Rp]];
        start = Rp + 100;
    %changed Rp=100 to 200
    else
        start = start + 150;
        %was 150
    end
end
% Now get the heart beat interval (set the first to 0)

RR = diff(ECGparams(:,15));
ECGparams(2:length(ECGparams),15) = RR;
ECGparams(1,15) = 0;
am = [];
as = [];
for i = 1:15
    am = [am mean(ECGparams(ECGparams(:,i)~= 0,i))];
    as = [as std(ECGparams(ECGparams(:,i)~= 0,i))];
end
ECGparams = [am; as; ECGparams];
```

BIBLIOGRAPHY

[1] J. M. Winters, Y. Wang, and J. M. Winters, "Wearable Sensors and Telerehabilitation : *Integrating Intelligent Telerehabilitiation Assistants with a Model for Optimizing Home Therapy*," *IEEE Engineering in Medicine and Biology Magazine,* pp. 56-65, 2003.

[2] E. Villalba, M. Ottaviano, M. T. Arredondo, A. Martinez, and S. Guillen, "Wearable Monitoring System for Heart failure Assessment in a Mobile Environment," *Computers in Cardiology,* vol. 33, pp. 237-240, 2006.

[3] G. Troster, "Review: The Agenda of Wearable Healthcare," *IMIA Yearbook of Medical Informatics: Ubiquitous Health Care Systems,* pp. 125-138, 2005.

[4] A. Lymberis and S. Olsson, "Intelligent Biomedical Clothing for Personal Health and Disease Management: State of the Art and Future Vision," *Telemedicine Journal and e-Health,* vol. 9, pp. 379-386, 2003.

[5] P. Bonato, "Advances in wearable technology and applications in physical medicine and rehabilitation," *Journal of NeuroEngineering and Rehabilitation,* vol. 2, 2005.

[6] A. Dittmar and A. Lymberis, "Smart Clothes and Associated Wearable devices for Biomedical Ambulatory Monitoring," in *13th International Conference on Solid-State Sensors, Actuators and Microsystems,Transducers*, Seoul, Korea, 2005, pp. 221-227.

[7] S. Park and S. Jayaraman, "Enhancing the quality of life through wearable technology," in *IEEE Engineering in Medicine and Biology Magazine*. vol. May/June, 2003, pp. 41-48.

[8] E. R. Post, M. Orth, P. R. Russo, and N. Gershenfeld, "E-broidery: Design and Fabrication of textile-based computing," *IBM Systems Journal,* vol. 39, pp. 840-860, 2000.

[9] D. De Rossi, F. Carpi, F. Lorussi, A. Mazzoldi, R. Paradiso, E. P. Scilingo, and A. Tognetti, "Electroactive Fabrics and Wearable Biomonitoring Devices," *AUTEX Research Journal,* vol. 3, 2003.

[10] D. De Rossi, F. Carpi, F. Lorussi, A. Mazzoldi, E. P. Scilingo, and A. Tognetti, "Electroactive Fabrics for Distributed, Conformable and Interactive Systems," in *Sensors 2002* 2002, pp. 1608-1613.

[11] F. H. Wilhelm, W. T. Roth, and M. A. Sackner, "The LifeShirt: An Advanced System for ambulatory measurement of respiratory and cardiac function. ," *Behaviour Modification,* vol. 27, pp. 671-691, 2003.

[12] VTAM Project, "http://www.medes.fr/VTAMN.html," accessed May 2007.

[13] E. P. Scilingo, F. Lorussi, A. Mazzoldi, and D. De Rossi, "Strain-Sensing Fabrics for Wearable Kinaesthetic-Like Systems," *IEEE Sensors Journal,* vol. 3, pp. 460-467, 2003.

[14] Sensatex, "http://www.gtwm.gatech.edu/gtwm.html," accessed May 2007.

[15] Y. A. Chizmadzhev, A. V. Indenbom, P. I. Kuzmin, S. V. Galichenko, J. C. Weaver, and R. O. Potts, "Electrical Properties of Skin at Moderate Voltages: Contribution of Appendageal Macropores," *Biophysical Journal,* vol. 74, pp. 843-856, 1998.

[16] C. Cullander and R. H. Guy, "Visualisation of iontophoretic pathways with confocal microscopy and the vibrating probe electrode," *Solid State Ionics,* vol. 53-56, pp. 197-206, 1992.
[17] S. Grimnes, "Pathways of Ionic Flow through Human Skin *in vivo*," *ACTA Derm Venereol(Stockh),* vol. 64, pp. 93-98, 1984.
[18] E. T. McAdams, J. Jossinet, A. Lackermeier, and F. Risacher, "Factors affecting electrode -gel-skin interface impedance in electrical impedance tomography," *Medical & Biological Engineering & Computing,* vol. 34, pp. 397-408, 1996.
[19] M. M. Puurtinen, S. M. Komulainen, P. K. Kauppinen, and J. A. V. Malmivuo, "Measurement of noise and impedance of dry and wet textile electrodes and textile electrodes with hydrogel," in *EMBS Annual International Conference*, New York City, USA, 2006, pp. 6012-6015.
[20] A. C. Williams, *Transdermal Drug Delivery: From theory to clinical practice*: Pharmaceutical Press, 2003.
[21] A. F. Coston and J. K. Li, "Transdermal Drug Delivery: An Assessment of Skin Impedance Models," *IEEE Transactions,* pp. 319-320, 2003.
[22] S. Grimnes and O. G. Martinsen, "Cole Electrical Impedance Model - A Critique and an Alternative," *IEEE Transactions on Biomedical Engineering,* vol. 52, pp. 132-135, 2005.
[23] Y. Yamamoto, "Measurement and Analysis of Skin Electrical Impedance," *Acta Derm Venereol,* vol. Suppl. 185, pp. 34-38, 1994.
[24] O. G. Martinsen, S. Grimnes, and O. Sveen, "Dielectric properties of some keritanised tissues. Part 1: *Stratum corneum and nail in situ.*," *Med Biol Eng Comput,* vol. 35, pp. 172-176, 1997.
[25] D. M. Ferreira, C. S. Silva, and M. N. Souza, "Electrical impedance model for evaluation of skin irritation in rabbits and humans," *Skin Research and Technology*pp. 1-9, 2007.
[26] R. Ivanic, I. Novotny, V. Rehacek, V. Tvarozek, and M. Weis, "Thin film non-symmetric microelectrode array for impedance monitoringof human skin," *Thin Solid Films,* pp. 332-336, 2003.
[27] IEC Standard, "IEC 60601-1 Ed 3.0 Medical Electrical Equipment -part 1, General requirements for basic safety and essential performance.," International, 2005.
[28] J. W. Clark, "Origin of Biopotentials," in *Medical Instrument: Application and Design*, 3rd ed, J. G. Webster, Ed. New York: John Wiley & Sons, Inc, 1998.
[29] O. G. Martinsen, S. Grimnes, and E. Haug, "Measuring depth depends on frequency in skin impedance measurements," *Skin Research and Technology,* vol. 5, pp. 179-181, 1999.
[30] O. G. Martinsen, S. Grimnes, and H. P. Schwan, "Interface Phenomena and Dielectric Properties of Biological Tissue," in *Encyclopedia of Surface and Colloid Science* Marcel Dekker Inc., 2002, pp. 2463-2652.
[31] D. J. Hewsen, J. Duchene, and J. Y. Hogrel, "Changes in impedance at the electrode-skin interface of surface EMG electrodes during long term recordings," in *23rd Annual EMBS International Conference*, Istanbul, Turkey, 2001, pp. 3345-3348.
[32] O. Pahlm and L. Sornmo, "Software QRS detection in ambulatory monitoring - a review," *Med Biol Eng Comput,,* vol. 22, pp. 289-297, 1984.
[33] R. Vigouroux, "The electrical resistance considered as a clinical sign," *Progres Medicale,* vol. 3, pp. 87-89, 1888.

[34] M. Kanebako, T. Inagi, and K. Takayama, "Evaluation of Skin Barrier function Using Direct Current I: Effects of Conductivity, Voltage , Distance between Electrodes and electrode Area," *Biol.Phar.Bull,* vol. 25, pp. 1456-1460, 2002.
[35] P. Aberg, P. Geladi, I. Nicander, and S. Ollmar, "Variation of skin properties within human forearms demonstrated by non-invasive detection and multi-way analysis," *Skin Research and Technology,* vol. 8, pp. 194-201, 2002.
[36] Philippot et al, "The Perception of Bodily Sensations during emotion: A cross-cultural perspective," *Polish Journal of Social Psychology,* 1997.
[37] J. Malmivuo and R. Plonsey, *Bioelectromagnetism: Principles and Application of Bioelectric and Biomagnetic Fields*. New York: Oxford University Press, 1995.
[38] BioSemi, "http://www.biosemi.com," accessed May 2007.
[39] B. J. Drew, R. M. Califf, M. Funk, E. S. Kaufman, M. W. Krucoff, P. W. Macfarlane, C. Sommargren, S. Swiryn, and G. F. Van Hare, "Practice Standards for Electrocardiograph Monitoring in Hospital Settings " *Journal of the American Heart Association,* vol. 110, pp. 2721-2746, 2004.
[40] G. Jelen, "Acrylate, a hidden allergen of electrocardiograph monitoring electrodes " *Contact Dermatitis,* vol. 45, pp. 315-316, 2001.
[41] M. Avenel-Audran, A. Goossens, E. Zimerson, and M. Bruze, "Contact Dermatitis from electrocardiograph monitoring electrodes: role of p-tert-butylphenolformaldehyde resin," *Contact Dermatitis,* vol. 48, pp. 108-111, 2003.
[42] W. Uter and H. Schwanitz, "Contact dermatitis from propylene glycol in ECG electrode gel," *Contact Dermatitis,* vol. 34, pp. 230-231, 1996.
[43] A. Searle and K. Kirkup, "A direct comparison of wet, dry and insulating bioelectric recording electrodes," *Physiological Measurement,* vol. 21, pp. 271-283, 2000.
[44] S. R. Wiese, P. Anheier, R. D. Connemara, A. T. Mollner, T. F. Neils, J. A. Kahn, and J. G. Webster, "Electrocardiograph Motion Artifact Versus Electrode Impedance," *IEEE Transactions on Biomedical Engineering,* vol. 52, pp. 136-139, 2005.
[45] R. Wijesiriwardana, K. Mitcham, and T. Dias, "Fibre-Meshed Transducers Based Real Time Wearable Physiological Information Monitoring System," in *Eighth International Symposium on Wearable Computers*, 2004.
[46] ECG Library, "www.ecglibrary.com," accessed June 2007.
[47] N. J. Outram, E. C. Ifeachor, P. W. J. Van Eetvelt, and J. S. H. Curnow, "Techniques for optimal enhancement and feature extraction of fetal electrocardiogram," in *IEE Proc. Sci. Meas. Technol.,*, 1995, pp. 482-489.
[48] C. D. McManus, U. Teppner, D. Neubert, and S. M. Lobodzinski, "Estimation and removal of baseline drift in the electrocardiogram," *Computers and Biomedical Research,* vol. 18, pp. 1-9, 1985.
[49] J. P. Couderc and W. Zareba, "Contribution of the Wavelet Analysis to the Noninvasive Electrocardiography," *A.N.E,* vol. 3, pp. 54-62, 1998.
[50] S. C. Saxena, V. Kumar, and S. T. Hamde, "QRS detection using new wavelets," *Journal of Medical Engineering & Technology,* vol. 26, pp. 7-15, 2002.
[51] P. Bhatia, J. Boudy, and R. V. Andreao, "Wavelet transformation and pre-selection of mother wavelets for ECG signal processing," in *24th IASTED International Conference on Biomedical Engineering*, Innsbruck,Austria, 2006, pp. 390-395.

[52] H. S. Shin, C. K. Lee, S. W. Yoon, D. J. Yoon, and M. Lee, "Heart rate Variability Analysis using Electric Fabric in Dry-Normal Condition," in *Engineering in Medicine and Bilogy 27th Annual Conference*, Shangai, China, 2005, pp. 3563-3566.

[53] J. P. Niskanen, M. P. Tarvainen, P. O. Ranta-aho, and P. A. Karjalainen, "Software for advanced HRV analysis," University of Kuopio, Dept. Applied Physics 2002.

[54] UniversityUtah, "http://library.med.utah.edu/kw/ecg/ecg_outline/Lesson2/index.html#measurements." vol. 2007, 2007, p. ECG Waveform.

[55] K. S. Kim, T. Yoon, J. W. Lee, D. Kim, and H. Koo, "A Robust Human Identification by Normalized Time-Domain Features of Electrocardiogram," in *Engineering in Medicine and Biology 27th Annual Conference*, Shanghai, China, 2005, pp. 1114-1117.

[56] K. Lund, H. Nygaard, and K. Pedersen, "Weighing the QT Intervals with the Slope or the Amplitude of the T wave," *A.N.E,* vol. 7, pp. 4-9, 2002.

[57] I. Goldenberg, A. J. Moss, and W. Zareba, "QT Interval: How to Measure it and What Is "Normal"," *Cardiovascular Electrophysiology,* vol. 17, pp. 333-336, 2006.

[58] B. Sredniawa, A. Musialik, P. Jarski, A. Sliwinska, and Z. Kalarus, "Methods of Assessment and Clinical Relevance of QT Dynamics," *Indian Pacing and Electrophysiology Journal,* vol. 5, pp. 221-232, 2005.

[59] E. Pueyo, P. Smetana, P. Caminal, A. Bayes de Luna, M. Malik, and P. Laguna, "Characterization of QT Interval Adaptation to RR Interval Changes and Its Use as a Risk-Stratifier of Arrhythimic Mortality in Amiodarone-Treated Survivors of Acute Myocardial Infarction" *IEEETransactions on Biomedical Engineering* vol. 51, pp. 1511-1520, 2004.

[60] V. Piotrovsky, "Pharmacokinetic-Pharmacodynamic Modelling in the Data Analysis and Interpretation of Drug-induced QT/QTc Prolongation," *AAPS Journal,* vol. 7, pp. E609-E624, 2005.

[61] J. Hill and A. Timmis, "ABC of clinical electrocardiology: Exercise Tolerance Testing," *BMJ,* vol. 324, pp. 1084-1087, 2002.

[62] M. Malik, P. Farbom, V. N. Batchvarov, K. Hnatkova, and A. J. Camm, "Relation between QT and RR intervals is highly individual among healthy subjects: implications for heart rate correction on the QT interval," *Heart,* vol. 87, pp. 220-228, 2002.

[63] J. H. Indik, E. C. Pearson, K. Fried, and R. L. Woosley, "Bazett and Fredericia QT correction formulas interfere with measurement of drug-induced changes in QT interval," *Heart Rhythm,* vol. 3, pp. 1003-1007, 2006.

[64] V. N. Batchvarov, A. Ghuran, P. Smetana, K. Hnatkova, M. Harries, P. Dilaveris, A. J. Camm, and M. Malik, "QT-RR relationship in healthy subjects exhibits substantial intersubject variability and high intrasubject stability" *Am J Physiol Heart Circ Physiol,* vol. 282, pp. 2356-2363, 2002.

[65] Y. Lokhandwala, "The fallacies of QT correction," *Indian Pacing and Electrophysiology Journal,* vol. 3, pp. 185-186, 2003.

[66] C. Dota, B. Skallefell, N. Edvardsson, and G. Fager, "Computer-Based Analysis of Dynamic QT Changes:*Toward High Precision and Individual Rate Correction*," *A.N.E,* vol. 7, pp. 289-301, 2002.

[67] G. C. Williams, K. M. Dunnington, and M.-Y. Hu, "The Impact of Posture on Cardiac Repolarisation: More Than Heart Rate?," *Journal of Cardiovascular Electrophysiology,* vol. 17, pp. 352-358, 2006.

[68] M. J. Burke and M. Nasor, "The time relationships of the constituent components of the human electrocardiogram," *Medical Engineering & Technology,* vol. 26, pp. 1-6, 2002.

[69] S. Luo, K. Michler, P. Johnston, and P. Macfarlane, "A Comparison of Commonly Used QT Correction Formulae: The Effect of Heart Rate on the QTc of Normal ECGs," *Journal of Electrocardiology,* vol. 37, pp. 81-90, 2004.

[70] A. M. Hekkala, H. Vaananen, H. Swan, L. Oikarinen, M. Viitasalo, and L. Toivonen, "Reproducibility of Computerised Measurements of QT Interval from Multiple Leads at Rest and During Exercise," *A.N.E,* vol. 11, pp. 318-326, 2006.

[71] H. C. Bazett, "An analysis of the time relations of electrocardiograms," *Heart,* vol. 7, p. 353, 1920.

[72] B. Hosmane, C. L. Locke, and D. Morris, "QT Interval:Correction for Heart Rate," *Journal of Applied Research,* vol. 6, pp. 288-299, 2006.

[73] M. Hodges, "Rate Correction of the QT Interval," *Cardiac Electrophysiology Review,* vol. 3, pp. 360-363, 1997.

[74] P. W. Macfarlane and J. Norrie, "The value of the electrocardiogram in risk assessment in primary prevention: Experience from the West of Scotland Coronary Prevention Study," *Journal of Electrocardiology,* vol. 40, pp. 101-109, 2007.

[75] F. Carpi and D. De Rossi, "Electroactive Polymer-Based Devices for e-Textiles in Biomedicine" *IEEE Transaction on Information in Biomedicine,* vol. 9, pp. 295-318, 2005.

[76] J. Edmison, D. Lehn, M. Jones, and T. Martin, "E-Textile Based Automatic Activity Diary for Medical Annotation and Analysis," in *International Workshop on Wearable and Implantable Body Sensor Networks*, 2006.

[77] N. Oliver and F. Flores-Mangas, "Healthgear: A Real-time Wearable System for Monitoring and Analysing Physiological Signals," in *International Workshop on Wearable and Implantable Body Sensor Networks*, 2006.

[78] C. Y. Ryu, S. H. Nam, and S. Kim, "Conductive rubber electrode for wearable health monitoring," in *Engineering in Medicine and Biology 27th Annual Conference*, Shangai, China, 2005, pp. 3279-3481.

[79] J. Muehlsteff and O. Such, "Dry electrodes for monitoring of vital signs," in *26th Annual International Conference of the IEEE EMBS*, San Francisco, 2004, pp. 2212-2215.

[80] C. Linti, H. Horter, P. Osterreicher, and H. Planck, "Sensory baby vest for the monitoring of infants," in *International Workshop on Wearable and Implantable Body Sensor Networks*, 2006.

[81] J. Muehlsteff, O. Such, R. Schmidt, M. Perkuhn, H. Reiter, J. Lauter, J. Thijs, G. Musch, and M. Harris, "Wearable approach for continuous ECG - and Activity Patient-Monitoring," in *26th Annual International Conference of the IEEE EMBS*, San Francisco, 2004, pp. 2184-2187.

[82] R. Paradiso, I. A. Gernignam, E. P. Scilingo, and D. De Rossi, "Knitted Bioclothes for Cardiopulmonary Monitoring," in *25 th Annual International Conference of the IEEE EMBS*, Cancun, Mexico, 2003, pp. 3720-3723.

[83] Tognetti A et al, "Strain Sensing Fabric Characterisation," in *3rd IEEE International Conference on Sensors*, Vienna, Austria, 2004, pp. 527-530.

[84] Georgia Tech, "http://www.sensatex.com/," accessed May 2007.

[85] Virginia Tech, "http:/www.ecpe.vt.edu/news/ar04/hokie.html." vol. April 2004, accessed 2004.
[86] MIT, "www.media.mit.edu/wearables," accessed May 2007.
[87] Georgia Tech., "Wearable Motherboard.www.wearables.gatech.edu," accessed May 2007.
[88] Philips-Healthcare., "http://www.research.philips.com/newscenter/archive/2005/050623-aachen-healthcare.html," accessed May 2007.
[89] Interactive Wear (ex Infineon), "www.interactive-wear.com," accessed May 2007.
[90] Fraunhofer IBMT, "Fraunhofer Projects http://www.ibmt.fraunhofer.de," accessed April 2006.
[91] ETH Wearables, "www.wearable.ethz.ch," accessed May 2007.
[92] J. Habetha, "The MyHeart Project- Fighting Cardiovascular Diseases by Prevention and Early Diagnosis," in *28th IEEE EMBS International Conference*, New York City, USA, 2006, pp. 6746-6749.
[93] G. Loriga, N. Taccini, D. De Rossi, and R. Paradiso, "Textile Sensing Interfaces for Cardiopulmonary Siogns Monitoring," in *Engineering in Medicine and Biology 27th Annual Conference*, Shangai, China, 2005.
[94] T. Linz, C. Kallmayer, R. Aschenbrenner, and H. Reichl, "Fully Integrated EKG Shirt based on Embroided Electrical Interconnections with Conductive Yarn and Miniaturised Flexible Electronics," in *International Workshop on Wearable and Implantable Body Sensor Networks*, 2006.
[95] E. P. Scilingo, A. Gemignani, Paradiso R, N. Taccini, B. Ghelarducci, and D. De Rossi, "Performance Evaluation of Sensing Fabrics for Monitoring Physiological and Biomechanical Variables" *IEEE Transactions on Information Technology in Biomedicine,* vol. 9, pp. 345-352, 2005.
[96] Bekaert, "www.bekaert.com/bft/products/Innovation%20textiles/Forms%20_%20products.html," accessed May 2007.
[97] P. Mirtaheri, S. Grimnes, and O. G. Martinsen, "Electrode Polarisation Impedance in Weak Na Cl Aqueous Solutions," *IEEE Transactions on Biomedical Engineering,* vol. 52, pp. 2093-2099, 2005.
[98] Shieldex Trading, "www.shieldextrading.com," accessed 2007.
[99] SWICOFIL, "www.swicofil.com/rstatconductivity.html," accessed May 2007.
[100] Elektrisola, "www.textile-wire.ch," accessed June 2007.
[101] T. A. Skotheim and J. R. Reynolds, "Handbook of Conducting Polymers," 3rd ed: CRC Press, 2007.
[102] S. Gimpel, U. Mohring, H. Mueller, A. Neudeck, and W. Scheibner, "Textile Based Electronic Substrate Technology," *Journal of Industrial Textiles,* vol. 33, Jan 2004 2004.
[103] A. C. Metting van Rijn, A. Peper, and C. A. Grimbergen, "High-quality recording of bioelectric events. Part 1 Interference reduction, theory and practice," *Medical & Biological Engineering & Computing,* pp. 389-397, 1990.
[104] M. Fernandez Chimeno and R. Pallas-Areny, "A Comprehensive Model for Power Line Interference Analysis," *IEEE Transactions on Instrumentation and Measurement,* vol. 49, pp. 535-540, 2000.
[105] E. M. Spinelli and M. A. Mayosky, "A practical approach to electrode-skin impedance unbalance measurement.," in *IEEE*, yet to be published.

[106] M. J. Burke and D. T. Gleeson, "A Micropower Dry-Electrode ECG Preamplifier," *IEEE Transactions on Biomedical Engineering,* vol. 47, pp. 155-162, 2000.
[107] C. Travis, "Nonlinear aspects of the bioelectrode-electrolyte interface," in *Biomedical electrode technology*, H. A. Miller, Ed. New York: Academic Press, 1974, pp. 143-159.
[108] P. Zipp and H. Ahrens, "A model of bioelectrode motion artifact and reduction of artifact by amplifier input stage design," *Journal Biomedical Engineering,* vol. 1, pp. 273-276, 1979.
[109] M. R. Neuman, "Biopotential electrodes," in *Medical Instrumentation, Application and Design*, 2nd ed, J. G. Webster, Ed. New York: John Wiley and Sons, 1995, pp. 227-287.
[110] E. S. Valchinov and N. E. Pallikarakis, "An active electrode for biopotential recording from small localized bio-sources" *Biomedical Engineering Online,* vol. 3, pp. 1-14, 2004.
[111] E. Huigen, A. Peper, and C. A. Grimbergen, "Investigation into the origin of the noise of surface electrodes," *Medical & Biological Engineering & Computing,* vol. 40, pp. 332-338, 2002.
[112] H. Tagami, Y. Kanamaru, K. Inoue, S. Suehisa, F. Inoue, K. Iwatsuki, K. Yoshikuni, and M. Yamada, "Water sorption -desorption Test of the Skin in Vivo for Functional Assessment of the Stratum Corneum," *The Journal of Investigative Dermatology* vol. 78, pp. 425-428, 1982.
[113] O. G. Martinsen and S. Grimnes, "Facts and Myths about Electrical Measurement of Stratum Corneum Hydration State," *Dermatology,* vol. 202, pp. 87-89, 2001.
[114] D. C. Salter, "Examination of Stratum corneum Hydration State by Electrical Methods," in *Skin Bioengineering Techniques and Applications in Dermatology and Cosmetology*. vol. 26, P. Elsner, A. O. Barel, E. Berardesca, B. Gabard, and J. Scrup, Eds.: Basel, Karger, 1998, pp. 38-47.
[115] B. H. Cornish, B. J. Thomas, and L. C. Ward, "Effect of Temperature and Sweating on Bioimpedance Measurements," *Appl. Radiat. Isot.,* vol. 49, 1998.
[116] M. Tronnier, M. Weibusch, and U. Heinrich, "Frictionometry on human skin," *Skin Research and Technology,* vol. 9, May 2003.
[117] P. Kenins, "Influence of Fibre Type and Moisture on Measured Fabric-to-Skin Friction," *Textile Research Journal,* vol. 64, pp. 722-728, 1994.
[118] S. Comaish and E. Bottoms, "The skin and friction: deviations from Amonton's laws, and the effects of hydration and lubrication," *British Journal Dermatology,* vol. 84, pp. 37-43, 1971.
[119] W. Besio and A. Prasad, "Analysis of Skin - Electrode Impedance Using Concentric Ring Electrode," in *28th Annual International Conference of the IEEE EMBS*, New York, , 2006, pp. 6414-6417.
[120] F. You, J. M. Wang, and X. N. Luo, "Garment's pressure sensation(1): subjective assessment and predicability for the sensation," *InternationalJournal of Clothing Science and Technology,* vol. 14, pp. 307-316, 2002.
[121] F. You, J. M. Wang, and X. N. Luo, "Garment's pressure sensation(2): the psychophysical mechanism for the sensation," *International Journal of Clothing Science and Technology,* vol. 14, pp. 317-327, 2002.
[122] A. Miyatsuji, T. Matsumoto, S. Mitarai, T. Kotabe, T. Takeshima, and S. Watanuki, "Effects of Clothing Pressure caused by different types of brassieres on Autonomic Nervous System Activity evaluated by Heart Rate Variability

Power Spectral Analysis," *Journal of Physiological Anthropology and Applied Human Sciences,* vol. 21, pp. 67-74, 2002.
[123] G. R. S. Naylor and D. G. Phillips, "Skin Comfort of Wool Fabrics," in *9th Int. Wool Textile Research Conference*, 1995, pp. 203-209.
[124] S. Rhee, B. H. Yang, and H. Asada, "Artifact-Resistant Power-Efficient design of Finger-Ring Plethysmographic Sensors," *IEEE Transactions on Biomedical Engineering,* vol. 48, pp. 795-805, 2001.
[125] P. Bonato, P. J. Mork, D. M. Sherrill, and R. H. Westgaard, "Data Mining of Motor Patterns Recorded with Wearable Technology," in *IEEE Engineering in Medicine and Biology Magazine*, 2003, pp. 110-119.
[126] NASA, "http://www.nasatech.com/Briefs/Feb00/NPO20651.html." vol. 2006, accessed May 2006.
[127] E. Berkeley, "http://robotics.eecs.berkeley.edu/~pister/SmartDust/," accessed May 2007.
[128] R. Paradiso and D. De Rossi, "Advances in textile technologies for unobtrusive monitoring of vital parameters and movements.," in *28th EMBS Annual International Conference*, New York City, USA, 2006, pp. 392-395.
[129] T. Vuorela, K. Kukkonen, J. Rantanen, T. Jarvinen, and J. Vanhala, "Bioimpedance Measurement System for Smart Clothing," in *Seventh IEEE International Symposium on Wearable Computers*, 2003.
[130] Bodymedia Inc, "SenseWear PRO Armband. http://www.bodymedia.com/main.jsp," accessed May 2007.
[131] Polar, "Heart Rate Monitor. http://www.polarusa.com," accessed May 2007.
[132] Y. Li and D.-Q. Dai, "Biomechanical engineering of textiles and clothing," Cambridge, England: Woodhead Publishing Ltd., 2006, p. 428.
[133] D. J. Spencer, *Knitting Technology: A Comprehensive Handbook & Practice Guide.*, 3rd ed.: Woodhead Publishing Ltd., 2001.
[134] K. Cole, "Permeability and impermeability of cell membranes for ions," in *Cold Springs Harbor Symposium, Quant. Biol.*, 1940, pp. 110-122.
[135] E. R. Wade and H. H. Asada, "DC Powerline Communication Network for a Wearable Health Monitoring System," *IEEE,* pp. 172-175, 2005.
[136] J. V. Basmajian and C. J. De Luca, *Muscles alive: Their functions revealed by electromyography*, 5th ed.: Williams and Wilkins, Baltimore, Maryland., 1985.
[137] B. Gerdle, S. Karlsson, S. Day, and M. Djubsjobacka, "Acquisition, Processing and Analysis of the Surface Electromyogram," in *Modern Techniques in Neuroscience*, W. a. Johansson, Ed. Berlin: Springer Verlag,, 1999, pp. 705-755.
[138] A. Rainoldi, J. E. Bullock-Saxton, F. Cavarretta, and N. Hogan, "Repeatability of maximal voluntary force and of the surface EMG variables during voluntary isometric contraction of quadriceps muscles in healthy subjects," *Journal of Electromyography and Kinesiology,* vol. 11, pp. 425-438, 2001.
[139] B. Larsson, C. Karlberg, J. Elert, and B. Gerdle, "Reproducibility of surface EMG during dynamic shoulder forward flexions: a study of clinically healthy subjects" *Clinical Physiology,* vol. 19, pp. 433-439, 1999.
[140] SENIUM, "www.seniam.org." vol. 2006, accessed May 2006.
[141] B. Taheri, R. T. Knight, and R. L. Smith, "A dry electrode for EEG recording," *Electroencephalography and clinical Neurophysiology,* vol. 90, 1994.
[142] C. A. Smith, "Dimensions of Appraisal and Physiological Response in Emotion," *Journal of Personality and Social Pshychology,* vol. 56, pp. 339-353, 1989.

[143] R. Helmer and M. Mestrovic, "System and Garment for Detecting Movement." vol. WO 2007/041806 A1, W. I. P. Organisation, Ed. Australia: CSIRO, 2006.
[144] B. J. Munro, J. R. Steele, T. E. Campbell, and G. G. Wallace, "Wearable Textile Biofeedback Systems: Are They Too Intelligent for the Wearer," *Studies in Health Technology and Informatics,* vol. 108, pp. 271-277, 2004.
[145] D. De Rossi and E. P. Scilingo, "Skin-like sensor arrays. www.piaggio.ccii.unipi.it/bio/corsi/modelli/2005-6/docs/systema%20sensoriale/skin_like_sensor_arrays.pdf," 2005.
[146] M. Y. Leung, X. M. Tao, X. Y. Cheng, J. Tsang, and M. C. W. Yuen, "Polypyrrole-coated conductive fabrics as a candidate for strain sensors," *Journal of Materials Science,* vol. 40, pp. 4093-4095, 2005.
[147] K. W. Oh, J. P. Park, and S. H. Kim, "Stretchable Conductive Fabric for Electrotherapy," *Journal of Applied Polymer Science,* vol. 88, pp. 1225-1229, 2003.
[148] X. Cheng, Y. Li, X. Tao, H. Y. J. Tsang, M. Y. Lueng, P. Xue, X. Cheng, and C. W. M. Yuen, "Polypyrrole -coated fabric Strain Sensor with High Sensitivity and Good Stability," in *1st International Conference on Nano/Micro Engineered and Molecular Systems*, Zhuhai, China, 2006, pp. 1245-1249.
[149] Oko, "Limit Values and Fastness. http://www.oeko-tex.com/xdesk/ximages/470/16132_grenzwerte.pdf."vol. 2007, accessed May 2007.
[150] Oko, "OKO-Tex Standard 100." vol. 2007, accessed May 2007.
[151] T. W. Shen and W. J. Tompkins, "Biometric Statistical Study of One-Lead ECG Features and Body Mass Index(BMI)," in *IEEE Engineering in Medicine and Biology 27th Annual Conference*, Shangai, China, 2005, pp. 1162-1165.
[152] M. L. Buist and A. J. Pullan, "The Effect of Torso Impedance on Epicardial and Body Surface Potentials: A Modelling Study," *IEEE Transactions on Biomedical Engineering,* vol. 50, pp. 816-824, 2003.
[153] A. Sagie, M. G. Larson, R. J. Goldberg, J. R. Bengtson, and D. Levy, "The Framingham Heart Study: An Improved method for adjusting the QT interval for heart rate.," *American Journal of Cardiology,* vol. 70, pp. 797-801, 1992.
[154] T.-H. Kang, C. Merritt, B. Karaguzel, and J. Wilson, "Sensors on Textile Substrates for Home-Based Healthcare Monitoring," in *1st Distributed Diagnosis and Home Healthcare Conference* Arlington,Virginia,USA: IEEE, 2006.
[155] S. Michielsen, "Device for Measuring Sliding Friction on Highloft Nonwovens," *Journal of Engineered Fibers and Fabrics,* vol. 1, pp. 23-31, 2006.
[156] R. J. Skotheim TA, "Handbook of Conducting Polymers," 3rd ed: CRC Press, 2007.